Computer-assisted Multiplicity Proofs
for Emden's Equation
on Domains with Hole

Zur Erlangung des akademischen Grades eines

Doktors der Naturwissenschaften

von der Fakultät für Mathematik des
Karlsruher Instituts für Technologie (KIT)
genehmigte

Dissertation

von

Dipl.-Math. Dagmar Rütters (geb. Roth)

aus Mühlhausen/Thür.

Declaration

The work described in this report is the result of my own investigations. All sections of the text and results that have been obtained from other work are fully referenced. I understand that cheating and plagiarism constitute a breach of University Regulations and will be dealt with accordingly.

Karlsruhe, July 8, 2014

Dagmar Rütters

Acknowledgement

At this point I would like to express my gratitude to a number of people who have helped me during the process of writing this thesis. In first place I would like to thank my supervisor Prof. Dr. Michael Plum who introduced me to the fascinating field of computer-assisted proofs. Many discussions with him and his helpful advice led to a successful completion of this thesis.
I would also like to thank my co-referee Prof. Dr. Filomena Pacella from the university "La Sapienza" in Rome. She originally suggested the topic of my thesis and gave valuable inspiration for related questions such as the problem considered in chapter 8.
Furthermore I thank Prof. Dr. Wolfgang Reichel for acting as co-referee.

The programs in my thesis are based on the Finite Element software M++. I would like to thank Prof. Dr. Christian Wieners for the possibility to use both his software and the cluster of his working group to execute the calculations for my results. Dr. Wolfgang Müller, Dr. Martin Sauter and in particular Dr. Daniel Maurer helped me in understanding M++ and answered my questions without complaining. I thank them a lot.

I would also like to thank Peter Rupp, Leonid Chaichenets and my husband for proofreading parts of this thesis.

Besides the people helping me on a mathematical level there are many more who supported me by building a pleasant office athmosphere, having lunch or coffee breaks with me or time for conversations: Dr. Maria Radosz, Marc Mitschele, Dr. Rainer Mandel, Dr. Hans-Jürgen Freisinger, Anton Verbitsky and particularly Marion Ewald.

Last but not least I would like to thank my family and my husband for their emotional support and encouragement during the last years.

Contents

1 Introduction

In this thesis we will mainly be concerned with the following parameter dependent problem for Emden's equation, given by

$$\begin{cases} -\Delta u & = & u^3 & \text{in } \Omega_t \\ u & = & 0 & \text{on } \partial\Omega_t \\ u & > & 0 & \text{in } \Omega_t, \end{cases} \qquad (1.1)$$

where $\Omega_t = (-t-1, t+1)^2 \backslash [-t, t]^2 \subset \mathbb{R}^2, t > 0$, is a square with quadratic hole. Our aim is to prove existence and multiplicity of solutions to this problem for various fixed values of t and, in some special cases, for whole intervals of t-values. It is easy to see that problem (1.1) is in fact equivalent to the problem of finding non-trivial solutions to

$$\begin{cases} -\Delta u & = & |u|^3 & \text{in } \Omega_t \\ u & = & 0 & \text{on } \partial\Omega_t, \end{cases} \qquad (1.2)$$

to which we will refer in the following.

As a motivation we will first summarize some results for Emden's equation on various domains in $\mathbb{R}^N$, $N \geq 2$, most of them of annulus type. For this purpose we consider the problem

$$\begin{cases} -\Delta u & = & |u|^p & \text{in } \Omega \\ u & = & 0 & \text{on } \partial\Omega, \end{cases} \qquad (1.3)$$

where $\Omega \subset \mathbb{R}^N$, $N \geq 2$, is a smoothly bounded domain and $p > 1$. It is well known that existence and also uniqueness of solutions to this problem depend strongly on the domain Ω and the parameter p. In case Ω is star-shaped and $p \geq \frac{N+2}{N-2}$, $N \geq 3$, Pohozaev's identity [60] proves that (1.3) admits no non-trivial solution. If however p is subcritical, existence of non-trivial solutions to (1.3) can be proved using e.g. the Mountain Pass Theorem [61]. Moreover, there are examples of domains for which existence of a solution implies also its uniqueness, e.g. in case of Ω being a ball [30] or Ω being symmetric and convex in N orthogonal directions and p close to the critical exponent [34]. It is even conjectured that for convex Ω and subcritical p there exists at most one non-trivial solution to (1.3) [22]. However, there are several examples showing that the conjecture cannot hold when the convexity assumption is dropped. In the following we will focus on some results for the case Ω being an annulus $A_R = \{x \in \mathbb{R}^N : R < |x| < R+1\}$ or another annulus type domain. In [14], [15], [20], [45], [46] and [47] the authors proved the existence of nonradial positive solutions in expanding annuli for sufficiently large R and moreover that the number of rotationally non-equivalent solutions tends to infinity as $R \to \infty$. Here some of the authors used the invariance of annuli w.r.t. different symmetry groups, e.g. in [45] the existence of critical points of the associated functional on subspaces of $H_0^1(\Omega)$ which are invariant under rotations by a fixed angle is proved.

If Ω is no longer an annulus, but still an annular-type domain, i.e. with expanding hole like our domain Ω_t above, one expects similar multiplicity results as in the above papers. Indeed, in [1], [15] and [25] the authors proved the existence of an increasing number of positive solutions as the domain expands. [2] covers also the case of sign changing solutions. The work of Ackerman et al. ([1] and [2]) is inspired by [25], and use ground state solutions of the limit problem in the open

strip (or cylinder in higher dimensions) as building blocks for solutions of (1.3) when the domain expands. The result is proved using a Lyapunov-Schmidt reduction argument. In contrast to the multibump solutions which are constructed in [1] and [2], the authors in [7] proved the existence of almost-radial solutions in annular-type domains. Here domains which are diffeomorphic to an annulus (by some diffeomorphism T) are considered and it is shown that there exist solutions (for sufficiently expanded domain) which are close to $\omega_R \circ T$, where ω_R is the unique positive solution of (1.3) on the corresponding annulus.

All results which are proved in the previously mentioned papers state existence and multiplicity in the asymptotic case, i.e. when the expansion parameter tends to infinity, and moreover the domain is smoothly bounded. We finally want to mention two papers by Dancer ([23] and [24]) where the opposite case, a domain with one or more small holes, is considered. It is proved that if the solutions of (1.3) on the domain without hole are non-degenerate and the holes are not too close to the boundary and sufficiently small, then the number of positive solutions on the domain with holes equals the number of positive solutions on the domain without hole. If the smoothness condition on the boundary of the domain could be dropped, this result applied to (1.2) would imply that there exists a unique positive solution of (1.2) if t is sufficiently small. Note that nondegeneracy and uniqueness of the positive solution of (1.2) with Ω_t replaced by $(-1, 1)^2$ has already been proven e.g. in [21].

The above papers motivate that also for problem (1.2) we expect multiplicity of solutions and moreover an increasing number of solutions as t grows. It is therefore our aim to prove existence and multiplicity of solutions to that problem for various fixed values of t or for whole parameter intervals. Since the methods in the cited papers gave results "only" in the asymptotic case we will use a completely different approach via a computer-assisted proof.

In the last decades the increasing performance of computers have led to a number of proofs in mathematics which are computer-assisted. The first major theorem proved with the help of a computer was the Four-Colour-Theorem (1976, [4]) but also the famous Kepler-conjecure was proven computer-aided.

In the following we mention some computer-assisted results concerning partial differential equations. We are aware of two major different approaches for proving existence of solutions to partial differential equations via computer-assistance: one is due to M.T. Nakao and the other one due to M. Plum. Both methods have in common that the given boundary value problem is reformulated as a fixed point equation, and the assumptions of a fixed point theorem to solve this problem are checked using the computer. However, the construction of the fixed point theorem and the methods for proving its assumptions differ, e.g. while Nakao's method requires verified solution of large linear and nonlinear systems in $\mathbb{R}^m$ and needs explicit a-priori projection error bounds, the method by Plum needs estimates on the spectrum of a self-adjoint operator. It depends on the given problem to decide which of both approaches is more suitable and easier to use. All results in this thesis have been obtained following the method of M. Plum. The main advantage is that it can also be applied to unbounded domains as it will be done in chapter 8.

Results proved by Nakao's method include e.g. verification of solutions to elliptic systems [63], parabolic [53] and hyperbolic [52] equations, stationary solutions for Navier-Stokes problems [36] and also verification of solution curves [51]. A recent survey paper [54] explains some variants of Nakao's method and includes many additional references. For the method of Plum we would like to mention [59], where the existence of an unknown solution branch for the Gelfand problem was proved, as well as [12] which is concerned with the verification of multiple travelling wave solutions of a nonlinear beam equation. In [50] and [49] it has been proved that the positive solution

of $-\Delta u - \lambda u - u^p = 0$ in $(0,1)^2$, with homogeneous Dirichlet boundary conditions, is unique and nondegenerate for all $\lambda \in [0, 2\pi^2)$ and $p = 2, 3$.

A general overview and introduction to the method of M. Plum is given in [58] and for some more examples we refer to [38], [13] and [44].

The main idea of Plum's method is to prove that in a suitable neighbourhood of some approximate solution ω to the given problem a true solution u exists. As already mentioned this is achieved by constructing an equivalent fixed point problem for the error $v = \omega - u$, similar to but a bit more general than the formulation in the Newton-Cantorovich Theorem. In proving that the corresponding fixed point operator maps a small ball into itself we need estimates for the defect of the approximate solution as well as a bound for the inverse of the linearization of the given problem at ω, which is obtained via eigenvalue bounds.

This thesis is organized as follows:

In chapter 2 we reformulate problem (1.2) as an equation of the form $\mathcal{F}(u) = 0$ with $\mathcal{F}$ being a map between Banach spaces. We will then explain how the fixed point problem mentioned above is constructed and formulate and prove the main existence and enclosure theorem. The subsequent three chapters are devoted to the computation of the main ingredients of this theorem: In chapter 3 we introduce methods to compute approximate solutions to (1.2), which provide a sufficiently small defect. The defect computation, which turns out to be rather technical, is explained in detail in chapter 4. Finally chapter 5 shows that a bound for the inverse of the linearization amounts to the computation of bounds for the spectrum of some self-adjoint operator. Therefore we will recall some methods concerning the calculation of upper and lower eigenvalues bounds and explain their application to the given problem.

In chapter 6 we present both purely approximate and rigorously verified results to problem (1.2) for fixed values of t in a grid $t_0 < t_1 < \ldots < t_n \leq 3$ where $t_i - t_{i-1}$ is small for all $i = 1, \ldots, n$. The results provide existence, multiplicity and moreover enclosure of solutions to problem (1.2).

The subsequent chapter 7 is concerned with an existence and enclosure result for solutions of (1.2) when $t \in [t_{i-1}, t_i]$ and t_i given as above. We present an interpolation/perturbation argument which yields approximate solutions, defect data and bounds for the inverse of the linearization for all $t \in [t_{i-1}, t_i]$ as well as an approach to verfiy the existence of smooth solution branches $(u_t)_{t \in (t_{i-1}, t_i)}$. The chapter concludes with some verified results.

In chapter 8 we consider the equation $-\Delta u = |u|^3$ with homogeneous Dirichlet boundary conditions on the unbounded L-shaped domain $\Omega = ((-1, \infty) \times (0, 1)) \cup ((-1, 0) \times (-\infty, 1))$. We prove the existence of a symmetric solution to this problem having a bump centered in the corner of the domain. Besides that this problem and the solution are interesting on their own, the solution might later also be used as a building block in expanding domains having rectangular corners. This is motivated by [1] and [2], where smoothly bounded domains are considered and the solution on the inifinite strip is used as a building block.

Chapter 9 revisits problem (1.2) for parameter values $t \geq 3$ (or $t \geq 1.5$ in some cases). By using basic corner and edgebumps as building blocks (similar to the idea in chapter 8) we prove existence and multiplicity of solutions to (1.2) for all $t \geq 3$ (or $t \geq 1.5$ in some cases).

2 Existence and Enclosure Theorem

In this chapter we will formulate and prove the main existence and enclosure Theorem for the problem

$$\begin{cases} -\Delta u &= |u|^3 & \text{in } \Omega \\ u &= 0 & \text{on } \partial\Omega, \end{cases} \tag{2.1}$$

where $\Omega \subset \mathbb{R}^2$ is a domain, not necessarily bounded. We first reformulate (2.1) as an equation $\mathcal{F}(u) = 0$ where X, Y and $\mathcal{F} : X \to Y$ are to be chosen appropriately and search for approximate solutions $\omega \in X$ of this equation. The crucial idea is to prove existence of a true solution in a suitable neighbourhood of some approximate solution ω. This will be done by rewriting the equation $\mathcal{F}(u) = 0$ as a fixed point problem for the error $v = u - \omega$ and using Schauder's or Banach's Fixed Point Theorem.

The main idea for the existence and enclosure theorem is due to Plum [56]. The proceeding in this chapter follows various papers by Plum or Plum et al., see [58],[50]. We repeat the main steps and results in the following.

2.1 Formulation as an Equation $\mathcal{F}(u) = 0$

By $H_0^1(\Omega)$ we denote the space of all functions in $L^2(\Omega)$ with zero Dirichlet boundary values (in the trace sense) and weak first derivatives in $L^2(\Omega)$. Endowed with the inner product $\langle u, v \rangle_{H_0^1} := \langle \nabla u, \nabla v \rangle_{L^2} + \langle u, v \rangle_{L^2}$, $H_0^1(\Omega)$ is a Hilbert space. Moreover, let $H^{-1}(\Omega)$ denote the dual space of $H_0^1(\Omega)$, i.e. the space of all bounded linear functionals on $H_0^1(\Omega)$, equipped with the usual operator sup-norm.

Let now $\mathcal{F} : H_0^1(\Omega) \to H^{-1}(\Omega)$, $\mathcal{F}(u) = -\Delta u - |u|^3$. We will first briefly repeat the well-known way of interpreting $-\Delta u$ and $|u|^3$ as elements of $H^{-1}(\Omega)$ for $u \in H_0^1(\Omega)$. For the Laplacian, we simply imitate partial integration:

$$(-\Delta u)[v] = \int_\Omega \nabla u \cdot \nabla v \, dx \quad \text{for all } v \in H_0^1(\Omega).$$

Then

$$|(-\Delta u)[v]| \le \int_\Omega |\nabla u \cdot \nabla v| \, dx \le \|\nabla u\|_{L^2} \|\nabla v\|_{L^2} \le \|\nabla u\|_{L^2} \|v\|_{H_0^1} \quad (v \in H_0^1(\Omega))$$

implies that $-\Delta u$ is indeed a bounded linear functional and

$$\| -\Delta u\|_{H^{-1}} \le \|\nabla u\|_{L^2} \le \|u\|_{H_0^1}.$$

Let now $f : \Omega \times \mathbb{R} \to \mathbb{R}$. In order to define some expression of the form $f(\cdot, u)$ as an element of $H^{-1}(\Omega)$, we recall Sobolev's Embedding Theorem. Since $\Omega \subset \mathbb{R}^2$ the theorem states that the embedding $H_0^1(\Omega) \hookrightarrow L^p(\Omega)$ is bounded for all $p \in [2, \infty)$, i.e. there exists some constant $C_p > 0$ such that $\|w\|_{L^p} \le C_p \|w\|_{H_0^1}$ for all $w \in H_0^1(\Omega)$. Denoting by p' the dual number to p (which is defined by the relation $\frac{1}{p} + \frac{1}{p'} = 1$) we obtain for any function $w \in L^{p'}(\Omega)$

$$\int_\Omega |wv| \, dx \le \|w\|_{L^{p'}} \|v\|_{L^p} \le C_p \|w\|_{L^{p'}} \|v\|_{H_0^1}, \quad (v \in H_0^1(\Omega)), \tag{2.2}$$

where we used Hölder's inequality and the above embedding. Thus for any $p' \in (1, 2]$ we can interpret $w \in L^{p'}(\Omega)$ as a bounded linear functional on $H_0^1(\Omega)$ via the definition

$$w[v] := \int_\Omega wv \, dx.$$

The crucial condition for $f(\cdot, u)$ being an element of $H^{-1}(\Omega)$ is therefore given by $f(\cdot, u) \in L^{p'}(\Omega)$ for some $p' \in (1, 2]$. This is for instance satisfied if $|f(\cdot, y)| \le C(|y| + |y|^q)$ for some $q \in (1, \infty)$, and hence in particular for $f(\cdot, u) = |u|^3$, $f(\cdot, u) = u$ or $f(\cdot, u) = 3|w|wu$, where $u, w \in H_0^1(\Omega)$. Therefore, $\mathcal{F}$ as stated above is well-defined and finding weak solutions of (2.1) is equivalent to find zeros of $\mathcal{F}$.

The mapping $\mathcal{F}$ is moreover Fréchet differentiable with Fréchet derivative (at some $w \in H_0^1(\Omega)$) given by

$$\mathcal{F}'(w)[v] = -\Delta v - 3|w|wv \quad \text{for all } v \in H_0^1(\Omega).$$

Note that also $\mathcal{F}'(w)[v] \in H^{-1}(\Omega)$ by the previous considerations. In the following we denote $L_\omega := \mathcal{F}'(\omega)$.

We assume that $\omega \in H_0^1(\Omega)$ is an approximate solution to $\mathcal{F}(u) = 0$ and that constants δ and K are known such that

(i) δ bounds the defect of the approximate solution in the H^{-1}-norm, i.e.

$$\|\mathcal{F}(\omega)\|_{H^{-1}} = \| -\Delta\omega - |\omega|^3 \|_{H^{-1}} \le \delta, \tag{2.3}$$

(ii) K bounds the inverse of the linearization of $\mathcal{F}$ at ω, i.e.

$$\|v\|_{H_0^1} \le K \, \|L_\omega[v]\|_{H^{-1}} \quad \text{for all } v \in H_0^1(\Omega). \tag{2.4}$$

Note that condition (2.4) immediately implies that L_ω is one-to-one. We will also need that L_ω is onto. For this purpose we introduce the linear mapping $\Phi : H_0^1(\Omega) \to H^{-1}(\Omega)$, given by

$$(\Phi[u])(v) := \langle u, v \rangle_{H_0^1} \quad (u, v \in H_0^1(\Omega)). \tag{2.5}$$

Φ is an isometry, since for all $u \in H_0^1(\Omega)$ we have

$$\|\Phi[u]\|_{H^{-1}} = \sup_{v \in H_0^1(\Omega) \setminus \{0\}} \frac{|(\Phi[u])(v)|}{\|v\|_{H_0^1}} = \sup_{v \in H_0^1(\Omega) \setminus \{0\}} \frac{\langle u, v \rangle_{H_0^1}}{\|v\|_{H_0^1}} = \|u\|_{H_0^1}$$

(where "$\le$" in the last step due to Cauchy-Schwarz and equality is attained for $v = u$). Using Riesz' representation theorem for bounded linear functionals on a Hilbert space, we can moreover prove that Φ is onto: For any $\varphi \in H^{-1}(\Omega)$ there exists some unique $u \in H_0^1(\Omega)$, such that $\varphi(v) = \langle u, v \rangle_{H_0^1}$ for all $v \in H_0^1(\Omega)$, i.e. $\Phi[u] = \varphi$ by (2.5). Φ is the usual canonical isometric isomorphism between $H_0^1(\Omega)$ and $H^{-1}(\Omega)$, and we can define an inner product on $H^{-1}(\Omega)$ by

$$\langle \varphi, \psi \rangle_{H^{-1}} := \langle \Phi^{-1}[\varphi], \Phi^{-1}[\psi] \rangle_{H_0^1} \quad (\varphi, \psi \in H^{-1}(\Omega)). \tag{2.6}$$

For the norm $||| \cdot |||$ generated by this inner product we observe, using that Φ is an isometric isomorphism,

$$|||\varphi|||^2 = \langle \Phi^{-1}[\varphi], \Phi^{-1}[\varphi] \rangle_{H_0^1} = \|\varphi\|_{H^{-1}}^2,$$

and therefore this norm coincides with the old operator norm. With the inner product defined in (2.6), $H^{-1}(\Omega)$ becomes a Hilbert space.

In order to prove that L_ω is onto, we will show that

(i) $(\Phi^{-1}L_\omega)(H_0^1(\Omega))$ is dense in $H_0^1(\Omega)$, implying $L_\omega(H_0^1(\Omega))$ is dense in $H^{-1}(\Omega)$,

(ii) $L_\omega(H_0^1(\Omega)) \subset H^{-1}(\Omega)$ is closed.

For proving (i) we first show that $\Phi^{-1}L_\omega : H_0^1(\Omega) \to H_0^1(\Omega)$ is symmetric w.r.t. $\langle\cdot,\cdot\rangle_{H_0^1}$. Let $u, v \in H_0^1(\Omega)$:

$$\langle \Phi^{-1}L_\omega[u], v \rangle_{H_0^1} \overset{(2.5)}{=} \left(\Phi\left(\Phi^{-1}L_\omega[u]\right)\right)[v] = (L_\omega[u])[v]$$
$$= \int_\Omega \left[\nabla v \cdot \nabla u - 3|\omega|\omega vu\right] dx = (L_\omega[v])[u] \overset{(2.5)}{=} \langle u, \Phi^{-1}L_\omega[v] \rangle_{H_0^1}.$$

Let now $u \in H_0^1(\Omega)$ be an element of the orthogonal complement of $(\Phi^{-1}L_\omega)(H_0^1(\Omega))$, i.e. we have

$$0 = \langle u, \Phi^{-1}L_\omega[v] \rangle_{H_0^1} \overset{\text{symmetry}}{=} \langle \Phi^{-1}L_\omega[u], v \rangle_{H_0^1} \quad \text{for all } v \in H_0^1(\Omega).$$

Therefore $\Phi^{-1}L_\omega[u] = 0$, which implies $L_\omega[u] = 0$ and since L_ω is one-to-one we finally conclude $u = 0$. Thus (i) follows.

To prove (ii), let $(L_\omega[u_n])_{n\in\mathbb{N}}$ be a sequence in $L_\omega(H_0^1(\Omega))$ converging to some $\varphi \in H^{-1}(\Omega)$. Condition (2.4) shows that $(u_n)_{n\in\mathbb{N}}$ is a Cauchy sequence in $H_0^1(\Omega)$ and thus converges to some $u \in H_0^1(\Omega)$. Since L_ω is bounded, we obtain $L_\omega[u_n] \to L[u]$ $(n \to \infty)$ which gives $\varphi = L[u] \in L(H_0^1(\Omega))$ and therefore the closedness of $L(H_0^1(\Omega))$ in $H^{-1}(\Omega)$.

We are now able to formulate and prove our main existence and enclosure theorem for problem (2.1), see also [50, Theorem 1].

Theorem 1. *Let $\omega \in H_0^1(\Omega)$ be an approximate solution to (2.1) and δ and K constants such that (2.3) and (2.4) are satisfied. Let moreover $C_4 > 0$ be an embedding constant for the embedding $H_0^1(\Omega) \hookrightarrow L^4(\Omega)$ and $\gamma := 3C_4^3$.*
Finally suppose that there exists some $\alpha > 0$ such that

$$\delta \leq \frac{\alpha}{K} - \gamma\alpha^2 \left(\|\omega\|_{L^4} + \tfrac{1}{3}C_4\alpha\right) \tag{2.7}$$

and

$$2K\gamma\alpha \left(\|\omega\|_{L^4} + \tfrac{1}{2}C_4\alpha\right) < 1. \tag{2.8}$$

Then there exists a solution $u \in H_0^1(\Omega)$ to problem (2.1) such that

$$\|\omega - u\|_{H_0^1} \leq \alpha, \tag{2.9}$$

which is moreover unique with the property (2.9).

We will need the following lemma (see [50, Lemmas 3.1 and 3.2]) to prove Theorem 1. For $p \in [2, \infty)$ we denote by C_p an embedding constant for the embedding $H_0^1(\Omega) \hookrightarrow L^p(\Omega)$.

Lemma 1. *Let $p_1, p_2, p_3, p_4 \in [2, \infty)$ such that $\frac{1}{p_1} + \frac{1}{p_2} + \frac{1}{p_2} + \frac{1}{p_4} = 1$.*

(a) *For all $u, \tilde{u}, v \in H_0^1(\Omega)$:*

$$\||u|u - |\tilde{u}|\tilde{u}] v\|_{H^{-1}} \leq C_{p_3}C_{p_4} \left(\|u\|_{L^{p_1}} + \|\tilde{u}\|_{L^{p_1}}\right) \|u - \tilde{u}\|_{L^{p_2}} \|v\|_{H_0^1}.$$

(b) *Let $u, \tilde{u} \in H_0^1(\Omega)$ and suppose that for some $K > 0$*

$$\|v\|_{H_0^1} \leq K \|L_{\tilde{u}}[v]\|_{H^{-1}} \quad \textit{for all } v \in H_0^1(\Omega)$$

(with L_w denoting the Fréchet derivative of $\mathcal{F}$ at $w \in H_0^1(\Omega)$) and

$$\kappa := 3 C_{p_3} C_{p_4} K \left(\|u\|_{L^{p_1}} + \|\tilde{u}\|_{L^{p_1}} \right) \|u - \tilde{u}\|_{L^{p_2}} < 1. \tag{2.10}$$

Then,

$$\|v\|_{H_0^1} \leq \frac{K}{1 - \kappa} \|L_u[v]\|_{H^{-1}} \quad \textit{for all } v \in H_0^1(\Omega).$$

Proof.   (a) The Mean Value Theorem gives

$$|u|u - |\tilde{u}|\tilde{u} = \int_0^1 2|tu + (1-t)\tilde{u}| \, dt \cdot (u - \tilde{u})$$

which, for all $\varphi \in H_0^1(\Omega)$, yields

$$\left| \int_\Omega \left[|u|u - |\tilde{u}|\tilde{u} \right] v\varphi \, dx \right| = 2 \left| \int_0^1 \int_\Omega |tu + (1-t)\tilde{u}|(u - \tilde{u})v\varphi \, dx \, dt \right|$$

$$\leq 2 \int_0^1 \|tu + (1-t)\tilde{u}\|_{L^{p_1}} \|u - \tilde{u}\|_{L^{p_2}} \|v\|_{L^{p_3}} \|\varphi\|_{L^{p_4}} \, dt$$

$$\leq 2 C_{p_3} C_{p_4} \int_0^1 \left[t\|u\|_{L^{p_1}} + (1-t)\|\tilde{u}\|_{L^{p_1}} \right] dt \cdot \|u - \tilde{u}\|_{L^{p_2}} \|v\|_{H_0^1} \|\varphi\|_{H_0^1}$$

$$= C_{p_3} C_{p_4} \left(\|u\|_{L^{p_1}} + \|\tilde{u}\|_{L^{p_1}} \right) \|u - \tilde{u}\|_{L^{p_2}} \|v\|_{H_0^1} \|\varphi\|_{H_0^1}.$$

(b) First note that $L_{\tilde{u}}[v] = -\Delta v - 3|\tilde{u}|\tilde{u}v = L_u[v] + 3 \left[|u|u - |\tilde{u}|\tilde{u} \right] v$. Using this equality and (a) we obtain

$$\|v\|_{H_0^1} \leq K \|L_{\tilde{u}}[v]\|_{H^{-1}} \leq K \left[\|L_u[v]\|_{H^{-1}} + \|3 \left[|u|u - |\tilde{u}|\tilde{u} \right] v\|_{H^{-1}} \right]$$
$$\leq K \|L_u[v]\|_{H^{-1}} + \kappa \|v\|_{H_0^1},$$

and since by assumption $\kappa < 1$, the assertion follows.

$\square$

Remark 1. Using the inequality $\|u - \tilde{u}\|_{L^{p_2}} \leq C_{p_2} \|u - \tilde{u}\|_{H_0^1}$ leads to a sufficient condition for (2.10). For the particular choice $p_1 = p_2 = p_3 = p_4 = 4$ condition (2.10) can be replaced by

$$\tilde{\kappa} := \gamma K \left(\|u\|_{L^4} + \|\tilde{u}\|_{L^4} \right) \|u - \tilde{u}\|_{H_0^1} < 1,$$

and the assertion of the lemma holds with $\tilde{\kappa}$ instead of κ.

Proof of Theorem 1, (see [50]). First rewrite problem (2.1) as follows: Find $u \in H_0^1(\Omega)$ such that

$$\underbrace{-\Delta u + \Delta\omega - 3|\omega|\omega(u - \omega)}_{L_\omega[u-\omega]} = \Delta\omega + |\omega|^3 + |u|^3 - |\omega|^3 - 3|\omega|\omega(u - \omega).$$

Denoting by $v := u - \omega$ the error between exact and approximate solution and using that L_ω is bijective, we can reformulate the problem as a fixed point problem for v:

$$v = T(v) := L_\omega^{-1} \left[\Delta\omega + |\omega|^3 + \left(|\omega + v|^3 - |\omega|^3 - 3|\omega|\omega v \right) \right]. \tag{2.11}$$

We will prove that the fixed point operator $T : H_0^1(\Omega) \to H_0^1(\Omega)$ maps $D := \{v \in H_0^1(\Omega) : \|v\|_{H_0^1} \leq \alpha\}$, with α satisfying (2.7), into itself and is contractive on D. Then Banach's Fixed Point Theorem ensures the existence of a unique fixed point $v^* \in D$ and therefore the existence of a solution $u = v^* + \omega$ to problem (3.10), which is unique in the ball with radius α centered at ω.

We first observe that for all $v, \tilde{v} \in H_0^1(\Omega)$

$$|\omega + v|^3 - |\omega + \tilde{v}|^3 - 3|\omega|\omega(v - \tilde{v}) = \int_0^1 \frac{d}{dt} \left[|\omega + tv + (1-t)\tilde{v}|^3 - 3t|\omega|\omega(v - \tilde{v}) \right] dt$$

$$= \int_0^1 3 \left[|\omega + tv + (1-t)\tilde{v}|(\omega + tv + (1-t)\tilde{v}) - |\omega|\omega \right] (v - \tilde{v}) \, dt.$$

Multiplying this equation by a test function, integrating over Ω and exchanging the order of integration on the right-hand-side yields

$$\left\| |\omega + v|^3 - |\omega + \tilde{v}|^3 - 3|\omega|\omega(v - \tilde{v}) \right\|_{H^{-1}}$$

$$\leq \sup_{\varphi \in H_0^1(\Omega) \setminus \{0\}} \|\varphi\|_{H_0^1}^{-1} \int_0^1 \left| \int_\Omega 3 \left[|\omega + tv + (1-t)\tilde{v}|(\omega + tv + (1-t)\tilde{v}) - |\omega|\omega \right] (v - \tilde{v})\varphi \, dx \right| dt$$

$$\leq \int_0^1 \gamma \left(\underbrace{\|\omega + tv + (1-t)\tilde{v}\|_{L^4}}_{\leq \|\omega\|_{L^4} + C_4 \|tv + (1-t)\tilde{v}\|_{H_0^1}} + \|\omega\|_{L^4} \right) \|tv + (1-t)\tilde{v}\|_{H_0^1} \|v - \tilde{v}\|_{H_0^1} \, dt$$

$$\leq \gamma \left[(\|v\|_{H_0^1} + \|\tilde{v}\|_{H_0^1})\|\omega\|_{L^4} + \tfrac{1}{3} C_4 (\|v\|_{H_0^1}^2 + \|\tilde{v}\|_{H_0^1}^2 + \|v\|_{H_0^1}\|\tilde{v}\|_{H_0^1}) \right] \|v - \tilde{v}\|_{H_0^1}. \tag{2.12}$$

Thus we obtain for any $v \in D$ (apply (2.12) with $\tilde{v} = 0$)

$$\|T(v)\|_{H_0^1} \overset{(2.4)}{\leq} K \| (\Delta\omega + |\omega|^3) + (|\omega + v|^3 - |\omega|^3 - 3|\omega|\omega v) \|_{H^{-1}}$$

$$\overset{(2.3),(2.12)}{\leq} K \left[\delta + \gamma \|\omega\|_{L^4} \|v\|_{H_0^1}^2 + \tfrac{1}{3}\gamma C_4 \|v\|_{H_0^1}^3 \right]$$

$$\leq K \left[\delta + \gamma(\|\omega\|_{L^4} + \tfrac{1}{3}C_4\alpha)\alpha^2 \right] \overset{(2.7)}{\leq} \alpha,$$

whence $T(D) \subset D$ follows.

To prove the contraction property on D, let $v, \tilde{v} \in D$. Then

$$\|T(v) - T(\tilde{v})\|_{H_0^1} \overset{(2.4)}{\leq} K \| |\omega + v|^3 - |\omega + \tilde{v}|^3 - 3|\omega|\omega(v - \tilde{v}) \|_{H^{-1}}$$

$$\overset{(2.12)}{\leq} K\gamma \left[(\|v\|_{H_0^1} + \|\tilde{v}\|_{H_0^1})\|\omega\|_{L^4} + \tfrac{1}{3}C_4(\|v\|_{H_0^1}^2 + \|\tilde{v}\|_{H_0^1}^2 + \|v\|_{H_0^1}\|\tilde{v}\|_{H_0^1}) \right] \|v - \tilde{v}\|_{H_0^1}$$

$$\leq 2K\gamma\alpha(\|\omega\|_{L^4} + \tfrac{1}{2}C_4\alpha)\|v - \tilde{v}\|_{H_0^1},$$

and the assertion follows using (2.8). □

Remark 2.   (a) Denote by $\psi(\alpha) := \frac{\alpha}{K} - \gamma\alpha^2\left(\|\omega\|_{L^4} + \frac{C_4}{3}\alpha\right)$ the right-hand-side of (2.7). Obviously ψ attains a positive maximum on $[0,\infty)$ and thus the existence of some $\alpha > 0$ satisfying (2.7) is equivalent to

$$\delta \leq \max_{\alpha\in[0,\infty)} \psi(\alpha). \tag{2.13}$$

This means that δ has to be sufficiently small, which will be satisfied if the approximate solution ω is computed with high accuracy.

Furthermore, a small defect bound δ will imply a small error bound α if K is not too large.

(b) Note that (2.7) will imply (2.8) if we require that δ satisfies (2.13) with a strict inequality, i.e.

$$\delta < \max_{\alpha\in[0,\infty)} \psi(\alpha)$$

and α is chosen appropriately. In order to prove this, let $\bar{\alpha} > 0$ such that

$$\psi(\bar{\alpha}) = \max_{\alpha\in[0,\infty)} \psi(\alpha).$$

Due to the structure of ψ, $\bar{\alpha}$ is unique and determined by $\psi'(\bar{\alpha}) = 0$. The latter equation implies

$$2\gamma K\bar{\alpha}(\|\omega\|_{L^4} + \tfrac{1}{2}C_4\bar{\alpha}) = 1$$

and therefore (2.7) and (2.8) will be satisfied for $\alpha < \bar{\alpha}$, α sufficiently close to $\bar{\alpha}$.

2.2   Computation of Embedding Constants

In the previous section we have made extensive use of the embedding constant C_4 for the embedding $H_0^1(\Omega) \hookrightarrow L^4(\Omega)$. The following lemma (see [58, Lemma 2]) provides an easy way to compute embedding constants for $H_0^1(\Omega) \hookrightarrow L^p(\Omega)$ for $p \in [2,\infty)$. Recall that $C_p > 0$ satisfies

$$\|u\|_{L^p} \leq C_p\|u\|_{H_0^1}\quad \text{for all } u \in H_0^1(\Omega), \tag{2.14}$$

where $\|u\|_{H_0^1}^2 = \|\nabla u\|_{L^2}^2 + \|u\|_{L^2}^2$.

Lemma 2. *Let $\Omega \subset \mathbb{R}^2$ and $p \in [2,\infty)$. Let $\rho^* \in [0,\infty)$ denote the minimal point of the spectrum of $-\Delta$ on $H_0^1(\Omega)$ and $\nu = \lfloor\frac{p}{2}\rfloor$. Then an embedding constant for $H_0^1(\Omega) \hookrightarrow L^p(\Omega)$ is given by*

$$C_p = \left(\frac{1}{2}\right)^{\frac{1}{2}+\frac{2\nu-3}{p}}\left[\frac{p}{2}\left(\frac{p}{2}-1\right)\cdots\left(\frac{p}{2}-\nu+2\right)\right]^{\frac{2}{p}}\frac{1}{\left(\rho^*+\frac{p}{2}\right)^{\frac{1}{p}}}.$$

(where the bracket-term is put equal to 1 if $\nu = 1$).

Applying Lemma 2 for $p = 2$, $p = 4$ and $p = 8$ gives

$$C_2 = \frac{1}{\sqrt{\rho^*+1}}, \qquad C_4 = \frac{1}{(2\rho^*+4)^{\frac{1}{4}}}, \qquad C_8 = \left(\frac{3}{2\sqrt{2}}\right)^{\frac{1}{4}}\frac{1}{(\rho^*+4)^{\frac{1}{8}}}.$$

The computation of a lower bound for ρ^* will be explained in section 6.3. It can be done using eigenvalue enclosure methods which are explained in section 5.2.

3 Approximate Solutions

In this chapter we will introduce and explain the methods used in this thesis to compute approximate solutions to problem (1.2). We will start with a brief review of the used Finite Element space and continue with algorithms to obtain the desired approximations. Finally we will show how to utilize corner singular functions in order to improve the quality of the approximate solutions.

3.1 Finite Elements

In this section we will briefly explain the Serendipity class of Finite Elements which we used throughout the computations. For a more general introduction into Finite Elements we refer to the books of Brenner and Scott [11] or Ciarlet [19].

Serendipity Elements were first described in 1968 by Ergatoudis, Irons and Zienkiewicz [29] and have become very popular for meshes discretized by parallelograms, and thus in particular rectangles. For these kinds of meshes the approximation order of Serendipity Elements of order $r = 1, 2$ in L^p and piecewise $W^{1,p}$ for $1 \leq p \leq \infty$ is the same as for Langrangian Finite Elements of order r, while simultaneously Serendipiy Elements have less degrees of freedom, resulting in lower computational cost.

For later purposes we will construct a Finite Element space which is suitable to discretize problems involving not only Dirichlet but also Neumann boundary conditions, i.e. problems of the form

$$\begin{cases} -\Delta u &=& f(u) \quad \text{in } \Omega \\ u &=& 0 \qquad \text{on } \Gamma_D \\ \frac{\partial u}{\partial \nu} &=& 0 \qquad \text{on } \partial\Omega \backslash \Gamma_D, \end{cases} \tag{3.1}$$

where $f : \mathbb{R} \to \mathbb{R}$ is a smooth function and $\Gamma_D \subset \partial\Omega$ is closed.

In the following, we will consider meshes discretized by both triangles and rectangles, and Serendipity Elements of order 2. We recall the constitution of a Finite Element space as it can be found in many textbooks about Finite Elements. We start with two reference elements $\hat{K}^t$ and $\hat{K}^q$, where $\hat{K}^t$ is the triangle with corners $(0,0), (1,0)$ and $(0,1)$ and $\hat{K}^q$ the unit square $(0,1)^2$. Sometimes it will not be necessary to distinguish between $\hat{K}^t$ and $\hat{K}^q$, hence we will omit the index and write $\hat{K}$ only. This will be a convention also for other variables to be introduced later on. On $\hat{K}$ we have a finite dimensional space $\hat{V}$ spanned by reference element shape functions, which are for Serendipity Elements of order 2 given by

$$\begin{aligned} \hat{s}_0^t(\hat{x}, \hat{y}) &=& (1 - \hat{x} - \hat{y})(1 - 2\hat{x} - 2\hat{y}) \\ \hat{s}_1^t(\hat{x}, \hat{y}) &=& \hat{x}(2\hat{x} - 1) \\ \hat{s}_2^t(\hat{x}, \hat{y}) &=& \hat{y}(2\hat{y} - 1) \\ \hat{s}_3^t(\hat{x}, \hat{y}) &=& 4\hat{x}(1 - \hat{x} - \hat{y}) \\ \hat{s}_4^t(\hat{x}, \hat{y}) &=& 4\hat{x}\hat{y} \\ \hat{s}_5^t(\hat{x}, \hat{y}) &=& 4\hat{y}(1 - \hat{x} - \hat{y}) \end{aligned} \qquad \text{for } (\hat{x}, \hat{y}) \in \hat{K}^t, \tag{3.2}$$

and

$$
\begin{aligned}
\hat{s}_0^q(\hat{x}, \hat{y}) &= (1 - \hat{x})(1 - \hat{y})(1 - 2\hat{x} - 2\hat{y}) \\
\hat{s}_1^q(\hat{x}, \hat{y}) &= -\hat{x}(1 - \hat{y})(1 - 2\hat{x} + 2\hat{y}) \\
\hat{s}_2^q(\hat{x}, \hat{y}) &= -\hat{x}\hat{y}(3 - 2\hat{x} - 2\hat{y}) \\
\hat{s}_3^q(\hat{x}, \hat{y}) &= -\hat{y}(1 - \hat{x})(1 + 2\hat{x} - 2\hat{y}) \\
\hat{s}_4^q(\hat{x}, \hat{y}) &= 4\hat{x}(1 - \hat{x})(1 - \hat{y}) \\
\hat{s}_5^q(\hat{x}, \hat{y}) &= 4\hat{x}\hat{y}(1 - \hat{y}) \\
\hat{s}_6^q(\hat{x}, \hat{y}) &= 4\hat{x}\hat{y}(1 - \hat{x}) \\
\hat{s}_7^q(\hat{x}, \hat{y}) &= 4\hat{y}(1 - \hat{x})(1 - \hat{y})
\end{aligned}
\qquad \text{for } (\hat{x}, \hat{y}) \in \hat{K}^q. \tag{3.3}
$$

More precisely we have

$$
\hat{V} = \hat{V}^q := \operatorname{span}\{\hat{s}_0^q, \ldots, \hat{s}_7^q\} \quad \text{or} \quad \hat{V} = \hat{V}^t := \operatorname{span}\{\hat{s}_0^t, \ldots, \hat{s}_5^t\}, \quad \text{respectively.}
$$

Each shape function is associated to a node of $\hat{K}$, which are vertices or midpoints of the edges, respectively. We denote the nodes of $\hat{K}^q$ by $\hat{\xi}_i^q$, $i = 0, \ldots, 7 =: m^q$ and $\hat{\xi}_i^t$, $i = 1, \ldots, 5 =: m^t$, thereby observing the identities

$$
\hat{s}_i(\hat{\xi}_j) = \delta_{ij} \quad i, j = 1, \ldots, m. \tag{3.4}
$$

Figure 3.1 shows the arrangement of nodes in the reference elements.
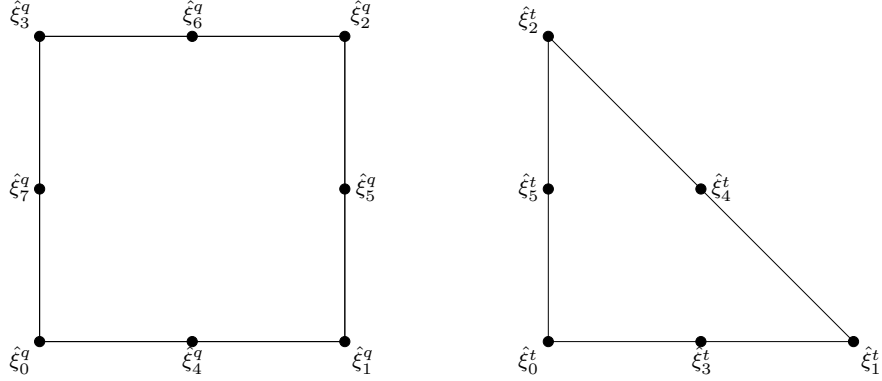
Figure 3.1: Reference elements with corresponding nodes

Let now $\mathcal{T}$ be a partition of a bounded polygonal domain $\Omega \subset \mathbb{R}^2$ into images of $\hat{K} = \hat{K}^q$ or $\hat{K} = \hat{K}^t$ under affine mappings. Note that we allow both reference elements here, so the resulting discretized domain may consist of both triangles and parallelograms. In case $\Omega = \Omega_t$, with Ω_t being the domain in problem (1.2), we may require the mappings not only to be affine, but to be an element of

$$
\mathrm{Aff}_{\mathrm{par}} := \left\{ F : \hat{K}^q \to \mathbb{R}^2 : F(\hat{x}, \hat{y}) = \begin{pmatrix} a & 0 \\ 0 & b \end{pmatrix} \begin{pmatrix} \hat{x} \\ \hat{y} \end{pmatrix} + \begin{pmatrix} c \\ d \end{pmatrix}, \ a, b \in \mathbb{R} \backslash \{0\}, c, d \in \mathbb{R} \right\} \cup
$$

$$
\left\{ F : \hat{K}^t \to \mathbb{R}^2 : F(\hat{x}, \hat{y}) = a \begin{pmatrix} \cos\alpha & -\sin\alpha \\ \sin\alpha & \cos\alpha \end{pmatrix} \begin{pmatrix} \hat{x} \\ \hat{y} \end{pmatrix} + \begin{pmatrix} c \\ d \end{pmatrix}, \ a \in \mathbb{R} \backslash \{0\}, \right.
$$

$$
\left. \alpha \in \{0, \tfrac{\pi}{2}, \pi, \tfrac{3\pi}{2}\}, \ c, d \in \mathbb{R} \right\},
$$

thereby obtaining a mesh involving only axis-parallel right-angled triangles and rectangles. For our purposes this will be sufficient, however for arbitrary polygonal domains Ω this restriction is too strong. We also remark that in order to discretize a domain into arbitrary triangles and quadrilaterals one has to permit bilinear mappings.

On an element $K = F(\hat{K})$ of $\mathcal{T}$ (with $F \in \text{Aff}_{\text{par}}$) we have a set of local shape functions

$$\{s_1^K, \ldots, s_m^K\} \quad \text{with} \quad s_i^K = \hat{s}_i \circ F^{-1}, \ i = 0, \ldots, m. \tag{3.5}$$

Again the local shape functions are associated to the nodes of K, given by $F(\hat{\xi}_i)$, $i = 0, \ldots, m$. Now we can define an affine equivalent Finite Element space V_{N,Γ_D} by

$$V_{N,\Gamma_D} := \left\{ v \in C(\overline{\Omega}) : \ v|_{\Gamma_D} = 0 \text{ and } v|_K \in \text{span}\{s_1^K, \ldots, s_m^K\}, \ K \in \mathcal{T} \right\}. \tag{3.6}$$

where $\Gamma_D \subset \partial\Omega$ denotes the part of the boundary where Dirichlet boundary conditions are imposed (cf. problem (3.1)). N indicates the number of unrestricted nodes in $\mathcal{T}$, i.e. the set $\mathcal{N} = \{\xi_1, \ldots, \xi_N\}$ consisting of all interior nodes together with nodes on $\partial\Omega \backslash \Gamma_D$. Note that the constructed Finite Element space is H^1-conforming. For later purposes we will also note that there is a basis $\{\varphi_1, \ldots, \varphi_N\}$ of V_{N,Γ_D}, which satisfies the conditions $\varphi_i(\xi_j) = \delta_{ij}$ for all $i, j = 1, \ldots, N$, ($\xi_j \in \mathcal{N}$). As an abbreviation we will use the notation $V_N := V_{N,\emptyset}$ and $V_N^D := V_{N,\partial\Omega}$. Clearly $V_N \supset V_{N,\Gamma_D}$ is true. In case the underlying domain Ω is not clear from the context, we will write $V_{N,\Gamma_D}(\Omega)$.

Moreover we define $I_{V_N} : C(\overline{\Omega}) \to V_N$ to be the interpolation operator for the Finite Element space, which maps a function $u \in C(\overline{\Omega})$ to its Finite Element interpolation, i.e. for $u \in C(\overline{\Omega})$ we have

$$I_{V_N}(u) = \sum_{i=1}^{N} u(\xi_i)\varphi_i. \tag{3.7}$$

Note that I_{V_N} maps $H_0^1(\Omega) \cap C(\overline{\Omega})$ into the space V_N^D.

As a motivation for using Serendipity Elements we recall a well-known result, which can e.g. be found in [19, Theorem 3.2.1]: Let $\mathcal{P}_r(\hat{K})$ be the space of polynomials of degree at most r on $\hat{K}$ and assume $\hat{V} \supseteq \mathcal{P}_r(\hat{K})$. Moreover let $\mathcal{T}_h$ be a regular family of decompositions of Ω, i.e.

a) there exists a constant $\sigma > 0$ such that for all $K \in \bigcup_h \mathcal{T}_h : \frac{h_K}{\rho_K} \leq \sigma$, where h_K denotes the diameter of the element K and ρ_K the diameter of the largest ball contained in K,

b) $h = \max\limits_{K \in \mathcal{T}_h} h_K$ tends to zero,

and V_N the corresponding Finite Element space, which is assumed to be constructed only from one single reference element. Then for any function $u \in H^{r+1}(\Omega)$ we have

$$\inf_{v \in V_N} \|u - v\|_{L^2(\Omega)} \leq Ch^{r+1}|v|_{r+1,\Omega} \tag{3.8}$$

$$\inf_{v \in V_N} \|u - v\|_{H^1(\Omega)} \leq Ch^{r}|v|_{r+1,\Omega}, \tag{3.9}$$

where C is a constant not depending on h and $|\cdot|_{r+1,\Omega}$ denotes the usual seminorm on $H^{r+1}(\Omega)$. The condition $\hat{V} \supseteq \mathcal{P}_r(\hat{K})$ is furthermore not only sufficient but also necessary for (3.8) and (3.9) to hold (see [5]).

Since $\mathcal{P}_2(\hat{K}) = \text{span}\{1, x, y, x^2, y^2, xy\}$ it is easy to see that $\hat{V} \supseteq P_2(\hat{K})$ and thus the above estimates hold with $r = 2$.

To compare, we briefly consider Langrangian Finite Elements, which in fact are constructed by the same space $\hat{V}^t$ as above in case of triangles and the space $\hat{V}^q$ plus a reference element shape funtion $\hat{s}_8^q(\hat{x}, \hat{y}) = 16\hat{x}\hat{y}(1 - \hat{x})(1 - \hat{y})$ in case of quadrilaterals. We introduce the notation $\hat{V}^L$ for the underlying space. Obviously $\hat{V}^L \supseteq \hat{V} \supseteq \mathcal{P}_2(\hat{K})$ and therefore we obtain the same approximation rate as for Serendipity Elements. Since moreover $\hat{V}^L \supseteq \mathcal{P}_3(\hat{K})$ is *not* true, this rate can not be improved and thus using Serendipity Elements instead of Langrangian Finite Elements does not lead to a loss of approximation quality in case of an affine equivalent Finite Element space.

However, it is immediately clear from the above, that the approximation rate is in both cases (Serendipity and Lagrangian Finite Elements) lower, if the function u is not smooth but e.g. only in $H^1(\Omega)$. This will also be the case in our applications, since our domain of interest has re-entrant corners. We will use corner singular functions to improve the approximations, see section 3.2.3 for details.

3.2   Algorithms

In order to compute approximate solutions to our given problem (1.2), we use a combination of the Mountain Pass Algorithm and a Newton method: A simplified version of the Mountain Pass Algorithm will give an approximate weak solution to our problem that serves as initial guess for a Newton method. Due to re-entrant corners of the domain, we will then introduce corner singular functions to obtain an improved approximate solution.

In this section we always consider the space $H_0^1(\Omega)$ equipped with norm $\|u\|_{H_0^1}^2 = \int_\Omega |\nabla u|^2 \, dx$, $(u \in H_0^1(\Omega))$.

3.2.1   Mountain Pass algorithm

Let $\Omega \subset \mathbb{R}^2$ be a domain. For the problem

$$\begin{cases} -\Delta u &= u^3 &\text{in } \Omega \\ u &= 0 &\text{on } \partial\Omega \end{cases} \tag{3.10}$$

the associated energy functional is given by

$$J(u) = \int_\Omega \left[\tfrac{1}{2}|\nabla u|^2 \, dx - \tfrac{1}{4}u^4 \right] \, dx, \qquad u \in H_0^1(\Omega). \tag{3.11}$$

We are now looking for critical points of the energy functional, since $J'(u) = 0$ implies that u is a weak solution of (3.10). Note that non-trivial solutions to (3.10) are not necessarily positive, but might also be negative or change sign. In particular, for any solution u to (3.10), also $-u$ is a solution. We are still only interested in positive solutions to (3.10), but for the equivalent formulation of finding critical points to the associated energy functional it is more convenient to drop this requirement for the moment. By choosing some parameters in the procedure below carefully we can hope for positive critical points, and check the desired positivity a-posteriori (see also the comments in the beginning of section 6.1).

For the functional J defined in (3.11) we have $J \in C^1(H_0^1(\Omega), \mathbb{R})$ and J satisfies the Palais-Smale condition (see [61]). Moreover we have $J(0) = 0$ and we can in addition prove that 0 is a local minimum of J: Since $\Omega \subset \mathbb{R}^2$ we have $H_0^1(\Omega) \hookrightarrow L^4(\Omega)$ and therefore $\|u\|_{L^4} \leq C_4 \|u\|_{H_0^1}$ for all $u \in H_0^1(\Omega)$. This yields

$$J(u) = \tfrac{1}{2}\|u\|_{H_0^1}^2 - \tfrac{1}{4}\|u\|_{L^4}^4 \geq \tfrac{1}{2}\|u\|_{H_0^1}^2 - \tfrac{C_4^4}{4}\|u\|_{H_0^1}^4 \geq 0 = J(0)$$

for all $u \in H_0^1(\Omega)$ such that

$$\|u\|_{H_0^1} \leq \frac{\sqrt{2}}{C_4^2}.$$

In particular this implies the existence of $\rho, \alpha > 0$ such that for all $u \in H_0^1(\Omega)$ with $\|u\|_{H_0^1} = \rho$ we have $J(u) > \alpha$. Since moreover for any $u \in H_0^1(\Omega)$ with $\|u\|_{H_0^1} = 1$, and $s > 0$ sufficiently large it holds

$$J(su) = \tfrac{1}{2}s^2 - \tfrac{1}{4}s^4\|u\|_{L^4} < 0, \tag{3.12}$$

the Mountain Pass Theorem (see e.g. [61]) implies the existence of at least one non-trivial critical point of J.

The original proof of the Mountain Pass Theorem is non-constructive and does not give insight how the critical point can be found in practise. A first algorithm to compute critical points arising from the Mountain Pass Theorem was presented by Choi and McKenna in [18]. The following simplified version is based on [17], where we modified some steps such that they are better suited to our cubic nonlinearity.

(i) Let $w_0 \in H_0^1(\Omega)$ be given such that $J(w_0) < 0$.

(ii) Find the maximum of J along the straight half-line connecting 0 and w_0, i.e. find $s^* > 0$ such that $J(s^* w_0) = \max_{s>0} J(sw_0)$. Define $w_1 := s^* w_0$.

(iii) Determine some $v \in H_0^1(\Omega)$ pointing into the direction of steepest descent at w_1 (approximately, with its length $\|v\|_{H_0^1}$ chosen appropriately); see below. If $\|v\|_{H_0^1}$ is less than a prescribed tolerance, stop the algorithm.

(iv) Go into the direction of steepest descent: Redefine $w_0 := w_1 + v$ and go to step (ii).

We want to comment on these steps when the algorithm is applied to the functional J given in (3.11). First note that (3.12) implies both the existence of a function $w_0 \in H_0^1(\Omega)$ as required in step (i), and the existence of a maximum of J on the half-line $\{sw_0 : s > 0\}$, which is needed in step (ii). An easy calculation shows

$$\frac{d}{ds} J(sw_0) = 0 \iff s \in \left\{ 0, \sqrt{\frac{\int_\Omega |\nabla w_0|^2 \, dx}{\int_\Omega w_0^4 \, dx}}, -\sqrt{\frac{\int_\Omega |\nabla w_0|^2 \, dx}{\int_\Omega w_0^4 \, dx}} \right\},$$

(note that $w_0 \neq 0$ due to $J(w_0) < 0$) and moreover for $s^* = \sqrt{\frac{\int_\Omega |\nabla w_0|^2 \, dx}{\int_\Omega w_0^4 \, dx}} > 0$ we have

$$\frac{d^2}{ds^2} J(sw) \Big|_{s=s^*} = -2 \int_\Omega |\nabla w_0|^2 \, dx < 0$$

and therefore the maximum of J on the half-line $\{sw_0 : s > 0\}$ is attained at $s^* w_0$.

We recall some considerations from [18] to find the direction of steepest descent at $w_1 \in H_0^1(\Omega)$. It corresponds to the function $\hat{v} \in H_0^1(\Omega)$ with $\|\hat{v}\|_{H_0^1} = 1$, such that

$$\lim_{\varepsilon \to 0} \frac{J(w_1 + \varepsilon \hat{v}) - J(w_1)}{\varepsilon}$$

becomes "as negative as possible", i.e. $\hat{v}$ minimizes the Fréchet derivative J' at w_1 applied to φ under the constraint $\|\varphi\|_{H_0^1(\Omega)} = 1$. For the minimizer $\hat{v}$ of that problem there exists a Lagrange parameter $\lambda \in \mathbb{R}$ such that

$$-2\lambda \Delta \hat{v} = \Delta w_1 + w_1^3. \tag{3.13}$$

Once a weak solution $w = 2\lambda \hat{v} \in H_0^1(\Omega)$ of $-\Delta w = \Delta w_1 + w_1^3$ is known, $|\lambda|$ can be determined such that $\|\hat{v}\|_{H_0^1} = 1$, and to find the sign of λ note that (as $\varepsilon \to 0$)

$$\frac{J(w_1 + \varepsilon \hat{v}) - J(w_1)}{\varepsilon} = \int_\Omega \left[\nabla w_1 \cdot \nabla \hat{v} - w_1^3 \hat{v} \right] \, dx + O(\varepsilon)$$

$$\overset{(3.13)}{=} \int_\Omega -2\lambda \nabla \hat{v} \cdot \nabla \hat{v} \, dx + O(\varepsilon) \overset{\|\hat{v}\|_{H_0^1} = 1}{=} -2\lambda + O(\varepsilon).$$

Since the left-hand-side becomes negative if w_1 is not a local minimum of J, λ must be positive. Finally we choose $v := 2\lambda \hat{v}$ in step (iii), which, due to $\lambda > 0$, points into the direction of steepest descent. Note that $-\Delta v$ equals the residual of the previous iteration and thus $\|v\|_{H_0^1} = 2\lambda$ will be small if w_1 is close to a solution of (3.10) and therefore close to a critical point of J. Numerical experience indicate that this choice of v is appropriate.

In our application to (1.2) the Mountain Pass Algorithm is used to find an approximate solution in terms of Finite Element functions. Thus we choose w_0 in (i), as well as $\hat{v}$ in (iii) to be elements of V_N^D. The latter leaves us with the computation of a Finite Element approximation of the weak solution to the linear problem (3.13). This can be done using a Ritz-method.

3.2.2 Newton method

We first recall the Newton method in Banach spaces (see also [6]).

Let X, Y be Banach-spaces, $\mathcal{F} : X \to Y$ a continuously Fréchet-differentiable mapping and $\omega^{(0)} \in X$ such that $\left[\mathcal{F}'(\omega^{(0)})\right]^{-1}$ is bounded and $\|\mathcal{F}(\omega^{(0)})\|$ is sufficiently small, i.e. $\omega^{(0)}$ is an approximate solution of $\mathcal{F}(\omega) = 0$. Then the sequence $\left(\hat{\omega}^{(n)}\right)_{n \in \mathbb{N}} \subset X$, which is defined by $\hat{\omega}^{(0)} = \omega^{(0)}, \hat{\omega}^{(n+1)} = \hat{\omega}^{(n)} + \hat{v}^{(n)}$, with $\hat{v}^{(n)} \in X$ being the solution of

$$\left(\mathcal{F}'(\hat{\omega}^{(n)})\right)[v] = -\mathcal{F}(\hat{\omega}^{(n)}) \tag{3.14}$$

(which exists if $\|\mathcal{F}(\hat{\omega}^{(0)})\|$ is small enough, see [6]) converges to a solution ω of the equation $\mathcal{F}(\omega) = 0$. Moreover ω is the only solution to this equation in a small neighbourhood of $\omega^{(0)}$.

The method can be used to construct a sequence of approximate solutions $\omega^{(1)}, \omega^{(2)}, \ldots \in X$ to $\mathcal{F}(u) = 0$ as follows: Instead of solving (3.14) exactly, we compute an approximate solution $v^{(n)} \in X$ to that problem (with $\hat{\omega}^{(n)}$ replaced by $\omega^{(n)}$) and define $\omega^{(n+1)} = \omega^{(n)} + v^{(n)}$. The iteration is stopped, when for some prescribed tolerance $\varepsilon > 0$ we have found $n_0 \in \mathbb{N}$ such that

$$\| \underbrace{\omega^{(n_0)} - \omega^{(n_0-1)}}_{=v^{(n_0-1)}} \| < \varepsilon.$$

$\omega^{(n_0)}$ will then serve as new approximate solution.

We will apply the Newton method twice in the process of computing approximate solutions. First it is used to improve the Finite Element approximation given by the Mountain Pass Algorithm. Here $X = H_0^1(\Omega_t)$, $Y = H^{-1}(\Omega_t)$ and $\mathcal{F}(u) := -\Delta u - |u|^3$. With the initial approximation $\omega^{(0)}$ being an element of $V_N^D \subset H_0^1(\Omega)$ and requiring the same for $v^{(n)}$, $n \in \mathbb{N}$ (again using a Ritz-method to solve the linear problems approximately) we finally obtain a Finite Element approximation $\omega^{(n_0)} \in V_N^D$. The second application will be explained in the end of section 3.2.3.

3.2.3 Corner singular functions

In this section will briefly recall some results from [32], [33] and [55], which state that the solution of the boundary value problem (1.2)

$$\begin{cases} -\Delta u &= |u|^3 \quad \text{in } \Omega_t \\ u &= 0 \quad\quad \text{on } \partial\Omega_t \end{cases}$$

can be split into a singular corner part and a regular part in $H^2(\Omega)$.

Recall that our domain is given by $\Omega_t = (-t+1, t+1)^2 \setminus [-t, t]^2$, and thus features four re-entrant corners $\xi_1 = (-t, t), \xi_2 = (t, t), \xi_3 = (t, -t)$ and $\xi_4 = (-t, -t)$. At each of these corners we introduce local polar coordinates (r_i, φ_i), where $r_i = |x - \xi_i|$ and φ_i ranges between 0 and $\theta := \frac{3\pi}{2}$, taking the minimal and maximal values on the two legs of the sector $\partial\Omega_t \cap B_r(\xi_i)$, respectively (where $r > 0$ is suitably chosen). Moreover, we define on $\overline{\Omega}_t$:

$$\gamma_i(r_i, \varphi_i) := r_i^{\frac{2}{3}} \sin\left(\tfrac{2}{3}\varphi_i\right), \qquad (i = 1, \dots, 4). \tag{3.15}$$

Obviously, $\gamma_i = 0$ on $\partial\Omega_t \cap B(\xi_i, r)$ when r is sufficiently small and one can easily check that $\Delta\gamma_i = 0$ in Ω_t $(i = 1, \dots, 4)$. For each $i \in \{1, \dots, 4\}$ we choose some fixed function $\lambda_i \in H^2(\Omega_t) \cap C^1(\overline{\Omega}_t)$ which vanishes on the part of $\partial\Omega_t$ where γ_i does not vanish and satisfies $\lambda_i(\xi_i) = 1$. Defining

$$w_i := \lambda_i \gamma_i \in H_0^1(\Omega_t) \qquad (i = 1, \dots, 4)$$

a solution $u \in H_0^1(\Omega_t)$ to (1.2) can be written as (see e.g. [55, Theorem 3.4])

$$u = \sum_{i=1}^{4} a_i w_i + v, \tag{3.16}$$

where $v \in H^2(\Omega_t) \cap H_0^1(\Omega_t)$ is the regular part and $a_i \in \mathbb{R}$ $(i = 1, \dots, 4)$ are the so-called stress-intensity-factors. We are now aiming at a computation of these factors: Using a dual singular function Γ_i we can represent a_i by means of the solution u. Let therefore

$$\Gamma_i(r_i, \varphi_i) = r_i^{-\frac{2}{3}} \sin\left(\tfrac{2}{3}\varphi_i\right)$$

and choose some fixed function $\Lambda_i \in H^2(\Omega_t) \cap C^1(\overline{\Omega}_t)$ with the following properties:

(i) Λ_i vanishes on the part of $\partial\Omega_t \setminus \{\xi_i\}$ where Γ_i does not vanish,

(ii) $\Lambda_i(\xi_i) = 1$,

(iii) $S := \Delta(\Lambda_i \Gamma_i) = (\Delta \Lambda_i)\Gamma_i + 2(\nabla \Lambda_i) \cdot (\nabla \Gamma_i) \in L^2(\Omega_t)$.

Then

$$W_i := \Lambda_i \Gamma_i$$

vanishes on $\partial \Omega_t \backslash \{\xi_i\}$ and the following theorem holds [55, Theorem 3.4]:

Theorem 2. *Let $u \in H_0^1(\Omega_t)$ be a weak solution of* (1.2)*, expressed in the form* (3.16)*. Then*

$$a_i = \frac{1}{\pi} \int_{\Omega_t} \left[W_i |u|^3 + S_i u \right] dx \qquad (i = 1, \dots, 4). \tag{3.17}$$

Clearly, a computation of the exact stress-intensity-factors by (3.17) is only possible if one knows also the exact solution u. For our purpose - the improvement of the approximate solution - it is however sufficient to know only approximations of a_i. So let the Finite Element function $\tilde{\omega}_t^{(n_0)} \in V_N^D$ be the approximate solution of (1.2) obtained by the Mountain Pass Algorithm and the Newton method (computed without separate singular part). Plugging this function into (3.17) yields approximate stress-intensity-factors

$$\tilde{a}_i := \frac{1}{\pi} \int_{\Omega_t} \left[W_i |\tilde{\omega}_t^{(n_0)}|^3 + S \tilde{\omega}_t^{(n_0)} \right] dx \qquad (i = 1, \dots, 4).$$

The approximation $\tilde{\omega}_t^{(n_0)}$ can now be improved as follows: Recall the Finite Element interpolation operator I_{V_N} defined in (3.7) and set $v_0 := \tilde{\omega}_t^{(n_0)} - I_{V_N}\left(\sum_{i=1}^4 \tilde{a}_i w_i\right)$, which is an initial guess for the regular part of the approximate solution to (1.2). Now apply a Newton method to improve the approximation of the regular part, i.e. use $X = H_0^1(\Omega_t)$, $Y = H^{-1}(\Omega_t)$ and

$$\mathcal{F}(v) = -\Delta v - \left| \sum_{i=1}^4 \tilde{a}_i w_i + v \right|^3 - \Delta \left(\sum_{i=1}^4 \tilde{a}_i w_i \right)$$

in the setting of section 3.2.2. We approximate the n-th iterate of this Newton method in V_N^D and denote it by v_m. The iteration is stopped when, for some $m_0 \in \mathbb{N}$ and a prescribed tolerance $\varepsilon > 0$,

$$\|v_{m_0} - v_{m_0-1}\| < \varepsilon$$

holds. We denote the final approximation of the regular part by $\tilde{v} := v_{m_0}$, whereby our final approximate solution to (1.2) is then given by:

$$\omega_t = \sum_{i=1}^4 \tilde{a}_i w_i + \tilde{v}. \tag{3.18}$$

4 Defect Computation

In this chapter we will explain how to compute a bound for the defect, i.e. some constant $\delta > 0$ such that

$$\| -\Delta\omega_t - |\omega_t|^3 \|_{H^{-1}} \le \delta,$$

where $\omega_t \in H_0^1(\Omega_t)$ is an approximate solution of (1.2).

4.1 Estimate by L^2-Norms

By definition, one has

$$\| -\Delta\omega_t - |\omega_t|^3 \|_{H^{-1}} = \sup_{\varphi \in H_0^1(\Omega_t)\setminus\{0\}} \frac{\left| \int_{\Omega_t} \left[\nabla\omega_t \cdot \nabla\varphi - |\omega_t|^3\varphi \right]\, dx \right|}{\|\varphi\|_{H_0^1}}, \tag{4.1}$$

which is, due to the supremum, disadvantageous for the computation of an upper bound.

We assume that $\hat{\rho} \in H(\mathrm{div},\Omega_t) = \{ u \in (L^2(\Omega_t))^2 \ : \ \mathrm{div}\, u \in L^2(\Omega_t)\}$ is an approximate minimizer of

$$\|\nabla\omega_t - \rho\|_{L^2}^2 + C_2^2 \|\,\mathrm{div}\,\rho + |\omega_t|^3\|_{L^2}^2.$$

Note that $\|\nabla\omega_t - \hat{\rho}\|_{L^2}^2 + C_2^2 \|\,\mathrm{div}\,\hat{\rho} + |\omega_t|^3\|_{L^2}^2$ is "small", since for $\nabla\omega_t \approx \hat{\rho}$ also $\mathrm{div}\,\hat{\rho} \approx \Delta\omega_t \approx -|\omega_t|^3$ follows (recall that $\omega_t \in H_0^1(\Omega_t)$ is an approximate solution to (1.2)).

Using the triangle inequality and $\|\,\mathrm{div}\, w\|_{H^{-1}} \le \|w\|_{L^2}$ for $w \in L^2(\Omega_t)$ we obtain:

$$\begin{aligned} \| -\Delta\omega_t - |\omega_t|^3 \|_{H^{-1}} &\le \| -\mathrm{div}(\nabla\omega_t) + \mathrm{div}\,\hat{\rho}\|_{H^{-1}} + \|\,\mathrm{div}\,\hat{\rho} + |\omega_t|^3\|_{H^{-1}} \\ &\le \|\nabla\omega_t - \hat{\rho}\|_{L^2} + \|\,\mathrm{div}\,\hat{\rho} + |\omega_t|^3\|_{H^{-1}}. \end{aligned}$$

Finally the embedding $L^2(\Omega_t) \hookrightarrow H^{-1}(\Omega_t)$ (with embedding constant C_2 being the one of the embedding $H_0^1(\Omega_t) \hookrightarrow L^2(\Omega_t)$) yields

$$\| -\Delta\omega_t - |\omega_t|^3 \|_{H^{-1}} \le \|\nabla\omega_t - \hat{\rho}\|_{L^2} + C_2 \|\,\mathrm{div}\,\hat{\rho} + |\omega_t|^3\|_{L^2}, \tag{4.2}$$

since $\mathrm{div}\,\hat{\rho} \in L^2(\Omega_t)$. Note that the right-hand-side of (4.2) will be small due to the (approximate) minimizing property of $\hat{\rho}$.

Remark 3. If $\Delta\omega_t + |\omega_t|^3$ was an element of $L^2(\Omega_t)$ (e.g. if ω_t was smooth enough), we could have used the dual embedding $L^2(\Omega_t) \hookrightarrow H^{-1}(\Omega_t)$ and thereby obtaining

$$\| -\Delta\omega_t - |\omega_t|^3 \|_{H^{-1}} \le C_2 \| -\Delta\omega_t - |\omega_t|^3 \|_{L^2}.$$

Equivalently, one can choose $\hat{\rho} := \nabla\omega_t$ in (4.2).

4.1.1 Application to the given problem

Recall that ω_t can be written as sum of a singular and an almost regular part, i.e.

$$\omega_t = \sum_{i=1}^{4} \tilde{a}_i\, w_i + \tilde{v},$$

where $w_i = \lambda_i \gamma_i$ with cut-off functions λ_i and singular functions $\gamma_i(r_i, \varphi_i) = r_i^{\frac{2}{3}} \sin\left(\frac{2}{3}\varphi_i\right)$ ((r_i, φ_i) local polar coordinates at the re-entrant corner ξ_i), $i = 1, \ldots, 4$ and $\tilde{v} \in V_N^D$.

Let now $\hat{\rho} = \sum_{i=1}^4 \tilde{a}_i \nabla w_i + \tilde{\rho}$ with $\tilde{\rho} \in (V_N)^2$ such that $\tilde{\rho} \approx \nabla v$ and $-\operatorname{div} \tilde{\rho} \approx \sum_{i=1}^4 \tilde{a}_i \Delta w_i + |\omega_t|^3$. Plugging this into (4.2) yields

$$\| -\Delta \omega_t - |\omega_t|^3 \|_{H^{-1}} \le \|\nabla \tilde{v} - \tilde{\rho}\|_{L^2} + C_2 \left\| -\operatorname{div} \tilde{\rho} - \sum_{i=1}^4 \tilde{a}_i \Delta w_i - \left| \sum_{i=1}^4 \tilde{a}_i w_i + \tilde{v} \right|^3 \right\|_{L^2}. \quad (4.3)$$

Both summands on the right-hand-side of (4.3) are square roots of integrals, so we are now left to compute upper bounds for integrals of non-negative functions. The first summand is an integral with integrand being a Finite Element function. It can be computed exactly using a quadrature rule of sufficiently high degree, applied in each element, and interval arithmetic. Our main concern in this section is the computation of a tight upper bound for the second summand in an effective way. The main problem is the mixture of cartesian coordinates and polar coordinates in this integral. Using the notations concerning Finite Elements introduced in section 3.1 and the abbreviation $\tilde{w} := \sum_{i=1}^4 \tilde{a}_i w_i$ we have:

$$\left\| -\operatorname{div} \tilde{\rho} - \Delta \tilde{w} - |\tilde{w} + \tilde{v}|^3 \right\|_{L^2}^2 = \int_{\Omega_t} \left[\operatorname{div} \tilde{\rho} + \Delta \tilde{w} + |\tilde{w} + \tilde{v}|^3 \right]^2 d(x,y)$$

$$= \sum_{i=1}^M \int_{K_i} \left[\operatorname{div} \tilde{\rho} + \Delta \tilde{w} + |\tilde{w} + \tilde{v}|^3 \right]^2 d(x,y).$$

We have made several attemps to treat these integrals directly, e.g. by representing the whole integrand either in polar coordinates or in cartesian coordinates and integrating or using quadrature rules. However, the resulting expressions turned out to be rather lengthy, which made such a treatment very technical and not successful.

Next we tried several approximation and interpolation techniques, e.g. substituting functions in polar coordinates by Taylor polynomials. This led to better resuls, but still the resulting error exceeded the value of the residuum. Finally we came up with the following interpolation idea, which turned out to be effective and produces also sufficiently small interpolation errors.

Before we start to explain the procedure in detail, we will fix the cut-off functions that we have used. For this purpose let

$$P(x) = \left(1 - \frac{x^2}{\tau^2}\right)^2, \quad x \in \mathbb{R}, \quad (4.4)$$

where $\tau = 1$ in case $t \ge 1$, and $\tau = t$ if $t < 1$ (recall that t is the parameter of our considered domain Ω_t). At a corner $\xi_i = (\zeta_i, \eta_i)$, $i = 1, \ldots, 4$, let $C_i := [\zeta_i - \tau, \zeta_i + \tau] \times [\eta_i - \tau, \eta_i + \tau]$, and define the cut-off function

$$\lambda_i(x,y) = \begin{cases} P(x - \zeta_i)P(y - \eta_i) & \text{if } (x,y) \in C_i \\ 0 & \text{else.} \end{cases} \quad (4.5)$$

Obviously $\lambda_i \in C^1(\overline{\Omega}_t)$ and $\frac{\partial \lambda_i}{\partial x}(x,y) = (x - \zeta_i)p(x - \zeta_i)P(y - \eta_i)$, $\frac{\partial \lambda_i}{\partial y}(x,y) = (y - \eta_i)P(x - \zeta_i)p(y - \eta_i)$ for $(x,y) \in C_i$ where $p(x) = -\frac{2}{\tau^2}\left(1 - \frac{x^2}{\tau^2}\right)$. Moreover, the cut-off functions satisfy

$$\lambda_i(x,y)\lambda_j(x,y) = 0 \quad \text{for all } (x,y) \in \overline{\Omega}_t \text{ and } i,j = 1, \ldots, 4 \text{ with } i \ne j. \quad (4.6)$$

With the above choice (4.5) the cut-off functions are piecewise polynomial in x and y, and we can therefore define $\hat{w}$ to be the following piecewise polynomial approximation of $\tilde{w} = \sum_{i=1}^{4} \tilde{a}_i w_i$:

$$\hat{w} = \sum_{i=1}^{4} \tilde{a}_i \lambda_i(x,y) I_{V_N}(\gamma_i), \tag{4.7}$$

with I_{V_N} being the interpolation operator into the Finite Element space V_N, defined in (3.7). Obviously $\hat{w} \in H_0^1(\Omega_t)$ is continuous on $\overline{\Omega}_t$ and smooth on each K_j ($j = 1, \ldots, M$).

Let furthermore $\mathcal{L}\tilde{w}$ be piecewise polynomial (continuous in $\overline{\Omega}_t$, smooth on each K_j, $j = 1, \ldots, M$), with $\mathcal{L}\tilde{w} \approx \sum_{i=1}^{4} \tilde{a}_i \Delta w_i = \Delta\tilde{w}$. We will comment on the actual choice later. Then we obtain:

$$
\begin{aligned}
\big\|\operatorname{div} &\tilde{\rho} + \Delta\tilde{w} + |\tilde{w} + \tilde{v}|^3 \big\|_{L^2} \\
&= \big\|\big(\operatorname{div}\tilde{\rho} + \mathcal{L}\tilde{w} + (\hat{w} + \tilde{v})^3\big) + (\Delta\tilde{w} - \mathcal{L}\tilde{w}) + \big(|\tilde{w} + \tilde{v}|^3 - (\hat{w} + \tilde{v})^3\big)\big\|_{L^2} \\
&\le \big\|\operatorname{div}\tilde{\rho} + \mathcal{L}\tilde{w} + (\hat{w} + \tilde{v})^3\big\|_{L^2} + \|\Delta\tilde{w} - \mathcal{L}\tilde{w}\|_{L^2} + \big\||\tilde{w} + \tilde{v}|^3 - (\hat{w} + \tilde{v})^3\big\|_{L^2}
\end{aligned}
\tag{4.8}
$$

Due to the choice of λ_i, $i = 1, \ldots, 4$, the term $\operatorname{div}\tilde{\rho} + \mathcal{L}\tilde{w} + (\hat{w} + v)^3$ is piecewise polynomial and its L^2-norm can in principle be computed using quadrature rules of sufficiently high degree, applied elementwise. We will first draw our attention to the other terms in (4.8) and comment on this purely polynomial part later.

Computation of $\big\||\tilde{w} + \tilde{v}|^3 - (\hat{w} + \tilde{v})^3\big\|_{L^2}$

At first we want to omit the modulus, which is possible if $\omega_t = \tilde{w} + \tilde{v} \ge 0$ in Ω_t. Since ω_t is explicitly known, it is only a matter of careful estimates and implementation to check whether $\omega_t \ge 0$ in Ω_t is true. Some estimates concerning the positivity check can be found in appendix A.2. In the following we will omit the modulus; indeed a rigorous check within our program showed that all approximate solutions ω_t are non-negative.

Clearly,

$$(\tilde{w} + \tilde{v})^3 - (\hat{w} + \tilde{v})^3 = (\tilde{w} - \hat{w})\big((\tilde{w} + \tilde{v})^2 + (\tilde{w} + \tilde{v})(\hat{w} + \tilde{v}) + (\hat{w} + \tilde{v})^2\big)$$

and thus recalling the definitions of $\tilde{w}$ and $\hat{w}$ this yields

$$(\tilde{w} + \tilde{v})^3 - (\hat{w} + \tilde{v})^3 = \underbrace{\big((\tilde{w} + \tilde{v})^2 + (\tilde{w} + \tilde{v})(\hat{w} + \tilde{v}) + (\hat{w} + \tilde{v})^2\big)}_{=:f} \sum_{i=1}^{4} \tilde{a}_i \lambda_i \big(\gamma_i - I_{V_N}(\gamma_i)\big).$$

The following computations provide an upper bound for $\|(\tilde{w} + \tilde{v})^3 - (\hat{w} + \tilde{v})^3\|_{L^2}^2$. Due to (4.6)

we have

$$\left\| (\tilde{w}+\tilde{v})^3 - (\hat{w}+\tilde{v})^3 \right\|_{L^2}^2 = \int\limits_{\Omega_t} \left((\tilde{w}+\tilde{v})^3 - (\hat{w}+\tilde{v})^3 \right)^2 \, d(x,y)$$

$$= \int\limits_{\Omega_t} f^2 \left(\sum_{i=1}^4 \tilde{a}_i \lambda_i (\gamma_i - I_{V_N}(\gamma_i)) \right)^2 \, d(x,y)$$

$$= \int\limits_{\Omega_t} f^2 \sum_{i=1}^4 \left(\tilde{a}_i \lambda_i (\gamma_i - I_{V_N}(\gamma_i)) \right)^2 \, d(x,y)$$

$$= \sum_{i=1}^4 \sum_{j=1}^M \int\limits_{K_j} f^2 \tilde{a}_i^2 \lambda_i^2 (\gamma_i - I_{V_N}(\gamma_i))^2 \, d(x,y)$$

$$\leq \sum_{i=1}^4 \sum_{j=1}^M \left(\max_{K_j} \left[f^2 \tilde{a}_i^2 \lambda_i^2 \right] \right) \cdot \int\limits_{K_j} (\gamma_i - I_{V_N}(\gamma_i))^2 \, d(x,y). \qquad (4.9)$$

Note that $\max_{K_j} [\tilde{a}_i^2 \lambda_i^2 f^2]$ $(i=1,\dots,4; j=1,\dots,M)$ can be computed using interval arithmetic.

We are now left to compute an upper bound for the integral in (4.9). For this purpose we will slightly enlarge the domain of integration such that the resulting integral can be calculated analytically using local polar coordinates. For simplicity, we will denote local polar coordinates by (r,φ), omitting the index i. Let $Q_j^k = (r_{\min}^{j,k}, r_{\max}^{j,k}) \times (\varphi_{\min}^{j,k}, \varphi_{\max}^{j,k})$ $(k=1,\dots,N_j$ with $N_j \in \mathbb{N}$ suitably chosen) such that $\bigcup_{k=1}^{N_j} \{(r\cos\varphi, r\sin\varphi) \ : \ (r,\varphi) \in Q_j^k\} \supseteq K_j$. By $I_{K_j} : C(\overline{\Omega}_t) \to$ span $\left\{ s_1^{K_j}, \dots, s_m^{K_j} \right\}$ $(j \in \{1,\dots,M\})$ we denote the local interpolation operator which satisfies $I_{V_N}(u)|_{K_j} = I_{K_j}(u|_{K_j})$. Therefore

$$\int\limits_{K_j} \left(\gamma_i - I_{V_N}(\gamma_i) \right)^2 \, d(x,y) = \int\limits_{K_j} \left(\gamma_i - I_{K_j}(\gamma_i) \right)^2 \, d(x,y),$$

and due to positivity of the integrand we have (denoting by $(I_{K_j}\gamma_i)(r,\varphi)$ the function $I_{K_j}\gamma_i$ written in polar coordinates)

$$\int\limits_{K_j} \left(\gamma_i - I_{K_j}(\gamma_i) \right)^2 \, d(x,y) \leq \sum_{k=1}^{N_j} \int\limits_{Q_j^k} \left[\gamma_i(r,\varphi) - \left(I_{K_j}\gamma_i \right)(r,\varphi) \right]^2 r \, d(r,\varphi)$$

$$= \sum_{k=1}^{N_j} \int\limits_{\varphi_{\min}^{j,k}}^{\varphi_{\max}^{j,k}} \int\limits_{r_{\min}^{j,k}}^{r_{\max}^{j,k}} \left[\gamma_i(r,\varphi) - (I_{K_j}\gamma_i)(r,\varphi) \right]^2 r \, dr \, d\varphi$$

$$= \sum_{k=1}^{N_j} \left[F_j \left(r_{\max}^{j,k}, \varphi_{\max}^{j,k} \right) - F_j \left(r_{\min}^{j,k}, \varphi_{\max}^{j,k} \right) - F_j \left(r_{\max}^{j,k}, \varphi_{\min}^{j,k} \right) + F_j \left(r_{\min}^{j,k}, \varphi_{\min}^{j,k} \right) \right].$$

Here, $F_j \in C^2((0,\infty) \times [0, \frac{3\pi}{2}], \mathbb{R})$ denotes a function with

$$\frac{\partial^2 F_j}{\partial r \partial \varphi}(r,\varphi) = \frac{\partial^2 F_j}{\partial \varphi \partial r}(r,\varphi) = \left[\gamma_i(r,\varphi) - \left(I_{K_j}\gamma_i \right)(r,\varphi) \right]^2 r.$$

This primitive can be computed using Maple [10], [48]. Note that $\gamma_i(r, \varphi) = r^{\frac{2}{3}} \sin\left(\frac{2}{3}\varphi\right)$ and for Serendipity Elements we have

$$(I_{K_j}\gamma_i)(x, y) = e_0 + e_1 x + e_2 y + e_3 xy + e_4 x^2 + e_5 y^2 + e_6 x^2 y + e_7 xy^2,$$

($e_6 = e_7 = 0$ in case of K_j being a triangle), resulting in an expression for $(I_{K_j}\gamma_i)(r, \varphi)$, which is polynomial in r, $\cos\varphi$ and $\sin\varphi$.

Computation of $\|\Delta\tilde{w} - \mathcal{L}\tilde{w}\|_{L^2}$

Recall that we first have to fix the choice of $\mathcal{L}\tilde{w}$. As before we denote local polar coordinates at a corner ξ_i, $i = 1, \ldots, 4$ by (r_i, φ_i) and define

$$
\begin{aligned}
f_1(r_1, \varphi_1) &:= -r_1^{\frac{2}{3}} \cos(\varphi_1) \sin\left(\tfrac{1}{3}\varphi_1\right) & g_1(r_1, \varphi_1) &:= r_1^{\frac{2}{3}} \sin(\varphi_1) \cos\left(\tfrac{1}{3}\varphi_1\right) \\
f_2(r_2, \varphi_2) &:= r_2^{\frac{2}{3}} \sin(\varphi_2) \cos\left(\tfrac{1}{3}\varphi_2\right) & g_2(r_2, \varphi_2) &:= -r_2^{\frac{2}{3}} \cos(\varphi_2) \sin\left(\tfrac{1}{3}\varphi_2\right) \\
f_3(r_3, \varphi_3) &:= -r_3^{\frac{2}{3}} \cos(\varphi_3) \sin\left(\tfrac{1}{3}\varphi_3\right) & g_3(r_3, \varphi_3) &:= r_3^{\frac{2}{3}} \sin(\varphi_3) \cos\left(\tfrac{1}{3}\varphi_3\right) \\
f_4(r_4, \varphi_4) &:= r_4^{\frac{2}{3}} \sin(\varphi_4) \cos\left(\tfrac{1}{3}\varphi_4\right) & g_4(r_4, \varphi_4) &:= -r_4^{\frac{2}{3}} \cos(\varphi_4) \sin\left(\tfrac{1}{3}\varphi_4\right).
\end{aligned}
\tag{4.10}
$$

f_i and g_i, $i = 1, \ldots, 4$ are continuous functions on $[0, \infty) \times [0, 2\pi]$ and therefore we can now define $\mathcal{L}\tilde{w}$ by

$$(\mathcal{L}\tilde{w})(x, y) := \sum_{i=1}^{4} \tilde{a}_i \Big[(I_{V_N}\gamma_i)(x, y)\Delta\lambda_i(x, y) + \underbrace{\tfrac{4}{3}p(x - \zeta_i)P(y - \eta_i)\chi_{C_i}(x, y)}_{=:\tilde{p}_i(x,y)} (I_{V_N} f_i)(x, y) +$$

$$\underbrace{\tfrac{4}{3}P(x - \zeta_i)p(y - \eta_i)\chi_{C_i}(x, y)}_{=:\tilde{q}_i(x,y)} (I_{V_N} g_i)(x, y) \Big], \quad (4.11)$$

with P as defined in (4.4) and p and C_i, $i = 1, \ldots, 4$ as in the text on page 22 thereafter. Since P and p are polynomials and λ_i is piecewise polynomial also $\mathcal{L}\tilde{w}$ is piecewise polynomial.

From the above definition of $\mathcal{L}\tilde{w}$ it is however not immediately clear that $\mathcal{L}\tilde{w}$ is in fact an approximation of $\Delta\tilde{w}$. To justify our choice we will consider the summand for $i = 1$ and show that $(I_{V_N}\gamma_1)\Delta\lambda_1 + \tilde{p}_1 I_{V_N} f_1 + \tilde{q}_1 I_{V_N} g_1$ is indeed an approximation of $w_1 = \lambda_1\gamma_1$. The cases $i = 2, 3, 4$ can be treated analogously but we will not write down the details here.

Recall that $\xi_1 = (\zeta_1, \eta_1) = (-t, t)$ is the upper left re-entrant corner of the domain Ω_t and thus for $(x, y) \in C_1 \cap \Omega_t$ we can switch between local polar and cartesian coordinates by

$$x - \zeta_1 = r_1 \cos\varphi_1, \quad y - \eta_1 = r_1 \sin\varphi_1,$$

$$r_1 = \sqrt{(x - \zeta_1)^2 + (y - \eta_1)^2},$$

$$\varphi_1 = \begin{cases} \arctan\left(\frac{y - \eta_1}{x - \zeta_1}\right), & x - \zeta_1 > 0, y - \eta_1 > 0 \\ \frac{\pi}{2}, & x - \zeta_1 = 0, y - \eta_1 > 0 \\ \arctan\left(\frac{y - \eta_1}{x - \zeta_1}\right) + \pi, & x - \zeta_1 < 0 \\ \frac{3\pi}{2}, & x - \zeta_1 = 0, y - \eta_1 < 0. \end{cases}$$

For simplicity of presentation we consider in the following only the case $x - \zeta_1 > 0, y - \eta_1 > 0$. Then w_1 can be expressed in cartesian coordinates by

$$w_1(x, y) = \lambda_1(x, y) \underbrace{\left((x - \zeta_1)^2 + (y - \eta_1)^2 \right)^{\frac{1}{3}} \sin\left(\tfrac{2}{3} \arctan\left(\tfrac{y - \eta_1}{x - \zeta_1} \right) \right)}_{= \gamma_1(x, y)}.$$

Computing $\Delta w_1(x, y)$ yields (note that $\Delta \gamma_1 = 0$)

$$\Delta w_1(x, y) = \gamma_1(x, y)\Delta\lambda_1(x, y) + 2\nabla\lambda_1(x, y) \cdot \nabla\gamma_1(x, y)$$
$$= \gamma_1(x, y)\Delta\lambda_1(x, y) + 2\tfrac{\partial\lambda_1}{\partial x}(x, y)\tfrac{\partial\gamma_1}{\partial x}(x, y) + 2\tfrac{\partial\lambda_1}{\partial y}(x, y)\tfrac{\partial\gamma_1}{\partial y}(x, y),$$

and comparing with the formula (4.11) for $\mathcal{L}\tilde{w}$ we will now show that $\tilde{p}_1 I_{V_N} f_1$ is an approximation of $2\tfrac{\partial\lambda_1}{\partial x}\tfrac{\partial\gamma_1}{\partial x}$ and $\tilde{q}_1 I_{V_N} g_1$ is an approximation of $2\tfrac{\partial\lambda_1}{\partial y}\tfrac{\partial\gamma_1}{\partial y}$ (clearly, $\Delta\lambda_1 I_{V_N}\gamma_1$ is an approximation of $(\Delta\lambda_1)\gamma_1$).

The derivatives of γ_1 in cartesian coordinates are given by

$$\frac{\partial\gamma_1}{\partial x}(x, y) = \frac{2}{3} \cdot \frac{(x - \zeta_1)\sin\left(\tfrac{2}{3}\arctan\left(\tfrac{y-\eta_1}{x-\zeta_1} \right) \right) - (y - \eta_1)\cos\left(\tfrac{2}{3}\arctan\left(\tfrac{y-\eta_1}{x-\zeta_1} \right) \right)}{\left((x - \zeta_1)^2 + (y - \eta_1)^2 \right)^{\frac{2}{3}}}$$

$$\frac{\partial\gamma_1}{\partial y}(x, y) = \frac{2}{3} \cdot \frac{(x - \zeta_1)\cos\left(\tfrac{2}{3}\arctan\left(\tfrac{y-\eta_1}{x-\zeta_1} \right) \right) + (y - \eta_1)\sin\left(\tfrac{2}{3}\arctan\left(\tfrac{y-\eta_1}{x-\zeta_1} \right) \right)}{\left((x - \zeta_1)^2 + (y - \eta_1)^2 \right)^{\frac{2}{3}}}.$$

We define

$$\tilde{f}_1(x, y) := \tfrac{3}{2}(x - \zeta_1)\frac{\partial\gamma_1}{\partial x}(x, y)$$
$$\tilde{g}_1(x, y) := \tfrac{3}{2}(y - \eta_1)\frac{\partial\gamma_1}{\partial y}(x, y)$$

and writing $\tilde{f}_1$ and $\tilde{g}_1$ in local polar coordinates we obtain

$$\tilde{f}_1(r_1\cos\varphi_1, r_1\sin\varphi_1) = r_1\cos\varphi_1\left(\sin\left(\tfrac{2}{3}\varphi_1\right)r_1\cos\varphi_1 - \cos\left(\tfrac{2}{3}\varphi_1\right)r_1\sin\varphi_1 \right)r_1^{-\frac{4}{3}}$$
$$= -r_1^{\frac{2}{3}}\cos\varphi_1\sin\left(\tfrac{1}{3}\varphi_1\right) = f_1(r_1, \varphi_1)$$
$$\tilde{g}_1(r_1\cos\varphi_1, r_1\sin\varphi_1) = r_1\sin\varphi_1\left(\cos\left(\tfrac{2}{3}\varphi_1\right)r_1\cos\varphi_1 + \sin\left(\tfrac{2}{3}\varphi_1\right)r_1\sin\varphi_1 \right)r_1^{-\frac{4}{3}}$$
$$= r_1^{\frac{2}{3}}\sin\varphi_1\cos\left(\tfrac{1}{3}\varphi_1\right) = g_1(r_1, \varphi_1)$$

with f_1, g_1 as defined in (4.10).

The properties of λ_1 (see (4.5) and the definition of p_1 thereafter) yield for $x, y \in C_1 \cap \Omega_t, x - \zeta_1 > 0, y - \eta_1 > 0$:

$$2\tfrac{\partial\lambda_1}{\partial x}(x, y)\tfrac{\partial\gamma_1}{\partial x}(x, y) = \tfrac{4}{3}p(x - \zeta_1)P(y - \eta_1)\tilde{f}_1(x, y) = \tilde{p}_1(x, y)\tilde{f}_1(x, y)$$
$$2\tfrac{\partial\lambda_1}{\partial y}(x, y)\tfrac{\partial\gamma_1}{\partial y}(x, y) = \tfrac{4}{3}P(x - \zeta_1)p(y - \eta_1)\tilde{f}_2(x, y) = \tilde{q}_1(x, y)\tilde{f}_2(x, y),$$

which completes our justification.

We will now continue with the computation of $\|\Delta \tilde{w} - \mathcal{L}\tilde{w}\|_{L^2}$. Using the triangle inequality we obtain

$$\|\Delta \tilde{w} - \mathcal{L}\tilde{w}\|_{L^2} = \left\|\sum_{i=1}^{4} \left[\tilde{a}_i \Delta \lambda_i (\gamma_i - I_{V_N} \gamma_i) + \tilde{a}_i \tilde{p}_i (f_i - I_{V_N} f_i) + \tilde{a}_i \tilde{q}_i (g_i - I_{V_N} g_i)\right]\right\|_{L^2}$$

$$\leq \sum_{i=1}^{4} \left[\|\tilde{a}_i \Delta \lambda_i (\gamma_i - I_{V_N} \gamma_i)\|_{L^2} + \|\tilde{a}_i \tilde{p}_i (f_i - I_{V_N} f_i)\|_{L^2} + \|\tilde{a}_i \tilde{q}_i (g_i - I_{V_N} g_i)\|_{L^2}\right].$$

Upper bounds for the summands can be obtained analogously as described above for $\|(\tilde{w} + \tilde{v})^3 - (\hat{w} + \tilde{v})^3\|_{L^2}$. They are given by:

$$\|\tilde{a} \Delta \lambda_i (\gamma_i - I_{V_N} \gamma_i)\|_{L^2}^2 = \int\limits_{\Omega_t \cap C_i} \left(\tilde{a}_i \Delta \lambda_i (\gamma_i - (I_{V_N} \gamma_i))\right)^2 \, d(x, y)$$

$$\leq \sum_{\substack{j=1 \\ K_j \subset C_i}}^{M} \tilde{a}_i^2 \max_{K_j} (\Delta \lambda_i)^2 \int\limits_{K_j} (\gamma_i - I_{K_j} \gamma_i)^2 \, d(x, y),$$

$$\|\tilde{a}_i \tilde{p}_i (f_i - I_{V_N} f_i)\|_{L^2}^2 \leq \sum_{\substack{j=1 \\ K_j \subset C_i}}^{M} \tilde{a}_i^2 \max_{K_j} \tilde{p}_i \int\limits_{K_j} (f_i - I_{K_j} f_i)^2 \, d(x, y), \tag{4.12}$$

$$\|\tilde{a}_i \tilde{q}_i (g_i - I_{V_N} g_i)\|_{L^2}^2 \leq \sum_{\substack{j=1 \\ K_j \subset C_i}}^{M} \tilde{a}_i^2 \max_{K_j} \tilde{q}_i \int\limits_{K_j} (g_i - I_{K_j} g_i)^2 \, d(x, y), \tag{4.13}$$

and the integrals over elements K_j in (4.12) and (4.13) can be bounded by a similar procedure as already explained for the integral $\int_{K_j} (\gamma_i - I_{V_N} \gamma_i)^2 \, d(x, y)$.

Summarizing the previous steps we obtain the following computable upper bound

$$\left\|\operatorname{div} \tilde{\rho} + \Delta \tilde{w} + (\tilde{w} + \tilde{v})^3\right\|_{L^2} \leq \left\|\operatorname{div} \tilde{\rho} + \mathcal{L}\tilde{w} + (\hat{w} + \tilde{v})^3\right\|_{L^2} + \left\|(a\tilde{w} + v)^3 - (a\hat{w} + v)^3\right\|_{L^2}$$

$$+ \sum_{i=1}^{4} \left[\|\tilde{a}_i \Delta \lambda_i (\gamma_i - I_{V_N} \gamma_i)\|_{L^2} + \|\tilde{a}_i \tilde{p}_i (f_i - I_{V_N} f_i)\|_{L^2} + \|\tilde{a}_i \tilde{q}_i (g_i - I_{V_N} g_i)\|_{L^2}\right].$$

Computation of polynomial parts: quadrature rules

We are now left to compute an enclosure or upper bound for $\|\operatorname{div} \tilde{\rho} + \mathcal{L}\tilde{w} + (\hat{w} + v)^3\|_{L^2}$. Since $\operatorname{div} \tilde{\rho} + \mathcal{L}\tilde{w} + (\hat{w} + \tilde{v})^3$ is piecewise polynomial we could, elementwise, use a quadrature rule of sufficiently high degree to obtain an enclosure for its L^2-norm. However, considering this polynomial on a rectangle, we would have to use a tensor-product quadrature rule of minimal degree 20 in each variable, which gives at least 400 quadrature points. Therefore we apply again an interpolation trick similar to the one at the beginning of the chapter: Let $\check{w} := I_{V_N}(\hat{w})$ be the interpolation of $\hat{w}$ in the Finite Element space. Then triangle inequality yields

$$\left\|\operatorname{div} \tilde{\rho} + \mathcal{L}\tilde{w} + (\hat{w} + v)^3\right\|_{L^2} \leq \left\|\operatorname{div} \tilde{\rho} + \mathcal{L}\tilde{w} + (\check{w} + v)^3\right\|_{L^2} + \left\|(\hat{w} + \tilde{v})^3 - (\check{w} + v)^3\right\|_{L^2},$$

and as before we can estimate:

$$\left\|(\hat{w}+\tilde{v})^3 - (\check{w}+\tilde{v})^3\right\|^2_{L^2(\Omega_t)} = \sum_{j=1}^{M}\left\|(\hat{w}-\check{w})\underbrace{\left((\hat{w}+\tilde{v})^2 + (\hat{w}+\tilde{v})(\check{w}+\tilde{v}) + (\check{w}+\tilde{v})^2\right)}_{=:h}\right\|^2_{L^2(K_j)}$$

$$\leq \sum_{j=1}^{M}\max_{K_j} h^2 \int_{K_j}(\hat{w}-\check{w})^2\, d(x,y).$$

If K_j is a rectangle, the integrand $(\hat{w}-\check{w})^2$ is a polynomial $\sum_{k,l=1}^{12} b_{kl}x^k y^l$ and thus a tensor-product quadrature rule of degree 7 in each variable, i.e. 49 quadrature points in K_j, will be sufficient for an exact computation of the integral.

Which degree is needed to compute $\|\operatorname{div}\tilde{\rho} + L\tilde{w} + (\check{w}+\tilde{v})^3\|^2_{L^2(K_j)}$ exactly by a quadrature rule when K_j is a rectangle? Since $\operatorname{div}\tilde{\rho} + L\tilde{w} + (\check{w}+\tilde{v})^3 = \sum_{k,l=1}^{6} c_{kl}x^k y^l$ we need again a tensor-product quadrature rule of degree at least 7 in each variable (when Gaussian quadrature rules are applied). Therefore the numerical effort will be reduced by paying the price of a very small additional defect-term.

Some explanations concerning quadrature rules and in particular construction of new cubature rules on triangles can be found in appendix A.3. For a brief introduction into interval arithmetic we refer to section 5.4.

5 Computation of a Bound for the Inverse of the Linearization

In this chapter we will describe how to find a bound for the inverse of the linearization at ω_t, i.e. a constant K satisfying

$$\|v\|_{H_0^1(\Omega_t)} \leq K \|L_{\omega_t}[v]\|_{H^{-1}(\Omega_t)} \qquad \text{for all } v \in H_0^1(\Omega_t), \tag{5.1}$$

where $\omega_t \in H_0^1(\Omega_t)$ is an approximate solution to problem (1.2). To begin with we will show that finding a constant K satisfying (5.1) is in fact equivalent to the computation of bounds for some parts of the spectrum of a self-adjoint operator. Therefore, the main part of this chapter covers methods to compute upper and lower eigenvalue bounds.

For simplicity of presentation we omit the index t in the following.

5.1 Formulation as an Eigenvalue Problem

Recall the isometric isomorphism $\Phi : H_0^1(\Omega) \to H^{-1}(\Omega)$ defined in (2.5). The isometry property of Φ yields

$$\|L_\omega[v]\|_{H^{-1}} = \|(\Phi^{-1}L_\omega)[v]\|_{H_0^1} \qquad \text{for all } v \in H_0^1(\Omega)$$

and thus condition (5.1) is equivalent to

$$\|v\|_{H_0^1} \leq K \|(\Phi^{-1}L_\omega)[v]\|_{H_0^1} \qquad \text{for all } v \in H_0^1(\Omega). \tag{5.2}$$

In section 2.1 we have already proved that the operator $\Phi^{-1}L_\omega : H_0^1(\Omega) \to H_0^1(\Omega)$ is symmetric. Moreover it is defined on the whole of $H_0^1(\Omega)$ and therefore self-adjoint. The following lemma shows an equivalent condition to (5.2), which will be the basis of our further considerations.

Lemma 3. *Condition* (5.2) *holds for some* $K > 0$ *if and only if*

$$\gamma := \min\{|\nu| : \nu \text{ is in the spectrum of } \Phi^{-1}L_\omega\} > 0,$$

and in the affirmative case one can choose any $K \geq \frac{1}{\gamma}$.

Proof. Since $\Phi^{-1}L_\omega$ is self-adjoint we have by the spectral theorem (see e.g. [37])

$$\Phi^{-1}L_\omega = \int_\mathbb{R} \nu \, dE_\nu$$

where (E_ν) is the spectral family of $\Phi^{-1}L_\omega$. Furthermore we can deduce from the properties of E_ν that, for all $v \in H_0^1(\Omega)$,

$$\|\Phi^{-1}L_\omega[v]\|^2 = \int_\mathbb{R} \nu^2 d\,\|E_\nu v\|^2 = \int_{\mathbb{R}\backslash(-\gamma,\gamma)} \nu^2 d\,\|E_\nu v\|^2$$

$$\geq \gamma^2 \int_{\mathbb{R}\backslash(-\gamma,\gamma)} d\,\|E_\nu v\|^2 = \gamma^2 \int_\mathbb{R} d\,\|E_\nu v\|^2 = \gamma^2 \|v\|^2,$$

since $\nu \mapsto E_\nu$ is constant on intervals contained in the resolvent set of $\Phi^{-1}L_\omega$.
Obviously (5.2) is satisfied with any $K \geq \frac{1}{\gamma}$ if and only if $\gamma > 0$. $\square$

We are now left to prove that the spectrum of $\Phi^{-1}L_\omega$ is bounded away from zero and to compute an explicit lower bound for the distance of $\sigma(\Phi^{-1}L_\omega)$ to zero. Self-adjointness of $\Phi^{-1}L_\omega$ implies that there is no residual spectrum and thus we have to consider the essential spectrum and eigenvalues of $\Phi^{-1}L_\omega$ in the following.

Let $I_{H_0^1}$ denote the identity map in $H_0^1(\Omega)$ and I the embedding $H_0^1(\Omega) \hookrightarrow L^2(\Omega)$.

Lemma 4. *The operator*

$$S : \begin{cases} H_0^1(\Omega) & \to & H_0^1(\Omega) \\ u & \mapsto & (I_{H_0^1} - \Phi^{-1}L_\omega)u \end{cases} \tag{5.3}$$

is compact.

Proof. We rewrite S as follows

$$S = \Phi^{-1}(\Phi - L_\omega) = \Phi^{-1}(1 + 3|\omega|\omega)I$$

and use the fact that the composition of compact and bounded linear operators is still compact. First, the embedding $H_0^1(\Omega) \hookrightarrow L^2(\Omega)$ is compact (recall that Ω is bounded). Since $(1 + 3|\omega|\omega) \in L^\infty(\Omega)$, the operator mapping $u \in L^2(\Omega)$ to $(1 + 3|\omega|\omega)u \in L^2(\Omega)$ is bounded. Using boundedness of both the embedding $L^2(\Omega) \hookrightarrow H^{-1}(\Omega)$ and Φ^{-1} we obtain the assertion. $\qquad\square$

Using $\omega \geq 0$ (see also the comments in the previous chapter) we immediately see that 0 is not an eigenvalue of S. Moreover, S is symmetric and linear and thus there exists a sequence $(\mu_n)_{n\in\mathbb{N}} \subset \mathbb{R}\backslash\{0\}$ of eigenvalues of S such that $\mu_n \to 0 \ (n \to \infty)$ and the corresponding eigenvectors form an orthonormal base $(u_n)_{n\in\mathbb{N}}$ of $H_0^1(\Omega)$. Thus $\Phi^{-1}L_\omega = I_{H_0^1} - S$ has eigenvalues $\nu_n = 1 - \mu_n$, $n \in \mathbb{N}$ and with the properties of $(\mu_n)_{n\in\mathbb{N}}$ we can conclude that

  (i) All eigenvalues ν_n, $n \in \mathbb{N}$ have finite multiplicity, since μ_n has.

 (ii) The essential spectrum of $\Phi^{-1}L_\omega$ consists only of the point $\{1\}$ because 0 is the only accumulation point of $(\mu_n)_{n\in\mathbb{N}}$.

This proves that the essential spectrum is indeed bounded away from zero and for the rest of the chapter we will turn our attention to the computation of upper and lower eigenvalue bounds.

For an eigenpair $(\nu, u) \in \mathbb{R} \times H_0^1(\Omega)$ of $\Phi^{-1}L_\omega$ we have by definition of Φ and L_ω:

$$-\Delta u + 3|\omega|\omega u = \nu(-\Delta u + u), \ \text{ i.e. } \ (1 - \nu)(-\Delta u + u) = u + 3|\omega|\omega u, \tag{5.4}$$

to be understood as equations in $H^{-1}(\Omega)$. Applying (5.4) to u yields

$$(1 - \nu) \int_\Omega (|\nabla u|^2 + u^2)\, dx = \int_\Omega (1 + 3|\omega|\omega)\, u^2\, dx.$$

Since $\omega \geq 0$ in Ω, we obtain $1 - \nu > 0$ and dividing (5.4) by $1 - \nu$ yields

$$-\Delta u + u = \underbrace{\frac{1}{1 - \nu}}_{=:\kappa} [1 + 3|\omega|\omega]\, u. \tag{5.5}$$

(5.5) is equivalent to

$$\int_\Omega [\nabla u \cdot \nabla \varphi + u\varphi]\, dx = \kappa \int_\Omega [1 + 3|\omega|\omega]u\varphi\, dx \qquad \text{for all } \varphi \in H_0^1(\Omega),$$

$$\text{i.e.} \quad \langle u, \varphi \rangle_{H_0^1} = \kappa N(u, \varphi) \qquad \text{for all } \varphi \in H_0^1(\Omega), \tag{5.6}$$

where

$$N(u, \varphi) := \int_\Omega [1 + 3|\omega|\omega]u\varphi\, dx \qquad \text{for all } u, \varphi \in H_0^1(\Omega). \tag{5.7}$$

Recall that we need to show that the spectrum of $\Phi^{-1}L_\omega$ is bounded away from zero, which, using the transformation $\kappa = \frac{1}{1-\nu}$, amounts to bounding κ away from 1. By the previous arguments we can furthermore conclude that all eigenvalues of (5.6), (5.7) are positive and tend to infinity. Thus we need an upper bound, which is smaller than 1, for the largest eigenvalue below 1 (if it exists), and a lower bound, which is larger than 1, for the smallest eigenvalue above 1.

5.2   Lower and Upper Eigenvalue Bounds

Although the eigenvalue problem (5.6), (5.7) does not have essential spectrum, we will in this section consider a more general case, where essential spectrum is allowed. This will be needed to treat an eigenvalue problem in one of the upcoming sections.

Let $(H, \langle \cdot, \cdot \rangle)$ be a seperable complex (real) Hilbert space and N a bounded, positive and hermitian sesquilinear (symmetric bilinear) form on H. Then the eigenvalue problem

$$\langle u, v \rangle = \kappa N(u, v) \quad \text{for all } v \in H \tag{5.8}$$

is equivalent to an eigenvalue problem for a self-adjoint operator $R : H \to H$. Note that for (5.6), (5.7) we have $H = H_0^1(\Omega)$ and $R = I_{H_0^1} - \Phi^{-1}L_\omega$. As usual we define the essential spectrum of (5.8) to be the one of the associated self-adjoint operator R and denote by $\sigma_0 \in \mathbb{R} \cup \{+\infty\}$ its infimum. Suppose moreover that $\sigma_0 > 0$. Upper bounds for eigenvalues of (5.8) *below* the essential spectrum can be computed by the well known method of Rayleigh-Ritz (see e.g. [64, Theorem 7.2]).

Theorem 3 (Rayleigh-Ritz-method). *Let $n \in \mathbb{N}$ and $v_1, \ldots, v_n \in H$ be linearly independent trial functions. Define the matrices*

$$A_0 := (\langle v_i, v_j \rangle)_{i,j=1,\ldots,n}, \qquad A_1 := (N(v_i, v_j))_{i,j=1,\ldots,n} \tag{5.9}$$

and let $\hat\kappa_1 \leq \hat\kappa_2 \leq \ldots \leq \hat\kappa_n$ denote the eigenvalues of

$$A_0 x = \hat\kappa A_1 x.$$

Then, if $\hat\kappa_n < \sigma_0$, there are at least n eigenvalues of (5.8) below σ_0 and the n smallest of these, denoted by $\kappa_1 \leq \kappa_2 \leq \ldots \leq \kappa_n$ and counted by multiplicity, satisfy

$$\kappa_j \leq \hat\kappa_j, \quad j = 1, \ldots, n.$$

The quality of upper bounds obtained by the Rayleigh-Ritz method depends strongly on the choice of $v_1, \ldots, v_n$. In order to get good bounds one should use approximate eigenfunctions as trial functions, which can as well be computed using Rayleigh-Ritz with simpler (but more) ansatz functions, e.g. Finite Element basis functions.

The verified computation of upper bounds is rather straightforward and simple if the dimension of the matrix eigenvalue problem is not too large. In our applications, most matrix eigenvalue problems have dimension 1 or 2 and the largest problems are of dimension 15.
On the other hand, computation of lower eigenvalue bounds is a more delicate task. We will use a method that has been developed by Lehmann and later been improved by Goerisch. The following version of this method can be found in [12].

Theorem 4. *Let $(X, b(\cdot, \cdot))$ denote a complex Hilbert space and $T : H \to X$ an isometric linear operator, i.e. $b(T\varphi, T\psi) = \langle \varphi, \psi \rangle$ for all $\varphi, \psi \in H$. Let $v_1, \ldots, v_n \in H$ be linearly independent and $w_1, \ldots, w_n \in X$ satisfying*

$$b(T\varphi, w_j) = N(\varphi, v_j) \qquad \text{for all } \varphi \in H, \ j = 1, \ldots, n. \tag{5.10}$$

In addition to the matrices A_0 and A_1 in (5.9) define the matrix

$$A_2 := (b(w_i, w_j))_{i,j=1\ldots,n}. \tag{5.11}$$

Let some $\rho \in (0, \sigma_0]$ be chosen such that there are at most finitely many eigenvalues of (5.8) below ρ, and such that

$$[v \in span\{v_1, \ldots, v_n\} \text{ and } \langle v, \varphi \rangle = \rho N(v, \varphi) \text{ for all } \varphi \in H] \Rightarrow v = 0. \tag{5.12}$$

Let $\tau_1 \leq \ldots \leq \tau_k < 0$ denote the negative eigenvalues (counted by multiplicity) of

$$(A_0 - \rho A_1)x = \tau(A_0 - 2\rho A_1 + \rho^2 A_2)x \tag{5.13}$$

(the matrix on the right-hand-side is positive definite). Then, there are at least k eigenvalues of (5.8) below ρ, and the k largest of these (counted by multiplicity), denoted by $\kappa_k^\rho \leq \kappa_{k-1}^\rho \leq \ldots \leq \kappa_1^\rho$, satisfy

$$\kappa_j^\rho \geq \rho - \frac{\rho}{1 - \tau_j} \quad (j = 1, \ldots, k).$$

To compute lower eigenvalue bounds using the previous theorem we need to specify the choice of various ingredients needed. As in the Rayleigh-Ritz method, we will choose $v_1, \ldots, v_n \in H$ to be approximate eigenfunctions of (5.8), and denote by $\hat{\kappa}_1 \leq \ldots \leq \hat{\kappa}_n$ upper bounds for the n smallest eigenvalues obtained by the Rayleigh-Ritz method (with $v_1, \ldots, v_n$ as ansatz functions). Here, n is chosen such that $\hat{\kappa}_n < \sigma_0$. If $n \geq 1$ (which is always true in our examples) the Rayleigh-Ritz method gives at least n eigenvalues $\kappa_1, \ldots, \kappa_n$ below σ_0, bounded from above by $\hat{\kappa}_j$ (indexwise). Assume moreover that we can find some $\rho > 0$ such that there are at most finitely many eigenvalues of (5.8) below ρ, and which satisfies

$$\hat{\kappa}_n < \rho \leq \kappa_{n+1} < \sigma_0, \tag{5.14}$$

if an $n + 1$-st eigenvalue of (5.8) exists. Otherwise we require $\hat{\kappa}_n < \rho < \sigma_0$. Due to the choice of $v_1, \ldots, v_n$, the first inequality in (5.14) implies condition (5.12). Furthermore the matrix on the

left-hand-side of (5.13) is now negative definite, whence (5.13) has precisely n negative eigen-values and thus the theorem gives lower bounds for the n largest eigenvalues of (5.8) below ρ. These eigenvalues are also the n smallest eigenvalues, since $\rho \leq \kappa_{n+1}$ by (5.14). Together with the Rayleigh-Ritz bounds we obtain two-sided eigenvalue bounds for the n smallest eigenvalues of (5.8).

However, to find ρ satisfying (5.14) is not trivial. The inequality means that we need a lower bound for the $n + 1$-st eigenvalue of (5.8) in order to computer lower bounds for the n smallest eigen-values. Fortunately, it is not necessary to have a good a-priori lower bound ρ, but a rather rough one will be sufficient to produce very precise eigenvalue bounds by Theorem 4. Such a rough bound can often be obtained by a homotopy method, which we will explain in the next section. During this homotopy, we will use Theorem 4 mostly in case $n = 1$, which results in the following Corollary:

Corollary 1. *Let X, b, T as in the previous theorem. Let $v \in H \backslash \{0\}$ and $w \in X$ such that*

$$b(T\varphi, w) = N(\varphi, v) \quad \text{for all } \varphi \in H.$$

(this is condition (5.10)). Moreover, let $\rho \in (0, \sigma_0]$ be chosen such that there are at most finitely many eigenvalues of (5.8) below ρ and

$$\frac{\langle v, v \rangle}{N(v, v)} < \rho \tag{5.15}$$

(this is the first inequality in (5.14) and implies (5.12)). Then, there is an eigenvalue κ of problem (5.8) satisfying

$$\frac{\rho N(v, v) - \langle v, v \rangle}{\rho b(w, w) - N(v, v)} \leq \kappa < \rho. \tag{5.16}$$

5.2.1 A homotopy method

In this subsection we will describe how to compute a constant ρ satisfying (5.14) as needed for Theorem 4. For this purpose we use a homotopy method which connects our given problem (5.8) to a "base problem", whereas we have some knowledge on the spectrum of this problem. The homotopy that we are going to describe here was first introduced in [12]. Its advantage over older homotopy-versions is low computational effort, as only matrix eigenvalue problems of very small dimension (usually 1 or 2) have to be solved rigorously.

Suppose that a bounded, positive definite, Hermitian sesquilinear (symmetric bilinear) form N_0 on $(H, \langle \cdot, \cdot \rangle)$ is at hand such that

$$N_0(u, u) \geq N(u, u) \quad \text{for all } u \in H. \tag{5.17}$$

We assume moreover, that there exists some $\rho \in \mathbb{R}$ and $n_0 \in \mathbb{N}_0$ such that the base problem

$$\langle u, \varphi \rangle = \kappa^{(0)} N_0(u, \varphi) \tag{5.18}$$

has exactly n_0 eigenvalues $\kappa_1^{(0)} \leq \ldots \leq \kappa_{n_0}^{(0)}$ (counted by multiplicity) in $(0, \rho_0)$ and $\rho_0 \leq \sigma_0^{(0)}$, with $\sigma_0^{(0)}$ denoting the infimum of the essential spectrum of (5.18) (to be defined as the essential spectrum of the associated self-adjoint operator $R^{(0)}$). We define

$$N_s(u, v) := (1 - s)N_0(u, v) + sN(u, v) \quad \text{for } u, v \in H, \ s \in [0, 1], \tag{5.19}$$

and consider the family of eigenvalue problems

$$\langle u, \varphi \rangle = \kappa^{(s)} N_s(u, \varphi) \quad \text{for all } \varphi \in H. \tag{5.20}$$

Analogously to the definition before $\sigma_0^{(s)}$ denotes the infimum of the essential spectrum of (5.20). Condition (5.17) together with definition (5.19) shows that $N_s(u, u)$ is non-increasing in s for each fixed $u \in H$. Therefore, with $\kappa_1^{(s)} \le \kappa_2^{(s)} \le \ldots$ denoting the eigenvalues of (5.20) below $\sigma_0^{(s)}$, we have for $0 \le s \le \tilde{s} \le 1$, by Poincaré's min-max-principle,

$$\kappa_j^{(s)} \le \kappa_j^{(\tilde{s})} \quad \text{for all } j \in \mathbb{N} \text{ such that } \kappa_j^{(\tilde{s})} < \sigma_0^{(\tilde{s})} \text{ exists.} \tag{5.21}$$

To start the homotopy (in case $n_0 \ge 1$) we suppose that the gap between $\kappa_{n_0}^{(0)}$ and ρ_0 is not too small. For some $s_1 > 0$ we compute approximate eigenpairs $\left(\tilde{\kappa}_j^{(s_1)}, \tilde{u}_j^{(s_1)} \right)$, $j = 1, \ldots, n_0$ of problem (5.20) (with $s = s_1$), with $\tilde{\kappa}_1^{(s_1)} \le \ldots \le \tilde{\kappa}_{n_0}^{(s_1)}$ ordered by magnitude and such that the Rayleigh quotient for $\tilde{u}_{n_0}^{(s_1)}$ satisfies

$$\frac{\left\langle \tilde{u}_{n_0}^{(s_1)}, \tilde{u}_{n_0}^{(s_1)} \right\rangle}{N_{s_1} \left(\tilde{u}_{n_0}^{(s_1)}, \tilde{u}_{n_0}^{(s_1)} \right)} < \rho_0. \tag{5.22}$$

We require furthermore that s_1 is chosen almost maximal with this property, i.e. the previous inequality is almost an equality, or $s_1 = 1$. In the latter case the argumentation further below completes already the homotopy. If $s_1 < 1$ we have to distinguish two different cases: On the basis of the approximations $\tilde{\kappa}_{n_0}^{(s_1)}, \tilde{\kappa}_{n_0-1}^{(s_1)}, \ldots, \tilde{\kappa}_1^{(s_1)}$ we can guess whether $\kappa_{n_0}^{(s_1)}$ is a well-isolated single eigenvalue or is part of an eigenvalue cluster (resp. a multiple eigenvalue). In the first case Corollary 1, applied to problem (5.20) with $s = s_1$ and $v := \tilde{u}_{n_0}^{(s_1)}$ implies the existence of an eigenvalue $\kappa^{(s_1)}$ of that problem in the interval given by (5.16). Denoting its lower bound by ρ_1, we obtain

$$\rho_1 \le \kappa^{(s_1)} < \rho_0. \tag{5.23}$$

Furthermore, since the base problem (5.18) has precisely n_0 eigenvalues in $(0, \rho_0)$, property (5.21) shows that problem (5.20) (with $s = s_1$) has at most n_0 eigenvalues in $(0, \rho_0)$, which together with (5.23) implies:

$$\text{problem (5.20) (with } s = s_1) \text{ has at most } n_0 - 1 \text{ eigenvalues in } (0, \rho_1). \tag{5.24}$$

If $\tilde{u}_{n_0}^{(s_1)}$ is computed with sufficient accuracy, the structure of ρ_1 shows that ρ_1 is not "far below" ρ_0. Consequently, if the gap between $\kappa_{n_0-1}^{(s_1)}$ and $\kappa_{n_0}^{(s_1)}$ is not too small, we expect that the only eigenvalue in $[\rho_1, \rho_0)$ is $\kappa_{n_0}^{(s_1)}$, and thus, that problem (5.20) has exactly $n_0 - 1$ eigenvalues in $(0, \rho_0)$.

In case $\kappa_{n_0}^{(s_1)}$ appears to belong to a cluster of eigenvalues (or appears to have higher multiplicity), we can apply Theorem 4 with $n = n_c \ge 2$ being the size of the cluster. This yields a lower bound ρ_1 for $\kappa_{n_0-n_c+1}^{(s_1)}, \ldots, \kappa_{n_0}^{(s_1)}$ and since the base problem has precisely n_0 eigenvalues in $(0, \rho_0)$, (5.21) shows that problem (5.19) (with $s = s_1$) has at most $n_0 - n_c$ eigenvalues in $(0, \rho_1)$. If furthermore $\kappa_{n_0-n_c+1}^{(s_1)}$ and $\kappa_{n_0-n_c}^{(s_1)}$ are well separated and ρ_1 is not too far below $\kappa_{n_0-n_c+1}^{(s_1)}$, we expect that the

only eigenvalues in $[\rho_1, \rho_0)$ will be $\kappa_{n_0-n_c+1}^{(s_1)}, \ldots, \kappa_{n_0}^{(s_1)}$ and therefore problem (5.20) (with $s = s_1$) has exactly $n_0 - n_c$ eigenvalues in $(0, \rho_1)$.

Altogether we conclude that problem (5.20) (with $s = s_1$) has at most $n_0 - n_1$ eigenvalues in $(0, \rho_1)$, where

$$n_1 = \begin{cases} 1 & \text{if } \kappa_{n_0}^{(s_1)} \text{ and } \kappa_{n_0-1}^{(s_1)} \text{ are well separated} \\ n_c & \text{else.} \end{cases} \qquad (5.25)$$

and we *expect* that problem (5.20) (with $s = s_1$) has exactly $n_0 - n_1$ eigenvalues in $(0, \rho_1)$. By a Rayleigh-Ritz computation we could check if this expectation is true, but it is not necessary. We simply continue on the basis of this expectation and the final Rayleigh-Ritz computation at the end of the homotopy will prove it a posteriori, or show that the homotopy was not successful.

In the second homotopy step (taking place if $n_0 - n_1 \geq 1$ and $s_1 < 1$) we repeat the above procedure with s_1 in place of 0, $n_0 - n_1$ in place of n_0 and ρ_1 in place of ρ_0: For some s_2 we compute approximate eigenpairs $\left(\tilde{\kappa}_j^{(s_2)}, \tilde{u}_j^{(s_2)}\right)$, $(j = 1, \ldots, n_0 - n_1)$ of problem (5.20) (with $s = s_2$), such that

$$\frac{\left\langle \tilde{u}_{n_0-n_1}^{(s_2)}, \tilde{u}_{n_0-n_1}^{(s_2)} \right\rangle}{N_{s_2}\left(\tilde{u}_{n_0-n_1}^{(s_2)}, \tilde{u}_{n_0-n_1}^{(s_2)}\right)} < \rho_1 \qquad (5.26)$$

and the inequality in (5.26) is almost an equality. We define

$$n_2 = \begin{cases} n_1 + 1 & \text{if } \kappa_{n_0-n_1}^{(s_2)} \text{ and } \kappa_{n_0-n_1-1}^{(s_2)} \text{ are well separated} \\ n_1 + n_c & \text{else,} \end{cases}$$

where n_c is the dimension of the eigenvalue cluster $\kappa_{n_0-n_1}^{(s_2)}$ possibly belongs to. Then either Corollary 1 or Theorem 4 with $N = n_c$, respectively, give a lower bound ρ_2 such that there are at least $n_1 - n_2$ eigenvalues in the interval $[\rho_2, \rho_1)$. Furthermore (5.24) and (5.21) show that problem (5.20) (with $s = s_2$) has at most $n_0 - n_1$ eigenvalues in $(0, \rho_1)$, and thus we can conclude

$$\text{problem (5.20) (with } s = s_2) \text{ has at most } n_0 - n_2 \text{ eigenvalues in } (0, \rho_2). \qquad (5.27)$$

As before, we expect that problem (5.20) (with $s = s_2$) has precisely $n_0 - n_2$ eigenvalues in $(0, \rho_2)$. We go on with this algorithm until for some $r \in \mathbb{N}_0$ either $s_r = 1$ and $n_r \leq n_0$ or $s_r < 1$ and $n_r = n_0$ (in which case the homotopy cannot be continued). For $s_r = 1$ we obtain in analogy to (5.24) and (5.27)

$$\text{problem (5.8) has at most } n_0 - n_r \text{ eigenvalues in } (0, \rho_r), \qquad (5.28)$$

implying that $\rho := \rho_r$ is a lower bound for the $n + 1$-st eigenvalue of (5.8) with $n := n_0 - n_r$. Finally, if $s_r = 1$ and $n \geq 1$, we perform a Rayleigh-Ritz computation for problem (5.8) and check if $\hat{\kappa}_n < \rho$ (cf. (5.14)) is satisfied (it will be satisfied if our expectations we made before are correct). If this check is successful, we can conclude that problem (5.8) has at least n eigenvalues in $(0, \rho)$, which, together with (5.28), shows that problem (5.8) has precisely n eigenvalues in $(0, \rho)$. By Theorem 4 we can now compute the desired lower bounds for the n smallest eigenvalues of problem (5.8).

In case $s_r < 1$ and $n_0 = n_r$ we have to restart the homotopy with new (larger) values of n_0 and ρ_0.

5.2.2 Application to the given eigenvalue problem

In the previous section we have presented a method to compute lower eigenvalue bounds. In order to apply it to our eigenvalue problem

$$\int_\Omega [\nabla u \cdot \nabla \varphi + u\varphi] \, dx = \kappa \underbrace{\int_\Omega (1 + 3|\omega|\omega)u\varphi \, dx}_{=N(u,\varphi)} \qquad \text{for all } \varphi \in H_0^1(\Omega)$$

we need to specify N_0, X, b and T.

To start with let $\overline{c} : \Omega \to \mathbb{R}$ be piecewise constant and such that

$$\overline{c}(x,y) \geq 3|\omega(x,y)|\omega(x,y) \quad \text{for all } (x,y) \in \Omega. \tag{5.29}$$

Defining $N_0 : H_0^1(\Omega) \times H_0^1(\Omega) \to \mathbb{R}$ by

$$N_0(u,v) := \int_\Omega (1 + \overline{c})uv \, dx \tag{5.30}$$

leads to

$$N_0(u,u) \geq N(u,u) \quad \text{for all } u \in H_0^1(\Omega),$$

i.e. condition (5.17) is satisfied. The eigenvalue problem

$$\int_\Omega [\nabla u \cdot \nabla \varphi + u\varphi] \, dx = \kappa^{(0)} \underbrace{\int_\Omega (1 + \overline{c})u\varphi \, dx}_{=N_0(u,\varphi)} \qquad \text{for all } \varphi \in H_0^1(\Omega) \tag{5.31}$$

$$\text{i.e.} \quad -\Delta u + u = \kappa^{(0)}(1 + \overline{c})u$$

(the latter equation to be understood as an equation in $H^{-1}(\Omega)$) will now serve as base problem. Note that if $\overline{c}$ was constant and Ω was a rectangle we could immediately write down the eigenvalues of (5.31). However, in our case there is no direct access to the eigenvalues, but a careful choice of $\overline{c}$ and another suitable comparison problem will enable us to compute lower bounds for certain eigenvalues of (5.31). We will explain this in section 5.3.

Now we adress the question how to choose X, b and T. In our application we have:

$$\begin{aligned} H &= H_0^1(\Omega), \\ \langle u, \varphi \rangle &= \langle \nabla u, \nabla \varphi \rangle_{L^2} + \langle u, \varphi \rangle_{L^2}, \\ N_s(u,\varphi) &= \int_\Omega (1 + 3s|\omega|\omega + (1-s)\overline{c})u\varphi \, dx \qquad \text{for } u, \varphi \in H_0^1(\Omega), \ s \in [0,1]. \end{aligned}$$

Define now

$$\begin{aligned} X &:= \left(L^2(\Omega)\right)^2 \times L^2(\Omega), \\ T\varphi &:= \begin{pmatrix} \nabla \varphi \\ \varphi \end{pmatrix} \qquad (\varphi \in H_0^1(\Omega)), \\ b\left(\begin{pmatrix} v^{(1)} \\ v^{(2)} \end{pmatrix}, \begin{pmatrix} w^{(1)} \\ w^{(2)} \end{pmatrix}\right) &:= \left\langle v^{(1)}, w^{(1)} \right\rangle_{L^2} + \left\langle v^{(2)}, w^{(2)} \right\rangle_{L^2}. \end{aligned}$$

Then the isometry condition on T is clearly satisfied. For given v_j, condition (5.10) for $w_j = \begin{pmatrix} w_j^{(1)} \\ w_j^{(2)} \end{pmatrix} \in X$, $j = 1, \ldots, n$ is equivalent to

$$\int_\Omega \left[\nabla\varphi \cdot w_j^{(1)} + \varphi w_j^{(2)} \right] dx = \int_\Omega (1 + 3s|\omega|\omega + (1-s)\bar{c})\varphi v_j \, dx \quad \text{for all } \varphi \in H_0^1(\Omega).$$

If we moreover require that $w_j^{(1)} \in H(\mathrm{div}, \Omega) = \{u \in (L^2(\Omega))^2 : \mathrm{div}\, u \in L^2(\Omega)\}$, partial integration gives

$$\int_\Omega \left[-\varphi \, \mathrm{div}\left(w_j^{(1)}\right) + \varphi w_j^{(2)} \right] dx = \int_\Omega (1 + 3s|\omega|\omega + (1-s)\bar{c})\varphi v_j \, dx \quad \text{for all } \varphi \in H_0^1(\Omega),$$

which is equivalent to

$$- \mathrm{div}\left(w_j^{(1)}\right) + w_j^{(2)} = (1 + 3s|\omega|\omega + (1-s)\bar{c})\, v_j,$$

since $H_0^1(\Omega)$ is dense in $L^2(\Omega)$. Therefore we choose

$$w_j^{(2)} = (1 + 3s|\omega|\omega + (1-s)\bar{c})v_j + \mathrm{div}\left(w_j^{(1)}\right). \tag{5.32}$$

By construction, any $\begin{pmatrix} w_j^{(1)} \\ w_j^{(2)} \end{pmatrix}$ satisfying $w_j^{(1)} \in H(\mathrm{div}, \Omega)$ and (5.32) can be used in Theorem 4 or Corollary 1 to compute lower eigenvalue bounds. However, not every choice of $w_j^{(1)}$ will lead to good bounds: an analysis of the proof of Theorem 4 shows that good bounds will be obtained when

$$w_j \approx T\breve{w}_j,$$

where $\breve{w}_j \in H_0^1(\Omega)$ is the solution of

$$\langle \varphi, \breve{w}_j \rangle = N_s(\varphi, v_j) \qquad (j = 1, \ldots, n). \tag{5.33}$$

Suppose that $v_1, \ldots, v_n$ are approximate eigenfunctions to (5.8) with corresponding approximate eigenvalues $\tilde{\kappa}_1, \ldots, \tilde{\kappa}_n$. Then $\frac{1}{\tilde{\kappa}_j}\langle \varphi, v_j \rangle \approx N_s(\varphi, v_j)$ for all $\varphi \in H_0^1(\Omega)$, which gives $\breve{w}_j \approx \frac{1}{\tilde{\kappa}_j} v_j$ and therefore $w_j \approx T\breve{w}_j$ if

$$w_j \approx \frac{1}{\tilde{\kappa}_j} T v_j = \frac{1}{\tilde{\kappa}_j} \begin{pmatrix} \nabla v_j \\ v_j \end{pmatrix} \qquad (j = 1, \ldots, n).$$

Since we have already chosen $w_j^{(2)}$ due to (5.32), only the first part of this "soft" condition is of use for us, i.e.

$$w_j^{(1)} \approx \frac{1}{\tilde{\kappa}_j} \nabla v_j \qquad (j = 1, \ldots, n).$$

Remark 4. (a) Problem (5.33) is part of the original theorem for lower eigenvalue bounds by Lehmann, whose application is strongly limited since (5.33) is usually not solvable in closed form. The Goerisch extension using X, b and T replaces (5.33) by (5.10), which can be solved in many cases when the parameters are chosen appropriately.

(b) A suitable approximation of ∇v_j is given by an approximate minimizer $\tilde{\rho} \in H(\mathrm{div}, \Omega)$ of

$$\|\nabla v_j - \rho\|_{L^2}^2 + \|\mathrm{div}\, \rho + (1 - \tilde{\kappa}_j(1 + 3s|\omega|\omega + (1-s)\bar{c}))v_j\|_{L^2}^2.$$

5.3   Domain Decomposition

We will now explain the general idea how to construct a suitable comparison problem for our base problem

$$\int_\Omega [\nabla u \cdot \nabla \varphi + u\varphi] \, dx = \kappa^{(0)} \int_\Omega (1+\bar{c})u\varphi \, dx \quad \text{for all } \varphi \in H_0^1(\Omega), \qquad (5.34)$$

thereby also briefly commenting on the choice of $\bar{c}$. The idea of the method is due to E.B. Davies and is explained in more detail in [8]. We will recall it in a more general setting.

Let therefore $U \subset \mathbb{R}^2$ be a domain (not necessarily bounded) with piecewise smooth boundary, $\Gamma \subset \partial U$ closed and $c \in L^\infty(U)$, $c \geq 0$ a.e. in U. We consider the eigenvalue problem (written here in strong formulation)

$$-\Delta u + u = \lambda(1+c)u \quad \text{in } U, \qquad u = 0 \quad \text{on } \Gamma, \qquad \frac{\partial u}{\partial \nu} = 0 \quad \text{on } \partial U \backslash \Gamma. \qquad (5.35)$$

Denoting by $H_\Gamma^1(U)$ the completion of $\{u \in C^\infty(U) : u = 0 \text{ in a neighbourhood of } \Gamma\}$ w.r.t. the H^1-norm, the weak formulation of that problem is given by

$$\int_U [\nabla u \cdot \nabla \varphi + u\varphi] \, dx = \lambda \int_U (1+c)u\varphi \, dx \quad \text{for all } \varphi \in H_\Gamma^1(U).$$

As before we denote the infimum of the essential spectrum of this problem by σ_0 and by $0 < \lambda_1 \leq \lambda_2 \leq \ldots$ its eigenvalues (note that $c \geq 0$ implies positivity of the eigenvalues).

Now we split U into two subdomains U_1 and U_2 such that their interface boundary $\Gamma_{01} = \partial U_1 \cap \partial U_2$ is smooth and consider (5.35) with U replaced by U_1 and U_2, respectively, and with Γ as before. We denote these eigenvalue problems by (5.35-1) and (5.35-2). Suppose now that for some fixed $0 < B < \sigma_0$ we know all eigenvalues of (5.35-1) and (5.35-2) below B and combine these to a single list of eigenvalues $\lambda_1^{(0)} \leq \lambda_2^{(0)} \leq \ldots \leq \lambda_L^{(0)}$ (counted by multiplicity). The corresponding eigenfunctions can be regarded as elements of $V := \{u \in L^2(U) : u|_{U_j} \in H^1(U_j), u|_\Gamma = 0 \text{ for } j = 1, 2\}$, by zero extension outside U_1 and U_2, respectively.

Then Poincaré's min-max-principle proves the following lemma:

Lemma 5. *For all $i = 1, \ldots, L$ we have: $\lambda_i^{(0)} \leq \lambda_i$ provided that $\lambda_i < \sigma_0$.*

Proof. Since $V \supset H_\Gamma^1(U)$ we have for all $i \in \{1, \ldots, L\}$ such that $\lambda_i < \sigma_0$:

$$\lambda_i^{(0)} = \inf_{\substack{V_i \subset V \text{ subspace} \\ \dim V_i = i}} \max_{u \in V_i \backslash \{0\}} \frac{\langle \nabla u, \nabla u \rangle_{L^2(U_1)} + \langle \nabla u, \nabla u \rangle_{L^2(U_2)} + \langle u, u \rangle_{L^2(U)}}{\langle (1+c)u, u \rangle_{L^2(U)}}$$

$$\leq \inf_{\substack{V_i \subset H_\Gamma^1(U) \text{ subspace} \\ \dim V_i = i}} \max_{u \in V_i \backslash \{0\}} \frac{\langle \nabla u, \nabla u \rangle_{L^2(U)} + \langle u, u \rangle_{L^2(U)}}{\langle (1+c)u, u \rangle_{L^2(U)}} = \lambda_i$$

$\square$

In principle, one can construct a homotopy joining the problems

$$\langle \nabla u, \nabla v \rangle_{L^2(U_1)} + \langle \nabla u, \nabla v \rangle_{L^2(U_2)} + \langle u, v \rangle_{L^2(U)} = \lambda^{(0)} \langle (1+c)u, v \rangle_{L^2(U)} \quad \text{for all } v \in V$$

and (5.35), as it is also described in [8]. However, in our application a pure comparision of these two problems is sufficient and therefore we will not describe the method in full generality here.

It is clear that the above procedure works as well, when U is splitted into more than two subdomains and Neumann boundary conditions are imposed at each interface edge.

For the application of the domain decomposition method to our eigenvalue problem (5.34) we will split $\Omega_t = (-t-1, t+1)^2\backslash[-t,t]^2$ into rectangles and squares and choose $\bar{c}$ to be constant (or piecewise constant in some cases) on these subdomains. Then the eigenvalues $\lambda_1^{(0)}, \ldots, \lambda_L^{(0)}$ are exactly computable (or can be enclosed). We will however postpone the details to section 6.2. Until then we have fixed the approximate solutions for which we will apply this method and can adapt our explanations to these cases.

5.4 Interval Arithmetic

A key ingredient for a computer-assisted proof as presented in this thesis is the calculation of various constants using the computer (e.g. δ and K satisfing (2.3) and (2.4), respectively), and in order to obtain results which can be used to complete an analytical proof the computations have to be rigorous. Since the computer can only represent finitely many numbers in an exact way (these are the machine numbers), rounding errors will occur which have to be captured in the computations. For this purpose one has to use interval arithmetic instead of the usual floating point arithmetic. A general introduction into interval arithmetic containing also various methods for rigorously solving nonlinear equations, linear systems and many more is given in the book of G. Alefeld and J. Herzberger [3].

For the implementation of interval arithmetic on a computer one can choose between various existing libraries. Since our programs are written in C++, we used the C-XSC library (see [43] and [39]), which provides all basic interval operations and standard functions as well as some sample algorithms.

For MATLAB we would also like to mention the toolbox INTLAB [62], which is very intuitive and easy to use and contains also a huge number of algorithms and applications, e.g. verified solvers for linear systems, eigenvalues or optimization routines.

5.4.1 Interval Newton method

We will now briefly recall the Interval Newton method, which is used at various points in this thesis to enclose all zeros of a function in a given compact interval. We will only consider the case of functions having simple roots, since this is satisfied in all our applications. However, there are more general versions of the Interval Newton method in the literature, treating also the case of multiple roots (see e.g. [3]). The algorithm that we are going to use can be found in [35]. By $[x]$ we denote an interval in $\mathbb{R}$ and by $m[x]$ its midpoint.

Let $f : \mathbb{R} \to \mathbb{R}$ be continuously differentiable and $[x]^0 \subset \mathbb{R}$ an interval satisfying $0 \notin f'([x]^{(0)})$. The latter condition implies that f has at most one zero $x^* \in [x]^0$. Defining

$$N([x]) := m([x]) - \frac{f(m[x])}{f'([x])}$$

the $(k + 1)$-st iterate of the interval Newton method is given by

$$[x]^{(k+1)} := [x]^{(k)} \cap N([x]^{(k)}), \quad k = 0, 1, 2, \ldots \tag{5.36}$$

Due to the intersection of $N([x]^k)$ with $[x]^k$ the Interval Newton method cannot diverge, i.e. the iterates of the Newton method cannot become unbounded. Moreover we have ([35, Theorem 6.1]):

a) Every zero $x^* \in [x]$ of f satisfies $x^* \in N([x])$.

b) If $N([x]) \cap [x] = \emptyset$, then there exists no zero of f in $[x]$.

c) If $N([x]) \overset{\circ}{\subset} [x]$, then there exists a unique zero of f in $[x]$ and hence in $N([x])$.

a) and b) imply in particular that if $[x]^{(k_0)} = \emptyset$ for some $k_0 \in \mathbb{N}$, then $[x]^{(0)}$ does not contain a zero of f.

To find all zeros of f on a given compact interval $[x] \subset \mathbb{R}$ we assume that there exists a subdivision of $[x]$ into smaller intervals $[x]_j$, $j = 1, \ldots, M$ ($M \geq 1$ suitable), such that $[x] = \bigcup_{j=1}^{M} [x]_j$ and either

(i) $0 \notin f([x]_j)$ or

(ii) $0 \notin f'([x]_j)$ and $f(\text{Inf}([x]_j)) f(\text{Sup}([x]_j)) < 0$.

The conditions in (i) and (ii) can be checked a-priori using Interval Arithmetic and the existence of the desired subdivision implies in particular that f has only simple roots. On each subinterval satisfying (ii) we perform the above Interval Newton iteration with starting interval $[x]^{(0)} = [x]_j$, and stop the alorithm if for some $k_1 \in \mathbb{N}$ we obtain $[x]^{(k_1+1)} = [x]^{(k_1)}$ or if the diameter of the interval $[x]^{(k_1+1)}$ is smaller than a prescribed tolerance. In both cases $[x]^{(k_1+1)}$ contains a new and tight enclosure of the zero in the interval $[x]_j$.

5.4.2 Matrix eigenvalue problems

We have seen in the previous sections that computation of bounds for eigenvalues also requires verified enclosure of matrix eigenvalues. This can be done using interval arithmetic, together with the following lemma (see [38]). By $[\mathbb{C}]^{N \times N}$ we denote the space of $N \times N$ matrices with complex interval coefficients. Note that N is "small" in our applications.

Lemma 6. *Let $[A], [B] \subset [\mathbb{C}]^{N \times N}$ be Hermitian matrices with interval entries and such that $B \in \mathbb{C}^{N \times N}$ is positive definite for all $B \in [B]$. For some fixed Hermitian $A_0 \in [A]$, $B_0 \in [B]$, let $(\tilde{\kappa}_j, \tilde{x}_j)$ $(j = 1, \ldots, N)$ denote approximate eigenpairs of $A_0 x = \kappa B_0 x$, with $\tilde{x}_i^* B_0 \tilde{x}_j \approx \delta_{ij}$. Suppose that, for some $r_0, r_1 > 0$,*

$$\|X^* A X - X^* B X K\|_\infty \leq r_0, \qquad \|X^* B X - I\|_\infty \leq r_1, \quad \text{for all } A \in [A], B \in [B]$$

where $X = (\tilde{x}_1, \ldots, \tilde{x}_N)$, $K = \text{diag}(\tilde{\kappa}_1, \ldots, \tilde{\kappa}_N)$. If $r_1 < 1$, we have for all $A \in [A]$, $B \in [B]$ and all eigenvalues κ of $Ax = \kappa Bx$:

$$\lambda \in \bigcup_{j=1}^{N} B(\tilde{\kappa}_j, r) \quad \text{where } r = \frac{r_0}{1 - r_1}, \quad \text{and } B(\kappa, r) = \{z \in \mathbb{C} : |z - \kappa| \leq r\}. \tag{5.37}$$

Moreover, each connected component of this union contains as many eigenvalues as midpoints $\tilde{\kappa}_i$.

6 Computations and Results

In this chapter we will present numerical results concerning our problem (1.2),

$$\begin{cases} -\Delta u &= |u|^3 \quad \text{in } \Omega_t \\ u &= 0 \quad\;\; \text{on } \partial\Omega_t \end{cases}$$

where t takes several values in the interval $(0,3]$. We start with some purely approximate results to show the variety of solutions that one can expect for the given problem. This includes also an approximate bifurcation diagram, which shows how approximate solutions behave when the parameter value t changes.

In the second part of this chapter we choose some special approximate solutions and show how the domain decomposition method can be applied to obtain lower bounds for eigenvalues of the corresponding base problem. Finally we present rigorous results for eigenvalue enclosures and defects, finally proving the existence of exact solutions to problem (1.2) by Theorem 1.

Hard- and software

All computations have been carried out on the parallel cluster OTTO of the Institute for Applied and Numerical Mathematics 3 at Karlsruhe Institute of Technology. We used the Finite Element Software M++, which has been developed by C. Wieners and his working group and is based on a programming model described in [65]. The software provides, amongst others, various parallel solvers for linear systems and eigenvalue problems. It is written in C++ and uses the MPI standard to realize parallel computations. Since we also extended the code by various routines that involve interval arithmetic, we did only use one processor for all our computations. This was still sufficient to carry out the calculations in reasonable time. For interval arithmetic we used the libraries C-XSC (see e.g. [43]) as well as MPFR and MPFI, which can be used in C-XSC via an interface (see [9]). Since both the MPFR and MPFI library are based on integer-arithmetic, they can use hardware ressources in their calculations which constitutes a significant reduction in computation time compared with the software-based arithemtic of pure C-XSC.

The programs for obtaining approximate and verified results comprise several (tens of) thousands lines of code and can clearly not be displayed in this thesis. The code may of course be inspected upon request to the author of this thesis.

6.1 Approximate Solutions

In order to find approximate solutions we use the combination of Mountain Pass Algorithm and Newton method as explained in sections 3.2.1 and 3.2.2. To start these methods we have to fix a suitable starting value for the Mountain Pass Algorithm. Our expectations are that there should be approximate solutions with various bumps centered at the corners or edges of the domain. Therefore we use starting values which have some kind of bump there, e.g. for $t = 1$ we put translated versions of $c \sin(\pi x) \sin(\pi y)$ $((x,y) \in (0,1)^2,\, c > 0)$ in one ore more corners or edges of the domain. By this technique we obtained the following approximate solutions to (1.2), all for $t = 1$.

(1) Onepeakcorner

(2) Onepeakedge

(3) Twopeakoppcorner

(4) Twopeakoppedge

(5) Fourpeakcorner

(6) Fourpeakedge
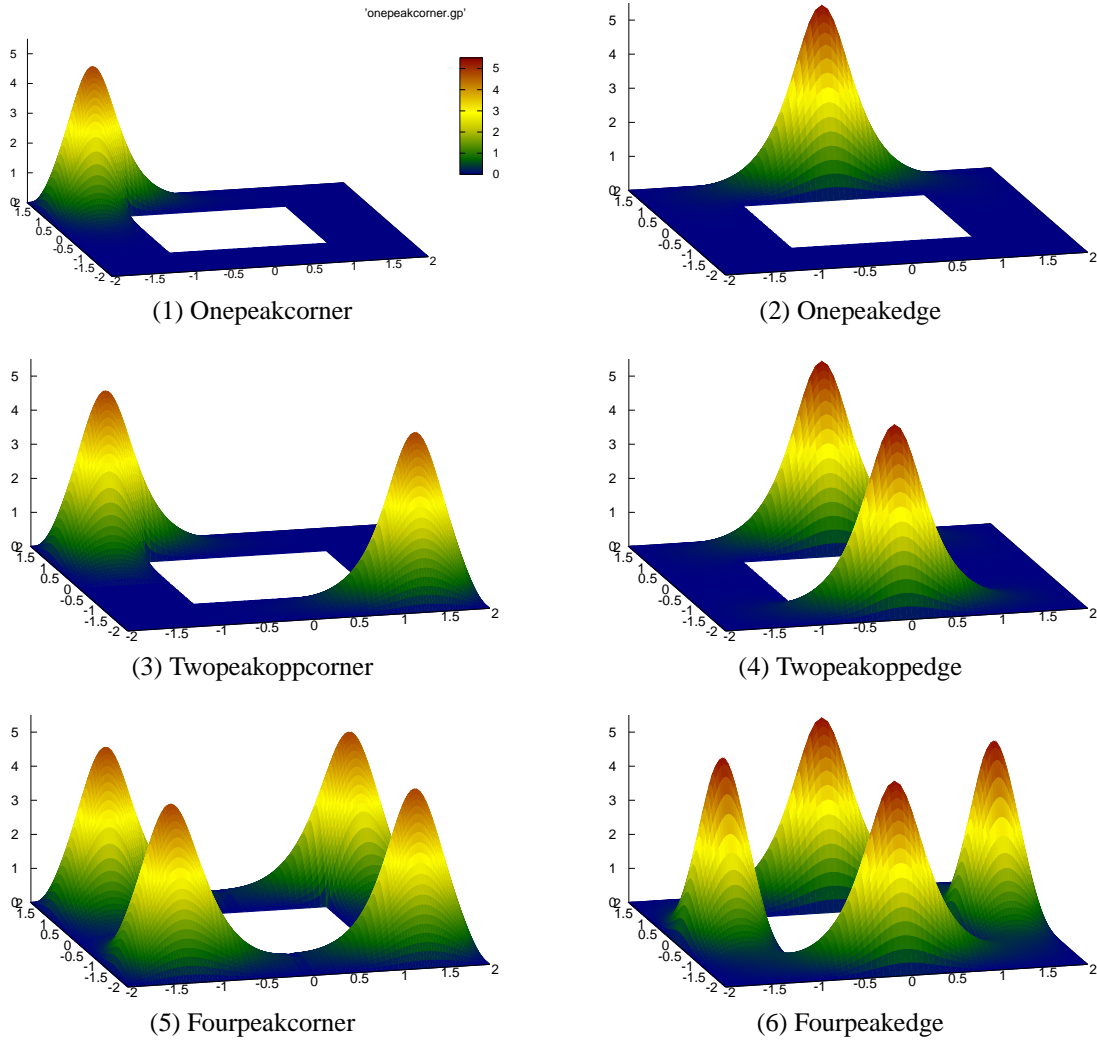
Figure 6.1: Approximate solutions - Part I

We remark that these will be the approximate solutions for which we will prove existence of an exact solution in a suitable neighbourhood (see also section 6.1.1).

6.1.1   More approximations and bifurcation diagrams

By putting suitable bumps in corners and edges of the domain and running Mountain Pass Algorithm and Newton method, we can even obtain more approximations for the parameter value $t = 1$. It is however clear that we cannot be sure to obtain all possible approximate solutions by this technique. In order to find more approximations we investigate branches of approximate solutions: Suppose that for some t_1 we have computed an approximate solution to (1.2) (with $t = t_1$) by means of Finite Elements. Let the approximation be given by

$$\omega_{t_1} = \sum_{i=1}^{N} c_i \varphi_i^{(t_1)}$$

where $\varphi_1^{(t_1)}, \ldots, \varphi_N^{(t_1)}$ denote a basis for the Finite Element space $V_N^D(\Omega_{t_1})$ and $c_1 \ldots, c_N \in \mathbb{R}$. If t_2 is "close" to t_1, we can define a function

$$\omega_{t_2}^{(0)} = \sum_{i=1}^{N} c_i \varphi_i^{(t_2)}$$

on $V_N^D(\Omega_{t_2})$, which can be used as initial approximation for a Newton method (for problem (1.2) with $t = t_2$). If the Newton method converges we obtain an approximate solution of problem (1.2) (with $t = t_2$). This technique is well-known as "continuation method" or "path-following method".

The procedure just presented may be used to investigate how a solution evolves when the parameter t becomes very small or very large. Figure 6.2 shows the evolution of the approximate solution that we introduced as fourpeakcorner solution in the previous section: for small t is looks almost radially symmetric and as t grows the bumps in the corners separate more and more.
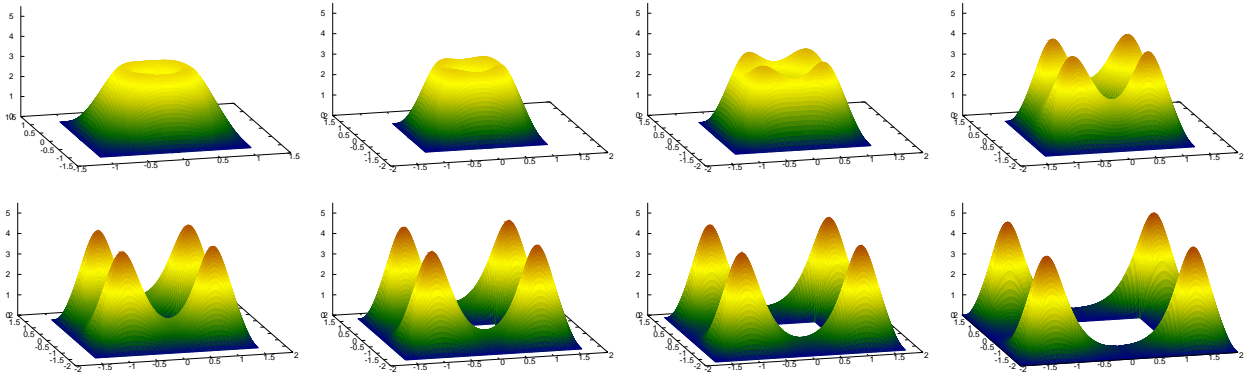
Figure 6.2: Evolution of Fourpeakcorner solution for $t \in \left\{ \frac{1}{16}, \frac{1}{8}, \frac{1}{4}, \frac{3}{8}, \frac{1}{2}, \frac{5}{8}, \frac{3}{4}, 1 \right\}$

However, this path-following method will not necessarily produce any new approximate solution types and thus we check if there might be bifurcations or turning points of these branches. Note that the following considerations are just a motivation and do not provide a rigorous proof of neither existence of solutions nor occurring bifurcations. By the Implicit Function Thorem, bifurcation from a solution branch or a turning point can only occur at some parameter value $t = t^*$ and solution u_{t^*} if for that value the solution is degenerate, i.e. 0 is an eigenvalue of the linearized operator at u_{t^*}.

To find a bifurcation or turning point, we therefore compute approximate eigenvalues of L_{ω_t} (using e.g. the Rayleigh-Ritz method). If for some value $t = t^*$ we have an eigenvalue of L_{ω_t} close to zero, Lyapunov-Schmidt Reduction (see e.g. [16, Chapter 1.3]) motivates the following approach: Compute approximate eigenfunctions $v_1, \ldots, v_d$ of $L_{\omega_{t^*}}$ corresponding to the eigenvalue close to zero. Choose $\varepsilon_1, \ldots, \varepsilon_d, \delta \in \mathbb{R} \setminus \{0\}$ suitable ("small") and set

$$\omega_{t^*+\delta}^{(0)} = \omega_{t^*+\delta} + \sum_{i=1}^{d} \varepsilon_i v_i.$$

This function may serve as an initial guess for a new approximate solution at the parameter value $t = t^* + \delta$, lying on a bifurcated branch (in case of a bifurcation point) or on another part of the original branch (in case of a turning point). One might have to "play" with the parameters $\varepsilon_i, i = 1, \ldots, d$ and δ in order to find an initial guess such that the Newton method converges.

We would like to remark that there are more sophisticated methods to compute branches past bifurcation or turning points, which are e.g. proposed by Keller, see [41] or [42]. However, it is more complicated and complex to implement these methods and since the above simple ansatz already led to the desired results we did not use Keller's methods.

Using the technique explained above (and an additional path-following on the new branches) we were able to find many more approximate solutions. Altogether we obtained 31 approximate solutions for $t = 1$, the first 6 were already displayed in Figure 6.1 and the following figures show the remaining approximations.

(7) Twopeak 1   (8) Twopeak 2   (9) Twopeak 3

(10) Twopeak 4   (11) Twopeak 5   (12) Threepeak 1

(13) Threepeak 2   (14) Threepeak 3   (15) Threepeak 4

(16) Threepeak 5   (17) Fourpeak 1   (18) Fourpeak 2

(19) Fourpeak 3   (20) Fourpeak 4   (21) Fourpeak 5

Figure 6.3: Approximate solutions - Part I

(22) Fourpeak 6

(23) Fourpeak 7

(24) Fivepeak 1

(25) Fivepeak 2

(26) Sixpeak 1

(27) Sixpeak 2

(28) Sixpeak 3

(29) Sixpeak 4

(30) Sevenpeak

(31) Eightpeak
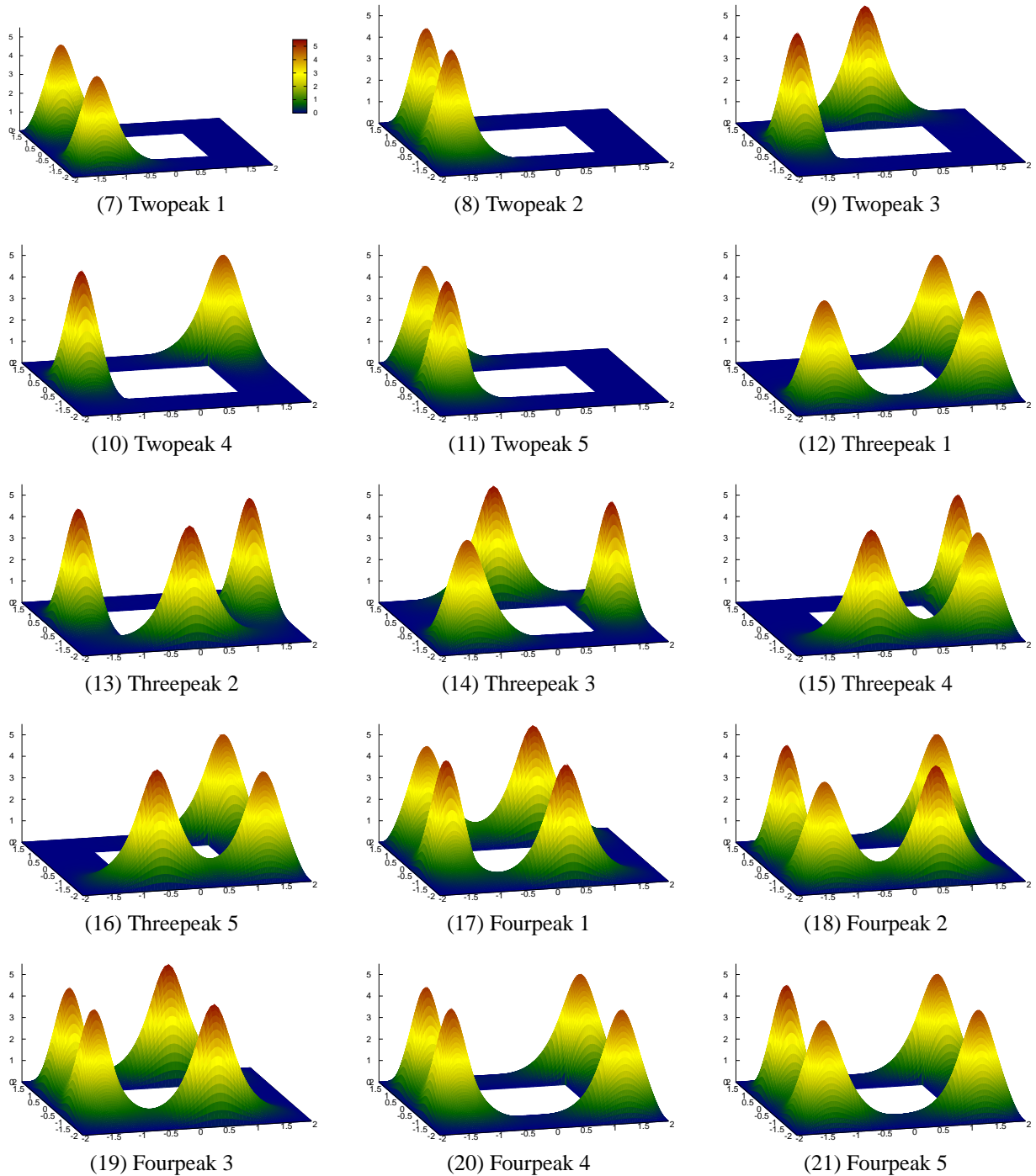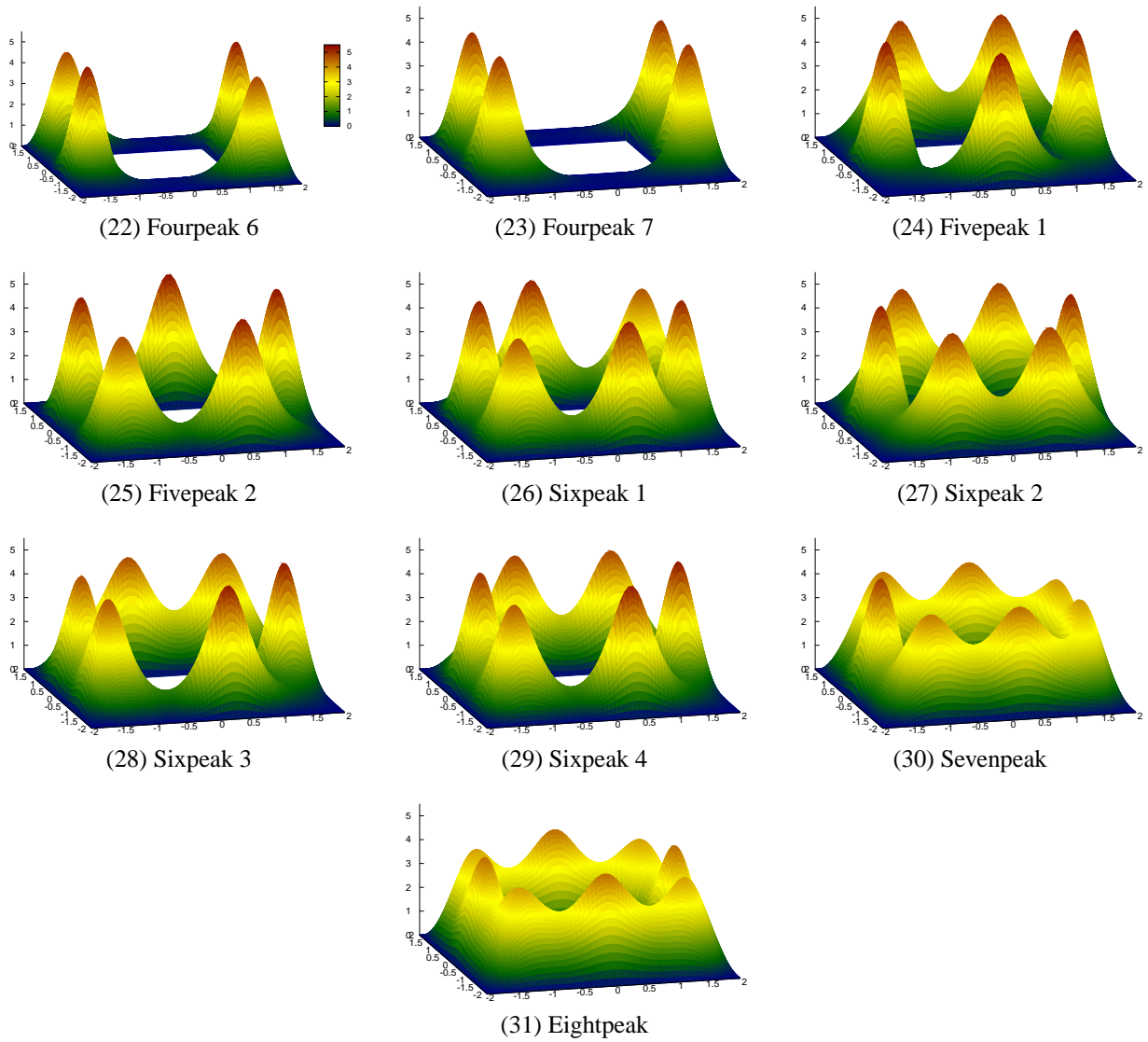
Figure 6.3: Approximate solutions - Part II

Since some of the solutions are hardly distinguishable from each other in the above plots we display the functions again, this time with a different point of view and thereby showing the level profile and symmetry.
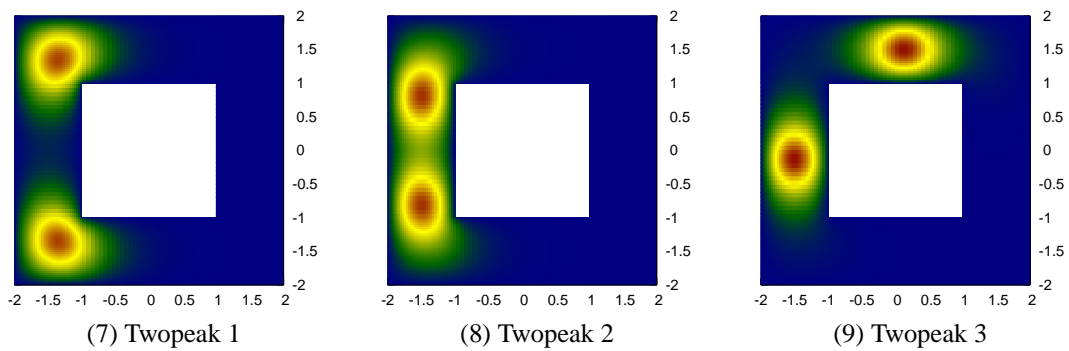
(7) Twopeak 1

(8) Twopeak 2

(9) Twopeak 3

Figure 6.4: Level sets and symmetry - Part I

(10) Twopeak 4

(11) Twopeak 5

(12) Threepeak 1

(13) Threepeak 2

(14) Threepeak 3

(15) Threepeak 4

(16) Threepeak 5

(17) Fourpeak 1

(18) Fourpeak 2

(19) Fourpeak 3

(20) Fourpeak 4

(21) Fourpeak 5

(22) Fourpeak 6

(23) Fourpeak 7

(24) Fivepeak 1

Figure 6.4: Level sets and symmetry - Part II

(25) Fivepeak 2

(26) Sixpeak 1

(27) Sixpeak 2

(28) Sixpeak 3

(29) Sixpeak 4

(30) Sevenpeak

(31) Eightpeak
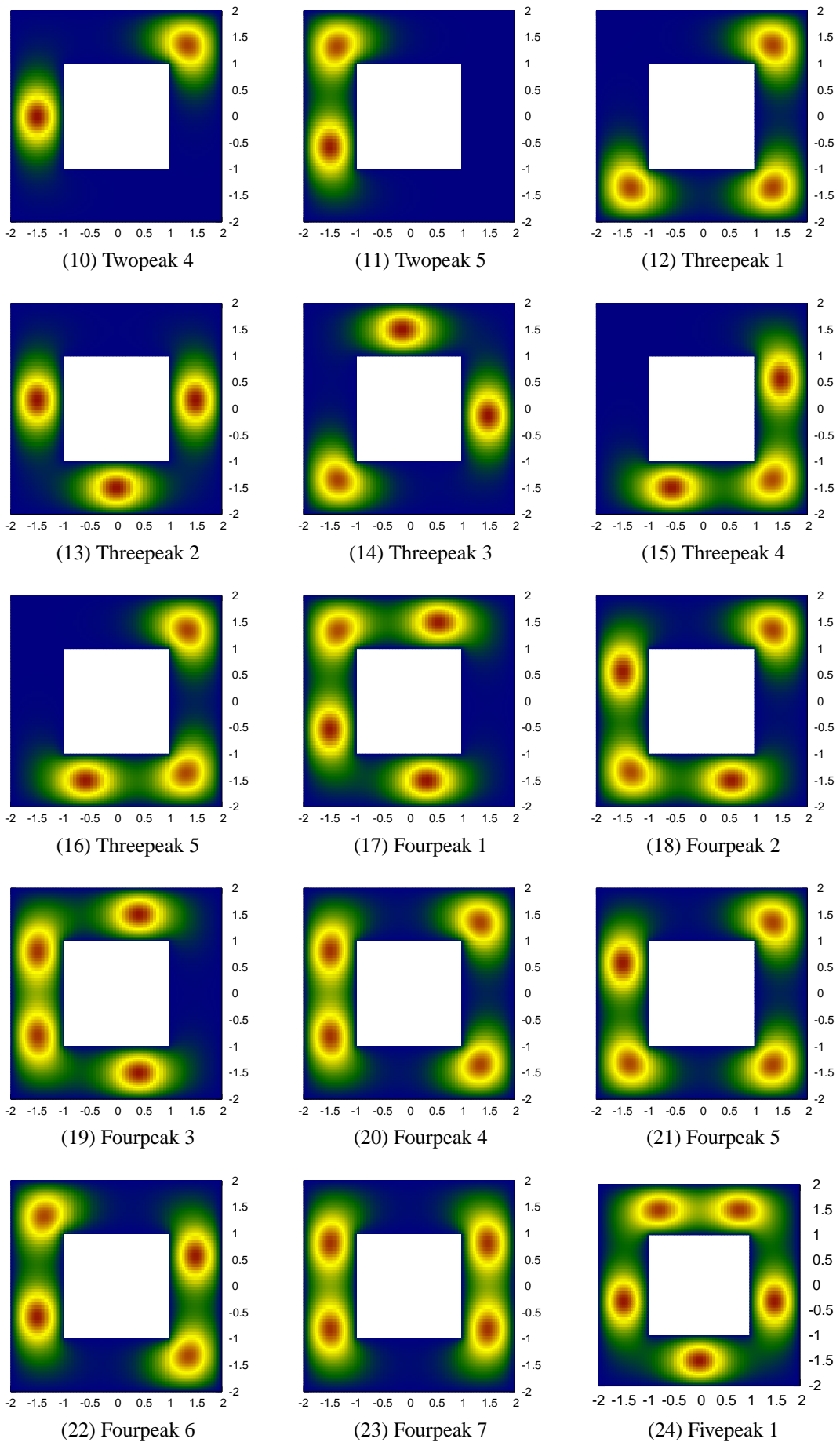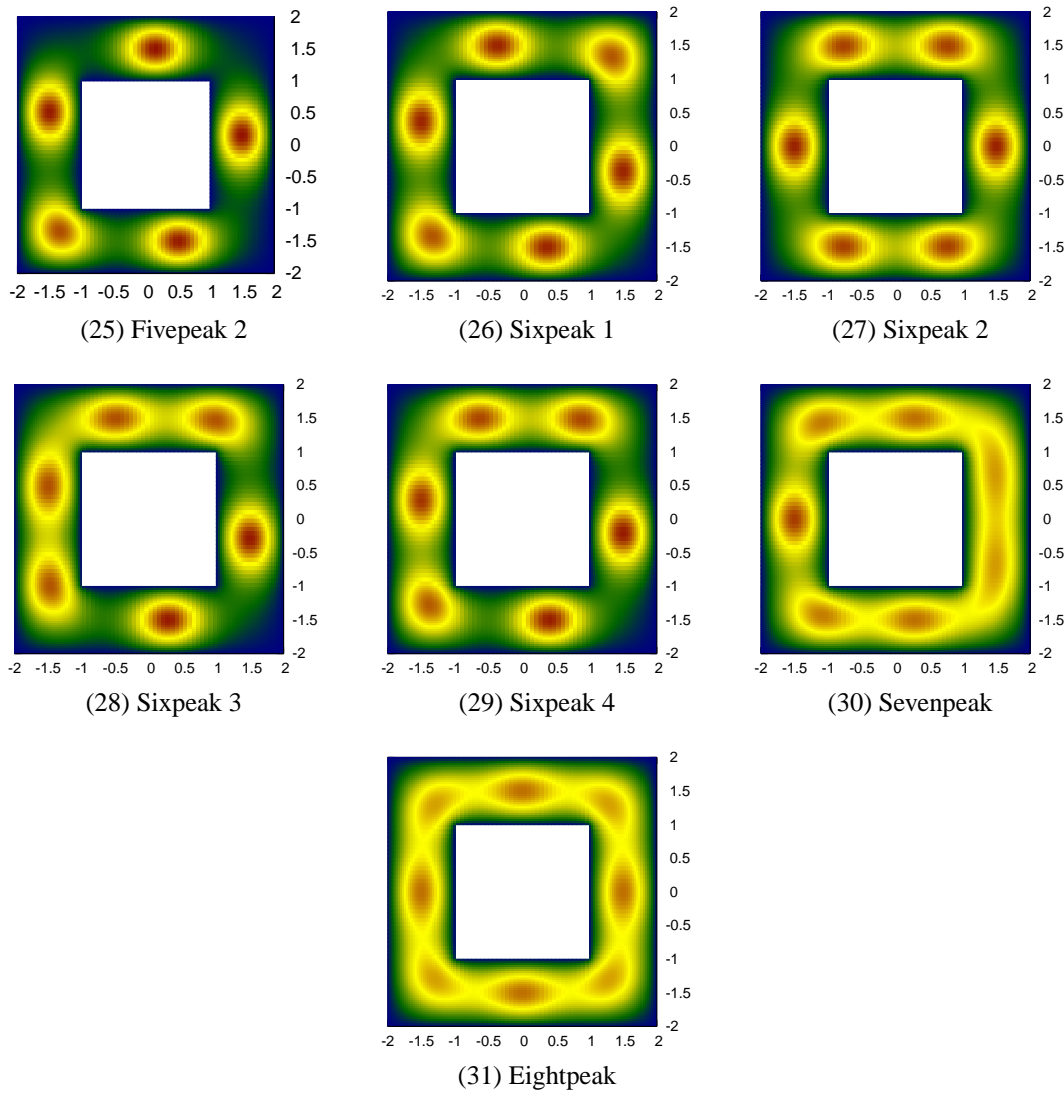
Figure 6.4: Level sets and symmetry - Part II

Finally, Figures 6.5 and 6.6 show bifurcation diagrams of the approximate solutions. Here we have the parameter t on the x-axis, the energy $J(\omega_t)$ (defined in (3.11)) on the y-axis and $\max_{\overline{\Omega}_t} \omega_t$ on the z-axis. In Figure 6.5 we displayed only the main branches without any bifurcations, while Figure 6.6 shows the full diagram including all occuring bifurcations. Note that we have only computed approximate solutions for $t \in \{t_0, \dots, t_n\}$ where the gridpoints t_i are "close". The continuous branches in the plots have been obtained by linear interpolation between the values in the gridpoints.

Remark 5. (a) In [23] it was proved that when $D \subset \mathbb{R}^m$ is a bounded domain with smooth boundary and U_n are small open star-shaped holes in D with $\operatorname{diam} U_n \to 0$ as $n \to \infty$, and if the positive solution of

$$\begin{cases} -\Delta u &= |u|^p \quad \text{in } D \\ u &= 0 \quad\quad \text{on } \partial D \end{cases} \tag{6.1}$$

($1 < p < \frac{m+2}{m-2}$ for $m > 2$, $1 < p < \infty$ for $m = 2$) is unique and non-degenerate, then also

the problem

$$\begin{cases} -\Delta u & = & |u|^p & \text{in } D\backslash U_n \\ u & = & 0 & \text{on } \partial(D\backslash U_n) \end{cases} \tag{6.2}$$

has a unique positive solution. Moreover, the solutions of (6.1) and (6.2) are close in L^q for all q. This result is not directly applicable to our problem since Ω_t does not have a smooth boundary. However, since the problem

$$\begin{cases} -\Delta u & = & |u|^p & \text{in } (-1,1)^2 \\ u & = & 0 & \text{on } \partial(-1,1)^2 \end{cases} \tag{6.3}$$

admits a unique non-degenerate solution (see e.g. [21]) we expect that for t close to zero there is only one solution to problem (1.2), which looks like the one of problem (6.3). An approximate shape of the solution to (6.3) is displayed in [50] and a comparision with Figure 6.2 for $t = \frac{1}{16}$ suggests the conjecture that for small t the only solution of (1.2) is the fourpeakcorner solution (looking almost "radial" for these small t-values). However, for all considered $t > 0.001$ we could also find the onepeakcorner and onepeakedge solutions as approximations. Besides the possibility that the approximate solutions are "ghosts", i.e. there does not exist an exact solution nearby, there are only two more options: either the theorem of [24] is false for domains not smoothly bounded or the onepeak solutions must "vanish" for very small values of t. We believe the latter is the case but we were not able to prove this.

(b) For larger values of t we could find many more approximate solutions having more than three bumps on the edges of the domain. For reasons of simplicity we did however not include these approximations in this thesis.

(1) onepeakcorner   (2) onepeakedge   (7) Twopeak 1   (8) Twopeak 2   (12) Threepeak 1   (15) Threepeak 4
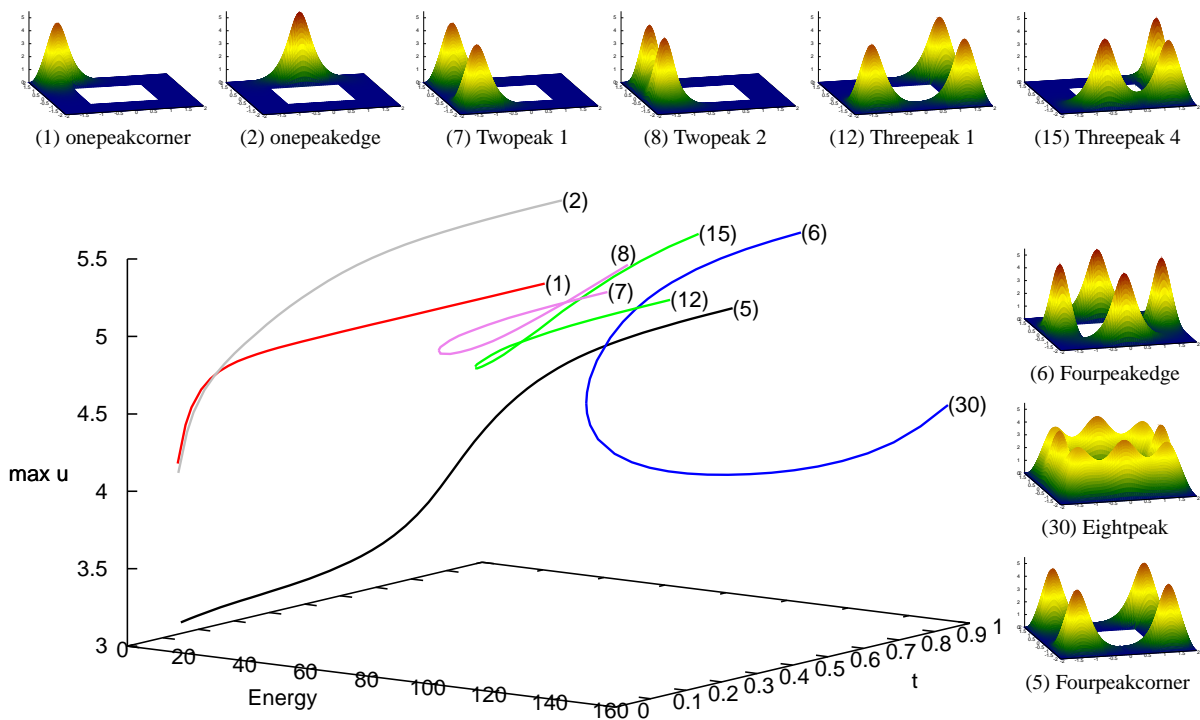
Figure 6.5: Bifurcation diagram including main branches
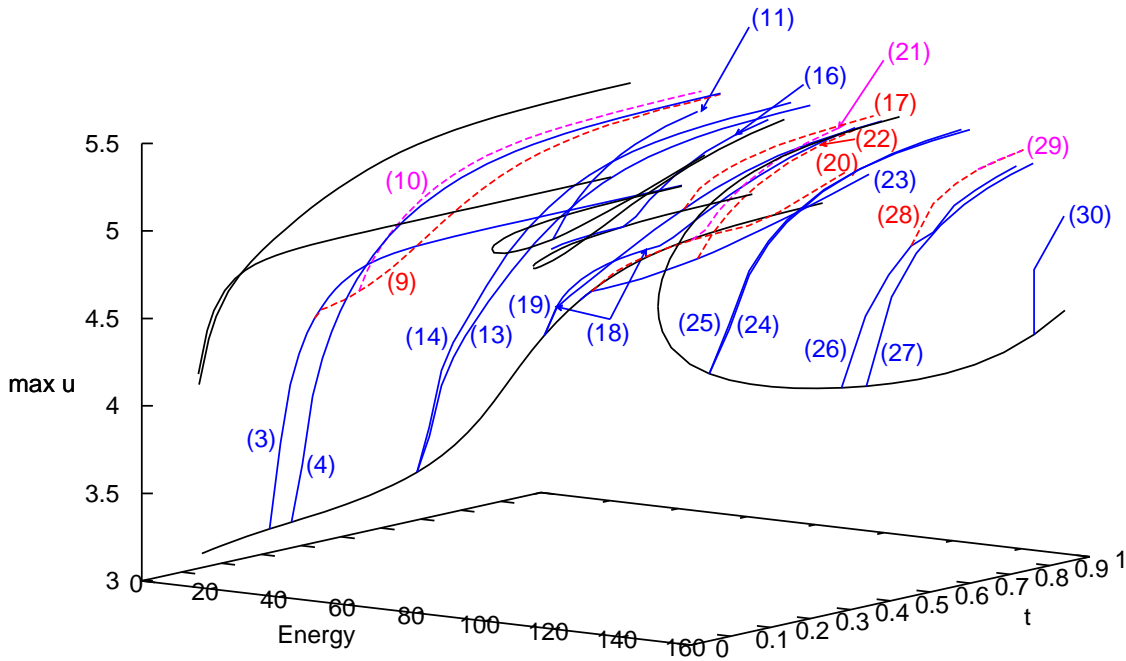
Figure 6.6: Full bifurcation diagram. The numbers correspond to the numbering in Figures 6.1 and 6.4. Main branches are displayed by straight black lines, bifurcations of main branches are displayed by straight blue lines and bifurcations from these branches by dottes lines.

Selection of candidates for verification

By purely numercial, i.e. non-verified, computations we can calculate approximations for the quantities that are needed to apply Theorem 1. This will give us some numerical evidence for which of the approximate solutions displayed above a verification of a true solution nearby might be successful. It turns out that for most of the approximate solutions the constant K, satisfying (2.4), will be too large to find some $\alpha > 0$ satisfying (2.7) and (2.8). We have seen in section 5.1 that the computation of K amounts to the computation of bounds for the spectrum of a selfadjoint operator involving the linearization of problem (1.2) at the approximate solution. Moreover we have seen that K becomes large if the spectrum is close to zero. In the above mentioned cases, when K is too large, we have one or more eigenvalues which are too close to zero. Fortunately, there are some approximate solutions which have certain symmetries and taking these symmetries into account in our computations can lead to a reduction of K: instead of working with the full space $H_0^1(\Omega_t)$ we will consider only the subspace of all $H_0^1(\Omega_t)$-functions exhibiting the same symmetry as the considered approximate solution. Then eigenvalues of the above mentioned operator corresponding to non-symmetric eigenfunctions do no longer contribute to the value of K and often these are the ones being closest to zero. Finally the verification process will lead to a true solution lying also in the space of symmetric $H_0^1(\Omega_t)$-functions.

It is clear that this procedure cannot be applied if the approximate solution does not have any symmetry at all. For the above considered approximate solutions it turned out that the most promising candidates for a successful verification are the ones displayed in Figure 6.1. Therefore we restricted ourselves to these approximate solutions in the rest of this thesis.

6.2   Application of Domain Decomposition

6.2.1   Computational domains and splitting into subdomains

As explained in the previous section we are going to prove existence of solutions to (1.2) in a neighbourhood of the approximations displayed in Figure 6.1 (1)-(6). The functions exhibit several symmetries:

a) The solutions are symmetric w.r.t. the axes $y = x$, $y = -x$, $y = 0$ and $x = 0$, i.e. they exhibit full symmetry of the domain. This is the case for the fourpeakcorner and the fourpeakedge solution.

b) The solutions are symmetric w.r.t. the axes $y = x$, $y = -x$. We refer to this as quarter symmetry I. It applies to the twopeakoppcorner solution.

c) The solutions are symmetric w.r.t. the axes $y = 0$, $x = 0$, which we call quarter symmetry II. This is the case for the twopeakoppedge solution.

d) The solutions are symmetric w.r.t. the axis $y = -x$. This is called half symmetry I and applies to the onepeakcorner solution.

e) The solutions are symmetric w.r.t. the axis $y = 0$, denoted by half symmetry II and is satisfied for the onepeakedge solution.

As already explained in the end of the previous section, and also to reduce computation time, we take all symmetry of the solutions into account and work only on suitable subdomains of Ω_t, imposing Neumann boundary conditions on the new parts of the boundary. Furthermore, we shift the remaining subdomain such that the upper left re-entrant corner is at the point $(0, 0)$. We write $\widehat{\Omega}_t$ for these computational domains and assume always that $\widehat{\Omega}_t$ is chosen according to the symmetries of the underlying approximate solution ω_t. Note that this restriction leads to lower bounds for those eigenvalues only, whose corresponding eigenfunctions have the same symmetry as ω_t and finally - provided the verification process is successful - to exact solutions also having this symmetry.

Figures 6.6 (a) to (e) show the computational domains and the splitting into subdomains as it will be used for the domain decomposition. Solid lines - in $\widehat{\Omega}_t$ - mark where the domain is split, at these lines we will impose additional Neumann boundary conditions in the course of the domain decomposition.
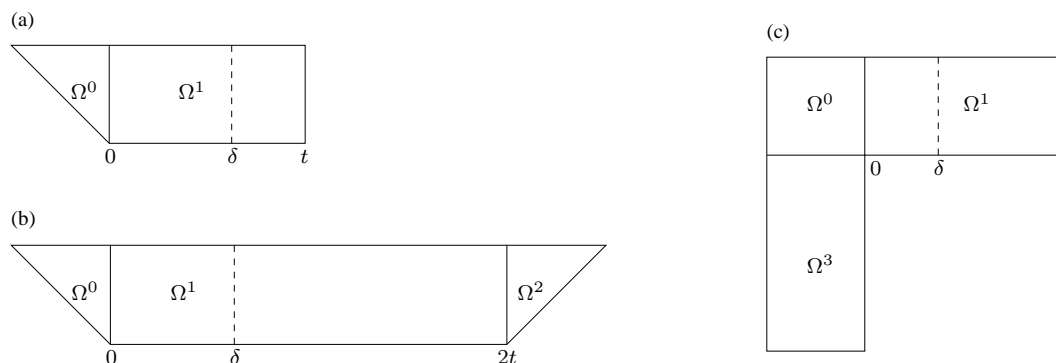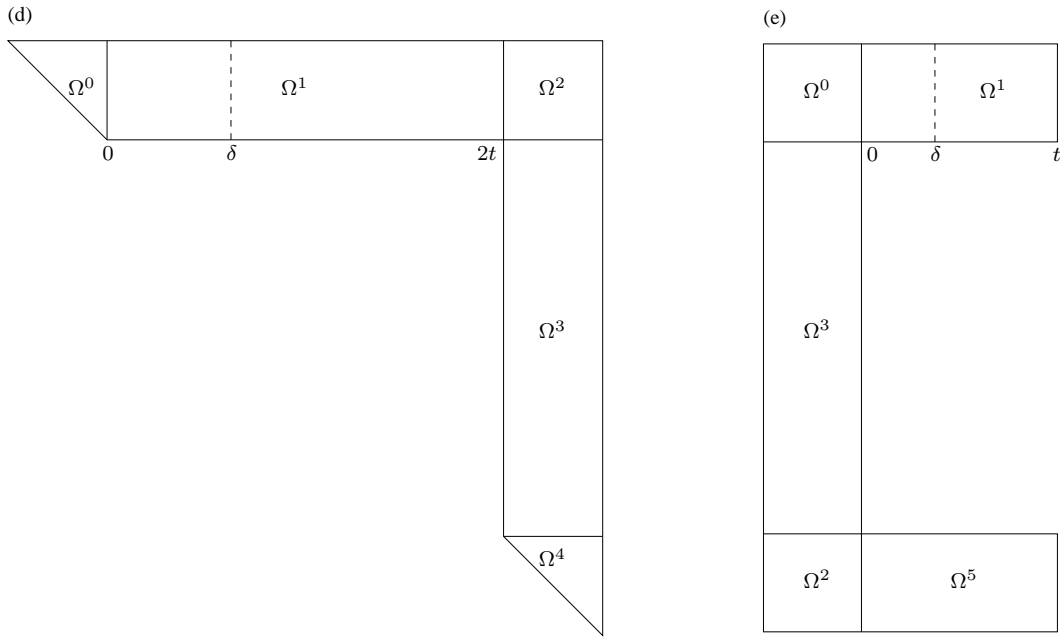
Figure 6.6: Computational domains for (a) fourpeakcorner and fourpeakedge, (b) twopeakopp-corner, (c) twopeakoppedge, (d) onepeakcorner, (e) onepeakedge

6.2.2   Eigenvalue bounds for the base-problem

We will now comment on the computation of lower eigenvalue bounds for the base problem (5.31), i.e. on the computation of eigenvalue bounds for the eigenvalue problems ($j \in \{0, \ldots, 5\}$)

$$\begin{cases} -\Delta u + u &=& \lambda(1 + \bar{c}(x,y))u & \text{in } \Omega^j \\ u &=& 0 & \text{on } \partial\Omega^j \cap \partial\Omega \\ \frac{\partial u}{\partial \nu} &=& 0 & \text{on } \partial\Omega^j \backslash \partial\Omega \end{cases} \qquad (6.4)$$

where $\bar{c} : \Omega_t \to \mathbb{R}$ is piecewise constant and such that $\bar{c} \geq 3|\omega_t|\omega_t$ on Ω_t. We used the subdomains Ω^j, $j = 0, \ldots, 5$ as marked in Figures 6.6 (a)-(e). To be more clear we write down the explicit definitions:

(a) $\Omega^0 = \text{conv}\{(0,0),(0,1),(-1,1)\}$
      $\Omega^1 = (0,t) \times (0,1)$

(b) $\Omega^0 = \text{conv}\{(0,0),(0,1),(-1,1)\}$
      $\Omega^1 = (0,2t) \times (0,1)$
      $\Omega^2 = \text{conv}\{(2t,0),(2t+1,1),(2t,1)\}$

(c) $\Omega^0 = (-1,0) \times (0,1)$
      $\Omega^1 = (0,2t) \times (0,1)$
      $\Omega^3 = (-1,0) \times (-t,0)$

(d) $\Omega^0 = \text{conv}\{(0,0),(0,1),(-1,1)\}$
      $\Omega^1 = (0,2t) \times (0,1)$
      $\Omega^2 = (2t,2t+1) \times (0,1)$
      $\Omega^3 = (2t,2t+1) \times (-2t,0)$
      $\Omega^4 = \text{conv}\{(2t,-2t),(2t+1,-2t-1),$
                           $(2t+1,-2t)\}$

(e) $\Omega^0 = (-1,0) \times (0,1)$
      $\Omega^1 = (0,t) \times (0,1)$
      $\Omega^2 = (-1,0) \times (-2t-1,-2t)$
      $\Omega^3 = (-1,0) \times (-2t,0)$
      $\Omega^5 = (0,t) \times (-2t-1,-2t)$

For a suitable definition of $\bar{c}$ it is helpful to take also the variation of the approximate solutions in the sudomains Ω^j into account: cornerbump functions have a bump centered (roughly) at $(-\frac{1}{2}, \frac{1}{2}) \in \Omega^0$ which fades in Ω^1 whereas edgebumps have a bump concentrating on the right part of Ω^1 (centered roughly at $(t, \frac{1}{2})$). On the remaining subdomains Ω^j, $j > 1$ the approximate solutions do not vary much and are close to zero. We will therefore choose $\bar{c}$ to be constant on each of the subdomains Ω^0 and Ω^j, $j > 1$, but piecewise constant on Ω^1: For some suitably chosen $\delta \in (0, t)$ we set $\Omega^{1,1} = (0, \delta) \times (0, 1)$, $\Omega^{1,2} = \Omega^1 \backslash \overline{\Omega^{1,1}}$ and define

$$
\bar{c}(x, y) := \begin{cases}
c_j := \max_{\overline{\Omega^j}} 3|\omega_t|\omega_t, & (x, y) \in \Omega^j & j = 0, 2, 3, 4, 5 \\
c_{1,1} := \max_{\overline{\Omega^{1,1}}} 3|\omega_t|\omega_t, & (x, y) \in \Omega^{1,1} \\
c_{1,2} := \max_{\overline{\Omega^{1,2}}} 3|\omega_t|\omega_t, & (x, y) \in \Omega^{1,2} \\
\max\{c_{1,1}, c_{1,2}\}, & (x, y) \in \partial\Omega^{1,1} \cap \partial\Omega^{1,2}.
\end{cases}
$$

On the interfaces $\partial\Omega^i \cap \partial\Omega^j$, $i \neq j$ we define $\bar{c}$ by the larger of the two values in the adjacent subdomains. We can check that $c_{1,1} \neq c_{1,2}$, which is also expectable from the shape of ω_t.
With this choice of $\bar{c}$ the base problem (5.31) is not "too far away" from the original eigenvalue problem (5.5), which results in a small number of homotopy steps to connect both problems.

Remark 6. Recall that we are aiming at bounds for the eigenvalues of problem (5.6), (5.7) neighbouring 1. Therefore we will restrict ourselves to the computation of eigenvalues λ of (6.4) which are smaller than a prescribed bound $C_L > 1$, and we will use the particular choice $C_L := 8$. Note that if there was no eigenvalue of (6.4) below C_L, then C_L would constitute a lower bound for the smallest eigenvalue of (5.6), (5.7) (in which case we would have obtained the desired eigenvalue bound). However, in all our applications this was never the case.

Eigenvalue problem in Ω^0

By the above definitions we have two different cases for Ω^0, namely $\Omega^0 = (-1, 0) \times (0, 1)$ (square case) and $\Omega^0 = \text{conv}\{(0, 0), (0, 1), (-1, 1)\}$ (triangle case). However, a closer look at the boundary conditions in (6.4) shows that in the triangle case the eigenvalues of (6.4), $j = 0$ are in fact eigenvalues of (6.4), $j = 0$ for the square case which correspond to eigenfunctions being symmetric w.r.t. $y = -x$. Therefore we can restrict ourselves to the computation of eigenvalues for the following problem (which is (6.4), $j = 0$ in the square case)

$$
\begin{cases}
-\Delta u + u = \lambda(1 + c_0)u & \text{in } (-1, 0) \times (0, 1) \\
u = 0 & \text{on } (\{-1\} \times [0, 1]) \cup ([-1, 0] \times \{1\}) =: \Gamma_{1,D} \\
\frac{\partial u}{\partial \nu} = 0 & \text{on } (\{0\} \times [0, 1]) \cup ([-1, 0] \times \{0\}).
\end{cases} \tag{6.5}
$$

Extracting from the eigenvalues of (6.5) all eigenvalues corresponding to eigenfunctions which are symmetric w.r.t. $y = -x$ finally yields eigenvalues of (6.4), $j = 0$, in the triangle case.

To solve (6.5) we use a separation ansatz $u(x, y) = v(x)w(y)$, leading to

$$
-\frac{v''(x)}{v(x)} = \frac{w''(y)}{w(y)} + \lambda(1 + c_0) - 1 = const. =: \tau
$$

and the boundary conditions give $v(-1) = v'(0) = 0$, $w'(0) = w(1) = 0$.

(i) $-v''(x) = \tau v(x)$, $v(-1) = v'(0) = 0$.

This problem has non-trivial solutions only if $\tau > 0$ and in this case the general solution is given by

$$v(x) = a\cos(\sqrt{\tau}(x+1)) + b\sin(\sqrt{\tau}(x+1)).$$

Using the boundary conditions we obtain $a = 0$ and

$$\sqrt{\tau} = \frac{\pi}{2} + k\pi, \quad k \in \mathbb{N}_0 \quad \text{i.e.} \quad \tau = \left(\frac{\pi + 2k\pi}{2}\right)^2, \quad k \in \mathbb{N}_0.$$

(ii) $w''(y) = \underbrace{(\tau - \lambda(1 + c_0) + 1)}_{=:\tilde{\tau}_k} w(y)$, $w'(0) = w(1) = 0$, $\tau = \left(\frac{\pi + 2k\pi}{2}\right)^2$ for some $k \in \mathbb{N}_0$.

We obtain non-trivial solutions only for $\tilde{\tau}_k < 0$ and the general solution in this case is given by

$$w(y) = a\cos(\sqrt{-\tilde{\tau}_k}y) + b\sin(\sqrt{-\tilde{\tau}_k}y).$$

The boundary conditions imply $b = 0$ and $\sqrt{-\tilde{\tau}_k} = \frac{\pi}{2} + l\pi$ for some $l \in \mathbb{N}_0$.

Altogether we obtain eigenvalues

$$\lambda_{kl} = \frac{\tau - \tilde{\tau}_k + 1}{1 + c_0} = \frac{(\pi + 2l\pi)^2 + (\pi + 2k\pi)^2 + 4}{4(1 + c_0)}, \quad k, l \in \mathbb{N}_0,$$

corresponding to eigenfunctions

$$u_{kl}(x, y) = \sin\left(\left(\tfrac{\pi}{2} + 2k\pi\right)x\right)\cos\left(\left(\tfrac{\pi}{2} + 2l\pi\right)y\right). \tag{6.6}$$

Since the space $\text{span}\{u_{kl} : k, l \in \mathbb{N}_0\}$ is dense in $H^1_{\Gamma_{1,D}}(\Omega_1)$ all eigenvalues of (6.5) are obtained by this separation ansatz.

For the triangle case we have to find all eigenvalues of (6.5) corresponding to eigenfunctions which are symmetric w.r.t. to $y = -x$: In case λ_{kl} is a simple eigenvalue its eigenfunction is symmetric, which can easily be seen from (6.6). For a double eigenvalue we also have one symmetric linearly independent eigenfunction, and in case of an eigenvalue with multiplicity 3 or 4 we have two linearly independent symmetric eigenfunctions. Eigenvalues with higher multiplicity do not occur if $\lambda_{kl} < C_L$ (see Remark 6).

Eigenvalue problems in Ω^j, $j > 1$

Since Ω^2 is a rotated and shifted version of Ω^0 (in both the triangle and square case) and moreover this transformation maps the Neumann and Dirichlet boundary of Ω^0, respectively, onto the Neumann and Dirichlet boundary of Ω^2, respectively, the eigenvalues of (6.4), $j = 2$ are given by eigenvalues of (6.4), $j = 0$ with c_0 replaced by c_2. The same argument applies for Ω^4.

For the eigenvalue problem in Ω^3 a separation ansatz leads to the eigenvalues

$$\lambda_{kl} = \frac{k^2\pi^2 + \frac{l^2\pi^2}{4t^2} + 1}{1 + c_3}, \quad k \in \mathbb{N}, l \in \mathbb{N}_0$$

and again a density argument shows that these are indeed all eigenvalues of (6.4), $j = 3$. The eigenvalue problem in Ω^5 can be treated similarly.

Eigenvalue problem in Ω^1

The eigenvalue problem to be solved in this section is given by

$$
\begin{cases}
-\Delta u + u &= \lambda(1 + \bar{c}(x,y))u \quad \text{in } (0,s) \times (0,1) \\
\frac{\partial u}{\partial x}(0,y) = \frac{\partial u}{\partial x}(s,y) &= 0 \qquad\qquad\qquad \text{for all } y \in [0,1] \\
u(x,0) = u(x,1) &= 0 \qquad\qquad\qquad \text{for all } x \in [0,s]
\end{cases}
\tag{6.7}
$$

with $s = t$ if ω_t is a cornerbump or the fourpeakedge solution and $s = 2t$ in the remaining cases. The separation ansatz $u(x,y) = v(x)w(y)$ leads to

$$
-\frac{w''(y)}{w(y)} = (\lambda(1 + \bar{c}) - 1) + \frac{v''(x)}{v(x)} = const. = \tau.
\tag{6.8}
$$

We will solve these equations, together with the corresponding boundary conditions from (6.7), in the subdomains $\Omega^{1,1} := (0,\delta) \times (0,1)$ and $\Omega^{1,2} := (\delta,s) \times (0,1)$.

(i) Differential equation in $\Omega^{1,1} = (0,\delta) \times (0,1)$.

The boundary conditions applying to this subdomain are $w(0) = w(1) = 0$ and $v'(0) = 0$. Clearly, non-trivial solutions to $-w''(y) = \tau w(y)$, $w(0) = w(1) = 0$ can only be obtained if $\tau > 0$ and in this case we have

$$
\tau = k^2\pi^2 \qquad (k \in \mathbb{N}), \quad w(y) = \sin(k\pi y).
$$

For v it remains to solve the differential equation

$$
v''(x) = (k^2\pi^2 - \lambda(1 + c_{1,1}) + 1)v(x)
$$

with boundary condition $v'(0) = 0$. We consider three different cases:

(a) $k^2\pi^2 - \lambda(1 + c_{1,1}) + 1 =: -\tau_1^2 < 0 \quad (\tau_1 \in \mathbb{R})$
In this case the general solution is given by $v_1(x) = a_1\sin(\tau_1 x) + b_1\cos(\tau_1 x)$ and $v_1'(0) = 0$ gives $v_1(x) = b_1\cos(\tau_1 x)$.

(b) $k^2\pi^2 - \lambda(1 + c_{1,1}) + 1 =: \tau_1^2 > 0 \quad (\tau_1 \in \mathbb{R})$
Now the general solution is $v_1(x) = a_1\sinh(\tau_1 x) + b_1\cosh(\tau_1 x)$ and using the boundary condition we obtain $v_1'(0) = a_1 = 0$, i.e. $v_1(x) = b_1\cosh(\tau_1 x)$.

(c) $k^2\pi^2 - \lambda(1 + c_{1,1}) + 1 = 0$, and we obtain $v_1(x) = b_1$ with $b_1 \in \mathbb{R}$.

(ii) Differential equation in $\Omega^{1,2} = (\delta,s) \times (0,1)$.

As before: $w(0) = w(1) = 0$, and thus $\tau = k^2\pi^2$ with $k \in \mathbb{N}$ and $w(y) = \sin(k\pi y)$. The differential equation for v reads

$$
v''(x) = (k^2\pi^2 - \lambda(1 + c_{1,2}) + 1)v(x)
$$

with boundary condition $v'(s) = 0$.

(a) $k^2\pi^2 - \lambda(1 + c_{1,2}) + 1 =: -\tau_2^2 < 0 \quad (\tau_2 \in \mathbb{R})$
General solution: $v_2(x) = a_2\sin(\tau_2(x - s)) + b_2\cos(\tau_2(x - s))$ and the boundary condition imply $a_2 = 0$, thus we have $v_2(x) = b_2\cos(\tau_2(x - s))$.

(b) $k^2\pi^2 - \lambda(1 + c_{1,2}) + 1 =: \tau_2^2 > 0 \quad (\tau_2 \in \mathbb{R})$

Now the general solution is given by $v_2(x) = a_2 \sinh(\tau_2(x - s)) + b_2 \cosh(\tau_2(x - s))$, the boundary condition yields $v_2'(s) = a_2 = 0$ and thus $v_2(x) = b_2 \cosh(\tau_2(x - s))$

(c) $k^2\pi^2 - \lambda(1 + c_{1,2}) + 1 = 0$, and we obtain $v_2(x) = b_2$, $b_2 \in \mathbb{R}$.

Altogether we obtain

$$v(x) = \begin{cases} v_1(x), & x \in (0, \delta) \\ v_2(x), & x \in (\delta, s) \end{cases}$$

with v_1, v_2 of the form determined before, and the additional smoothness conditions

$$v_1(\delta) = v_2(\delta), \qquad v_1'(\delta) = v_2'(\delta).$$

Note that the number k occuring in v_1 and v_2 must be the same, since the resulting eigenfunction will not be continuous at $x = \delta$ otherwise.

Case A: (i)(a) and (ii)(b), i.e. $\tau_1 = \sqrt{\lambda(1 + c_{1,1}) - 1 - k^2\pi^2}$, $\tau_2 = \sqrt{k^2\pi^2 + 1 - \lambda(1 + c_{1,2})}$ (note that due to the form of v_1, v_2 we may assume $\tau_1, \tau_2 \geq 0$) and we have the following restrictions for λ :

$$\frac{1 + k^2\pi^2}{1 + c_{1,1}} < \lambda < \frac{1 + k^2\pi^2}{1 + c_{1,2}}, \tag{6.9}$$

which can only be satisfied if $c_{1,1} > c_{1,2}$.

We have to find non-trivial solutions b_1, b_2 of the following system of equations

$$\begin{aligned} b_1 \cos(\tau_1\delta) &= b_2 \cosh(\tau_2(\delta - s)) \\ -b_1\tau_1(\sin \tau_1\delta) &= b_2\tau_2 \sinh(\tau_2(\delta - s)), \end{aligned}$$

which is equivalent to

$$\underbrace{\begin{pmatrix} \cos(\tau_1\delta) & -2\cosh(\tau_2(\delta - s)) \\ -\tau_1 \sin(\tau_1\delta) & -2\tau_2 \sinh(\tau_2(\delta - s)) \end{pmatrix}}_{=:A} \begin{pmatrix} b_1 \\ b_2 \end{pmatrix} = \begin{pmatrix} 0 \\ 0 \end{pmatrix}.$$

Non-trivial solutions do exist if and only if $\det A = 0$, and this leads to

$$\tau_2 \cos(\tau_1\delta) \sinh(\tau_2(\delta - s)) + \tau_1 \sin(\tau_1\delta) \cosh(\tau_2(\delta - s)) = 0.$$

For a fixed value of k we can enclose all solutions to this nonlinear equation on the interval determined by (6.9) using an Interval Newton method (see section 5.4.1) as follows: we first apply the Interval Newton method to the closure of the interval determined by (6.9) and check a-posteriori that the enclosed solutions are lying in the interior of the interval determined by (6.9) (which is indeed satisfied in all our computations). In the following cases we will always implicitly refer to this procedure when the Interval Newton method is applied to an open interval.

Note that we have to consider only finitely many values of k, since we are only interested in eigenvalues $\lambda < C_L$ (see Remark 6).

Case B: (i)(a) and (ii)(a), i.e. $\tau_1 = \sqrt{\lambda(1 + c_{1,1}) - 1 - k^2\pi^2}$, $\tau_2 = \sqrt{\lambda(1 + c_{1,2}) - k^2\pi^2 - 1}$ and we have the following restrictions for λ :

$$\lambda > \max\left\{\frac{1 + k^2\pi^2}{1 + c_{1,1}}, \frac{1 + k^2\pi^2}{1 + c_{1,2}}\right\} =: B_k. \tag{6.10}$$

In this case the system to be solved is given by

$$\underbrace{\begin{pmatrix} \cos(\tau_1\delta) & -\cos(\tau_2(\delta - s)) \\ -\tau_1\sin(\tau_1\delta) & \tau_2\sin(\tau_2(\delta - s)) \end{pmatrix}}_{=:B} \begin{pmatrix} b_1 \\ b_2 \end{pmatrix} = \begin{pmatrix} 0 \\ 0 \end{pmatrix}$$

and $\det B = 0$ is equivalent to

$$\tau_2\cos(\tau_1\delta)\sin(\tau_2(\delta - s)) - \tau_1\sin(\tau_1\delta)\cos(\tau_2(\delta - s)) = 0.$$

Recall that we are only aiming at eigenvalues $\lambda < C_L$ and therefore only at solutions to the previous equation in the interval (B_k, C_L), provided $B_k < C_L$, with B_k as defined in (6.10). Note that $B_k < C_L$ is satisfied for only finitely many values of k and in these cases all solutions in the interval (B_k, C_L) can be enclosed using an Interval Newton method.

Case C: (i)(b) and (ii)(b), i.e. $\tau_1 = \sqrt{1 + k^2\pi^2 - \lambda(1 + c_{1,1})}$, $\tau_2 = \sqrt{k^2\pi^2 + 1 - \lambda(1 + c_{1,2})}$. Restrictions for λ :
$$\lambda < \min\left\{\frac{1 + k^2\pi^2}{1 + c_{1,1}}, \frac{1 + k^2\pi^2}{1 + c_{1,2}}\right\}.$$

The system to be solved in this case is

$$\underbrace{\begin{pmatrix} \cosh(\tau_1\delta) & -\cosh(\tau_2(\delta - s)) \\ \tau_1\sinh(\tau_1\delta) & -\tau_2\sinh(\tau_2(\delta - s)) \end{pmatrix}}_{=:C} \begin{pmatrix} b_1 \\ b_2 \end{pmatrix} = \begin{pmatrix} 0 \\ 0 \end{pmatrix}.$$

Obviously,

$$\det C = 0 \iff \tau_2\sinh(\tau_2(\delta - s))\cosh(\tau_1\delta) - \tau_1\sinh(\tau_1\delta)\cosh(\tau_2(\delta - s)) = 0$$
$$\iff \tau_2\tanh(\tau_2(\delta - s)) = \tau_1\tanh(\tau_1\delta).$$

Since $0 < \delta < t \leq s$ and $\tau_1, \tau_2 > 0$, the term on the left-hand-side is negative while the expression on the right-hand-side is positive. Thus there are no non-trivial solutions in this case.

Case D: (i)(b) and (ii)(a), i.e. $\tau_1 = \sqrt{1 + k^2\pi^2 - \lambda(1 + c_{1,1})}$, $\tau_2 = \sqrt{\lambda(1 + c_{1,2}) - k^2\pi^2 - 1}$. We have the following restrictions for λ :

$$\frac{1 + k^2\pi^2}{1 + c_{1,2}} < \lambda < \frac{1 + k^2\pi^2}{1 + c_{1,1}}, \tag{6.11}$$

which can only be satisfied if $c_{1,1} < c_{1,2}$. In case $c_{1,2} < c_{1,1}$ we do not obtain eigenvalues.

The system to be solved is the following:

$$\underbrace{\begin{pmatrix} \cosh(\tau_1\delta) & -\cos(\tau_2(\delta-s)) \\ \tau_1\sinh(\tau_1\delta) & \tau_2\sin(\tau_2(\delta-s)) \end{pmatrix}}_{=:D} \begin{pmatrix} b_1 \\ b_2 \end{pmatrix} = \begin{pmatrix} 0 \\ 0 \end{pmatrix}.$$

Again non-trivial solutions will occur only for

$$\det D = 0 \iff \tau_2\cosh(\tau_1\delta)\sin(\tau_2(\delta-s)) + \tau_1\sinh(\tau_1\delta)\cos(\tau_2(\delta-s)) = 0.$$

We use an Interval Newton method on the interval determined by (6.11) to enclose zeros of this nonlinear equation for fixed k. As before we have to consider only finitely many values of k, since we are aiming at eigenvalues $\lambda < C_L$ only.

Case E1: (i)(a) and (ii)(c), i.e.

$$\lambda = \frac{k^2\pi^2+1}{1+c_{1,2}}, \quad \tau_1 = \sqrt{(k^2\pi^2+1)\frac{1+c_{1,1}}{1+c_{1,2}} - k^2\pi^2 - 1} \neq 0,$$

since $c_{1,1} \neq c_{1,2}$. Note that this case can only occur if $c_{1,1} > c_{1,2}$.

The smoothness conditions on v_1 imply

$$b_1\cos(\tau_1\delta) = b_2 \quad \text{and} \quad -b_1\tau_1\sin(\tau_1\delta) = 0.$$

Since $b_1 = 0$ or $b_2 = 0$ yield $v \equiv 0$ the second equation implies $\tau_1\delta = j\pi$ for some $j \in \mathbb{N}$, and therefore

$$\sqrt{(k^2\pi^2+1)\frac{1+c_{1,1}}{1+c_{1,2}} - k^2\pi^2 - 1} = \frac{j\pi}{\delta}.$$

For a given value of k we can check if there exists some $j \in \mathbb{N}$ such that the previous equality is satisfied. Note that we have to consider only finitely many cases, since we are aiming at $\lambda < C_L$.

Case E2: (i)(b) and (ii)(c)

In this case the smoothness conditions on v read

$$b_1\cosh(\tau_1\delta) = b_2 \quad \text{and} \quad \tau_1 b_1\sinh(\tau_1\delta) = 0$$

which, due to $\tau_1 \neq 0$ and $\delta \neq 0$ implies $b_1 = b_2 = 0$ and therefore $v \equiv 0$.

Case E3: (i)(c) and (ii)(b)

Now the smoothness conditions on v give

$$b_1 = b_2\cosh(\tau_2(\delta-s)) \quad \text{and} \quad 0 = \tau_2 b_2\sinh(\tau_2(\delta-s))$$

which, due to $\tau_2 \neq 0$ and $\delta - s \neq 0$ implies $b_1 = b_2 = 0$ and therefore $v \equiv 0$.

Case E4: (i)(c) and (ii)(a), i.e.

$$\lambda = \frac{k^2\pi^2 + 1}{1 + c_{1,1}}, \quad \tau_2 = \sqrt{(k^2\pi^2 + 1)\frac{1 + c_{1,2}}{1 + c_{1,1}} - k^2\pi^2 - 1} \neq 0.$$

This case occurs only if $c_{1,1} < c_{1,2}$.

As in case E1 the smoothness conditions on v imply the existence of some $j \in \mathbb{N}$ such that

$$\sqrt{(k^2\pi^2 + 1)\frac{1 + c_{1,2}}{1 + c_{1,1}} - k^2\pi^2 - 1} = \frac{j\pi}{\delta - s}$$

and we can check for given k (k small since only $\lambda < C_L$ is of interest to us) whether this can be satisfied.

Case E5: (i)(c) and (ii)(c), which is not possible since $c_{1,1} \neq c_{1,2}$.

Remark 7. In the actual computations for eigenvalue bounds we did not work with the approximate solution $\omega_t = \sum_{i=1}^4 \tilde{a}_i w_i + \tilde{v}_i$ ($w_i = \lambda_i \gamma_i$ and $\tilde{v}_i \in V_N$) but with the Finite Element interpolation $\breve{\omega}_t^{(2)} = I_{V_{\tilde{N}}}(\omega_t)$ where $\tilde{N} < N$ (i.e. $V_{\tilde{N}}$ is coarser than the Finite Element space V_N). This avoids complicated integration during the homotopies and saves computation time. Eventually we obtain a bound for the inverse of the linearization at $\breve{\omega}_t^{(2)}$, which can then be used to compute the corresponding bound for L_{ω_t} by Lemma 1 (b) (see also appendix A.4 for some details).

6.3   Lower Bound for the First Eigenvalue of the Laplacian

For the computation of embedding constants for the embeddings $H_0^1(\Omega_t) \hookrightarrow L^p(\Omega_t)$, $p > 2$, via Lemma 2 we need a lower bound for the first eigenvalue of the Laplacian on Ω_t (with homogeneous Dirichlet boundary conditions). Such a bound can be obtained using a domain decomposition method. We first divide the domain into 8 subdomains, where the subdomains marked with A are congruent to $(0, 1) \times (0, 1)$ and the ones marked with B are congruent to $(0, 2t) \times (0, 1)$. We use

	1	2t	
1	A	B	A
2t	B		B
	A	B	A

a domain decomposition ansatz to compute a lower bound of the first eigenvalue of the Dirichlet-Laplacian on Ω. We first compute the eigenvalues in the subdomains A and B with zero Dirichlet boundary conditions on $\partial\Omega$ and zero Neumann boundary conditions on $\partial A \cap \partial B$.

A) Let $\Omega_A := (0,1)^2$. The eigenvalue problem is given by: Find eigenpairs (λ_A, u) such that

$$\begin{cases} -\Delta u = \lambda_A u & \text{in} \quad \Omega_A \\ u(0,y) = u(x,1) = 0 & \text{for all} \quad x, y \in [0,1] \\ \frac{\partial u}{\partial x}(1,y) = \frac{\partial u}{\partial y}(x,0) = 0 & \text{for all} \quad x, y \in [0,1]. \end{cases}$$

A separation ansatz $u(x,y) = v(x)w(y)$ leads to the following eigenvalues:

$$\lambda_A = \frac{(\pi + 2l\pi)^2 + (\pi + 2k\pi)^2}{4}, \quad l, k \in \mathbb{N}_0.$$

B) Let $\Omega_B = (0, 2t) \times (0,1)$. Now we have to solve the eigenvalue problem: Find (λ_B, u) such that

$$\begin{cases} -\Delta u = \lambda_B u & \text{in} \quad \Omega_B \\ u(x,0) = u(x,1) = 0 & \text{for all} \quad x \in [0, 2t] \\ \frac{\partial u}{\partial x}(0,y) = \frac{\partial u}{\partial x}(2t,y) = 0 & \text{for all} \quad y \in [0,1]. \end{cases}$$

Again, by separation of variables we obtain

$$\lambda_B = k^2\pi^2 + \frac{l^2\pi^2}{4t^2}, \quad k \in \mathbb{N}, l \in \mathbb{N}_0.$$

The smallest eigenvalues in the union of all λ_A and λ_B are $\frac{\pi^2}{2}$ (smallest eigenvalue in A) and π^2 (smallest eigenvalue in B). Thus (by domain decomposition), a lower bound for the 5-th eigenvalue in of $-\Delta$ in Ω is given by $\pi^2 - \frac{1}{10}$. This lower bound is independent of t and can be used to compute a lower bound for the first eigenvalue of $-\Delta$ via the Lehmann-Goerisch method. We denote the final bound by $\underline{\lambda}$.

For some selected values of t we display $\underline{\lambda}$, as well as upper bounds $\overline{\lambda}$, which we computed using the Rayleigh-Ritz method. The eigenvalue bounds have been computed on a rather coarse mesh, resulting in low computation time but still sufficiently tight bounds.

t	$\underline{\lambda}$	$\overline{\lambda}$
0.384765625	8.441616	8.461986
0.501953125	8.588606	8.610882
0.765625	8.795805	8.822743
1	8.903686	8.934723
1.5	9.024702	9.063226
2	9.077287	9.121176
2.5	9.100550	9.147982
3	9.110544	9.160245

Table 6.1: Lower bound for the smallest eigenvalue of the Dirichlet Laplacian on Ω_t

6.4   Verified Results for some Discrete Values of t

We choose the grid $\frac{257}{512} = t_0 < t_1 < \ldots < t_{17} = 1 < t_{18} < \ldots < t_{49} = 3$, where the grid points $t_0, \ldots, t_{17}$ and $t_{17}, \ldots, t_{49}$ are equally spaced with $d_1 = \frac{15}{512}$ and $d_2 = \frac{1}{16}$, respectively. By this choice all nodes in the Finite Element grid are machine numbers and thus exactly representable by the computer. In case of the fourpeakcorner solution we also present some verified results for parameter values $t \leq t_0$, thereby showing that our method is not limited to the chosen grid.

In the first part of the section we show results of our computations for the different solution types. The second part is concerned with proving multiplicity of solutions for a fixed value of t.

6.4.1   Existence of solutions

In the following we summarize our verified results for:

  (i) bounds for the smallest eigenvalues of (5.6), (5.7) (with ω_t replaced by $\breve{\omega}_t^{(2)}$, see Remark 7), i.e. an upper bound for the largest eigenvalue below 1 and a lower bound for the smallest eigenvalue above 1,

 (ii) a bound for the inverse of the linearization at ω_t satisfying

$$\|v\|_{H_0^1} \leq K_t \|L_{\omega_t}[v]\|_{H^{-1}} \quad \text{for all } v \in H_0^1(\Omega_t, \text{sym}),$$

        where $H_0^1(\Omega_t, \text{sym})$ denotes the space of all functions having the same symmetry as the approximate solution ω_t,

(iii) an upper bound for the defect-norm of ω_t,

 (iv) a constant α_t satisfying (2.7) and (2.8), if existent.

The existence of some α_t in (iv) and the final check $\|\omega_t\|_{H_0^1} > \alpha_t$ proves the existence of an exact non-trivial solution $u_t \in H_0^1(\Omega_t, \text{sym})$ to problem (1.2) such that $\|u_t - \omega_t\|_{H_0^1} < \alpha_t$.

Here we will display the results for selected values of t only. Complete lists containing the results for all grid values can be found in Appendix A.1.

Fourpeakcorner

As already mentioned we extended our grid by some t-values smaller than t_0. In case we could not find a value $\alpha_t > 0$ satisfying (2.7), we note also the value of $\max \psi$ with ψ defined as in Remark 2 (a). Note that all values are rounded (downwards if the value constitutes a lower bound and upwards otherwise).

(1) $t = \frac{197}{512}$ (2) $t = 1$ (3) $t = 3$
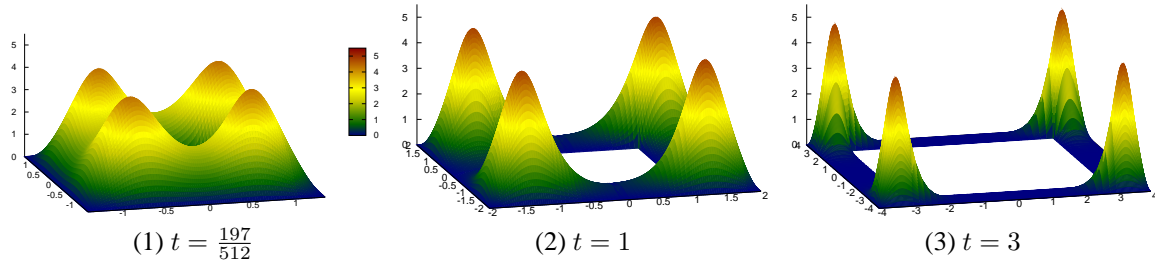
Figure 6.7: Approximate solution "fourpeakcorner" for different values of t

t	$\overline{\kappa}_1$	$\underline{\kappa}_2$	K_t	δ_t	α_t	$\max \psi$
0.208984375	0.35886	1.46450	3.15489	0.0257979	-	0.0206708
0.267578125	0.35837	1.29394	4.40575	0.0162102	-	0.0104117
0.326171875	0.35759	1.23600	5.24225	0.0112234	-	0.0072413
0.35546875	0.35700	1.25520	4.92280	0.0095729	-	0.0081590
0.384765625	0.35637	1.28913	4.46259	0.0083061	0.0529693	-
0.4140625	0.35579	1.32103	4.11833	0.0733333	0.0376470	-
0.47265625	0.35485	1.35813	3.79517	0.0059516	0.0258406	-
0.53125	0.35419	1.36966	3.70819	0.0049660	0.0204041	-
0.6484375	0.35340	1.37157	3.69441	0.0035973	0.0142616	-
0.765625	0.35302	1.36993	3.70615	0.0029272	0.0114808	-
0.8828125	0.35282	1.36847	3.71728	0.0027233	0.0106701	-
1	0.35272	1.36782	3.72185	0.0026960	0.0105702	-
1.25	0.35264	1.36723	3.72630	0.0027001	0.0105984	-
1.5	0.35262	1.36710	3.72704	0.0026982	0.0105912	-
1.75	0.35262	1.36706	3.72779	0.0026960	0.0105832	-
2	0.35262	1.36704	3.72778	0.0026943	0.0105754	-
2.25	0.35262	1.36703	3.72778	0.0026932	0.0105702	-
2.5	0.35262	1.36703	3.72778	0.0026925	0.0105670	-
2.75	0.35262	1.36703	3.72778	0.0026922	0.0105653	-
3	0.35262	1.36702	3.72779	0.0026920	0.0105647	-

From the table we can read that the defect bound δ_t becomes larger as t decreases. This is due to the fact that the cut-off functions λ_i, which are defined in (4.5), have support in $\{(x, y) \in \mathbb{R}^2 : |\zeta_i - x| < t$ and $|\eta_i - y| < t\} \cap \overline{\Omega}_t$ (where $\xi_i = (\zeta_i, \eta_i)$ denotes a re-entrant corner of Ω_t) and satisfy $\lambda_i(\xi_i) = 1$. Therefore the cut-off functions become steeper as t decreases and since $\nabla \lambda_i$ and $\Delta \lambda_i$ enter the defect computation this has direct influence of the value δ_t.

Fourpeakedge

Our approximate bifurcation diagrams indicate that the fourpeakedge solution lies on a branch which has a turning point close to $t = 0.5$. Indeed our verified results show that close to this parameter value the bound for the inverse of the linearization at the approximate solution increases rapidly. However, we did not prove that a turning point exists in some neighbourhood of $t = 0.5$.

(1) $t = \frac{272}{512}$ (2) $t = 1$ (3) $t = 3$
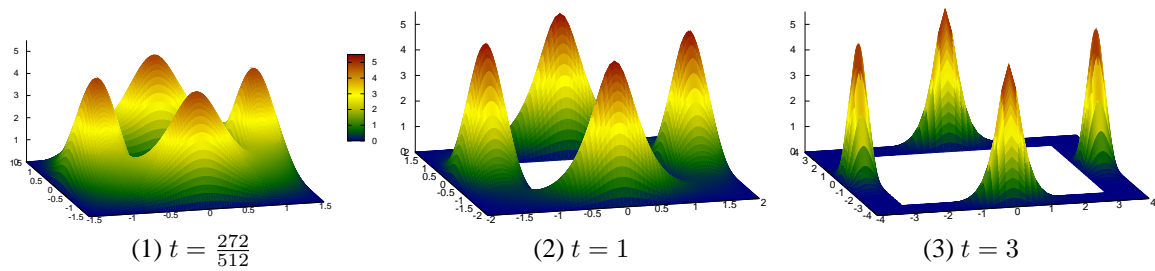
Figure 6.8: Approximate solution "fourpeakedge" for different values of t

t	$\overline{\kappa}_1$	$\underline{\kappa}_2$	K_t	δ_t	α_t	$\max \psi$
0.501953125	0.35423	1.06716	15.97879	0.0041423	-	0.0007329
0.53125	0.35286	1.24676	5.05846	0.0034592	0.0203114	-
0.6484375	0.35077	1.56669	2.76567	0.0026737	0.0076181	-
0.765625	0.34994	1.54170	2.84700	0.0027014	0.0079404	-
0.8828125	0.34954	1.52943	2.88992	0.0028066	0.0083929	-
1	0.34935	1.52380	2.91018	0.0029412	0.0088759	-
1.25	0.34920	1.51987	2.92472	0.0027142	0.0082100	-
1.5	0.34916	1.51908	2.92764	0.0026696	0.0080783	-
1.75	0.34915	1.51897	2.92804	0.0027713	0.0083975	-
2	0.34915	1.51888	2.92858	0.0030319	0.0092189	-
2.25	0.34915	1.51885	2.92901	0.0035123	0.0107472	-
2.5	0.34915	1.51865	2.93055	0.0042391	0.0131032	-
2.75	0.34915	1.51878	2.93136	0.0052125	0.0163329	-
3	0.34915	1.51868	2.93337	0.0064216	0.0204903	-

Onepeakcorner

We display only results for grid values smaller than or equal to 1.5. In chapter 9 we will show that a solution of onepeakcorner-type exists for all parameter values $t \geq 1.5$.

(1) $t = \frac{257}{512}$ (2) $t = 1$ (3) $t = 3$
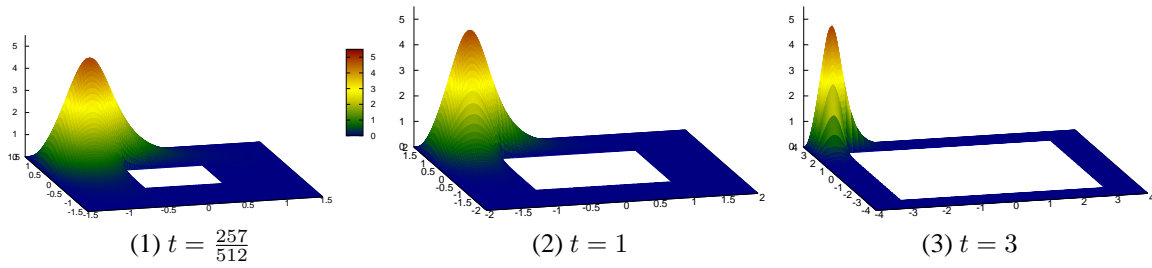
Figure 6.9: Approximate solution "onepeakcorner" for different values of t

t	$\overline{\kappa}_1$	$\underline{\kappa}_2$	K_t	δ_t	α_t
0.501953125	0.35262	1.36707	3.72550	0.0047839	0.0190828
0.53125	0.35262	1.36705	3.72560	0.0041881	0.0165515
0.6484375	0.35262	1.36698	3.72600	0.0025596	0.0098762
0.765625	0.35262	1.36722	3.72418	0.0017697	0.0067501
0.8828125	0.35262	1.36712	3.72493	0.0014677	0.0055765
1	0.35262	1.36702	3.72570	0.0013807	0.0052407
1.125	0.35262	1.36702	3.72571	0.0013593	0.0051577
1.25	0.35262	1.36702	3.72571	0.0013531	0.0051335
1.375	0.35262	1.36702	3.72571	0.0013509	0.0051248
1.5	0.35262	1.36702	3.72571	0.0013498	0.0051205

Onepeakedge

(1) $t = \frac{257}{512}$ (2) $t = 1$ (3) $t = 3$
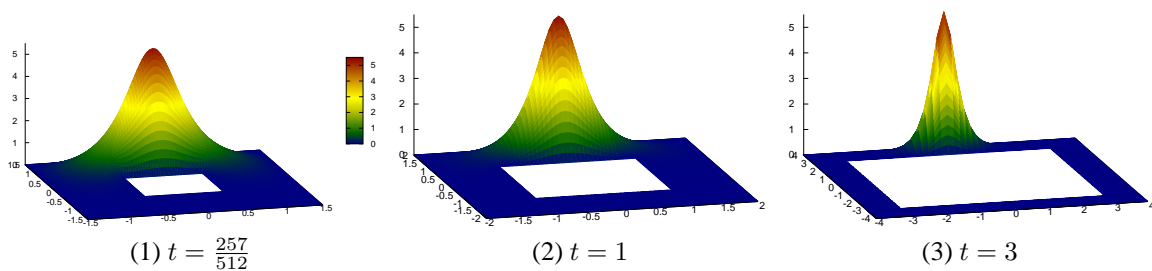
Figure 6.10: Approximate solution "onepeakedge" for different values of t

t	$\overline{\kappa}_1$	$\underline{\kappa}_2$	K_t	δ_t	α_t
0.501953125	0.34980	1.53720	2.86448	0.0021935	0.0064033
0.53125	0.34971	1.53469	2.87327	0.0020107	0.0058791
0.6484375	0.34945	1.52717	2.89999	0.0017023	0.0050115
0.765625	0.34931	1.52278	2.91576	0.0016161	0.0047805
0.8828125	0.34923	1.52089	2.92242	0.0015804	0.0046844

1	0.34919	1.51976	2.92628	0.0015857	0.0047065
1.25	0.34916	1.51905	2.92709	0.0013685	0.0040551
1.5	0.34915	1.51881	2.92786	0.0013392	0.0039682
1.75	0.34915	1.51893	2.92738	0.0013875	0.0041123
2	0.34915	1.51887	2.92765	0.0015168	0.0045007
2.25	0.34915	1.51885	2.92787	0.0017565	0.0052229
2.5	0.34915	1.51864	2.92893	0.0021197	0.0063246
2.75	0.34915	1.51830	2.93062	0.0026063	0.0078136
3	0.34915	1.51871	2.92966	0.0032109	0.0096732

Twopeakoppcorner

Again we display only results for grid values smaller than or equal to 1.5. The method in chapter 9 will prove that a solution of twopeakoppcorner-type exists for all parameter values $t \geq 1.5$.

(1) $t = \frac{257}{512}$ (2) $t = 1$ (3) $t = 3$
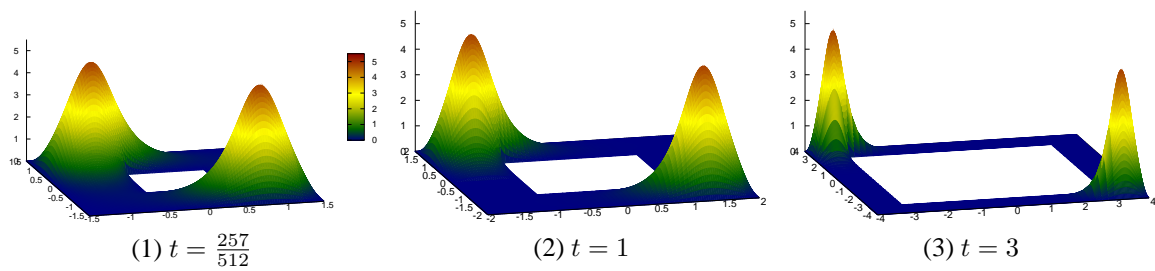
Figure 6.11: Approximate solution "twopeakoppcorner" for different values of t

t	$\overline{\kappa}_1$	$\underline{\kappa}_2$	K_t	δ_t	α_t
0.501953125	0.35264	1.36689	3.72722	0.0160981	0.1054400
0.53125	0.35264	1.36688	3.72730	0.0135297	0.0709231
0.6484375	0.35262	1.36677	3.72819	0.0069463	0.0294037
0.765625	0.35262	1.36713	3.72569	0.0039136	0.0155638
0.8828125	0.35262	1.36686	3.72803	0.0026440	0.0102880
1	0.35262	1.36699	3.72758	0.0022034	0.0085089
1.125	0.35262	1.36702	3.72571	0.0013825	0.0052473
1.25	0.35262	1.36702	3.72571	0.0013596	0.0051589
1.375	0.35262	1.36702	3.72571	0.0013526	0.0051316
1.5	0.35262	1.36702	3.72571	0.0013502	0.0051223

Twopeakoppedge

(1) $t = \frac{257}{512}$ (2) $t = 1$ (3) $t = 3$
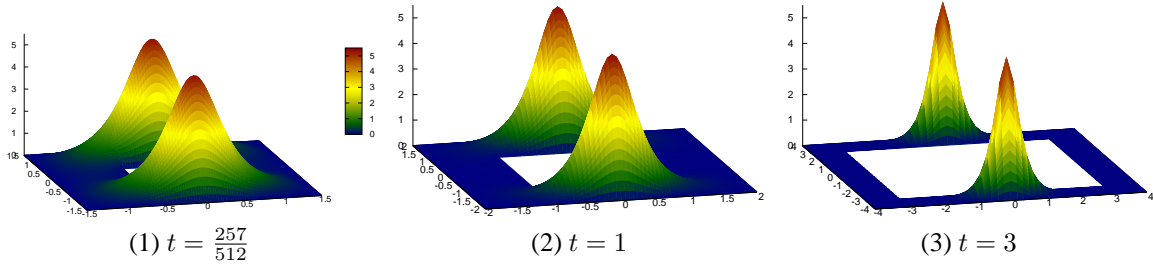
Figure 6.12: Approximate solution "twopeakoppedge" for different values of t

t	$\overline{\kappa}_1$	$\underline{\kappa}_2$	K_t	δ_t	α_t
0.501953125	0.34983	1.53786	2.86108	0.0025267	0.0074174
0.53125	0.34973	1.53514	2.87054	0.0023319	0.0068555
0.6484375	0.34945	1.52728	2.89834	0.0020558	0.0060872
0.765625	0.34931	1.52281	2.91444	0.0020373	0.0060655
0.8828125	0.34923	1.52090	2.92130	0.0020653	0.0061653
1	0.34919	1.51976	2.92536	0.0021303	0.0063725
1.25	0.34916	1.51905	2.92709	0.0013685	0.0040551
1.5	0.34915	1.51881	2.92786	0.0013392	0.0039682
1.75	0.34915	1.51893	2.92738	0.0013875	0.0041123
2	0.34915	1.51887	2.92765	0.0015168	0.0045007
2.25	0.34915	1.51885	2.92787	0.0017565	0.0052229
2.5	0.34915	1.51864	2.92893	0.0021197	0.0063246
2.75	0.34915	1.51830	2.93062	0.0026063	0.0078136
3	0.34915	1.51871	2.92966	0.0032109	0.0096732

6.4.2 Multiplicity

In order to prove that for some fixed value of t two exact solutions $u_t^{(1)}$ and $u_t^{(2)}$ do not coincide it is sufficient to prove

$$\|u_t^{(1)} - u_t^{(2)}\|_{H_0^1} > 0.$$

Suppose that we know approximate solutions $\omega_t^{(1)}, \omega_t^{(2)} \in H_0^1(\Omega_t)$ as well as constants $\alpha_t^{(1)}, \alpha_t^{(2)} > 0$ such that

$$\|u_t^{(1)} - \omega_t^{(1)}\|_{H_0^1} \leq \alpha_t^{(1)} \quad \text{and} \quad \|u_t^{(2)} - \omega_t^{(2)}\|_{H_0^1} \leq \alpha_t^{(2)}.$$

Using reverse triangle inequality we can estimate

$$\begin{aligned}
\|u_t^{(1)} - u_t^{(2)}\|_{H_0^1} &\geq \|\omega_t^{(1)} - \omega_t^{(2)}\|_{H_0^1} - \|u_t^{(1)} - \omega_t^{(1)}\|_{H_0^1} - \|u_t^{(2)} - \omega_t^{(2)}\|_{H_0^1} \\
&\geq \|\omega_t^{(1)} - \omega_t^{(2)}\|_{L^2} - \alpha_t^{(1)} - \alpha_t^{(2)} \\
&\geq \|I_{V_N}(\omega_t^{(1)}) - I_{V_N}(\omega_t^{(2)})\|_{L^2} - \|\omega_t^{(1)} - I_{V_N}(\omega_t^{(1)})\|_{L^2} - \|\omega_t^{(2)} - I_{V_N}(\omega_t^{(2)})\|_{L^2} \\
&\quad - \alpha_t^{(1)} - \alpha_t^{(2)}.
\end{aligned}$$

Since $I_{V_N}(\omega_t^{(1)})$ and $I_{V_N}(\omega_t^{(2)})$ are Finite Element functions, the L^2-norms of the first term can easily be enclosed using a quadrature rule of sufficiently high degree, applied elementwise. Upper bounds for the remaining norms have already been computed during the defect computations and thus a multiplicity check does not require a lot of additional effort.

A successful multiplicity check finally proves

Theorem 5. *(a) For all $t \in \left\{ \frac{197}{512} + i\frac{15}{512} : i = 0, 1, 2, 3 \right\}$ there exists at least one non-trivial solution to problem* (1.2) *(type fourpeakcorner).*

(b) For $t = \frac{257}{512}$ there exist at least five non-trivial solutions to problem (1.2) *(types fourpeakcorner, onepeakcorner, onepeakedge, twopeakoppcorner and twopeakoppedge).*

(c) For $t \in \left\{ \frac{272}{512} + i\frac{15}{512} : i = 0, \ldots, 16 \right\} \cup \left\{ 1 + \frac{i}{16} : i = 1, \ldots, 8 \right\}$ there exist at least six non-trivial solutions to problem (1.2).

(d) For $t \in \left\{ 1.5 + \frac{i}{16} : i = 1, \ldots, 24 \right\}$ there exist at least four non-trivial solutions to problem (1.2) *(types fourpeakcorner, fourpeakedge, onepeakedge, twopeakoppedge).*

7 Verification of Solution Branches

Suppose now, that for two approximate solutions $\omega_{t_1} \in H_0^1(\Omega_{t_1})$ and $\omega_{t_2} \in H_0^1(\Omega_{t_2})$ to problem (1.2) (with $t = t_1$ and $t = t_2$, respectively) which are close, i.e. $t_2 - t_1$ is small and and both solutions are of the same type (fourpeakcorner, onepeakcorner, etc.), we have proved the existence of two exact solutions $u_{t_1} \in H_0^1(\Omega_{t_1})$ and $u_{t_2} \in H_0^1(\Omega_{t_2})$ in some neighbourhood of ω_{t_1} and ω_{t_2}, respectively. In this chapter we will introduce a method to prove the existence of solutions $u_t \in H_0^1(\Omega_t)$ for all $t \in [t_1, t_2]$, and to show that $(u_t)_{t \in (t_1, t_2)}$ is a smooth branch, with a suitable notion of continuity to be defined. The main idea is to transform the approximate solutions ω_{t_1} and ω_{t_2} to a fixed reference domain and to define (transformed) approximate solutions for $t \in [t_1, t_2]$ by linear interpolation of the transformed approximations.

In our given problem the parameter t occurs in the domain and the equation is not depending on the parameter. For the opposite case, i.e. a parameter-dependent equation on a fixed domain, we refer to [57], where computer-assisted existence and enclosure results for semilinear elliptic problems (with parameter-dependent equation) are presented. A further application of this method is also given in [50]. However, the basic ideas of [57] can be transferred also to our problem.

7.1 Construction of Branches

We start with a grid $t_0 < t_1 < \ldots < t_i < t_{i+1} < \ldots < t_n$ and suppose that for each t_i, $i \in \{0, \ldots n\}$, we have computed an approximate solution $\omega_{t_i} \in H_0^1(\Omega_{t_i})$ to problem (1.2) (with $t = t_i$) as well as constants δ_{t_i} and K_{t_i} such that

(i) $\left\| -\Delta \omega_{t_i} - |\omega_{t_i}|^3 \right\|_{H^{-1}(\Omega_{t_i})} \leq \delta_{t_i}$,

(ii) $\|v\|_{H_0^1(\Omega_{t_i})} \leq K_{t_i} \left\| L_{\omega_{t_i}}[v] \right\|_{H^{-1}(\Omega_{t_i})}$ for all $v \in H_0^1(\Omega_{t_i})$.

It will be convention, that when speaking of a grid of functions, we always consider functions of the same type, e.g. approximate solutions with full symmetry of the domain and a bump in each corner, or approximate solutions with only one bump in the upper left corner etc.

We furthermore assume that, by using Theorem 1, we have proved that there exists a number $\alpha_{t_i} > 0$ and a solution $u_{t_i} \in H_0^1(\Omega_{t_i})$ satisfying

$$\|u_{t_i} - \omega_{t_i}\|_{H_0^1(\Omega_{t_i})} \leq \alpha_{t_i}$$

for all $i \in \{0, \ldots, n\}$.

Let now $i \in \{1, \ldots, n\}$ be fixed and $t \in [t_{i-1}, t_{i+1}]$. We assume that $\phi_t^{(i)}$ is a Lipschitz continuous function mapping the domain Ω_{t_i} onto Ω_t and satisfying $(\phi_t^{(i)})^{-1} \in C^{0,1}(\Omega_t, \Omega_{t_i})$, i.e. $\phi_t^{(i)}$ is a Lipschitz homeomorphism. Furthermore we assume $\phi_{t_i}^{(i)} = Id$. By [31, Problem 7.5], $w_t \circ \phi_t^{(i)} \in H_0^1(\Omega_{t_i})$ for all $w_t \in H_0^1(\Omega_t)$ and $w_{t_i} \circ (\phi_t^{(i)})^{-1} \in H_0^1(\Omega_t)$ for all $w_{t_i} \in H_0^1(\Omega_{t_i})$. It follows, that

$$\Theta_t^{(i)} : \begin{cases} H_0^1(\Omega_t) & \to & H_0^1(\Omega_{t_i}) \\ w_t & \mapsto & w_t \circ \phi_t^{(i)} \end{cases} \tag{7.1}$$

is bijective. In the following we denote variables in Ω_{t_i} by $(\tilde{x}, \tilde{y})$ and variables in Ω_t by (x, y), and using moreover the notation

$$\tilde{w}_t(\tilde{x}, \tilde{y}) := w_t(\phi_t^{(i)}(\tilde{x}, \tilde{y})), \qquad (\tilde{x}, \tilde{y}) \in \Omega_{t_i},$$

for $w_t \in H_0^1(\Omega_t)$, we obtain

$$w_t(x, y) = \tilde{w}_t((\phi_t^{(i)})^{-1}(x, y)), \quad (x, y) \in \Omega_t$$
$$(\nabla w_t(x, y))^T = (\nabla \tilde{w}_t)((\phi_t^{(i)})^{-1}(x, y))^T J[\phi_t^{-1}](x, y)$$

(where J denotes the Jacobian matrix).

Definition of interpolating approximations ω_t

For $t \in (t_{i-1}, t_i]$ we define $\tilde{\omega}_t$ by linear interpolation of $\tilde{\omega}_{t_{i-1}} = \omega_{t_{i-1}} \circ \phi_{t_{i-1}}^{(i)}$ and $\tilde{\omega}_{t_i} = \omega_{t_i} \circ \phi_{t_i}^{(i)} = \omega_{t_i}$:

$$\tilde{\omega}_t = \frac{t_i - t}{t_i - t_{i-1}} \tilde{\omega}_{t_{i-1}} + \frac{t - t_{i-1}}{t_i - t_{i-1}} \tilde{\omega}_{t_i} \tag{7.2}$$

Finally, $\omega_t \in H_0^1(\Omega_t)$ is given by

$$\omega_t := \tilde{\omega}_t \circ (\phi_t^{(i)})^{-1} \tag{7.3}$$

and will serve as approximate solution to problem (1.2).

Remark 8. In the following sections we will usually consider $t \in (t_{i-1}, t_i]$ for some fixed $i \in \{0, \dots, n\}$ and thus in most cases the transformation $\phi_t^{(i)}$ is used. If no confusion can arise we will often omit the superscript (i) in the notion of $\phi_t^{(i)}$ and write only ϕ_t. However, also in case of this shortened notation we always assume that $\phi_t : \Omega_{t_i} \to \Omega_t$.

7.1.1 Defect computation

As before let $i \in \{1, \dots, n\}$ be fixed. Our aim is to compute a uniform bound $\delta^{(i)}$ such that

$$\| - \Delta \omega_t - |\omega_t|^3 \|_{H^{-1}(\Omega_t)} \leq \delta^{(i)} \quad \text{for all } t \in (t_{i-1}, t_i],$$

where $\omega_t \in H_0^1(\Omega_t)$ is the approximate solution of (1.2) given by (7.2), (7.3). In contrast to the procedure for the defect computation for fixed t in section 4.1, where we estimated the H^{-1}-norm of the defect by the sum of two L^2-norms, we will now work with the usual sup-formulation of the H^{-1}-norm. In the following we will use the notation $f(\omega_t) := |\omega_t|^3$.

For $\varphi \in H_0^1(\Omega_t)$ we have, denoting $\tilde{\varphi} := \varphi \circ \phi_t$,

$$(-\Delta \omega_t - f(\omega_t))[\varphi] = \int_{\Omega_t} [\nabla \omega_t \cdot \nabla \varphi - f(\omega_t)\varphi] \, d(x, y)$$

$$\overset{(x,y)=\phi_t(\tilde{x},\tilde{y})}{=} \int_{\Omega_{t_i}} |\det J[\phi_t]| \Big(\left[(\nabla \tilde{\omega}_t)(\tilde{x}, \tilde{y})^T \left(J[\phi_t^{-1}] \circ \phi_t \right)(\tilde{x}, \tilde{y}) \right] \cdot$$

$$\left[(\nabla \tilde{\varphi})(\tilde{x}, \tilde{y})^T \left(J[\phi_t^{-1}] \circ \phi_t \right)(\tilde{x}, \tilde{y}) \right] - f(\tilde{\omega}_t(\tilde{x}, \tilde{y}))\tilde{\varphi}(\tilde{x}, \tilde{y}) \Big) \, d(\tilde{x}, \tilde{y})$$

$$= \int_{\Omega_{t_i}} |\det J[\phi_t]| \Big((\nabla \tilde{\omega}_t)^T J[\phi_t]^{-1} J[\phi_t]^{-T} \nabla \tilde{\varphi} - f(\tilde{\omega}_t)\tilde{\varphi} \Big) \, d(\tilde{x}, \tilde{y}).$$

Assume now that functions $\gamma_i^{(1)}, \gamma_i^{(2)} \in L^2(\Omega_{t_i})$ are at hand such that for all $t \in [t_{i-1}, t_i]$

$$\left| \frac{d^2}{dt^2} \left[|\det J[\phi_t]| (\nabla \tilde{\omega}_t)^T J[\phi_t]^{-1} J[\phi_t]^{-T} \right] \right| \leq \gamma_i^{(1)} \tag{7.4}$$

$$\left| \frac{d^2}{dt^2} \left[|\det J[\phi_t]| f(\tilde{\omega}_t) \right] \right| \leq \gamma_i^{(2)}. \tag{7.5}$$

Then by the usual interpolation error estimate for linear interpolation we obtain for $t \in [t_{i-1}, t_i]$ and $\varphi_i \in H_0^1(\Omega_{t_i})$:

$$\left| \int_{\Omega_{t_i}} |\det J[\phi_t]| \left[(\nabla \tilde{\omega}_t)^T J[\phi_t]^{-1} J[\phi_t]^{-T} \nabla \varphi_i - f(\tilde{\omega}_t) \varphi_i \right] d(\tilde{x}, \tilde{y}) \right.$$

$$- \frac{t_i - t}{t_i - t_{i-1}} \int_{\Omega_{t_i}} |\det J[\phi_{t_{i-1}}]| \left[(\nabla \tilde{\omega}_{t_{i-1}})^T J[\phi_{t_{i-1}}]^{-1} J[\phi_{t_{i-1}}]^{-T} \nabla \varphi_i - f(\tilde{\omega}_{t_{i-1}}) \varphi_i \right] d(\tilde{x}, \tilde{y})$$

$$\left. - \frac{t - t_{i-1}}{t_i - t_{i-1}} \int_{\Omega_{t_i}} |\det J[\phi_{t_i}]| \left[(\nabla \tilde{\omega}_{t_i})^T J[\phi_{t_i}]^{-1} J[\phi_{t_i}]^{-T} \nabla \varphi_i - f(\tilde{\omega}_{t_i}) \varphi_i \right] d(\tilde{x}, \tilde{y}) \right|$$

$$\leq \left[\int_{\Omega_{t_i}} \gamma_i^{(1)} |\nabla \varphi_i| \, d(\tilde{x}, \tilde{y}) + \int_{\Omega_{t_i}} \gamma_i^{(2)} |\varphi_i| \, d(\tilde{x}, \tilde{y}) \right] \frac{(t_i - t_{i-1})^2}{8}. \tag{7.6}$$

Before we start to consider the right-hand-side of (7.6), we will comment on the transformation that will be used during the process. We have already mentioned that ϕ_t has to be Lipschitz continuous (ensuring that Θ_t maps $H_0^1(\Omega_t)$ onto $H_0^1(\Omega_{t_i})$). In addition, we will construct ϕ_t such that it is piecewise linear and the linear mappings are compositions of dilations and translations, i.e. such that

$$\phi_t(\tilde{x}, \tilde{y}) = \sum_{j=1}^{k} \phi_t^j(\tilde{x}, \tilde{y}) \chi_{\Omega_{t_i}^j}(\tilde{x}, \tilde{y}) \tag{7.7}$$

with

$$\phi_t^j(\tilde{x}, \tilde{y}) = \begin{pmatrix} a_j(t) & 0 \\ 0 & b_j(t) \end{pmatrix} \begin{pmatrix} \tilde{x} \\ \tilde{y} \end{pmatrix} + \begin{pmatrix} c_j^{(1)}(t) \\ c_j^{(2)}(t) \end{pmatrix} \tag{7.8}$$

and $\Omega_{t_i}^j \subset \Omega_{t_i}$ satisfying

$$\Omega_{t_i}^j \cap \Omega_{t_i}^l = \emptyset \text{ for } j \neq l \quad \text{and} \quad \Omega_{t_i} = \text{int} \left(\bigcup_{j=1}^{k} \overline{\Omega_{t_i}^j} \right).$$

The coefficients $a_j, b_j, c_j^{(1)}, c_j^{(2)}$ have to be acoordingly to guarantee Lipschitz continuity and the required mapping properties of ϕ_t. Moreover we assume $t \mapsto a_j(t)$, $t \mapsto b_j(t)$, and $t \mapsto c_j^{(l)}(t)$, $l = 1, 2$, to be continuous in $[t_{i-1}, t_i]$ and $|a_j(t)|, |b_j(t)| > \delta > 0$ for all $t \in [t_{i-1}, t_i]$ (ensuring that ϕ_t^{-1} exists for all $t \in [t_{i-1}, t_i]$). To guarantee $\phi_{t_i} = Id$ we assume furthermore $a_j(t_i) = b_j(t_i) = 1$ and $c_j^{(l)}(t_i) = 0$, $l = 1, 2$. The actual choice of ϕ_t will be fixed in section 7.1.3.

(7.8) implies in particular: $|J[\phi_t^j] \xi| \leq \max\{|a_j(t)|, |b_j(t)|\} |\xi|$ for all $\xi \in \mathbb{R}^2$ and considering the

first summand on the right-hand-side of (7.6) we obtain

$$
\int_{\Omega_{t_i}} \gamma_i^{(1)} |\nabla \varphi_i| \, d(\tilde{x}, \tilde{y}) = \sum_{j=1}^{k} \int_{\Omega_{t_i}^j} \gamma_i^{(1)} \frac{\sqrt{|\det J[\phi_t^j]|}}{\sqrt{|\det J[\phi_t^j]|}} \left| J[\phi_t^j]^T J[\phi_t^j]^{-T} \nabla \varphi_i \right| \, d(\tilde{x}, \tilde{y})
$$

$$
\leq \left[\max_{j=1,\dots,k} \max_{t \in [t_{i-1}, t_i]} \left(\frac{\max\{|a_j(t)|, |b_j(t)|\}}{\sqrt{|\det J[\phi_t^j]|}} \right) \right] \sum_{j=1}^{k} \int_{\Omega_{t_i}^j} \gamma_i^{(1)} \sqrt{|\det J[\phi_t^j]|} \, |J[\phi_t^j]^{-T} \nabla \varphi_i| \, d(\tilde{x}, \tilde{y})
$$

$$
\leq \left[\max_{j=1,\dots,k} \max_{t \in [t_{i-1}, t_i]} \left(\frac{\max\{|a_j(t)|, |b_j(t)|\}}{\sqrt{|\det J[\phi_t^j]|}} \right) \right] \|\gamma_i^{(1)}\|_{L^2(\Omega_{t_i})} \left(\int_{\Omega_{t_i}} |\det J[\phi_t^j]| |J[\phi_t^j]^{-T} \nabla \varphi_i|^2 \, d(\tilde{x}, \tilde{y}) \right)^{\frac{1}{2}}
$$

$$
= \underbrace{\left[\max_{j=1,\dots,k} \max_{t \in [t_{i-1}, t_i]} \left(\frac{\max\{|a_j(t)|, |b_j(t)|\}}{\sqrt{|\det J[\phi_t^j]|}} \right) \right] \|\gamma_i^{(1)}\|_{L^2(\Omega_{t_i})}}_{=:C_{t_{i-1}t_i}^{(1)}} \|\nabla \varphi\|_{L^2(\Omega_t)},
$$

where $\varphi = \varphi_i \circ \phi_t^{-1} \in H_0^1(\Omega_t)$. In a similar way we can estimate the second summand on the right-hand side of (7.6):

$$
\int_{\Omega_{t_i}} \gamma_i^{(2)} |\varphi_i| \, d(\tilde{x}, \tilde{y}) = \sum_{j=1}^{k} \int_{\Omega_{t_i}^j} \frac{\sqrt{|\det J[\phi_t^j]|}}{\sqrt{|\det J[\phi_t^j]|}} \gamma_i^{(2)} |\varphi_i| \, d(\tilde{x}, \tilde{y})
$$

$$
\leq \underbrace{\left[\max_{j=1,\dots,k} \max_{t \in [t_{i-1}, t_i]} \frac{1}{\sqrt{|\det J[\phi_t^j]|}} \right] \|\gamma_i^{(2)}\|_{L^2(\Omega_{t_i})}}_{=:C_{t_{i-1}t_i}^{(2)}} \|\varphi\|_{L^2(\Omega_t)}.
$$

Putting these two estimates together yields

$$
\int_{\Omega_{t_i}} \gamma_i^{(1)} |\nabla \varphi_i| \, d(\tilde{x}, \tilde{y}) + \int_{\Omega_{t_i}} \gamma_i^{(2)} |\varphi_i| \, d(\tilde{x}, \tilde{y}) \leq \max \left\{ C_{t_{i-1}t_i}^{(1)}, C_{t_{i-1}t_i}^{(2)} \right\} \|\varphi\|_{H_0^1(\Omega_t)}.
$$

Thus the inequality in (7.6) leads to

$$
\frac{|(-\Delta \omega_t - f(\omega_t))[\varphi]|}{\|\varphi\|_{H_0^1(\Omega_t)}} \leq \max \left\{ C_{t_{i-1}t_i}^{(1)}, C_{t_{i-1}t_i}^{(2)} \right\} \frac{(t_i - t_{i-1})^2}{8} +
$$

$$
\frac{t_i - t}{t_i - t_{i-1}} \frac{|(-\Delta \omega_{t_{i-1}} - f(\omega_{t_{i-1}}))[\varphi_{i-1}]|}{\|\varphi\|_{H_0^1(\Omega_t)}} + \frac{t - t_{i-1}}{t_i - t_{i-1}} \frac{|(-\Delta \omega_{t_i} - f(\omega_{t_i}))[\varphi_i]|}{\|\varphi\|_{H_0^1(\Omega_t)}}, \quad (7.9)
$$

where $\varphi_{i-1} = \varphi \circ \phi_t \circ \phi_{t_{i-1}}^{-1} \in H_0^1(\Omega_{t_{i-1}})$ (note that by our convention $\phi_{t_{i-1}}^{-1} = (\phi_{t_{i-1}}^{(i)})^{-1}$). Therefore, with (x_1, y_1) denoting coordinates in $\Omega_{t_{i-1}}$, we have

$$
\|\varphi\|_{H_0^1(\Omega_t)}^2 = \int_{\Omega_t} \left[|\nabla \varphi|^2 + \varphi^2 \right] \, d(x, y)
$$

$$
= \int_{\Omega_{t_{i-1}}} |\det J[\phi_t] \circ \phi_{t_{i-1}}^{-1}| |\det J[\phi_{t_{i-1}}^{-1}]| \cdot
$$

$$
\left[\left| (J[\phi_t]^{-T} \circ \phi_{t_{i-1}}^{-1})(J[\phi_{t_{i-1}}]^T \circ \phi_{t_{i-1}}^{-1}) \nabla \varphi_{i-1} \right|^2 + \varphi_{i-1}^2 \right] \, d(x_1, y_1)
$$

$$\geq \underbrace{\left[\min_{j=1,\dots,k} \min_{t \in [t_{i-1},t_i]} \left(\min \left\{ \left| \frac{a_j(t_{i-1})}{a_j(t)} \right|^2, \left| \frac{b_j(t_{i-1})}{b_j(t)} \right|^2, 1 \right\} \frac{|a_j(t)b_j(t)|}{|a_j(t_{i-1})b_j(t_{i-1})|} \right) \right]}_{=: C^{(3)}_{t_{i-1} t_i}} \cdot$$

$$\int_{\Omega_{t_{i-1}}} \left[|\nabla \varphi_{i-1}|^2 + \varphi_{i-1}^2 \right] d(x_1, y_1)$$

$$= C^{(3)}_{t_{i-1} t_i} \|\varphi_{i-1}\|^2_{H^1_0(\Omega_{t_{i-1}})},$$

and moreover

$$\|\varphi\|^2_{H^1_0(\Omega_t)} = \int_{\Omega_{t_i}} |\det J[\phi_t]| \left[|J[\phi_t]^{-T} \nabla \varphi_i|^2 + \varphi_i^2 \right] d(\tilde{x}, \tilde{y})$$

$$\geq \underbrace{\left[\min_{j=1,\dots,k} \min_{t \in [t_{i-1},t_i]} \left(\min \left\{ \left| \frac{1}{a_j(t)} \right|^2, \left| \frac{1}{b_j(t)} \right|^2, 1 \right\} |a_j(t)b_j(t)| \right) \right]}_{=: C^{(4)}_{t_{i-1} t_i}} \int_{\Omega_{t_i}} \left[|\nabla \varphi_i|^2 + \varphi_i^2 \right] d(\tilde{x}, \tilde{y})$$

$$= C^{(4)}_{t_{i-1} t_i} \|\varphi_i\|^2_{H^1_0(\Omega_{t_i})}. \tag{7.10}$$

Plugging these two estimates into (7.9) and taking the supremum over all $\varphi \in H^1_0(\Omega)$ (which is, due to the mapping properties of Θ_t, equivalent to taking the supremum over all $\varphi_{i-1} \in H^1_0(\Omega_{t_{i-1}})$ or $\varphi_i \in H^1_0(\Omega_{t_i})$), we obtain

$$\| - \Delta \omega_t - f(\omega_t) \|_{H^{-1}(\Omega_t)} \leq \frac{(t_i - t_{i-1})^2}{8} \max \left\{ C^{(1)}_{t_{i-1} t_i}, C^{(2)}_{t_{i-1} t_i} \right\} +$$

$$\max \left\{ \frac{1}{\sqrt{C^{(3)}_{t_{i-1} t_i}}} \| - \Delta \omega_{t_{i-1}} - f(\omega_{t_{i-1}}) \|_{H^{-1}(\Omega_{t_{i-1}})}, \frac{1}{\sqrt{C^{(4)}_{t_{i-1} t_i}}} \| - \Delta \omega_{t_i} - f(\omega_{t_i}) \|_{H^{-1}(\Omega_{t_i})} \right\}$$

$$\leq \frac{(t_i - t_{i-1})^2}{8} \max \left\{ C^{(1)}_{t_{i-1} t_i}, C^{(2)}_{t_{i-1} t_i} \right\} + \max \left\{ \frac{\delta_{t_{i-1}}}{\sqrt{C^{(3)}_{t_{i-1} t_i}}}, \frac{\delta_{t_i}}{\sqrt{C^{(4)}_{t_{i-1} t_i}}} \right\}.$$

7.1.2 Bound for the inverse of the linearization

Let $i \in \{1, \dots, n\}$ be fixed and denote by I a given subinterval of $[t_{i-1}, t_i]$. Our goal is to compute constants K_I such that

$$\|v\|_{H^1_0(\Omega_t)} \leq K_I \|L_{\omega_t}[v]\|_{H^{-1}(\Omega_t)} \quad \text{for all } v \in H^1_0(\Omega_t) \text{ and for all } t \in I. \tag{7.11}$$

As before we will make strong use of the Transformation Theorem and in addition apply Poincaré's min-max principle.

Recall that by Lemma 3 in section 5.1 a constant K satisfying

$$\|v\|_{H^1_0(\Omega_t)} \leq K \|L_{\omega_t}[v]\|_{H^{-1}(\Omega_t)} \quad \text{for all } v \in H^1_0(\Omega_t) \quad \text{(for } t > 0 \text{ being fixed)}$$

exists if and only if

$$\gamma := \min\{|\nu| : \nu \text{ is in the spectrum of } \Phi^{-1} L_{\omega_t}\} > 0$$

and in the affirmative case one can choose any $K \geq \frac{1}{\gamma}$. The isometric isomorphism $\Phi : H^1_0(\Omega_t) \to H^{-1}(\Omega_t)$ has been introduced in (2.5).

We have already seen in section 5.1 that $\sigma_{\mathrm{ess}}\left(\Phi^{-1} L_{\omega_t}\right) = \{1\}$ and therefore it suffices to compute upper and lower bounds for the eigenvalues of $\Phi^{-1} L_{\omega_t}$ neighbouring 0. Equivalently to (5.5), which is the eigenvalue problem for $\Phi^{-1} L_{\omega_t}$, we consider the eigenvalue problem

$$
\int_{\Omega_t} (1 + 3|\omega_t|\omega_t)\, u\varphi\, d(x,y) = \eta \int_{\Omega_t} \left[\nabla u \cdot \nabla \varphi + u\varphi \right] d(x,y) \quad \text{for all } \varphi \in H_0^1(\Omega_t), \quad (7.12)
$$

and the transformation $\eta = 1 - \nu$ yields eigenvalues ν of $\Phi^{-1} L_{\omega_t}$.

Let now $t_{i-1/2} = \frac{1}{2}(t_{i-1} + t_i)$ and $I := \left[t_{i-1/2}, t_i \right]$. For $t \in I$ we denote by $\eta_1^{(t)} \geq \eta_2^{(t)} \geq \dots$ the eigenvalues of (7.12), ordered by magnitude and counted by multiplicity. By Poincaré's min-max-principle we have for all $m \in \mathbb{N}$ (note that in section 5.1 we have proved that there exists an infinite sequence of eigenvalues of (7.12) which converges to 0):

$$
\eta_m^{(t)} = \max_{\substack{U \subset H_0^1(\Omega_t) \\ \dim U = m}} \min_{u \in U} \frac{\int_{\Omega_t} (1 + 3|\omega_t|\omega_t)\, u^2\, d(x,y)}{\int_{\Omega_t} \left[|\nabla u|^2 + u^2 \right] d(x,y)}. \quad (7.13)
$$

Estimating the Rayleigh quotient, where we compute analogously as in (7.10) and use the notation $\tilde{u} = u \circ \phi_t,\ \tilde{\omega}_t = \omega_t \circ \phi_t$, yields for all $t \in I$

$$
\frac{\int_{\Omega_t} (1 + 3|\omega_t|\omega_t)\, u^2\, d(x,y)}{\int_{\Omega_t} \left[|\nabla u|^2 + u^2 \right] d(x,y)} = \frac{\int_{\Omega_{t_i}} |\det J[\phi_t]|\, (1 + 3|\tilde{\omega}_t|\tilde{\omega}_t)\, \tilde{u}^2\, d(\tilde{x},\tilde{y})}{\int_{\Omega_{t_i}} |\det J[\phi_t]|\, \left[|J[\phi_t]^{-T} \nabla \tilde{u}|^2 + \tilde{u}^2 \right] d(\tilde{x},\tilde{y})}
$$

$$
\begin{cases} \leq C_{t_{i-1/2} t_i}^{(1)} \dfrac{\int_{\Omega_{t_i}} (1 + 3|\tilde{\omega}_t|\tilde{\omega}_t)\tilde{u}^2\, d(\tilde{x},\tilde{y})}{\int_{\Omega_{t_i}} \left[|\nabla \tilde{u}|^2 + \tilde{u}^2 \right] d(\tilde{x},\tilde{y})} \\[3mm] \geq C_{t_{i-1/2} t_i}^{(2)} \dfrac{\int_{\Omega_{t_i}} (1 + 3|\tilde{\omega}_t|\tilde{\omega}_t)\tilde{u}^2\, d(\tilde{x},\tilde{y})}{\int_{\Omega_{t_i}} \left[|\nabla \tilde{u}|^2 + \tilde{u}^2 \right] d(\tilde{x},\tilde{y})}, \end{cases} \quad (7.14)
$$

where

$$
C_{t_{i-1/2} t_i}^{(1)} = \max_{t \in [t_{i-1/2}, t_i]} \left(\frac{\max\limits_{j=1,\dots,k} |a_j(t) b_j(t)|}{\min\limits_{j=1,\dots,k} \left(\min \left\{ \left| \frac{1}{a_j(t)} \right|^2, \left| \frac{1}{b_j(t)} \right|^2, 1 \right\} |a_j(t) b_j(t)| \right)} \right)
$$

$$
C_{t_{i-1/2} t_i}^{(2)} = \min_{t \in [t_{i-1/2}, t_i]} \left(\frac{\min\limits_{j=1,\dots,k} |a_j(t) b_j(t)|}{\max\limits_{j=1,\dots,k} \left(\max \left\{ \left| \frac{1}{a_j(t)} \right|^2, \left| \frac{1}{b_j(t)} \right|^2, 1 \right\} |a_j(t) b_j(t)| \right)} \right). \quad (7.15)
$$

For the numerators of the new Rayleighquotients on the right-hand-side of (7.14) we write

$$
\int_{\Omega_{t_i}} (1 + 3|\tilde{\omega}_t|\tilde{\omega}_t)\tilde{u}^2\, d(\tilde{x},\tilde{y}) = \int_{\Omega_{t_i}} 3\left[|\tilde{\omega}_t|\tilde{\omega}_t - |\omega_{t_i}|\omega_{t_i} \right] \tilde{u}^2\, d(\tilde{x},\tilde{y}) + \int_{\Omega_{t_i}} (1 + 3|\omega_{t_i}|\omega_{t_i})\tilde{u}^2\, d(\tilde{x},\tilde{y}).
$$
$$
(7.16)
$$

The modulus of the the first summand can be estimated as in the proof of Lemma 1(a), with $p_1, \dots, p_4 \in [2, \infty)$ such that $\frac{1}{p_1} + \frac{1}{p_2} + \frac{1}{p_3} + \frac{1}{p_4} = 1$ and denoting by C_{p_j} an embedding constant for the embedding $H_0^1(\Omega_{t_i}) \hookrightarrow L^{p_j}(\Omega_{t_i})$. Using moreover $\omega_{t_i} - \tilde{\omega}_t = \frac{t_i - t}{t_i - t_{i-1}}(\omega_{t_i} - \tilde{\omega}_{t_{i-1}})$ and

$t \in [t_{i-1/2}, t_i]$ we obtain

$$3\left| \int_{\Omega_{t_i}} \left[|\tilde{\omega}_t|\tilde{\omega}_t - |\omega_{t_i}|\omega_{t_i} \right] \tilde{u}^2 \, d(\tilde{x}, \tilde{y}) \right|$$

$$\leq 3C_{p3}C_{p4} \left(\|\omega_{t_i}\|_{L^{p_1}(\Omega_{t_i})} + \|\tilde{\omega}_t\|_{L^{p_1}(\Omega_{t_i})} \right) \|\omega_{t_i} - \tilde{\omega}_t\|_{L^{p_2}(\Omega_{t_i})} \|\tilde{u}\|^2_{H_0^1(\Omega_{t_i})}$$

$$\leq \tfrac{3}{2}C_{p3}C_{p4} \left(\|\omega_{t_i}\|_{L^{p_1}(\Omega_{t_i})} + \max\{ \|\omega_{t_i}\|_{L^{p_1}(\Omega_{t_i})}, \tfrac{1}{2}(\|\tilde{\omega}_{t_{i-1}}\|_{L^{p_1}(\Omega_{t_i})} + \|\omega_{t_i}\|_{L^{p_1}(\Omega_{t_i})}) \} \right) \cdot$$
$$\|\omega_{t_i} - \tilde{\omega}_{t_{i-1}}\|_{L^{p_2}(\Omega_{t_i})} \|\tilde{u}\|^2_{H_0^1(\Omega_{t_i})}$$

$$=: \tau_i^- \|\tilde{u}\|^2_{H_0^1(\Omega_{t_i})} \qquad \text{for all } t \in \left[t_{i-1/2}, t_i \right]. \tag{7.17}$$

Note that by choosing the interval $I = [t_{i-1/2}, t_i]$ (instead of $[t_{i-1}, t_i]$) we gained a factor $\frac{1}{2}$ in τ_i^-. Combining (7.16) and (7.17) yields

$$\frac{\int_{\Omega_{t_i}} (1 + 3|\tilde{\omega}_t|\tilde{\omega}_t) \tilde{u}^2 \, d(\tilde{x}, \tilde{y})}{\int_{\Omega_{t_i}} \left[|\nabla\tilde{u}|^2 + \tilde{u}^2 \right] d(\tilde{x}, \tilde{y})} \leq \frac{\int_{\Omega_{t_i}} (1 + 3|\omega_{t_i}|\omega_{t_i}) \tilde{u}^2 \, d(\tilde{x}, \tilde{y})}{\int_{\Omega_{t_i}} \left[|\nabla\tilde{u}|^2 + \tilde{u}^2 \right] d(\tilde{x}, \tilde{y})} + \tau_i^-, \tag{7.18}$$

and analogously we obtain:

$$\frac{\int_{\Omega_{t_i}} (1 + 3|\tilde{\omega}_t|\tilde{\omega}_t) \tilde{u}^2 \, d(\tilde{x}, \tilde{y})}{\int_{\Omega_{t_i}} \left[|\nabla\tilde{u}|^2 + \tilde{u}^2 \right] d(\tilde{x}, \tilde{y})} \geq \frac{\int_{\Omega_{t_i}} (1 + 3|\omega_{t_i}|\omega_{t_i}) \tilde{u}^2 \, d(\tilde{x}, \tilde{y})}{\int_{\Omega_{t_i}} \left[|\nabla\tilde{u}|^2 + \tilde{u}^2 \right] d(\tilde{x}, \tilde{y})} - \tau_i^-.$$

Recall that the mapping properties of ϕ_t ensured bijectivity of the operator Θ_t defined in (7.1). Therefore also any m-dimensional subspace U of $H_0^1(\Omega_t)$ is mapped to an m-dimensional subspace $\tilde{U} \subset H_0^1(\Omega_{t_i})$ and for $u \in U$ we have $\tilde{u} = u \circ \phi_t \in \tilde{U}$. These considerations imply for all $t \in [t_{i-1/2}, t_i]$:

$$\eta_m^{(t)} \stackrel{(7.13)}{=} \max_{\substack{U \subset H_0^1(\Omega_t) \\ \dim U = m}} \min_{u \in U} \frac{\int_{\Omega_t} (1 + 3|\omega_t|\omega_t) u^2 \, d(x, y)}{\int_{\Omega_t} \left[|\nabla u|^2 + u^2 \right] d(x, y)}$$

$$\stackrel{(7.14)}{\leq} C^{(1)}_{t_{i-1/2}t_i} \max_{\substack{\tilde{U} \subset H_0^1(\Omega_{t_i}) \\ \dim \tilde{U} = m}} \min_{\tilde{u} \in \tilde{U}} \frac{\int_{\Omega_{t_i}} (1 + 3|\tilde{\omega}_t|\tilde{\omega}_t) \tilde{u}^2 \, d(\tilde{x}, \tilde{y})}{\int_{\Omega_{t_i}} \left[|\nabla\tilde{u}|^2 + \tilde{u}^2 \right] d(\tilde{x}, \tilde{y})}$$

$$\stackrel{(7.18),(7.13)}{\leq} C^{(1)}_{t_{i-1/2}t_i} \left(\eta_m^{(t_i)} + \tau_i^- \right), \tag{7.19}$$

and analogously

$$\eta_m^{(t)} \geq C^{(2)}_{t_{i-1/2}t_i} \left(\eta_m^{(t_i)} - \tau_i^- \right). \tag{7.20}$$

Denoting by $\nu_m^{(t)}$ the m-th eigenvalue of $\Phi^{-1}L_{\omega_t} : H_0^1(\Omega_t) \to H_0^1(\Omega_t)$ we therefore obtain, using the transformation $\nu_m^{(t)} = 1 - \eta_m^{(t)}$ and the estimates (7.19), (7.20)

$$\underline{\nu}_m^{i-} := 1 - C^{(1)}_{t_{i-1/2}t_i} \left(\eta_m^{(t_i)} + \tau_i^- \right) \leq \nu_m^{(t)} \leq 1 - C^{(2)}_{t_{i-1/2}t_i} \left(\eta_m^{(t_i)} - \tau_i^- \right) =: \overline{\nu}_m^{i-}$$
$$\text{for all } t \in \left[t_{i-1/2}, t_i \right] = I \text{ and } m \in \mathbb{N}.$$

If there exists an index $m_0 \in \mathbb{N}_0$ for which $\overline{\nu}_{m_0}^{i-} < 0$ (only in case $m_0 > 0$) and $\underline{\nu}_{m_0+1}^{i-} > 0$, Lemma 3 implies that

$$K_I = \left(\min\left\{ |\overline{\nu}_{m_0}^{i-}|, \underline{\nu}_{m_0+1}^{i-} \right\} \right)^{-1}$$

is a constant satisfying (7.11) for all $t \in I = \left[t_{i-1/2}, t_i \right]$.

We will now consider the interval $I := \left[t_i, t_{i+1/2} \right]$, with $t_{i+1/2} = \frac{1}{2}(t_i + t_{i+1})$. Note that in this case the function $\tilde{\omega}_t$ is defined by linear interpolation of $\omega_{t_i} \circ \phi_{t_i}^{(i+1)}$ and $\omega_{t_{i+1}}$ on $\Omega_{t_{i+1}}$, and $\omega_t = \tilde{\omega}_t \circ (\phi_t^{(i+1)})^{-1}$. For the next steps, we transform to Ω_{t_i} and use the notation $\hat{\omega}_t = \omega_t \circ \phi_t^{(i)}$ and $\hat{u} = u \circ \phi_t^{(i)}$ for $\omega_t, u \in H_0^1(\Omega_t)$. Then we obtain for all $t \in I = [t_i, t_{i+1/2}]$:

$$\frac{\int_{\Omega_t} (1 + 3|\omega_t|\omega_t) \, u^2 \, d(x,y)}{\int_{\Omega_t} \left[|\nabla u|^2 + u^2 \right] d(x,y)} = \frac{\int_{\Omega_{t_i}} |\det J[\phi_t]| \, (1 + 3|\hat{\omega}_t|\hat{\omega}_t) \, \hat{u}^2 \, d(\tilde{x},\tilde{y})}{\int_{\Omega_{t_i}} |\det J[\phi_t]| \left[\, |J[\phi_t]^{-T}\nabla\hat{u}|^2 + \hat{u}^2 \right] d(\tilde{x},\tilde{y})}$$

$$\begin{cases} \le C_{t_i t_{i+1/2}}^{(1)} \dfrac{\int_{\Omega_{t_i}} (1+3|\hat{\omega}_t|\hat{\omega}_t)\hat{u}^2 \, d(\tilde{x},\tilde{y})}{\int_{\Omega_{t_i}} \left[|\nabla\hat{u}|^2+\hat{u}^2 \right] d(\tilde{x},\tilde{y})} \\[2ex] \ge C_{t_i t_{i+1/2}}^{(2)} \dfrac{\int_{\Omega_{t_i}} (1+3|\hat{\omega}_t|\hat{\omega}_t)\hat{u}^2 \, d(\tilde{x},\tilde{y})}{\int_{\Omega_{t_i}} \left[|\nabla\hat{u}|^2+\hat{u}^2 \right] d(\tilde{x},\tilde{y})}, \end{cases} \tag{7.21}$$

where

$$C_{t_i t_{i+1/2}}^{(1)} = \max_{t \in [t_i, t_{i+1/2}]} \left(\frac{\displaystyle\max_{j=1,\dots,k} |a_j(t)b_j(t)|}{\displaystyle\min_{j=1,\dots,k} \left(\min\left\{ \left|\frac{1}{a_j(t)}\right|^2, \left|\frac{1}{b_j(t)}\right|^2, 1 \right\} |a_j(t)b_j(t)| \right)} \right)$$

$$C_{t_i t_{i+1/2}}^{(2)} = \min_{t \in [t_i, t_{i+1/2}]} \left(\frac{\displaystyle\min_{j=1,\dots,k} |a_j(t)b_j(t)|}{\displaystyle\max_{j=1,\dots,k} \left(\max\left\{ \left|\frac{1}{a_j(t)}\right|^2, \left|\frac{1}{b_j(t)}\right|^2, 1 \right\} |a_j(t)b_j(t)| \right)} \right). \tag{7.22}$$

Using

$$\hat{\omega}_t = \omega_t \circ \phi_t^{(i)} = \tilde{\omega}_t \circ (\phi_t^{(i+1)})^{-1} \circ \phi_t^{(i)}$$
$$= \frac{t_{i+1}-t}{t_{i+1}-t_i} \omega_{t_i} \circ \phi_{t_i}^{(i+1)} \circ (\phi_t^{(i+1)})^{-1} \circ \phi_t^{(i)} + \frac{t-t_i}{t_{i+1}-t_i} \omega_{t_{i+1}} \circ (\phi_t^{(i+1)})^{-1} \circ \phi_t^{(i)},$$

leads to

$$\omega_{t_i} - \hat{\omega}_t = \omega_{t_i} - \omega_{t_i} \circ \phi_{t_i}^{(i+1)} \circ (\phi_t^{(i+1)})^{-1} \circ \phi_t^{(i)}$$
$$+ \frac{t-t_i}{t_{i+1}-t_i} \left[\omega_{t_i} \circ \phi_{t_i}^{(i+1)} \circ (\phi_t^{(i+1)})^{-1} \circ \phi_t^{(i)} - \omega_{t_{i+1}} \circ (\phi_t^{(i+1)})^{-1} \circ \phi_t^{(i)} \right],$$

and therefore, estimating as before yields:

$$\underline{\nu}_m^{i+} := 1 - C_{t_i t_{i+1/2}}^{(1)} \left(\eta_m^{(t_i)} + \tau_i^+ \right) \le \nu_m^{(t)} \le 1 - C_{t_i t_{i+1/2}}^{(2)} \left(\eta_m^{(t_i)} - \tau_i^+ \right) =: \overline{\nu}_m^{i+}$$
$$\text{for all } t \in \left[t_i, t_{i+1/2} \right] = I \text{ and } m \in \mathbb{N}. \quad (7.23)$$

Here, the constant τ_i^+ is given by

$$\tau_i^+ = \frac{3}{2} C_{p_3} C_{p_4} \left[\|\omega_{t_i}\|_{L^{p_1}(\Omega_{t_i})} + \max\left\{ \|\omega_{t_i} \circ \phi_{t_i}^{(i+1)} \circ (\phi_t^{(i+1)})^{-1} \circ \phi_t^{(i)}\|_{L^{p_1}(\Omega_{t_i})}, \right. \right.$$
$$\left. \frac{1}{2} \left(\|\omega_{t_i} \circ \phi_{t_i}^{(i+1)} \circ (\phi_t^{(i+1)})^{-1} \circ \phi_t^{(i)}\|_{L^{p_1}(\Omega_{t_i})} + \|\hat{\omega}_{t_{i+1}} \circ (\phi_t^{(i+1)})^{-1} \circ \phi_t^{(i)}\|_{L^{p_1}(\Omega_{t_i})} \right) \right\} \right] \cdot$$
$$\left[2 \left\| \omega_{t_i} - \omega_{t_i} \circ \phi_{t_i}^{(i+1)} \circ (\phi_t^{(i+1)})^{-1} \circ \phi_t^{(i)} \right\|_{L^{p_2}(\Omega_{t_i})} \right.$$
$$\left. + \left\| \omega_{t_i} \circ \phi_{t_i}^{(i+1)} \circ (\phi_t^{(i+1)})^{-1} \circ \phi_t^{(i)} - \omega_{t_{i+1}} \circ (\phi_t^{(i+1)})^{-1} \circ \phi_t^{(i)} \right\|_{L^{p_2}(\Omega_{t_i})} \right]. \tag{7.24}$$

If there exists an index $m_0 \in \mathbb{N}_0$ for which $\overline{\nu}_{m_0}^{i+} < 0$ (only in case $m_0 > 0$) and $\underline{\nu}_{m_0+1}^{i+} > 0$, Lemma 3 implies that

$$K_I = \left(\min \left\{ |\overline{\nu}_{m_0}^{i+}|, \underline{\nu}_{m_0+1}^{i+} \right\} \right)^{-1} \tag{7.25}$$

is a constant satisfying (7.11) for all $t \in I = \left[t_i, t_{i+1/2} \right]$.

7.1.3 Transformations and computation of the relevant constants

Before we continue we fix the transformations in (7.7) and (7.8) and use the concrete definitions to calculate the second derivative in (7.4) and (7.5) as well as constans $C_{t_{i-1}t_i}^{(1)}, \ldots, C_{t_{i-1}t_i}^{(4)}$, $C_{t_{i-1/2}t_i}^{(1)}, C_{t_{i-1/2}t_i}^{(2)}, C_{t_i t_{i+1/2}}^{(1)}, C_{t_i t_{i+1/2}}^{(2)}, \tau_i^-$ and τ_i^+. We will consider a shifted version of the domain $(-t-1, t+1)^2 \setminus [-t, t]^2$, which has its upper left re-entrant corner at the point $(0, 0)$, i.e. we use

$$\Omega_t = \left((-1, 2t+1) \times (-2t-1, 1) \right) \setminus \left([0, 2t] \times [-2t, 0] \right).$$

Moreover, we will take symmetries of the domain and the considered solutions, respectively, into account. This will simplify the upcoming definitions and calculations.

Remark 9. It turned out that only in case of the fourpeakcorner solution we are able to prove the existence of a solution branch for $t \in [1.5, 3]$. For all other solution types or parameter values of t the grid that we chose in our numerical computations was not fine enough. Due to time reasons we were not able to use a finer grid in our computations, which would eventually lead to solution branches for other solutions types.
In the following, we will therefore only consider the case of functions having full symmetry.

Full symmetry

We distinguish the cases $t < 1$ and $t > 1$ and set

$$\varepsilon = \begin{cases} \frac{1}{16}, & t \in (\frac{1}{16}, 1) \\ 1, & t \in (1, 3). \end{cases}$$

Let now

$$\Omega_t^1 = \text{conv}\{(0,0), (\varepsilon, 0), (\varepsilon, 1), (-1, 1)\}, \qquad \Omega_t^2 = (\varepsilon, t) \times (0, 1),$$

then $\widehat{\Omega}_t := \text{int}\left(\overline{\Omega_t^1} \cup \overline{\Omega_t^2} \right)$ denotes the upper left eighth of the domain Ω_t. Note that it will be enough to define the transformation ϕ_t on $\widehat{\Omega}_{t_i}$ as it can be symmetrically extended to the whole of Ω_{t_i}. In the following we always assume $t_i < \varepsilon$ or $t_{i-1} > \varepsilon$. We set

$$\begin{cases} \phi_t^1(\tilde{x}, \tilde{y}) = \begin{pmatrix} \tilde{x} \\ \tilde{y} \end{pmatrix}, & (\tilde{x}, \tilde{y}) \in \Omega_{t_i}^1 \cup \{(\varepsilon, \tilde{y}) : y \in (0,1)\} \\[2ex] \phi_t^2(\tilde{x}, \tilde{y}) = \begin{pmatrix} \frac{t-\varepsilon}{t_i-\varepsilon} & 0 \\ 0 & 1 \end{pmatrix} \begin{pmatrix} \tilde{x} \\ \tilde{y} \end{pmatrix} + \begin{pmatrix} \varepsilon \frac{t_i-t}{t_i-\varepsilon} \\ 0 \end{pmatrix}, & (\tilde{x}, \tilde{y}) \in \Omega_{t_i}^2, \end{cases} \tag{7.26}$$

and observe $\lim_{\tilde{x} \to \varepsilon^-} \phi_t^2(\tilde{x}, \tilde{y}) = \left(\frac{t-\varepsilon}{t_i-\varepsilon} \varepsilon + \varepsilon \frac{t_i-t}{t_i-\varepsilon}, \tilde{y} \right) = \left(\varepsilon \frac{t_i-\varepsilon}{t_i-\varepsilon}, \tilde{y} \right) = (\varepsilon, \tilde{y}) = \phi_t^1(\varepsilon, \tilde{y})$. Moreover, $\phi_t^1(\Omega_{t_i}^1) = \Omega_t^1$, $\phi_t^1(\Omega_{t_i}^2) = \Omega_t^2$ and therefore $\phi_t(x_1, y_1) = \phi_t(x_2, y_2)$ for some $(x_1, y_1), (x_2, y_2) \in \widehat{\Omega}_t$ implies $(x_1, y_1), (x_2, y_2) \in \Omega_t^1$ or $(x_1, y_1), (x_2, y_2) \in \Omega_t^2$ or $x_1 = x_2 = \varepsilon$. In either case linearity of ϕ_t^i $i = 1, 2$ and $\det J[\phi_t^i] \neq 0$ implies $(x_1, y_1) = (x_2, y_2)$. Thus ϕ_t is continuous, bijective, piecewise linear and therefore Lipschitz-continous.

The inverse $\phi_t^{-1} : \Omega_t \to \Omega_{t_i}$, defined on $\widehat{\Omega}_t$ (and symmetrically extended to the whole of Ω_t), is given by:

$$
\phi_t^{-1}(x, y) := \begin{cases}
(\phi_t^1)^{-1}(x, y) = \begin{pmatrix} x \\ y \end{pmatrix}, & (x, y) \in \Omega_t^1 \cup \{ (\varepsilon, y) : y \in (0, 1) \} \\[2ex]
(\phi_t^2)^{-1}(x, y) = \begin{pmatrix} \frac{t_i-\varepsilon}{t-\varepsilon} & 0 \\ 0 & 1 \end{pmatrix} \begin{pmatrix} x \\ y \end{pmatrix} - \begin{pmatrix} \varepsilon \frac{t_i-t}{t-\varepsilon} \\ 0 \end{pmatrix}, & (x, y) \in \Omega_t^2.
\end{cases}
$$

Indeed $\phi_t \circ \phi_t^{-1} = \phi_t \circ \phi_t^{-1} = Id$ and continuity of ϕ_t^{-1} can be checked as done for ϕ_t. Since ϕ_t^{-1} is also piecewise linear, it follows that ϕ_t is a Lipschitz homeomorphism.

We will now compute $\gamma_i^{(1)}, \gamma_i^{(2)}$ satisfying (7.4) and (7.5). An easy calculation shows

$$
\left| \frac{d^2}{dt^2} \left[|\det J[\phi_t^1]| (\nabla \tilde{\omega}_t)^T J[\phi_t^1]^{-1} J[\phi_t^1]^{-T} \right] \right| = 0
$$

$$
\left| \frac{d^2}{dt^2} \left[|\det J[\phi_t^2]| (\nabla \tilde{\omega}_t)^T J[\phi_t^2]^{-1} J[\phi_t^2]^{-T} \right] \right| =
$$

$$
\left| \left[\frac{2(t_i-\varepsilon)}{(t-\varepsilon)^3} \left(\frac{t_i-t}{t_i-t_{i-1}} \frac{\partial \tilde{\omega}_{t_{i-1}}}{\partial \tilde{x}} + \frac{(t-t_{i-1})}{(t_i-t_{i-1})} \frac{\partial \tilde{\omega}_{t_i}}{\partial \tilde{x}}, 0 \right) + \left(\frac{-2(t_i-\varepsilon)}{(t-\varepsilon)^2} \frac{\frac{\partial \tilde{\omega}_{t_i}}{\partial \tilde{x}} - \frac{\partial \tilde{\omega}_{t_{i-1}}}{\partial \tilde{x}}}{t_i-t_{i-1}}, \frac{2}{t_i-\varepsilon} \frac{\frac{\partial \tilde{\omega}_{t_i}}{\partial \tilde{y}} - \frac{\partial \tilde{\omega}_{t_{i-1}}}{\partial \tilde{y}}}{t_i-t_{i-1}} \right) \right] \right|
$$

$$
\leq \zeta_{i,1} \qquad \text{for all } \varepsilon < t_{i-1} \leq t \leq t_i.
$$

where

$$
\zeta_{i,1} := \frac{2(t_i-\varepsilon)}{(t_{i-1}-\varepsilon)^3} \left(\left| \frac{\partial \tilde{\omega}_{t_i}}{\partial \tilde{x}} \right| + \left| \frac{\partial \tilde{\omega}_{t_i}}{\partial \tilde{x}} - \frac{\partial \tilde{\omega}_{t_{i-1}}}{\partial \tilde{x}} \right| \right) + \frac{2(t_i-\varepsilon)}{(t_{i-1}-\varepsilon)^2(t_i-t_{i-1})} \left| \frac{\partial \tilde{\omega}_{t_i}}{\partial \tilde{x}} - \frac{\partial \tilde{\omega}_{t_{i-1}}}{\partial \tilde{x}} \right| +
$$

$$
\frac{2}{(t_i-\varepsilon)(t_i-t_{i-1})} \left| \frac{\partial \tilde{\omega}_{t_i}}{\partial \tilde{y}} - \frac{\partial \tilde{\omega}_{t_{i-1}}}{\partial \tilde{y}} \right|.
$$

Here we used

$$
\max \left\{ \left| \frac{\partial \tilde{\omega}_{t_{i-1}}}{\partial \tilde{x}} \right|, \left| \frac{\partial \tilde{\omega}_{t_i}}{\partial \tilde{x}} \right| \right\} \leq \left| \frac{\partial \tilde{\omega}_{t_i}}{\partial \tilde{x}} \right| + \left| \frac{\partial \tilde{\omega}_{t_i}}{\partial \tilde{x}} - \frac{\partial \tilde{\omega}_{t_{i-1}}}{\partial \tilde{x}} \right|.
$$

Thus we obtain (7.4) with

$$
\| \gamma_i^{(1)} \|_{L^2(\Omega_{t_i})} = \sqrt{8} \| \gamma_i^{(1)} \|_{L^2(\widehat{\Omega}_{t_i})}
$$

$$
\leq \frac{2\sqrt{8}(t_i-\varepsilon)}{(t_{i-1}-\varepsilon)^3} \left\| \frac{\partial \tilde{\omega}_{t_i}}{\partial \tilde{x}} \right\|_{L^2(\Omega_{t_i}^2)} + \frac{2\sqrt{8}(t_i-\varepsilon)}{(t_{i-1}-\varepsilon)^2} \left(\frac{1}{t_{i-1}-\varepsilon} + \frac{1}{t_i-t_{i-1}} \right) \left\| \frac{\partial \tilde{\omega}_{t_i}}{\partial \tilde{x}} - \frac{\partial \tilde{\omega}_{t_{i-1}}}{\partial \tilde{x}} \right\|_{L^2(\Omega_{t_i}^2)} +
$$

$$
\frac{2\sqrt{8}(t_i-\varepsilon)}{(t_i-t_{i-1})} \left\| \frac{\partial \tilde{\omega}_{t_i}}{\partial \tilde{y}} - \frac{\partial \tilde{\omega}_{t_{i-1}}}{\partial \tilde{y}} \right\|_{L^2(\Omega_{t_i}^2)}.
$$

For the computation of $\gamma_i^{(2)}$ we note that $f(\tilde{\omega}_t) = \tilde{\omega}_t^3$ and thus

$$\left| \frac{d^2}{dt^2} \left[|\det J[\phi_t^1] f(\tilde{\omega}_t)] \right] \right| = 0$$

$$\left| \frac{d^2}{dt^2} \left[|\det J[\phi_t^2] f(\tilde{\omega}_t)] \right] \right| = \left| \frac{6\,\tilde{\omega}_t^2}{t_i - \varepsilon} \frac{\tilde{\omega}_{t_i} - \tilde{\omega}_{t_{i-1}}}{t_i - t_{i-1}} \hat{\varphi} + 6\,\tilde{\omega}_t \frac{t - \varepsilon}{t_i - \varepsilon} \left(\frac{\tilde{\omega}_{t_i} - \tilde{\omega}_{t_{i-1}}}{t_i - t_{i-1}} \right)^2 \right|$$

$$\leq \zeta_{i,2} \qquad \text{for all } \varepsilon < t_{i-1} \leq t \leq t_i,$$

where

$$\zeta_{i,2} = 6 \left[\frac{1}{t_i - \varepsilon} \max \left\{ \left\| \tilde{\omega}_{t_{i-1}} \right\|_{\infty,\Omega_t^2}^2, \left\| \tilde{\omega}_{t_i} \right\|_{\infty,\Omega_t^2}^2 \right\} \left| \frac{\tilde{\omega}_{t_i} - \tilde{\omega}_{t_{i-1}}}{t_i - t_{i-1}} \right| + \right.$$

$$\left. \max \left\{ \left\| \tilde{\omega}_{t_{i-1}} \right\|_{\infty,\Omega_t^2}, \left\| \tilde{\omega}_{t_i} \right\|_{\infty,\Omega_t^2} \right\} \left| \frac{\tilde{\omega}_{t_i} - \tilde{\omega}_{t_{i-1}}}{t_i - t_{i-1}} \right|^2 \right].$$

Thus, (7.5) holds with

$$\left\| \gamma_i^{(2)} \right\|_{L^2(\Omega_{t_i})} \leq 6\sqrt{8} \left(\frac{1}{t_i - \varepsilon} \max \left\{ \left\| \tilde{\omega}_{t_{i-1}} \right\|_{\infty,\Omega_t^2}^2, \left\| \tilde{\omega}_{t_i} \right\|_{\infty,\Omega_t^2}^2 \right\} \frac{\left\| \tilde{\omega}_{t_i} - \tilde{\omega}_{t_{i-1}} \right\|_{L^2(\Omega_{t_i}^2)}}{t_i - t_{i-1}} + \right.$$

$$\left. \max \left\{ \left\| \tilde{\omega}_{t_{i-1}} \right\|_{\infty,\Omega_t^2}, \left\| \tilde{\omega}_{t_i} \right\|_{\infty,\Omega_t^2} \right\} \frac{\left\| \tilde{\omega}_{t_i} - \tilde{\omega}_{t_{i-1}} \right\|_{L^4(\Omega_{t_i}^2)}^2}{(t_i - t_{i-1})^2} \right).$$

Computation of the relevant constants

With ϕ_t defined as in (7.26) we can now easily compute the desired constants. Note that for the computation of τ_i^+ in (7.24) we need compositions of different transformations. It is easy to see that with the definition in (7.26) we have:

$$(\phi_t^{(i+1)})^{-1} \circ \phi_t^{(i)} = (\phi_{t_i}^{(i+1)})^{-1} \quad \text{and} \quad \phi_{t_i}^{(i+1)} \circ (\phi_t^{(i+1)})^{-1} \circ \phi_t^{(i)} = Id_{\Omega_{t_i}}.$$

This simplifies the formula for τ_i^+ significantly.

$$C_{t_{i-1}t_i}^{(1)} = \max_{j=1,2} \max_{t \in [t_{i-1},t_i]} \left(\frac{\max\{|a_j(t)|,|b_j(t)|\}}{\sqrt{|\det J[\phi_t^j]|}} \left\| \gamma_i^{(1)} \right\|_{L^2(\Omega_{t_i})} \right) = \left\| \gamma_i^{(1)} \right\|_{L^2(\Omega_{t_2})} \max_{t \in [t_{i-1},t_i]} \sqrt{\frac{t_i - \varepsilon}{t - \varepsilon}}$$

$$= \left\| \gamma_i^{(1)} \right\|_{L^2(\Omega_{t_i})} \sqrt{\frac{t_i - \varepsilon}{t_{i-1} - \varepsilon}}$$

$$C_{t_{i-1}t_i}^{(2)} = \max_{j=1,2} \max_{t \in [t_{i-1},t_i]} \frac{1}{\sqrt{|\det J[\phi_t^j]|}} \left\| \gamma_i^{(2)} \right\|_{L^2(\Omega_{t_i})} = \left\| \gamma_i^{(2)} \right\|_{L^2(\Omega_{t_i})} \sqrt{\frac{t_i - \varepsilon}{t_{i-1} - \varepsilon}}$$

$$C_{t_{i-1}t_i}^{(3)} = \min_{j=1,2} \min_{t \in [t_{i-1},t_i]} \left(\min \left\{ \left| \frac{a_j(t_{i-1})}{a_j(t)} \right|^2, \left| \frac{b_j(t_{i-1})}{b_j(t)} \right|^2, 1 \right\} \frac{|a_j(t)b_j(t)|}{|a_j(t_{i-1})b_j(t_{i-1})|} \right)$$

$$= \min_{j=1,2} \min_{t \in [t_{i-1},t_i]} \left(\underbrace{\min \left\{ \left| \frac{t_{i-1} - \varepsilon}{t - \varepsilon} \right|^2, 1 \right\}}_{= \left| \frac{t_{i-1}-\varepsilon}{t-\varepsilon} \right|^2} \frac{t - \varepsilon}{t_{i-1} - \varepsilon} \right) = \frac{t_{i-1} - \varepsilon}{t_i - \varepsilon}$$

$$C_{t_{i-1}t_i}^{(4)} = \min_{j=1,2} \min_{t \in [t_{i-1},t_i]} \left(\min \left\{ \left| \frac{1}{a_j(t)} \right|^2, \left| \frac{1}{b_j(t)} \right|^2, 1 \right\} |a_j(t)b_j(t)| \right)$$

$$= \min_{j=1,2} \min_{t\in[t_{i-1},t_i]} \left(\underbrace{\left\{ \left|\tfrac{t_i-\varepsilon}{t-\varepsilon}\right|^2 , 1 \right\}}_{=1} \left|\tfrac{t-\varepsilon}{t_i-\varepsilon}\right| \right) = \tfrac{t_{i-1}-\varepsilon}{t_i-\varepsilon}$$

$$C^{(1)}_{t_{i-1/2}t_i} = \max_{t\in[t_{i-1/2},t_i]} \left(\frac{\max\limits_{j=1,2} |a_j(t)b_j(t)|}{\min\limits_{j=1,2}\left(\min\left\{\left|\tfrac{1}{a_j(t)}\right|^2,\left|\tfrac{1}{b_j(t)}\right|^2,1\right\}|a_j(t)b_j(t)|\right)} \right) = \max_{t\in[t_{i-1/2},t_i]} \frac{1}{\min\left\{\tfrac{t-\varepsilon}{t_i-\varepsilon},1\right\}}$$

$$= \max_{t\in[t_{i-1/2},t_i]} \tfrac{t_i-\varepsilon}{t-\varepsilon} = \tfrac{t_i-\varepsilon}{t_{i-1/2}-\varepsilon}$$

$$C^{(2)}_{t_{i-1/2}t_i} = \min_{t\in[t_{i-1/2},t_i]} \left(\frac{\min\limits_{j=1,2} |a_j(t)b_j(t)|}{\max\limits_{j=1,2}\left(\max\left\{\left|\tfrac{1}{a_j(t)}\right|^2,\left|\tfrac{1}{b_j(t)}\right|^2,1\right\}|a_j(t)b_j(t)|\right)} \right) = \min_{t\in[t_{i-1/2},t_i]} \frac{\tfrac{t-\varepsilon}{t_i-\varepsilon}}{\max\left\{1,\tfrac{t-\varepsilon}{t_i-\varepsilon}\right\}}$$

$$= \min_{t\in[t_{i-1/2},t_i]} \left(\tfrac{t-\varepsilon}{t_i-\varepsilon}\right)^2 = \left(\tfrac{t_{i-1/2}-\varepsilon}{t_i-\varepsilon}\right)^2$$

$$C^{(1)}_{t_it_{i+1/2}} = \max_{t\in[t_i,t_{i+1/2}]} \left(\frac{\max\limits_{j=1,2} |a_j(t)b_j(t)|}{\min\limits_{j=1,2}\left(\min\left\{\left|\tfrac{1}{a_j(t)}\right|^2,\left|\tfrac{1}{b_j(t)}\right|^2,1\right\}|a_j(t)b_j(t)|\right)} \right) = \max_{t\in[t_i,t_{i+1/2}]} \frac{\tfrac{t-\varepsilon}{t_i-\varepsilon}}{\min\left\{\tfrac{t_i-\varepsilon}{t-\varepsilon},1\right\}}$$

$$= \max_{t\in[t_i,t_{i+1/2}]} \left(\tfrac{t-\varepsilon}{t_i-\varepsilon}\right)^2 = \left(\tfrac{t_{i+1/2}-\varepsilon}{t_i-\varepsilon}\right)^2$$

$$C^{(2)}_{t_it_{i+1/2}} = \min_{t\in[t_i,t_{i+1/2}]} \left(\frac{\min\limits_{j=1,2} |a_j(t)b_j(t)|}{\max\limits_{j=1,2}\left(\max\left\{\left|\tfrac{1}{a_j(t)}\right|^2,\left|\tfrac{1}{b_j(t)}\right|^2,1\right\}|a_j(t)b_j(t)|\right)} \right) = \min_{t\in[t_i,t_{i+1/2}]} \frac{1}{\max\left\{1,\tfrac{t-\varepsilon}{t_i-\varepsilon}\right\}}$$

$$= \min_{t\in[t_i,t_{i+1/2}]} \tfrac{t_i-\varepsilon}{t-\varepsilon} = \tfrac{t_i-\varepsilon}{t_{i+1/2}-\varepsilon}. \tag{7.27}$$

Computation of embedding constants for a parameter interval

An embedding constant $C_p = C_p(\Omega_t)$ for the embedding $H_0^1(\Omega_t) \hookrightarrow L^p(\Omega_t)$ for all $t \in [t_{i-1}, t_i]$ can be obtained using the following lemma:

Lemma 7. *Let $C_p(\Omega_s)$ be an embedding constant for the embedding $H_0^1(\Omega_s) \hookrightarrow L^p(\Omega_s)$ which has been computed via Lemma 2. Then, for all $t \geq s$, $C_p(\Omega_t) = C_p(\Omega_s)$ is also a valid embedding constant for $H_0^1(\Omega_t) \hookrightarrow L^p(\Omega_t)$.*

Proof. Denote by $\lambda_1(\Omega_t)$ the smallest Dirichlet eigenvalue of $-\Delta$ on Ω_t. By Lemma 2 it suffices to prove $\lambda_1(\Omega_s) \leq \lambda_1(\Omega_t)$ for all $t \geq s$.

For this purpose we consider a suitable domain decomposition of Ω_t (see section 5.3) and use Lemma 5. Let $t > s$ and split the domain Ω_t as shown in Figure 7.1.

The subdomains marked with C are congruent to $C_0 := ((-1,s) \times (0,1)) \cup ((-1,0) \times (-s,1))$ and the ones marked with D are congruent to $D_0 := (0, 2t - 2s) \times (0,1)$. We consider the eigenvalue problem for $-\Delta$ on the subdomains C, D, with zero Neumann boundary conditions at the interface and zero Dirichlet boundary conditions on the remaining part of the boundary. The resulting problem can equivalently be stated on the prototype domains C_0 and D_0, respectively:
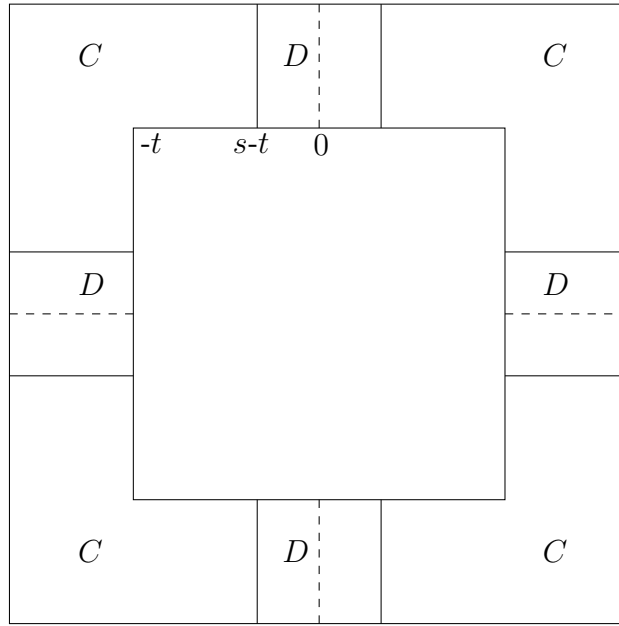
Figure 7.1: Domain decomposition for Ω_t

(C)

$$
\begin{cases}
-\Delta u = \lambda_C u & \text{in } C_0 \\
\quad\quad u = 0 & \text{on } \partial C_0 \backslash \{(x,y) \in \overline{C}_0 : \ x = s \text{ or } y = -s\} \\
\frac{\partial u}{\partial x}(s,y) = \frac{\partial u}{\partial y}(x,-s) = 0 & \text{for all } x \in [-1,0], \ y \in [0,1]
\end{cases}
\tag{7.28}
$$

Due to symmetry the smallest eigenvalue of this problem equals $\lambda_1(\Omega_s)$: We first note that for any eigenfunction u corresponding to the smallest eigenvalue $\lambda_1(\Omega_s)$ also the function $\tilde{u}$, given by $\tilde{u}(x,y) = u(-x,y)$ for $(x,y) \in \Omega_s$ is an eigenfunction corresponding to the eigenvalue $\lambda_1(\Omega_s)$. Since this eigenvalue is simple, u and $\tilde{u}$ must be linearly dependent. Using in addition that u does not have zeros in Ω_s, this implies $u(x,y) = u(-x,y)$ for all $(x,y) \in \Omega_s$ and therefore symmetry of u w.r.t. the axis $x = 0$. Other symmetries can be proven analogously. Since Ω_s can be split into four congruent copies of C_0, the symmetry of the first eigenfunction implies indeed that the smallest eigenvalue of problem (C) is equal to $\lambda_1(\Omega_s)$. Moreover it is clear that the L-shaped domain $U_s := ((-s-1,-s+1) \times (s-1,s+1))$ $\backslash \, ([-s,-s+1] \times [s-1,s]) \subset \Omega_s$ for all $s > 0$ and therefore Poincaré's min-max-principle implies $\lambda_1(\Omega_s) \leq \lambda_1(U_s) = \lambda_1(U_0)$. An easy and verified Rayleigh-Ritz computation for the first Dirichlet eigenvalue $\lambda_1(U_0)$ of $-\Delta$ on U_0 shows $\lambda_1(U_0) \leq 9.642$, which in particular is smaller than π^2. Hence $\lambda_1(\Omega_s) \leq \pi^2$ follows.

(D)

$$
\begin{cases}
-\Delta u = \lambda_D u & \text{in } D_0 \\
u(x,0) = u(x,1) = 0 & \text{for all } x \in [0, 2t - 2s\,] \\
\frac{\partial u}{\partial x}(0,y) = \frac{\partial u}{\partial y}(2t - 2s, y) = 0 & \text{for all } y \in [0,1]
\end{cases}
\tag{7.29}
$$

The eigenvalues of this problem are larger than π^2.

Lemma 5, applied to the domain decomposition as given in Figure 7.1, implies that a lower bound for the smallest eigenvalue of $-\Delta$ in Ω_t with homogeneous Dirichlet boundary conditions is given

by the smallest eigenvalue in the union of all λ_C and λ_D. The smallest eigenvalue of problem (C), which by the above considerations is equal to $\lambda_1(\Omega_s)$, occurs four times in this union and is smaller than π^2, whereas all eigenvalues λ_D are larger than π^2. Therefore $\lambda_1(\Omega_s) \le \lambda_1(\Omega_t)$ follows.   □

7.1.4   Numerical results

In the following we present verified results proving the existence of a solution u_t to problem (1.2) for all $t \in [1.5, 3]$. As already mentioned in Remark 9 we will restrict ourselves to the fourpeakcorner solution, since the grid we chose was too coarse to verify other branches of solutions. However, this is a purely technical restriction and no general limitation of the method we presented.

We chose the grid $t_0 = 1.5 < 1.53125 < 1.5625 < 1.625 < 1.6875 < \ldots < 2.9375 < 3 = t_{25}$, i.e. $t_i - t_{i-1} = \frac{1}{16}$ for all $i \in \{3, \ldots, 25\}$ and $t_2 - t_1 = t_1 - t_0 = \frac{1}{32}$.

The following table shows for the t-intervals $(t_{i-1/2}, t_i)$ and $(t_i, t_{i+1/2})$ (where $t_{i-1/2} = \frac{1}{2}(t_{i-1}+t_i)$ and $t_{i+1/2} = \frac{1}{2}(t_i + t_{i+1})$) constants K_t, δ_t and α_t such that for all t in the given parameter interval

  (i) K_t bounds the inverse of the linearization at ω_t, i.e.

$$\|v\|_{H_0^1(\Omega_t)} \le K_t \|L_{\omega_t}[v]\|_{H^{-1}(\Omega_t)} \quad \text{for all } v \in H_0^1(\Omega_t, \text{sym}),$$

   where $H_0^1(\Omega_t, \text{sym})$ denotes the space of all functions having full symmetry

  (ii) δ_t is an upper bound for the defect-norm of ω_t, i.e.

$$\| - \Delta\omega_t - |\omega_t|^3 \|_{H^{-1}(\Omega_t)} \le \delta_t,$$

  (iii) α_t satisfies (2.7) and (2.8).

Recall that the existence of $\alpha_t > 0$ satisfying (2.7) and (2.8) implies, by Theorem 1, that there exists a solution $u_t \in H_0^1(\Omega_t)$ of problem (1.2) such that $\|\omega_t - u_t\|_{H_0^1(\Omega_t)} < \alpha_t$.

t-interval	K_t	δ_t	α_t
[1.5,1.515625]	4.79893	0.0034096	0.018427
[1.515625,1.53125]	4.43140	0.0034096	0.016672
[1.53125,1.546875]	4.88362	0.0033413	0.018416
[1.546875,1.5625]	4.25373	0.0033413	0.015514
[1.5625,1.59375]	6.19434	0.0050492	0.054182
[1.59375,1.625]	4.82656	0.0050492	0.029767
[1.625,1.65625]	5.76800	0.0046496	0.036495
[1.65625,1.6875]	4.67152	0.0046496	0.025580
[1.6875,1.71875]	5.46148	0.0043524	0.029937
[1.71875,1.75]	4.55093	0.0043524	0.022793
[1.75,1.78125]	5.23175	0.0041257	0.026063
[1.78125,1.8125]	4.45535	0.0041257	0.020821

[1.8125,1.84375]	5.05417	0.0039489	0.023467
[1.84375,1.875]	4.37846	0.0039489	0.019365
[1.875,1.90625]	4.91354	0.0038084	0.021605
[1.90625,1.9375]	4.31584	0.0038084	0.018254
[1.9375,1.96875]	4.79996	0.0036948	0.020207
[1.96875,2]	4.26426	0.0036948	0.017385
[2,2.03125]	4.70665	0.0036016	0.019123
[2.03125,2.0625]	4.22131	0.0036016	0.016691
[2.0625,2.09375]	4.62880	0.0035242	0.018261
[2.09375,2.125]	4.18515	0.0035242	0.016126
[2.125,2.15625]	4.56294	0.0034592	0.017561
[2.15625,2.1875]	4.15436	0.0034592	0.015660
[2.1875,2.21875]	4.50651	0.0034042	0.016982
[2.21875,2.25]	4.12782	0.0034042	0.015270
[2.25,2.28125]	4.45758	0.0033572	0.016497
[2.28125,2.3125]	4.10469	0.0033572	0.014940
[2.3125,2.34375]	4.41470	0.0033168	0.016086
[2.34375,2.375]	4.08433	0.0033168	0.014658
[2.375,2.40625]	4.37679	0.0032819	0.015733
[2.40625,2.4375]	4.06623	0.0032819	0.014414
[2.4375,2.46875]	4.34299	0.0032514	0.015427
[2.46875,2.5]	4.05000	0.0032514	0.014203
[2.5,2.53125]	4.31263	0.0032248	0.015160
[2.53125,2.5625]	4.03535	0.0032248	0.014017
[2.5625,2.59375]	4.28520	0.0032013	0.014925
[2.59375,2.625]	4.02203	0.0032013	0.013853
[2.625,2.65625]	4.26028	0.0031805	0.014716
[2.65625,2.6875]	4.00986	0.0031805	0.013708
[2.6875,2.71875]	4.23753	0.0031621	0.014531
[2.71875,2.75]	3.99869	0.0031621	0.013578
[2.75,2.78125]	4.21666	0.0031456	0.014364
[2.78125,2.8125]	3.98839	0.0031456	0.013461
[2.8125,2.84375]	4.19745	0.0031308	0.014214
[2.84375,2.875]	3.97886	0.0031308	0.013356
[2.875,2.90625]	4.17970	0.0031175	0.014078
[2.90625,2.9375]	3.97002	0.0031175	0.013261
[2.9375,2.96875]	4.16326	0.0031054	0.013954
[2.96875,3]	3.96177	0.0031054	0.013174

With α_t given as in the above table we obtain the following theorem:

Theorem 6. *For every $t \in [1.5, 3]$ there exists a solution $u_t \in H_0^1(\Omega_t)$ of problem (1.2) (type fourpeakcorner), such that*

$$\|u_t - \omega_t\|_{H_0^1(\Omega_t)} \le \alpha_t.$$

Remark 10.   (a) Comparing with the results for fixed values of t in section 6.4.1 we observe that the values of K_t for t in a parameter interval $(t_{i-1/2}, t_i)$ or $(t_i, t_{i+1/2})$ are significantly larger than the value of K_t for $t = t_i$. The difference is due to the error terms τ_i^-, τ_i^+ and the constants $C_{t_{i-1/2}t_i}^{(l)}, C_{t_i t_{i+1/2}}^{(l)}$, $l = 1, 2$, defined in (7.15), (7.16), and (7.22), (7.24). Moreover, the calculations in (7.27) show that (in case of equally spaced grid-points) $C_{t_{i-1/2}, t_i}^{(1)} < C_{t_{i-1/2}, t_i}^{(2)}$ and $C_{t_i, t_{i+1/2}}^{(1)} > C_{t_i, t_{i+1/2}}^{(2)}$ and the difference between the constants grows in inverse proportion with the distance of t_i to ε (note that $\varepsilon = 1$ for our chosen grid). These differences are also responsible for the jumps of K_t: We observe that the value of K_t for $t \in (t_i, t_{i+1/2})$ is larger than the value of K_t in $(t_{i-1/2}, t_i)$. This is due to the fact that in the first case the larger constant $C_{t_i t_{i+1/2}}^{(1)}$ acts on the eigenvalue with smallest distance to zero, which finally determines K_t (cf. (7.23) and (7.25)), while in the second case the smaller constant $C_{t_{i-1/2}t_i}^{(1)}$ is active. Note that the eigenvalue with smallest distance to zero is always the second one, which is indicated by the verified eigenvalue bounds in section 6.4.1.

(b) Using the values in the above table for $t \in [t_{i-1/2}, t_i]$ and $t \in [t_i, t_{i+1/2}]$ we can define a piecewise constant and lower semicontinuous function $t \mapsto \alpha_t$ ($t \in [1.5, 3]$) such that α_t satisfies (2.7) and (2.8) for all $t \in [1.5, 3]$. To achieve lower semicontinuity we redefine α_t in the points of double definition to be the minimum of the two values in the adjacent intervals.

Since α_t satisfies (2.8) with a strict inequality for all $t \in [1.5, 3]$, and moreover α_t is piecewise constant, we can choose some uniform $\eta > 0$ such that (2.8) is satisfied with $\alpha_t + \eta$ instead of α_t. This fact will be essential for proving that the obtained solutions u_t for $t \in [1.5, 3]$ form a continuous branch of solutions, as it will be done in the next section.

7.2   Smoothness of Solution Branches

With a grid $t_0 < t_1 < \ldots t_{i-1} < t_i < \ldots < t_n$, e.g. chosen as in the previous section, we assume again that for every $i \in \{0, \ldots, n\}$ we have computed an approximate solution $\omega_{t_i} \in H_0^1(\Omega_{t_i})$ of (1.2) (with $t = t_i$). Then using the definition in (7.2) and (7.3) we can construct approximate solutions $\omega_t \in H_0^1(\Omega_t)$ of problem (1.2) for each $t \in I := [t_0, t_n]$. We assume now that for every $t \in I$ a defect bound δ_t satisfying (2.3), a bound K_t for the inverse of the linearization at ω_t (satisfying (2.4)) and a constant α_t satisfying (2.7) and (2.8) is known, implying that for every $t \in I$ there exists a solution $u_t \in H_0^1(\Omega_t)$ with $\|\omega_t - u_t\|_{H_0^1} \le \alpha_t$. We will now consider the mapping $t \mapsto u_t$ and to prove that it is continuously differentiable in a suitable sense, thereby obtaining a continuously differentiable branch of solutions to problem (1.2).

In addition to the above we assume that $t \mapsto \alpha_t$ is lower semicontinuous and that we can choose some uniform (i.e. t-independent) $\eta > 0$ such that (2.8) holds with $\alpha_t + \eta$ instead of α_t, i.e. we

have

$$2K_t\gamma(\alpha_t + \eta)\left(\|\omega_t\|_{L^4(\Omega_t)} + \tfrac{1}{2}C_4(\alpha_t + \eta)\right) < 1 \quad \text{for all } t \in I, \tag{7.30}$$

where C_4 denotes an embedding constant for the embedding $H_0^1(\Omega_t) \hookrightarrow L^4(\Omega_t)$ and $\gamma := 3C_4^3$.

We will use two results of Theorem 3.1 in [50], which constitute an extension of Theorem 1 (assumptions on ω_t, α_t and η just as stated above):

(U) If $u \in H_0^1(\Omega_t)$ is a solution of (1.2) satisfying $\|u - \omega_t\|_{H_0^1} \le \alpha_t + \eta$ it follows that $u = u_t$, i.e. the solution u_t is locally unique.

(N) Let $u \in H_0^1(\Omega)$ with $\|u - \omega_t\|_{H_0^1} \le \alpha_t$. Then $L_u : H_0^1(\Omega_t) \to H^{-1}(\Omega_t)$ is bijective, whence in particular L_{u_t} is bijective.

We will use a similar approach as in [50] to prove that $(u_t)_{t \in I}$ is a smooth branch, with a suitable notion of differentiability still to be defined. In contrast to the problem studied in [50], where the parameter was part of the equation, the parameter in our problem (1.2) occurs in the domain Ω_t. We therefore transform our problem to a fixed reference domain, thereby obtaining an equivalent parameter-dependent problem where the parameter does no longer appear in the domain, but only in the transformed equation. We will then call the branch $t \mapsto u_t$ continuously differentiable if the branch $t \mapsto \breve{u}_t$ has this property (with $\breve{u}_t$ denoting the transformed solution on the reference domain).

Transformation of the problem

Let $s \in I$ be fixed and $\varepsilon > 0$ small (to be chosen later). The domain Ω_s will serve as reference domain for all $t \in U_\varepsilon(s) := (s - \varepsilon, s + \varepsilon) \cap I$ and we will denote variables in Ω_s by $(\breve{x}, \breve{y})$. As before (x, y) denote variables in Ω_t. Recall that the "old" transformations $\phi_t^{(i)}$, which have been used troughout the previous section, were piecewise linear and Lipschitz continuous, which simplified many calculations. In this section it will however be necessary to define a new and smoother transformation $\psi_t : \overline{\Omega}_s \to \overline{\Omega}_t$ $(t \in U_\varepsilon(s))$, since the smoothness of the transformation is needed to prove differentiability of the transformed solution branch.

For $t \in U_\varepsilon(s)$ denote $\Gamma_t^{\text{in}} = \partial\left((-t, t)^2\right)$ and $\Gamma_t^{\text{out}} = \partial\left((-t - 1, t + 1)^2\right)$. We fix a smooth cut-off function $\chi_s \in C^\infty(\overline{\Omega}_s)$ with the following properties:

$$\begin{aligned}
\chi_s(\breve{x}, \breve{y}) &= 1 & \text{for all } (\breve{x}, \breve{y}) \in \Gamma_s^{\text{in}} \\
\chi_s(\breve{x}, \breve{y}) &= 0 & \text{for all } (\breve{x}, \breve{y}) \in \Gamma_s^{\text{out}} \\
\chi_s(\breve{x}, \breve{y}) &\in [0, 1] & \text{for all } (\breve{x}, \breve{y}) \in \Omega_s,
\end{aligned}$$

and define for $t \in U_\varepsilon(s)$:

$$\psi_t : \begin{cases} \overline{\Omega}_s &\to \overline{\Omega}_t \\ (\breve{x}, \breve{y}) &\mapsto \left(\tfrac{t}{s}\chi_s(\breve{x}, \breve{y}) + \tfrac{t+1}{s+1}\left(1 - \chi_s(\breve{x}, \breve{y})\right)\right)(\breve{x}, \breve{y}). \end{cases} \tag{7.31}$$

Clearly, $\psi_t \in C^\infty(\overline{\Omega}_t)$ and we have

$$\psi_t\left(\Gamma_s^{\text{in}}\right) = \left(\Gamma_t^{\text{in}}\right) \quad \text{and} \quad \psi_t\left(\Gamma_s^{\text{out}}\right) = \Gamma_t^{\text{out}}. \tag{7.32}$$

We will now prove that $\psi_t : \overline{\Omega}_s \to \overline{\Omega}_t$ is bijective if t is sufficiently close to s. For this purpose note that ψ_t can also be written as

$$\psi_t(\check{x}, \check{y}) = \left(\frac{t+1}{s+1} + \frac{t-s}{s(s+1)} \chi_s(\check{x}, \check{y}) \right) (\check{x}, \check{y}), \quad (\check{x}, \check{y}) \in \Omega_s.$$

Let $\varphi \in [0, 2\pi)$ be a fixed angle and consider the ray $R_\varphi := \{(r \cos \varphi, r \sin \varphi) \in \mathbb{R}^2, r > 0\}$. Since $\psi_t(\check{x}, \check{y}) = \lambda(\check{x}, \check{y})(\check{x}, \check{y})$ with $\lambda(\check{x}, \check{y}) \in \mathbb{R}$ it is immediately clear that $\psi_t(R_\varphi) \cap \overline{\Omega}_s \subset R_\varphi$. Moreover we have

$$\frac{\partial}{\partial r} \left(\psi_t(r \cos \varphi, r \sin \varphi) \right) =$$

$$\underbrace{\left[\frac{t+1}{s+1} + \frac{t-s}{s(s+1)} \left(\chi_s(r \cos \varphi, r \sin \varphi) + r(\nabla \chi_s)(r \cos \varphi, r \sin \varphi) \cdot \begin{pmatrix} \cos \varphi \\ \sin \varphi \end{pmatrix} \right) \right]}_{=:\zeta_s(t, r, \varphi)} (\cos \varphi, \sin \varphi).$$

$$(7.33)$$

Since $\chi_s \in C^\infty(\overline{\Omega}_s)$ we obtain

$$\max \left\{ \left| \chi_s(r \cos \varphi, r \sin \varphi) + r(\nabla \chi_s)(r \cos \varphi, r \sin \varphi) \cdot \begin{pmatrix} \cos \varphi \\ \sin \varphi \end{pmatrix} \right| : (r \cos \varphi, r \sin \varphi) \in \overline{\Omega}_s \right\} < \infty$$

and we can therefore choose $\varepsilon > 0$ such that for some prescribed $0 < \delta < \frac{1}{2}$ we obtain

$$\zeta_s(t, r, \varphi) > \delta > 0 \text{ for all } (r, \varphi) \text{ such that } (r \cos \varphi, r \sin \varphi) \in \overline{\Omega}_s \text{ and } |t - s| < \varepsilon.$$

Then (7.33), (7.32) imply that $\psi_t|_{R_\varphi \cap \overline{\Omega}_s} : R_\varphi \cap \overline{\Omega}_s \to R_\varphi \cap \overline{\Omega}_t$ is bijective for each $\varphi \in (0, 2\pi]$ and all $t \in U_\varepsilon(s)$, whence bijectivity of ψ_t follows for $t \in U_\varepsilon(s)$. With similar arguments, and by possibly decreasing ε a little further, $\det J[\psi_t](\check{x}, \check{y}) > 0$ for all $t \in U_\varepsilon(s)$ and $(\check{x}, \check{y}) \in \overline{\Omega}_s$ (note that $\psi_s = Id$ and therefore $\det J[\psi_s] = 1 > 0$). Thus the local inversion Theorem implies that for each $(x, y) \in \overline{\Omega}_t$ there exists a neighbourhood $U_{(\check{x}, \check{y})} \subset \overline{\Omega}_s$ of $(\check{x}, \check{y}) = \psi_t^{-1}(x, y)$ and a neighbourhood $V_{(x,y)} \subset \overline{\Omega}_t$ of (x, y) such that $\psi_t : U_{(\check{x}, \check{y})} \to V_{(x,y)}$ is bijective and $\psi_t^{-1} \in C^\infty(V_{(x,y)})$ since $\psi_t \in C^\infty(\overline{\Omega}_t)$. Thus we obtain $\psi_t^{-1} \in C^\infty(\overline{\Omega}_t)$ for all $t \in U_\varepsilon(s)$.

By denoting $\check{u} = u \circ \psi_t \in H_0^1(\Omega_s)$ and $\check{\varphi} = \varphi \circ \psi_t \in H_0^1(\Omega_s)$ for $u, \varphi \in H_0^1(\Omega_t)$, we obtain an equivalent transformed formulation of our given problem (1.2) as follows ($t \in U_\varepsilon(s)$):

$$\int_{\Omega_t} \nabla u \cdot \nabla \varphi \, d(x, y) = \int_{\Omega_t} |u|^3 \varphi \, d(x, y)$$

$$\iff \int_{\Omega_s} |\det J[\psi_t]| (\nabla \check{u})^T \left(J[\psi_t]^{-1} \circ \psi_t \right) \left(J[\psi_t]^{-T} \circ \psi_t \right) (\nabla \check{\varphi}) \, d(\check{x}, \check{y})$$

$$= \int_{\Omega_s} |\det J[\psi_t]| |\check{u}|^3 \check{\varphi} \, d(\check{x}, \check{y})$$

and therefore in strong formulation we have:

$$\begin{cases} -\Delta u = |u|^3 & \text{in } \Omega_t \\ u = 0 & \text{on } \partial \Omega_t \end{cases}$$

$$\iff \begin{cases} -\operatorname{div} \left(|\det J[\psi_t]| \left(J[\psi_t]^{-1} \circ \psi_t \right) \left(J[\psi_t]^{-T} \circ \psi_t \right) \nabla \check{u} \right) = |\det J[\psi_t]| |\check{u}|^3 & \text{in } \Omega_s \\ \check{u} = 0 & \text{on } \partial \Omega_s. \end{cases}$$

$$(7.34)$$

Defining

$$\breve{\mathcal{F}} : \begin{cases} U_\varepsilon(s) \times H_0^1(\Omega_s) & \to & H^{-1}(\Omega_s) \\ (t, \breve{u}) & \mapsto & -\operatorname{div}\left(|\det J[\psi_t]| \left(J[\psi_t]^{-1} \circ \psi_t\right)\left(J[\psi_t]^{-T} \circ \psi_t\right) \nabla \breve{u}\right) \\ & & -|\det J[\psi_t]||\breve{u}|^3 \end{cases} \quad (7.35)$$

(7.34), and therefore (1.2), is equivalent to

$$\breve{\mathcal{F}}(t, \breve{u}) = 0.$$

Note that since u_t is a solution of (1.2) for $t \in U_\varepsilon(s)$, we have $\breve{\mathcal{F}}(t, \breve{u}_t) = 0$ for all $t \in U_\varepsilon(s)$ where $\breve{u}_t = u_t \circ \psi_t$. The following theorem proves the desired smoothness of the solution branch:

Theorem 7. *The solution branch*

$$\begin{cases} U_\varepsilon(s) & \to & H_0^1(\Omega_s) \\ t & \mapsto & \breve{u}_t \end{cases}$$

is continuously differentiable.

Remark 11. We call the solution branch $(u_t)_{t \in U_\varepsilon(s)}$ continuously differentiable if the associated transformed branch $(\breve{u}_t)_{t \in U_\varepsilon(s)}$ has this property.

The main idea for the proof is similar to the one in the proof of [50, Theorem 4.1]. However, due to the construction of ω_t in (7.2) and (7.3), some technical difficulties arise and therefore we need the following three lemmas before we can prove Theorem 7.

Lemma 8. *Let $\hat{\psi}_\tau : \Omega_s \to \Omega_s$ be a C^0-family of Lipschitz-homeomorphisms such that $\|\hat{\psi}_\tau - Id\|_{L^\infty(\Omega_s)} \to 0$ and $\|J[\hat{\psi}_\tau] - I\|_{L^\infty(\Omega_s)} \to 0$ as $\tau \to 0$. Then*

$$\lim_{\tau \to 0} \|u \circ \hat{\psi}_\tau - u\|_{H_0^1(\Omega_s)} = 0 \quad \text{for all } u \in H_0^1(\Omega_s).$$

Note that in this Lemma and its proof we omit the accent $\breve{\ }$, since we are always working in the domain Ω_s and no confusion with other variables can arise.

Proof.   (i) As a first step we prove for all $u \in C_0^\infty(\Omega_s)$:

$$\|u \circ \hat{\psi}_\tau - u\|_{L^2(\Omega_s)} \to 0 \quad \text{as} \quad \tau \to 0.$$

For this purpose we fix $(x, y) \in \Omega_s$ and choose $\gamma \subset \overline{\Omega}_s$ to be the shortest piecewise C^1-path connecting $(x, y) =: \gamma(0)$ and $\hat{\psi}_\tau(x, y) =: \gamma(1)$. Then

$$\left|u(\hat{\psi}_\tau(x, y)) - u(x, y)\right| = \left|\int_0^1 (\nabla u)(\gamma(t)) \cdot \gamma'(t)| \, dt\right|$$

$$\leq \|\nabla u\|_{L^\infty} \int_0^1 |\gamma'(t)| \, dt = \|\nabla u\|_{L^\infty} L(\gamma),$$

where $L(\gamma)$ denotes the arc-length of the path γ. Since $\|\hat{\psi}_\tau - Id\|_{L^\infty} \to 0$ as $\tau \to 0$, $L(\gamma)$ is bounded by $2|(x, y) - \hat{\psi}_\tau(x, y)|$ for τ sufficiently small (recall $\Omega_s = (-s - 1, s + 1)^2 \backslash [-s, s]^2$). Therefore

$$\|u \circ \hat{\psi}_\tau - u\|_{L^2}^2 \leq 4\|\nabla u\|_{L^\infty}^2 \int_\Omega |(x, y) - \hat{\psi}_\tau(x, y)|^2 \, d(x, y) \leq C\|\hat{\psi}_\tau - Id\|_{L^\infty}^2 \to 0$$

$$(\tau \to 0).$$

(ii) We will now prove the assertion of the lemma for $u \in C_0^\infty(\Omega_s)$. Since $\|u\|_{H_0^1(\Omega_s)} \leq C\|\nabla u\|_{L^2(\Omega_s)}$ it suffices to show

$$\left\| \tfrac{\partial}{\partial x}(u \circ \hat{\psi}_\tau) - \tfrac{\partial u}{\partial x} \right\|_{L^2(\Omega_s)} \to 0 \quad \text{as} \quad \tau \to 0,$$

(and hence analogously $\|\tfrac{\partial}{\partial y}(u \circ \hat{\psi}_\tau) - \tfrac{\partial u}{\partial y}\|_{L^2(\Omega_s)} \to 0$ as $\tau \to 0$ follows).

Using the triangle inequality and $u \in C_0^\infty(\Omega_s)$ we obtain

$$
\begin{aligned}
\left\| \tfrac{\partial}{\partial x}(u \circ \hat{\psi}_\tau) - \tfrac{\partial u}{\partial x} \right\|_{L^2} &\leq \left\| \left((\nabla u)^T \circ \hat{\psi}_\tau - (\nabla u)^T \right) \tfrac{\partial \hat{\psi}_\tau}{\partial x} \right\|_{L^2} + \left\| (\nabla u)^T \left(\tfrac{\partial \hat{\psi}_\tau}{\partial x} - \left(\begin{smallmatrix}1\\0\end{smallmatrix}\right) \right) \right\|_{L^2} \\
&\leq \left\| \left((\nabla u)^T \circ \hat{\psi}_\tau - (\nabla u)^T \right) \left(\tfrac{\partial \hat{\psi}_\tau}{\partial x} - \left(\begin{smallmatrix}1\\0\end{smallmatrix}\right) \right) \right\|_{L^2} + \left\| \nabla u \circ \hat{\psi}_\tau - \nabla u \right\|_{L^2} \\
&\qquad\qquad\qquad\qquad\qquad\qquad + C \left\| J[\hat{\psi}_\tau] - I \right\|_{L^\infty} \\
&\leq \left(\left\| \tfrac{\partial u}{\partial x} \circ \hat{\psi}_\tau - \tfrac{\partial u}{\partial x} \right\|_{L^2} + \left\| \tfrac{\partial u}{\partial y} \circ \hat{\psi}_\tau - \tfrac{\partial u}{\partial y} \right\|_{L^2} \right) \left(\left\| J[\hat{\psi}_\tau] - I \right\|_{L^\infty} + 1 \right) \\
&\qquad\qquad\qquad\qquad\qquad\qquad + C \left\| J[\hat{\psi}_\tau] - I \right\|_{L^\infty}, \qquad\qquad (7.36)
\end{aligned}
$$

where the constant C depends on u. Since $\tfrac{\partial u}{\partial x}, \tfrac{\partial u}{\partial y} \in C_0^\infty(\Omega_s)$, step (i) and $\|J[\hat{\psi}_\tau] - I\|_{L^\infty} \to 0$, $\tau \to 0$, imply the assertion.

(iii) Let $u \in H_0^1(\Omega_s)$ and $\delta > 0$ be arbitrary. Then there exists $v \in C_0^\infty(\Omega_s)$ such that, for all τ sufficiently small ($|\tau| < \tilde{\tau}(\delta)$),

$$\|u \circ \hat{\psi}_\tau - v \circ \hat{\psi}_\tau\|_{H_0^1} < \tfrac{\delta}{3}$$

as well as

$$\|u - v\|_{H_0^1} < \tfrac{\delta}{3}.$$

This follows from the fact that $C_0^\infty(\Omega_s) \subset H_0^1(\Omega_s)$ is dense and

$$
\begin{aligned}
\|u \circ \hat{\psi}_\tau - v \circ \hat{\psi}_\tau\|_{H_0^1}^2 &= \int_{\Omega_s} \left[|\nabla(u \circ \hat{\psi}_\tau) - \nabla(v \circ \hat{\psi}_\tau)|^2 + (u \circ \hat{\psi}_\tau - v \circ \hat{\psi}_\tau)^2 \right] d(x,y) \\
&\leq \int_{\Omega_s} |\det(J[\hat{\psi}_\tau]^{-1}) \circ \hat{\psi}_\tau^{-1}| \left(|J[\hat{\psi}_\tau] \circ \hat{\psi}_\tau^{-1}|^2 |\nabla u - \nabla v|^2 + |u - v|^2 \right) d(x,y) \\
&\leq C\|u - v\|_{H_0^1},
\end{aligned}
$$

where we used $\|J[\hat{\psi}_\tau] - I\|_{L^\infty} \to 0$, implying in particular boundedness of $J[\hat{\psi}_\tau]^{-1}$.

By step (ii) we have

$$\|v \circ \hat{\psi}_\tau - v\|_{H_0^1} < \tfrac{\delta}{3}$$

for all τ sufficiently small and together with the above we obtain

$$\|u \circ \hat{\psi}_\tau - u\|_{H_0^1} \leq \|u \circ \hat{\psi}_\tau - v \circ \hat{\psi}_\tau\|_{H_0^1} + \|v \circ \hat{\psi}_\tau - v\|_{H_0^1} + \|u - v\|_{H_0^1} < \delta.$$

Since $\delta > 0$ was arbitrary the assertion of the lemma follows.

$\square$

Before we state and prove the next lemma, we recall the definition of approximate solutions $\omega_t \in H_0^1(\Omega_t)$ for $t \in (t_{i-1}, t_i]$ (given in (7.2) and (7.3)). Using the transformation $\phi_t^{(i)} : \Omega_{t_i} \to \Omega_t$, given in (7.7) and (7.8), we have

$$\tilde{\omega}_t = \frac{t_i - t}{t_i - t_{i-1}} \underbrace{\omega_{t_{i-1}} \circ \phi_{t_{i-1}}^{(i)}}_{=\tilde{\omega}_{t_{i-1}}} + \frac{t - t_{i-1}}{t_i - t_{i-1}} \omega_{t_i} \in H_0^1(\Omega_{t_i})$$

$$\omega_t = \tilde{\omega}_{t_i} \circ (\phi_t^{(i)})^{-1} \in H_0^1(\Omega_t),$$

where $\omega_{t_{i-1}} \in H_0^1(\Omega_{t_{i-1}})$ and $\omega_{t_i} \in H_0^1(\Omega_{t_i})$ are approximate solutions to (1.2) with $t = t_{i-1}$ and $t = t_i$, respectively.

Lemma 9. *There exists some $0 < \varepsilon_2 \leq \varepsilon$ such that the mapping*

$$\begin{cases} U_{\varepsilon_2}(s) & \to & H_0^1(\Omega_s) \\ t & \mapsto & \breve{\omega}_t = \omega_t \circ \psi_t \end{cases} \tag{7.37}$$

is continuous.

Proof. <u>Case 1:</u> $s \neq t_j$ for all $j \in \{0, \ldots, n\}$, i.e. there exists a unique $i \in \{0, \ldots, n\}$ and some $\varepsilon_2 > 0$ such that $(s - \varepsilon_2, s + \varepsilon_2) \subset (t_{i-1}, t_i)$. In this case we have for all $t \in (s - \varepsilon_2, s + \varepsilon_2)$: $\omega_t = \tilde{\omega}_t \circ (\phi_t^{(i)})^{-1}$ and thus

$$\breve{\omega}_t = \omega_t \circ \psi_t = \tilde{\omega}_t \circ (\phi_t^{(i)})^{-1} \circ \psi_t \in H_0^1(\Omega_s).$$

Since $t \in (t_{i-1}, t_i)$, the mappings

$$\begin{cases} (s - \varepsilon_2, s + \varepsilon_2) & \to & H_0^1(\Omega_{t_i}) \\ t & \mapsto & \tilde{\omega}_t \end{cases}$$

and

$$\begin{cases} (s - \varepsilon_2, s + \varepsilon_2) & \to & C(\Omega_s, \Omega_{t_i}) \\ t & \mapsto & (\phi_t^{(i)})^{-1} \circ \psi_t \end{cases}$$

are continuous by construction of $\tilde{\omega}_t$, $\phi_t^{(i)}$ and ψ_t. This proves the desired continuity of the mapping in (7.37) in $s \neq t_j$ $(j = 1, \ldots, n)$.

<u>Case 2:</u> There exists some $i \in \{1, \ldots, n\}$ such that $s = t_{i-1}$. We choose some $\varepsilon_2 > 0$ such that $(s, s + \varepsilon_2) \subset (t_{i-1}, t_i]$. Note that in this case it is sufficient to prove right-hand continuity in s, since left-hand continuity follows as in case 1.

For $t \in (s, s + \varepsilon_2) \subset (t_{i-1}, t_i]$ we have again $\omega_t = \tilde{\omega}_t \circ (\phi_t^{(i)})^{-1}$ and thus

$$\breve{\omega}_t = \omega_t \circ \psi_t = \tilde{\omega}_t \circ (\phi_t^{(i)})^{-1} \circ \psi_t \in H_0^1(\Omega_s).$$

For $t = s = t_{i-1}$ we have $\breve{\omega}_s = \omega_s \circ \psi_s \overset{\psi_s = Id}{=} \omega_{t_{i-1}}$ and the desired right-continuity follows if we can prove

$$\lim_{t \to t_{i-1}^+} \|\omega_t \circ \psi_t - \omega_{t_{i-1}}\|_{H_0^1(\Omega_{t_{i-1}})} = 0.$$

Using the definition of $\tilde{\omega}_t$ (by linear interpolation, see (7.2)) we obtain

$$
\begin{aligned}
\omega_t \circ \psi_t - \omega_{t_{i-1}} &= \tilde{\omega}_t \circ (\phi_t^{(i)})^{-1} \circ \psi_t - \omega_{t_{i-1}} \\
&= \tfrac{t_i - t}{t_i - t_{i-1}} \tilde{\omega}_{t_{i-1}} \circ (\phi_t^{(i)})^{-1} \circ \psi_t + \tfrac{t - t_{i-1}}{t_i - t_{i-1}} \omega_{t_i} \circ (\phi_t^{(i)})^{-1} \circ \psi_t - \omega_{t_{i-1}} \\
&\overset{\tilde{\omega}_{t_{i-1}} = \omega_{t_{i-1}} \circ \phi_{t_{i-1}}^{(i)}}{=} \tfrac{t_i - t}{t_i - t_{i-1}} \omega_{t_{i-1}} \circ \phi_{t_{i-1}}^{(i)} \circ (\phi_t^{(i)})^{-1} \circ \psi_t + \tfrac{t - t_{i-1}}{t_i - t_{i-1}} \omega_{t_i} \circ (\phi_t^{(i)})^{-1} \circ \psi_t - \omega_{t_{i-1}} \\
&= \omega_{t_{i-1}} \circ \phi_{t_{i-1}}^{(i)} \circ (\phi_t^{(i)})^{-1} \circ \psi_t - \omega_{t_{i-1}} \\
&\quad + \tfrac{t - t_{i-1}}{t_i - t_{i-1}} \left[\omega_{t_i} \circ (\phi_t^{(i)})^{-1} \circ \psi_t - \omega_{t_{i-1}} \circ \phi_{t_{i-1}}^{(i)} \circ (\phi_t^{(i)})^{-1} \circ \psi_t \right].
\end{aligned} \tag{7.38}
$$

First consider $(\phi_t^{(i)})^{-1} \circ \psi_t : \Omega_{t_{i-1}} \to \Omega_{t_i}$ (note that $\psi_t : \Omega_{t_{i-1}} \to \Omega_t$ since $s = t_{i-1}$). Using the definition of $\phi_t^{(i)}$ in (7.7), (7.8), together with the required properties of the coefficients $a_j, b_j, c_j^{(1)}, c_j^{(2)}$ thereafter, and the construction of ψ_t in (7.31), we immediately obtain that $\left((\phi_t^{(i)})^{-1} \circ \psi_t \right)_{t \in (t_{i-1}, t_{i-1} + \varepsilon_2)}$ is a C^0-family of Lipschitz homeomorphisms satisfying

$$
\| (\phi_t^{(i)})^{-1} \circ \psi_t - Id \|_{L^\infty(\Omega_{t_{i-1}})} \to 0 \quad \text{as} \quad t \to t_{i-1}^+ \tag{7.39}
$$

and

$$
\| J[(\phi_t^{(i)})^{-1} \circ \psi_t] - I \|_{L^\infty(\Omega_{t_{i-1}})} \to 0 \quad \text{as} \quad t \to t_{i-1}^+. \tag{7.40}
$$

Moreover, (7.39) and (7.40) imply that $\left(\phi_{t_{i-1}}^{(i)} \circ (\phi_t^{(i)})^{-1} \circ \psi_t \right)_{t \in (t_{i-1}, t_{i-1} + \varepsilon_2)}$ is a C^0-family of Lipschitz homeomorphisms on $\Omega_{t_{i-1}}$ satisfying

$$
\| \phi_{t_{i-1}}^{(i)} \circ (\phi_t^{(i)})^{-1} \circ \psi_t - Id \|_{L^\infty(\Omega_{t_{i-1}})} \to 0 \quad \text{as} \quad t \to t_{i-1}^+ \tag{7.41}
$$

and

$$
\| J[\phi_{t_{i-1}}^{(i)} \circ (\phi_t^{(i)})^{-1} \circ \psi_t] - I \|_{L^\infty(\Omega_{t_{i-1}})} \to 0 \quad \text{as} \quad t \to t_{i-1}^+. \tag{7.42}
$$

By Lemma 8 it therefore follows that

$$
\| \omega_{t_{i-1}} \circ \phi_{t_{i-1}}^{(i)} \circ (\phi_t^{(i)})^{-1} \circ \psi_t - \omega_{t_{i-1}} \|_{H_0^1(\Omega_{t_{i-1}})} \to 0 \quad \text{as} \quad t \to t_{i-1}^+.
$$

To prove that the H_0^1- norm of the second part in (7.38) tends to zero it is sufficient to show that

$$
\| \omega_{t_i} \circ (\phi_t^{(i)})^{-1} \circ \psi_t \|_{H_0^1(\Omega_{t_{i-1}})} \tag{7.43}
$$

as well as

$$
\| \omega_{t_{i-1}} \circ \phi_{t_{i-1}}^{(i)} \circ (\phi_t^{(i)})^{-1} \circ \psi_t \|_{H_0^1(\Omega_{t_{i-1}})} \tag{7.44}
$$

are uniformly bounded for $t \in (t_{i-1}, t_{i-1} + \varepsilon_2)$. For (7.43) this follows directly from (7.39) and (7.40) and similarly (7.41) and (7.42) imply the assertion for (7.44).

This finally proves right-hand continuity in $s = t_{i-1}$. $\square$

Lemma 10. *Let* $0 < \varepsilon_1 < \varepsilon$ *and*

$$
\begin{cases}
U_{\varepsilon_1}(s) & \to & H_0^1(\Omega_s) \\
t & \mapsto & \breve{u}_t
\end{cases}
$$

be a C^1-smooth mapping. Then the mapping

$$\begin{cases} U_{\varepsilon_1}(s) & \to & \mathbb{R} \\ t & \mapsto & \|\breve{u}_t \circ \psi_t^{-1} - \omega_t\|_{H_0^1(\Omega_t)} \end{cases} \tag{7.45}$$

is continuous.

Proof. We will only prove continuity of $t \mapsto \|\nabla(\breve{u}_t \circ \psi_t^{-1} - \omega_t)\|_{L^2(\Omega_t)}$, since continuity of $t \mapsto \|\breve{u}_t \circ \psi_t^{-1} - \omega_t\|_{L^2}$ can be proven by similar ideas, but with much less effort. Using the Transformation Theorem again, we obtain (note that $\omega_t = \omega_t \circ \psi_t \circ \psi_t^{-1} = \breve{\omega}_t \circ \psi_t^{-1}$):

$$\left\|\nabla(\breve{u}_t \circ \psi_t^{-1} - \omega_t)\right\|_{L^2(\Omega_t)}^2 =$$
$$\int_{\Omega_s} |\det J[\psi_t]| \left[(\nabla\breve{u}_t - \nabla\breve{\omega}_t)^T (J[\psi_t]^{-1}\circ\psi_t)(J[\psi_t]^{-T}\circ\psi_t)(\nabla\breve{u}_t - \nabla\breve{\omega}_t) \right] d(\breve{x}, \breve{y}).$$

Let $t_0 \in U_{\varepsilon_1}(s)$ be fixed and $t \in U_{\varepsilon_1}(s)$. Then, using the triangle inequality, we can estimate (writing $J[t] := J[\psi_t]^{-T}\circ\psi_t$ to shorten the notation):

$$\left| \int_{\Omega_s} |\det J[\psi_t]| \left[(\nabla\breve{u}_t - \nabla\breve{\omega}_t)^T J[t]^T J[t](\nabla\breve{u}_t - \nabla\breve{\omega}_t) \right] d(\breve{x}, \breve{y}) - \right.$$
$$\left. \int_{\Omega_s} |\det J[\psi_{t_0}]| \left[(\nabla\breve{u}_{t_0} - \nabla\breve{\omega}_{t_0})^T J[t_0]^T J[t_0](\nabla\breve{u}_{t_0} - \nabla\breve{\omega}_{t_0}) \right] d(\breve{x}, \breve{y}) \right|$$
$$\leq \int_{\Omega_s} \left| |\det J[\psi_t]| - |\det J[\psi_{t_0}]| \right| |J[t]|^2 |\nabla\breve{u}_t - \nabla\breve{\omega}_t|^2 \, d(\breve{x}, \breve{y})$$
$$+ \int_{\Omega_s} |\det J[\psi_{t_0}]| \left| J[t]^T J[t] - J[t_0]^T J[t_0] \right| |\nabla\breve{u}_t - \nabla\breve{\omega}_t|^2 \, d(\breve{x}, \breve{y})$$
$$+ 2\int_{\Omega_s} |\det J[\psi_{t_0}]| |J[t_0]^T J[t_0]| |\nabla\breve{u}_t - \nabla\breve{u}_{t_0} - (\nabla\breve{\omega}_t - \nabla\breve{\omega}_{t_0})| |\nabla\breve{u}_{t_0} - \nabla\breve{\omega}_{t_0}| \, d(\breve{x}, \breve{y})$$
$$+ \int_{\Omega_s} |\det J[\psi_{t_0}]| |J[t_0]^T J[t_0]| |\nabla\breve{u}_t - \nabla\breve{u}_{t_0} - (\nabla\breve{\omega}_t - \nabla\breve{\omega}_{t_0})|^2 \, d(\breve{x}, \breve{y}). \tag{7.46}$$

By assumption $t \mapsto \breve{u}_t$ is a C^1-smooth branch and Lemma 9 yields continuity of $t \mapsto \breve{\omega}_t$. Since moreover $t \to \psi_t$ is continuous it follows that all terms on the right-hand side of (7.46) tend to 0 as $t \to t_0$ (note that continuity of the mappings implies in particular boundedness of the terms depending on t, for t close to t_0). $\qquad\square$

Proof of Theorem 7. The mapping $\breve{\mathcal{F}}$ defined in (7.35) is continuously differentiable since $\varepsilon > 0$ was chosen such that ψ_t is invertible and $\psi_t^{-1} \in C^\infty(\Omega_t)$ for all $t \in U_\varepsilon(s)$. Using $\psi_s = Id$, implying $\breve{u}_s = u_s \circ \psi_s = u_s$, we obtain

$$\frac{\partial\breve{\mathcal{F}}}{\partial\breve{u}}(s, \breve{u}_s) = -\Delta - 3|u_s|u_s = L_{u_s},$$

which is bijective by (N) from page 83. Thus by the Implicit Function Theorem there exists $0 < \varepsilon_1 \leq \varepsilon$ and a branch

$$\begin{cases} U_{\varepsilon_1}(s) & \to & H_0^1(\Omega_s) \\ t & \mapsto & \hat{u}_t, \end{cases}$$

which is a C^1-smooth solution branch of problem (7.34) with $\hat{u}_s = \breve{u}_s = u_s$. By assumption we have (note that $\breve{\omega}_s = \omega_s$):

$$\|\hat{u}_s - \omega_s\|_{H_0^1(\Omega_s)} \leq \alpha_s. \tag{7.47}$$

By Lemma 10 the mapping

$$\begin{cases} U_{\varepsilon_1}(s) & \to & \mathbb{R} \\ t & \mapsto & \|\hat{u}_t \circ \psi_t^{-1} - \omega_t\|_{H_0^1(\Omega_t)} \end{cases} \tag{7.48}$$

is continuous and since moreover $t \mapsto \alpha_t$ is lower semicontinuous, (7.47) implies the existence of $0 < \varepsilon_2 \leq \varepsilon_1$ such that

$$\|\hat{u}_t \circ \psi_t^{-1} - \omega_t\|_{H_0^1(\Omega_t)} \leq \alpha_t + \eta, \quad \text{for all } t \in U_{\varepsilon_2}(s).$$

Hence, (U) from page 83 implies

$$\hat{u}_t \circ \psi_t^{-1} = u_t \qquad \text{for all } t \in U_{\varepsilon_2}(s)$$

and therefore

$$\hat{u}_t = u_t \circ \psi_t = \breve{u}_t \qquad \text{for all } t \in U_{\varepsilon_2}(s).$$

Thus the desired smoothness of $t \mapsto \breve{u}_t$ in some neighbourhood of s follows. $\qquad\square$

Theorem 7 proves continuous differentiability of $t \mapsto u_t$ (with continuous differentiability of this mapping as defined in Remark 11) in a neighbourhood of $s \in I$. Repeating the argument for any $s \in I$, we therefore obtain a continuously differentiable branch $(u_t)_{t \in I}$ of solutions to problem (1.2).

In particular, Theorem 7 can be applied to the solutions u_t, $t \in [1.5, 3]$ obtained in Theorem 6; cf. Remark 9 (b) for lower semicontinuity of $t \mapsto \alpha_t$ and the existence of η satisfying (7.30).

8 Unbounded L-shaped Domain

In the previous chapters we were concerned with the equation $-\Delta u - |u|^3 = 0$ on some bounded domain with homogeneous Dirichlet boundary conditions. We will now consider a similar problem, but stated on the unbounded L-shaped domain $\Omega = ((-1, \infty) \times (0, 1)) \cup (-1, 0) \times (-\infty, 1))$. We will start with a motivation for this problem and then recall the main steps for a computer-assisted proof.

8.1 Motivation

The main inspiration for considering our problem on an unbounded L-shaped domain is given by two papers of Ackermann, Clapp and Pacella ([1] and [2]) which are both concerned with the equation $-\Delta u + \lambda u = f(u)$ on expanding tubular domains together with Dirichlet boundary conditions. In order to understand their approach, we will repeat some of the main results and ideas here. We will focus on [1], in which only positive solutions are considered.

Let $N \geq 2$, $1 \leq k \leq N-1$ and M be a compact k-dimensional smooth submanifold of $\mathbb{R}^N$ without boundary. For $R > 0$ sufficiently large define Ω_R to be the open tubular neighbourhood of radius 1 of the expanded manifold $M_R := \{Rx : x \in M\}$, i.e.

$$\Omega_R := \bigcup_{x \in M} \left\{ Rx + v : v \in (T_x M)^\perp, |v| < 1 \right\},$$

where $T_x M$ denotes the tangent space of M at x. For $\lambda > -\lambda_1$ (λ_1 being the first Dirichlet eigenvalue of $-\Delta$ in the unit ball in $\mathbb{R}^{N-k}$) consider the problem

$$\begin{cases} -\Delta u + \lambda u &= f(u) \quad \text{in } \Omega_R \\ u &= 0 \qquad \text{on } \partial \Omega_R. \end{cases} \tag{8.1}$$

There are some general hypotheses on differentiability and growth of f which we do not repeat here, but which are e.g. satisfied in case $f(u) = |u|^3$.

Next, define

$$\mathbb{L} := \{(\xi, \eta) \in \mathbb{R}^k \times \mathbb{R}^{N-k} : |\eta| < 1\},$$

which is the open cylinder (or in case $N = 1, k = 1$ an open strip) and describes locally the limit of Ω_R as $R \to \infty$. The main idea is to use ground state solutions of the problem

$$\begin{cases} -\Delta u + \lambda u &= f(u) \quad \text{in } \mathbb{L} \\ u &= 0 \qquad \text{on } \partial \mathbb{L} \end{cases} \tag{8.2}$$

as building blocks for multibump solutions of (8.1). Assume that (8.2) has a positive solution U which is radially symmetric in ξ and η separately, and is non-degenerate in the sense that the solution space to the problem

$$-\Delta u + \lambda u = f'(U)u, \quad u \in H_0^1(\mathbb{L})$$

has dimension k. Finally, for each $x \in M_R$ let $A_x \in O(N)$ be a linear isometry mapping the tangent space $T_x M$ onto $\mathbb{R}^k \times \{0\}$ and $(T_x M)^\perp$ onto $\{0\} \times \mathbb{R}^{N-k}$, and set

$$U_{x,R} := U(A_x(y-x)) \quad (y \in \mathbb{R}^N),$$

where U is extended by 0 to all of $\mathbb{R}^N$. The main theorem of [1] proves the existence of solutions to (8.1) for sufficiently large R:

Theorem 8. *For each $n \in \mathbb{N}$ there exist $R_n > 0$ such that for every $R \geq R_n$ there are n points $x_{R,1}, \ldots, x_{R,n} \in M_R$ and a positive solution u_R of* (8.1) *of the form*

$$u_R = \sum_{i=1}^{n} U_{x_{R,i},R} + o(1)$$

in $H^1(\mathbb{R}^N)$ as $R \to \infty$. Moreover $|x_{R,i} - x_{R,j}| \to \infty$ as $R \to \infty$ for $i \neq j$.

The basic idea of the proof is glueing rotated translates of the positive ground state solution U and using a Lyapunov-Schmidt reduction argument.

Due to corners in our domain Ω_t this result cannot be applied directly to problem (1.2), although it might be possible, with some additional arguments, to construct solutions with bumps on the edges of Ω_t (far away from the corners). Our aim is to prove - by computer-assisted means - a suitable "one-bump" solution $u \in H_0^1(\Omega)$ that may serve as a building block for solutions of (3.10), as $t \to \infty$, with bumps in the corners of Ω_t. The actual construction of these kinds of solutions will is not part of this thesis, instead we present another method to prove existence of certain bump-solutions for all $t > \hat{t}$ for some suitable $\hat{t}$ in section 9.

8.2   Existence of a Solution by Computer-assistance

We first note that Theorem 1, which is our main existence and enclosure theorem, is also valid in case of unbounded domains. In order to apply this theorem to

$$\begin{cases} -\Delta u &= |u|^3 \quad \text{in } \Omega \\ u &= 0 \qquad \text{on } \partial\Omega, \end{cases} \tag{8.3}$$

with $\Omega = ((-1,\infty) \times (0,1)) \cup (-1,0) \times (-\infty, 1))$, we need to compute an approximate solution $\omega \in H_0^1(\Omega)$ as well as constants δ and K such that

$$\| - \Delta\omega - |\omega|^3 \|_{H^{-1}(\Omega)} \leq \delta \tag{8.4}$$

and

$$\|v\|_{H_0^1(\Omega)} \leq K \|L_\omega[v]\|_{H^{-1}(\Omega)} \quad \text{for all } v \in H_0^1(\Omega) \tag{8.5}$$

are satisfied. As before,

$$L_\omega : H_0^1(\Omega) \to H^{-1}(\Omega), \; L_\omega[v] = -\Delta v - 3|\omega|\omega v$$

denotes the linearized operator at the approximate solution ω.

8.2.1   Computation of an approximate solution

For the computation of an approximate solution we will use a similar procedure as for the problem on a bounded domain, i.e. we first compute an approximate solution by means of Finite Elements and improve it by using a corner singular function. Since the computer cannot handle an unbounded domain, we have to restrict ourselves to a bounded subdomain $\Omega^T = \Omega \cap (-T, T)^2$ ($T > 0$), which contains the corner part of Ω and cuts off the infinite legs of the domain. Using the methods described in chapter 3 (Mountain Pass Algorithm and Newton method), we compute an approximate solution $\omega^c \in V_N^D(\Omega^T)$ of the following problem:

$$\begin{cases} -\Delta u & = & |u|^3 & \text{in } \Omega^T \\ u & = & 0 & \text{on } \partial\Omega^T. \end{cases} \tag{8.6}$$

Starting the Mountain Pass Algorithm with an initial guess possessing a bump centered in the corner we obtain an approximate solution having the same property. Figure 8.1 shows ω^c.
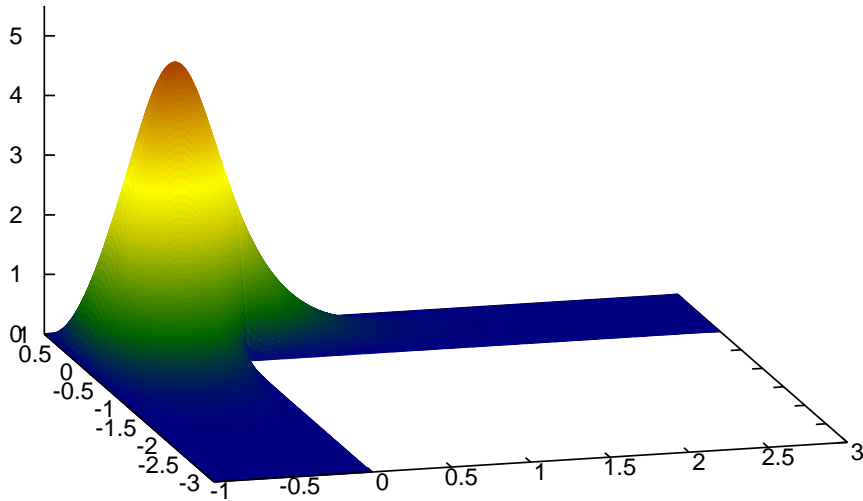
Figure 8.1: Plot of ω^c

Since Ω^T has a re-entrant corner, we will again use a corner singular function to obtain an approximate solution with improved (i.e. smaller) defect. Denoting by (x, y) cartesian coordinates and by (r, φ) local polar coordinates at $(0, 0)$, we define

corner singular function: $\gamma(r, \varphi) = r^{\frac{2}{3}} \sin\left(\frac{2}{3}\varphi\right)$

cut-off function: $\lambda(x, y) = (1 - x^2)^2(1 - y^2)^2 \chi_{(-1,1)^2}(x, y)$

and the new approximate solution (denoted by ω^c again)

$$\omega^c = \tilde{a}\lambda\gamma + \tilde{v}^c, \tag{8.7}$$

where $\tilde{a} \in \mathbb{R}$ denotes the corresponding approximate stress intensity factor and $\tilde{v}^c \in V_N^D(\Omega^T)$ a Finite Element approximation of the regular part. The computation of $\tilde{a}$ and $\tilde{v}^c$ can be done analogously to section 3.2.3 (keeping in mind that we have only one re-entrant corner here).

In order to obtain an approximate solution on Ω, we extend ω^c and $\tilde{v}^c$ by zero in $\Omega \backslash \overline{\Omega^T}$:

$$\omega = \begin{cases} \omega^c & \text{in } \Omega^T \\ 0 & \text{in } \Omega \backslash \overline{\Omega^T} \end{cases}, \qquad \tilde{v} = \begin{cases} \tilde{v}^c & \text{in } \Omega^T \\ 0 & \text{in } \Omega \backslash \overline{\Omega^T} \end{cases}. \tag{8.8}$$

Since $\omega^c, \tilde{v}^c \in H_0^1(\Omega^T)$ we have $\omega, \tilde{v} \in H_0^1(\Omega)$.

8.2.2   Computation of the defect

To compute a bound for the defect we follow the procedure in section 4.1 and estimate the H^{-1}-norm by a sum of two L^2-norms. For this purpose we need an approximation $\tilde{\rho} \in H(\mathrm{div}, \Omega)$ of the gradient $\nabla \omega$, which is constructed as follows: First compute $\tilde{\rho}^c = \begin{pmatrix} \tilde{\rho}_1^c \\ \tilde{\rho}_2^c \end{pmatrix} \in (V_N)^2$ such that $\tilde{\rho}^c \approx \nabla \tilde{v}$ and $-\mathrm{div}\,\tilde{\rho}^c \approx \tilde{a}\Delta(\lambda\gamma) + |\omega^c|^3$. Moreover we require $\tilde{\rho}_1^c(T, y) = \tilde{\rho}_2^c(x, -T) = 0$ for $x, y \in (0, 1)$. The latter condition assures that

$$\tilde{\rho} = \begin{cases} \tilde{\rho}^c & \text{in} & \Omega^T \\ 0 & \text{in} & \Omega \backslash \overline{\Omega^T} \end{cases}$$

is an element of $H(\mathrm{div}, \Omega)$.

Analogously as in the beginning of section 4.1 we can estimate

$$\| -\Delta\omega - |\omega|^3 \|_{H^{-1}(\Omega)} \leq \| \nabla\tilde{v} - \tilde{\rho} \|_{L^2(\Omega)} + C_2 \left\| -\mathrm{div}\,\tilde{\rho} - \tilde{a}\Delta(\lambda\gamma) - |\tilde{a}\lambda\gamma + \tilde{v}|^3 \right\|_{L^2(\Omega)}$$
$$= \| \nabla\tilde{v}^c - \tilde{\rho}^c \|_{L^2(\Omega^T)} + C_2 \left\| -\mathrm{div}\,\tilde{\rho}^c - \tilde{a}\Delta(\lambda\gamma) - |\tilde{a}\lambda\gamma + \tilde{v}^c|^3 \right\|_{L^2(\Omega^T)},$$

where C_2 denotes an embedding constant for the embedding $H_0^1(\Omega) \hookrightarrow L^2(\Omega)$. Upper bounds for the L^2-norms can be computed as described before.

For later purposes we define $\rho^c := \tilde{a}\nabla(\lambda\gamma) + \tilde{\rho}^c$ and remark that $\omega^c = \tilde{a}\lambda\gamma + \tilde{v}^c$ gives

$$\| \nabla\tilde{v}^c - \tilde{\rho}^c \|_{L^2(\Omega^T)} = \| \nabla\omega^c - \rho^c \|_{L^2(\Omega^T)}$$
$$\left\| -\mathrm{div}\,\tilde{\rho}^c - \tilde{a}\Delta(\lambda\gamma) - |\tilde{a}\lambda\gamma + \tilde{v}^c|^3 \right\|_{L^2(\Omega^T)} = \left\| -\mathrm{div}\,\rho^c - |\omega^c|^3 \right\|_{L^2(\Omega^T)}.$$

8.2.3   Bound for the inverse of the linearization

As in section 5.1 we use the isometric isomorphism $\Phi : H_0^1(\Omega) \to H^{-1}(\Omega)$ defined in (2.5), to obtain
$$\| L_\omega[v] \|_{H^{-1}} = \| (\Phi^{-1}L_\omega)[v] \|_{H_0^1} \qquad \text{for all } v \in H_0^1(\Omega),$$
which shows that condition (8.5) is equivalent to

$$\| v \|_{H_0^1} \leq K \| (\Phi^{-1}L_\omega)[v] \|_{H_0^1}.$$

By Lemma 3 it follows that the previous inequality is satisfied if

$$\gamma := \min\{|\nu| : \nu \text{ is in the spectrum of } \Phi^{-1}L_\omega\} > 0$$

and in the affirmative case one can choose any $K \geq \frac{1}{\gamma}$. Thus we are again left to compute bounds for the spectrum of $\Phi^{-1}L_\omega$. In section 5.1 we continued by showing that a certain operator was compact, thereby proving that the essential spectrum of $\Phi^{-1}L_\omega$ consisted only of the point $\{1\}$. This compactness is however lacking in our case since the domain Ω is now unbounded and we

have to use a different approach to bound the essential spectrum of $\Phi^{-1}L_\omega$. We follow the procedure in [26, Example 1.8].

First consider the operator $L_0 : H_0^1(\Omega) \to H^{-1}(\Omega)$, $v \mapsto -\Delta v + \left(\frac{\pi^2}{\pi^2+1} \chi_{\Omega^0} \right) v$, where $\Omega^0 = (-1,0) \times (0,1)$. Since both ω and χ_{Ω^0} have compact support, $\Phi^{-1}L_\omega - \Phi^{-1}L_0 : H_0^1(\Omega) \to H_0^1(\Omega)$ is compact and hence a well-known perturbation result in [40] yields $\sigma_{\mathrm{ess}}(\Phi^{-1}L_\omega) = \sigma_{\mathrm{ess}}(\Phi^{-1}L_0)$. To bound $\sigma_{\mathrm{ess}}(\Phi^{-1}L_0)$ we consider Rayleigh quotients: $\Omega \backslash \Omega^0$ is the union of two semi-infinite strips, on each of which the Rayleigh quotient $\frac{\|\nabla u\|_{L^2}^2}{\|u\|_{L^2}^2}$ is bounded from below by π^2. Thus we obtain for all $u \in H_0^1(\Omega)$:

$$\int_{\Omega \backslash \Omega^0} |\nabla u|^2 \, dx \geq \frac{\pi^2}{\pi^2+1} \int_{\Omega \backslash \Omega^0} \left[|\nabla u|^2 + u^2 \right] \, dx. \tag{8.9}$$

Furthermore the trivial estimate $1 > \frac{\pi^2}{\pi^2+1}$ implies

$$\int_{\Omega^0} \left[|\nabla u|^2 + \frac{\pi^2}{\pi^2+1} u^2 \right] \, dx \geq \frac{\pi^2}{\pi^2+1} \int_{\Omega^0} \left[|\nabla u|^2 + u^2 \right] \, dx. \tag{8.10}$$

Adding (8.9) and (8.10) gives, for all $u \in H_0^1(\Omega)$:

$$\int_{\Omega} \left[|\nabla u|^2 + \left(\frac{\pi^2}{\pi^2+1} \chi_{\Omega^0} \right) u^2 \right] \, dx \geq \frac{\pi^2}{\pi^2+1} \|u\|_{H_0^1}^2$$

and the left-hand side equals $\langle \Phi^{-1}L_0 u, u \rangle_{H_0^1}$. So the Rayleigh quotient, and hence the spectrum, and in particular the essential spectrum of $\Phi^{-1}L_0$ is bounded from below by $\frac{\pi^2}{\pi^2+1}$. Hence we conclude $\sigma_{\mathrm{ess}}(\Phi^{-1}L_\omega) \subset \left[\frac{\pi^2}{\pi^2+1}, \infty \right)$, implying that the essential spectrum of $\Phi^{-1}L_\omega$ is indeed bounded away from zero.

As in section 5.1 we see that for an eigenpair $(\nu, u) \in \mathbb{R} \times H_0^1(\Omega)$ of $\Phi^{-1}L_\omega$ we have

$$\underbrace{\int_{\Omega} [\nabla u \cdot \nabla \varphi + u\varphi] \, dx}_{=\langle u, \varphi \rangle_{H_0^1}} = \kappa \underbrace{\int_{\Omega} (1 + 3|\omega|\omega)u\varphi \, dx}_{=:N(u,\varphi)} \quad \text{for all } \varphi \in H_0^1(\Omega) \tag{8.11}$$

where $\kappa := \frac{1}{1-\nu}$. N is a symmetric bilinear form and due to non-negativity of ω, which can be checked using computer-assistance, also positive definite. Therefore, $1 - \nu > 0$ for all possible eigenvalues ν and we are left to compute upper and lower bounds for eigenvalues κ of (8.11) neighbouring 1. The essential spectrum of (8.11), which is defined in the usual way by the essential spectrum of the associated operator $R = \left(I_{H_0^1} - \Phi^{-1}L_\omega \right)^{-1}$, is bounded below by $(1 - \min \sigma_{\mathrm{ess}}(\Phi^{-1}L_\omega))^{-1} = 1 + \pi^2$. The methods in section 5.2, which were formulated for eigenvalue problems allowing essential spectrum, can therefore be used to compute lower and upper bounds for eigenvalues κ of (8.11) below the essential spectrum, i.e. below $1 + \pi^2$. Thus we will in particular obtain bounds for eigenvalues neighbouring 1.

We will briefly comment on the choice of ansatz functions to be used in the Rayleigh-Ritz and the Lehmann-Goerisch method: Analogously to the construction of ω, let $n \in \mathbb{N}$ and $v_1^c, \ldots, v_n^c \in H_0^1(\Omega^T)$ be approximate eigenfunctions of

$$\int_{\Omega^T} [\nabla u \cdot \nabla \varphi + u\varphi] \, dx = \kappa \int_{\Omega^T} (1 + 3|\omega^c|\omega^c)u\varphi \, dx \quad \text{for all } \varphi \in H_0^1(\Omega^T). \tag{8.12}$$

Setting

$$v_i := \begin{cases} v_i^c, & \text{in } \Omega^T \\ 0, & \text{in } \Omega \backslash \Omega^T \end{cases} \qquad (i = 1, \dots, n),$$

i.e. extending the functions by zero outside Ω^T yields functions $v_i, \dots, v_n \in H_0^1(\Omega)$, which can be used as approximate eigenfunctions of (8.11). In fact, using these ansatz functions replaces the eigenvalue problem (8.11) in the actual computations by the eigenvalue problem (8.12). But still we have to be aware that the bounds are only valid for eigenvalues below the essential spectrum.

Homotopy and domain decomposition

Recall that a crucial ingredient for the Lehmann-Goerisch method is an a-priori lower bound for some eigenvalue of (8.11), i.e. we need some ρ such that $\hat{\kappa}_n \leq \rho < \kappa_{n+1}$ for some $n \in \mathbb{N}$ (with $\hat{\kappa}_n$ denoting an upper bound for κ_n, which can be obtained using the Rayleigh-Ritz method). Recall from section 5.2 that the base problem

$$\langle u, \varphi \rangle_{H_0^1(\Omega)} = \kappa^{(0)} \int_\Omega (1 + \overline{c}) u\varphi \, dx, \quad \text{for all } \varphi \in H_0^1(\Omega), \tag{8.13}$$

where $\overline{c} \geq 3|\omega|\omega$ in Ω, can be connected to (8.11) by the family of eigenvalue problems

$$\langle u, \varphi \rangle_{H_0^1(\Omega)} = \kappa^{(s)} \int_\Omega (1 + (1-s)\overline{c} + 3s|\omega|\omega) u\varphi \, dx \quad \text{for all } \varphi \in H_0^1(\Omega),$$

defined for $s \in [0,1]$. We will now explain how to compute lower bounds for (8.13) in order to find an a-priori lower bound to start the homotopy. For the homotopy itself we refer to section 5.2.1.

As before we take symmetry of ω into account and restrict ourselves to the computational domain $\widehat{\Omega} := \Omega^{0,\mathrm{sym}} \cup ([0,\infty) \times (0,1))$ where $\Omega^{0,\mathrm{sym}} := \mathrm{conv}\{(0,0), (0,1), (-1,1)\}$, imposing Neumann boundary conditions on $\partial\widehat{\Omega}\backslash\partial\Omega$. A decomposition into subdomains $\Omega^{0,\mathrm{sym}}$ and $(0,\infty) \times (0,1)$ leads to the eigenvalue problems

$$\begin{cases} -\Delta u + u &= \lambda(1+\overline{c})u, & \text{in } \Omega^{0,\mathrm{sym}} \\ u &= 0, & \text{on } (-1,0) \times \{1\} =: \Gamma_D \\ \frac{\partial u}{\partial \nu} &= 0, & \text{on } \partial\Omega^{0,\mathrm{sym}}\backslash\Gamma_D \end{cases} \tag{8.14}$$

and

$$\begin{cases} -\Delta u + u &= \lambda(1+\overline{c})u, & \text{in } (0,\infty) \times (0,1) \\ u &= 0, & \text{on } ((0,\infty) \times \{0\}) \cup ((0,\infty) \times \{1\}) \\ \frac{\partial u}{\partial \nu} &= 0, & \text{on } \{0\} \times (0,1) \\ u(x,y) &\to 0, & \text{as } x \to \infty \end{cases} \tag{8.15}$$

and the union of their eigenvalues, ordered by magnitude, counted by multiplicity and denoted by $\lambda_1 \leq \lambda_2 \leq \dots$ constitute indexwise lower bounds for the eigenvalues of (8.13) by Lemma 5. We define

$$\overline{c}(x,y) = \begin{cases} c_0 & := & \max_{\overline{\Omega^{0,\mathrm{sym}}}} 3|\omega|\omega, & (x,y) \in \overline{\Omega^{0,\mathrm{sym}}} \\ c_1 & := & \max_{[0,1]\times[0,1]} 3|\omega|\omega, & (x,y) \in (0,1] \times (0,1) \\ c_2 & := & \max_{[1,3]\times[0,1]} 3|\omega|\omega, & (x,y) \in (1,3] \times (0,1) \\ 0 & & & (x,y) \in (3,\infty) \times (0,1). \end{cases}$$

Then $\bar{c}: \widehat{\Omega} \to \mathbb{R}$ is piecewise constant and satisfies $\bar{c} \geq 3|\omega|\omega$ in $\widehat{\Omega}$. We can check that $c_0 > c_1 > c_2 > 0$, which is expectable from the shape of ω.

Note that we are aiming at bounds for eigenvalues of (8.11) neighbouring 1. As mentioned in Remark 6 it will be sufficient to compute only eigenvalues λ of (8.14) and (8.15) below a prescribed value C_L and we will choose $C_L := \frac{\pi^2+1}{2}$ here.

For the computation of eigenvalues for (8.14) we refer to section 6.2.2, where we can also find a guideline for the treatment of (8.15). For the latter, we use a separation ansatz $u(x,y) = v(x)w(y)$ with

$$
v(x) = \begin{cases} v_1(x), & x \in (0,1) \\ v_2(x), & x \in (1,3) \\ v_3(x), & x \in (3,\infty), \end{cases}
$$

with the requirements $v \in C^1((0,\infty))$, $w \in C^1((0,1))$. Clearly, $w(y) = \sin(k\pi y)$ for some $k \in \mathbb{N}$. For v_1, v_2, v_3 we obtain the following ($\tau_i \in \mathbb{R}$, $i = 1, 2, 3$):

(1) $x \in (0,1)$.

    (1.1) $k^2\pi^2 + 1 - \lambda(1 + c_1) =: -\tau_1^2 < 0$, i.e. $\lambda > \frac{k^2\pi^2+1}{1+c_1}$.
         The differential equation for v_1 and boundary condition $v_1'(0) = 0$ imply $v_1(x) = b_1 \cos(\tau_1 x)$.

    (1.2) $k^2\pi^2 + 1 - \lambda(1 + c_1) =: \tau_1^2 > 0$, i.e. $\lambda < \frac{k^2\pi^2+1}{1+c_1}$.
         Now we obtain $v_1(x) = b_1 \cosh(\tau_1 x)$.

    (1.3) $k^2\pi^2 + 1 - \lambda(1 + c_1) = 0$, i.e. $\lambda = \frac{k^2\pi^2+1}{1+c_1}$.
         In this case we have $v_1(x) = b_1$, $b_1 \in \mathbb{R}$

(2) $x \in (1,3)$.

    (2.1) $k^2\pi^2 + 1 - \lambda(1 + c_2) = -\tau_2^2 \leq 0$, i.e. $\lambda \geq \frac{k^2\pi^2+1}{1+c_2}$. We will later see that $c_2 < 1$, thus only eigenvalues larger than or equal to $C_L = \frac{\pi^2+1}{2}$ will be obtained in this case.

    (2.2) $k^2\pi^2 + 1 - \lambda(1 + c_2) = \tau_2^2 \geq 0$, i.e. $\lambda \leq \frac{k^2\pi^2+1}{1+c_2}$.
         Then, $v_2(x) = a_2 e^{\tau_2 x} + b_2 e^{-\tau_2 x}$.

(3) $x \in (3,\infty)$.

     The boundary condition implies $\tau_3^2 := k^2\pi^2 - \lambda + 1 > 0$, whence $\lambda < k^2\pi^2 + 1$ and $v_3(x) = a_3 e^{-\tau_3 x}$ follows.

The continuity and differentiability conditions on v lead to transcendental equations whose solutions are eigenvalues of (8.15). Leaving out the case (2.1) we obtain:

Cases (1.1), (2.2), (3): We have the restriction

$$
\frac{k^2\pi^2 + 1}{1 + c_1} < \lambda < \min\left\{\frac{k^2\pi^2 + 1}{1 + c_2}, C_L\right\} \tag{8.16}
$$

for λ and the resulting equation is given by

$$
e^{-3\tau_3}\big(e^{-2\tau_2}(\tau_2 - \tau_3)(\cos(\tau_1)\tau_2 + \tau_1 \sin(\tau_1)) +
$$
$$
e^{2\tau_2}(\tau_2 + \tau_3)(-\cos(\tau_1)\tau_2 + \tau_1 \sin(\tau_1))\big) = 0. \tag{8.17}
$$

For fixed k we can compute all solutions to this nonlinear equation in the interval determined by (8.16) using an Interval Newton method (see section 5.4.1). Clearly, the interval in (8.16) will be non-empty for only finitely many values of k.

Cases (1.2), (2.2), (3): We have the restriction $\lambda < \min\left\{\frac{k^2\pi^2+1}{1+c_1}, C_L\right\}$ and the resulting equation is

$$e^{-3\tau_3}\left[e^{2\tau_2}(\tau_2+\tau_3)(-\cosh(\tau_1)\tau_2+\tau_1\sinh(\tau_1))+\right.$$
$$\left. e^{-2\tau_2}(\tau_2-\tau_3)(\cosh(\tau_1)\tau_2+\tau_1\sinh(\tau_1)\right]=0. \quad (8.18)$$

Since $c_1 > c_2 > c_3 > 0$ we have $0 < \tau_1 < \tau_2 < \tau_3$ and therefore $\tau_2 - \tau_3 < 0$ as well as $-\cosh(\tau_1)\tau_2 + \tau_1\sinh(\tau_1) < 0$. Note that the latter inequality is equivalent to $\tanh(\tau_1) < \frac{\tau_2}{\tau_1}$, which is true since $|\tanh(x)| < 1$ for all $x \in \mathbb{R}$.

Therefore the left-hand-side of equation (8.18) is negative for all λ in the considered range and we do not obtain eigenvalues in this case.

Cases (1.3), (2.2), (3): Now we have $\lambda = \frac{k^2\pi^2+1}{1+c_1}$ and the equation for λ is given by

$$e^{-3\tau_3}\left((\tau_2-\tau_3)e^{-2\tau_2} - e^{2\tau_2}(\tau_2+\tau_3)\right) = 0.$$

Since $0 < \tau_2 < \tau_3$ the left-hand-side of this equation is strictly negative and we do not obtain eigenvalues.

Table 8.1 shows lower bounds for the union of eigenvalues of problems (8.14) and (8.15) below 3, denoted by $\underline{\lambda}_1 \leq, \underline{\lambda}_2 \leq \ldots$, and upper bounds for the smallest eigenvalues of the base problem (8.13), denoted by $\hat{\kappa}_1^{(0)} \leq \hat{\kappa}_2^{(0)} \leq \ldots$ and obtained using the Rayleigh-Ritz method.

We can read from the table that there are various indices n satisfying $\hat{\kappa}_n^{(0)} < \underline{\lambda}_{n+1} \leq \lambda_{n+1} \leq \kappa_{n+1}^{(0)}$, where the last two inequalities are always satisfied (the latter following from Lemma 5). Choosing one of these indices and setting $\rho_0 := \underline{\lambda}_{n+1}$ leads to a suitable a-priori lower bound as needed to start the homotopy. In our calculations we used $n = 11$ and $\rho_0 = 2.35653$.

n	$\underline{\lambda}_n$	$\hat{\kappa}_n^{(0)}$	n	$\underline{\lambda}_n$	$\hat{\kappa}_n^{(0)}$
1	0.08291115	0.18116190	9	1.73749089	1.97597235
2	0.35867444	0.48072268	10	1.79188325	2.07091923
3	0.52231225	0.69817471	11	2.01325418	2.27738840
4	0.63443773	0.84523449	12	2.35653704	2.75039604
5	0.91020102	1.02707258	13	2.43367893	2.86291360
6	1.08005919	1.43594363	14	2.56478076	3.00029477
7	1.18596431	1.52508408	15	2.84054405	3.41282185
8	1.73749089	1.93535659			

Table 8.1: Eigenvalues of the base problem and corresponding lower bounds

Smallest eigenvalue of the Laplacian

To compute the defect as well as for the computation of $\alpha > 0$ satisfying (2.7) we need a embedding constants for the embedding $H_0^1(\Omega) \hookrightarrow L^p(\Omega)$ for different values of p. Lemma 2 proved that these embedding constants can easily be computed once a lower bound for the smallest eigenvalue of $-\Delta$ on Ω with homogeneous Dirichlet boundary conditions in known. We could use zero as a lower bound for this eigenvalue, but a better bound can be computed using the domain decomposition method.

Analogous to the above considerations we can prove that the essential spectrum of $-\Delta$ is contained in $[\pi^2, \infty)$. Splitting Ω at $\{x = 0\}$ and $\{y = 0\}$ leads to the subdomains $\Omega^0 = (-1, 0) \times (0, 1)$, $\{(x, y) \in \Omega : x > 0\}$ and $\{(x, y) \in \Omega : y < 0\}$ and as before we observe that the spectrum of the two semi-infinite strips (with Neumann boundary conditions at $\{x = 0\}$ and $\{y = 0\}$, respectively) starts at π^2 and moreover does not contain eigenvalues. An easy calculation shows that there is only one eigenvalue of

$$\begin{cases} -\Delta u &= \lambda u \quad \text{in } \Omega^0 \\ u &= 0 \quad\;\; \text{on } \partial\Omega^0 \cap \partial\Omega \\ \frac{\partial u}{\partial \nu} &= 0 \quad\;\; \text{on } \partial\Omega^0 \backslash \partial\Omega \end{cases}$$

below π^2, given by $\frac{\pi^2}{2}$. With Lemma 5 it follows that also $-\Delta$ on Ω has precisely one eigenvalue, denoted κ_1, below the essential spectrum and a rough lower bound for it is given by $\frac{\pi^2}{2}$. However, using the Lehmann-Goerisch method it is possible to obtain a better lower bound: Computing (via the Rayleigh-Ritz method) an upper bound $\hat{\kappa}_1$ for κ_1, any $\rho \in (\hat{\kappa}_1, \pi^2)$ provides a suitable constant satisfying (5.12). Now Theorem 4 yields the improved lower bound

$$\kappa_1 \geq 8.974967.$$

8.2.4 Numerical results

As before we used an interpolation $I_{V_{\tilde{N}}}(\omega^c)$ of ω^c in a Finite Element space $V_{\tilde{N}}$ as approximate solution in the eigenvalue computations and computed a bound for the inverse of the linearization at ω via Lemma 1. Summarizing our results we have (cf. section 8.2.2 for the definition of ρ^c):

$$\|\nabla\omega^c - \rho^c\|_{L^2(\Omega^T)} \leq 0.000781513 \tag{8.19}$$
$$\|\operatorname{div}(\rho^c) + |\omega^c|^3\|_{L^2(\Omega^T)} \leq 0.002897424 \tag{8.20}$$
$$\|\omega^c\|_{L^4(\Omega^T)} = \|\omega\|_{L^4(\Omega)} \leq 3.014332566 \tag{8.21}$$
$$\| -\Delta\omega - |\omega|^3\|_{H^{-1}(\Omega)} \leq 0.001698908$$
$$K^{\text{sym}} = 3.722883900$$
$$C_4 = 0.461999702$$
$$\alpha = 0.006470065$$

where K^{sym} is a constant satisfying

$$\|v\|_{H_0^1(\Omega)} \leq K^{\text{sym}}\|L_\omega[v]\|_{H^{-1}(\Omega)} \quad \text{for all } v \in H_0^1(\Omega) \text{ symmetric w.r.t. } y = -x.$$

This proves the following

Theorem 9. *Problem* (8.3) *has a non-trivial solution* $u \in H_0^1(\Omega)$ *satisfying*

$$\|u - \omega\|_{H_0^1(\Omega)} \leq \alpha$$

and being symmetric w.r.t $y = -x$.

Remark 12. In a continuative joint paper with F. Pacella and M. Plum (in preparation) we prove that the solution u obtained by our computer-assisted proof is moreover non-degenerate and decays exponentially as $x \to \infty$ and $y \to -\infty$, respectively. Thus the solution has similar properties as the ground state of (8.2), and we hope to prove a similar result as stated in Theorem 8 for expanding domains with corners and using our solution u instead of of the ground state from (8.2).

9 Solutions for Domains with Large *t*

In this chapter we revisit problem (1.2) on domains Ω_t with $t > 3$ (or $t > 1.5$ in some special cases). Our aim is to prove the existence of solutions of the previously considered types (fourpeak-corner, fourpeakedge, twopeakoppcorner, twopeakoppedge, onepeakcorner and onepeakedge) for all $t > \hat{t}$ (with $\hat{t} = 3$ or $\hat{t} = 1.5$, respecively). More precisely we are going to prove the following:

Theorem 10. *(a) For all $t \geq 1.5$ there exist at least three different non-trivial solutions to problem (1.2) (types: onepeakcorner, twopeakoppcorner and fourpeakcorner).*

(b) For all $t \geq 3$ there exist at least six different non-trivial solutions to problem (1.2).

Moreover we will show that the solution branches $(u_t)_{t \in [\hat{t}, \infty)}$, given by the solutions in Theorem 10, are continuously differentiable.

To motivate our proceeding in this chapter we will start with some observations based on numerical experiments. If one considers, for a fixed solution type, the evolution of the approximate solution as t varies, one oberserves the following for sufficiently large and growing t (see also Figures 6.2 and 6.7 - 6.12):

- cornerbumps are centered in the cornerparts of the domain and do not change their shape

- edgebumps are centered in the middle of the edgeparts of the domain and do not change their shape

- between the corner- or edgebumps the approximate solution is close to zero and these regions are enlarged as t grows

Therefore the basic idea is to construct an approximate solution by putting bumps in the cornerparts or edgeparts of the domain, extending by zero outside, and to prove the existence of an exact solution nearby, using computer-assistance. We take these bumps as the computed approximate solution for

- the unbounded L-shaped domain from chapter 8, in case of a cornerbump

- the infinite strip domain, in case of an edgebump,

(after obvious shifts and rotations).

Using the notations of section 8.2.1 we choose $T = 3$, and consider the computational L-shaped domain $\Omega^T := ((-1, 0) \times (-3, 1)) \cup ((-1, 3) \times (0, 1))$. We recall that $\omega^c \in H_0^1(\Omega^T)$ as defined in (8.7) is an approximate solution to the problem

$$\begin{cases} -\Delta u &= |u|^3 \quad \text{in } \Omega^T \\ u &= 0 \qquad \text{on } \partial\Omega^T, \end{cases}$$

which is symmetric w.r.t. $y = -x$ and has one bump centered in the corner part of Ω^T. We will refer to this approximate solution as the basic cornerbump.

Analogously, we can define a basic edgebump: Let therefore $\Omega^e := (0,6) \times (0,1)$ and $\omega^e \in H_0^1(\Omega^e)$ be an approximate solution to

$$\begin{cases} -\Delta u & = & |u|^3 & \text{in } \Omega^e \\ u & = & 0 & \text{on } \partial\Omega^e, \end{cases} \tag{9.1}$$

which has a bump centered at $(3, \frac{1}{2})$ and is symmetric w.r.t. $x = 3$. Note that ω^e can be chosen to be a pure Finite Element function since Ω^e does not contain re-entrant corners.

We will use these two functions to construct various approximate solutions to our original problem on Ω_t, which have bumps in corner parts or on edges of the domain. In the following, we always consider a shifted version of Ω_t, having the upper left re-entrant corner at the point $(0,0)$.

9.1   Construction of Approximate Solutions

Cornerbumps

We define four subdomains of $\Omega_t = ((-1, 2t+1) \times (-2t-1, 1)) \setminus ([0, 2t] \times [-2t, 0])$:

$$\Omega_t^{(c,0)} := \Omega^T$$
$$\Omega_t^{(c,1)} := ((2t-3, 2t+1) \times (0,1)) \cup ((2t, 2t+1) \times (-3, 1))$$
$$\Omega_t^{(c,2)} := ((2t-3, 2t+1) \times (-2t-1, -2t)) \cup ((2t, 2t+1) \times (-2t-1, -2t+3))$$
$$\Omega_t^{(c,3)} := ((-1, 3) \times (-2t-1, -2t)) \cup ((-1, 0) \times (-2t-1, -2t+3)),$$

which are also displayed in Figure 9.1 (1).
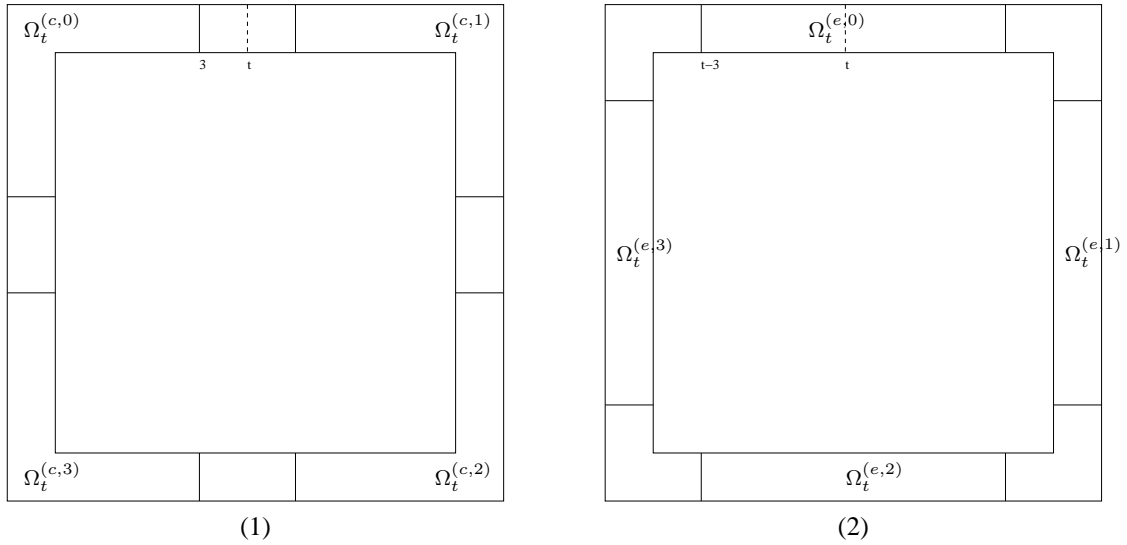
Figure 9.1: Subdomains for the definition of (1) cornerbump and (2) edgebump functions

By using shifted and rotated versions of ω^c in $\Omega_t^{(c,i)}$, $i \in \{0, \dots, 3\}$ and extending by zero in the remaining part of Ω_t, we can define several approximations of cornerpeak-solutions:

(C1)

$$\omega_t^{c_1}(x,y) := \begin{cases} \omega^c(x,y), & (x,y) \in \Omega_t^{(c,0)} \\ 0, & \text{else.} \end{cases}$$

By construction, ω_t is symmetric w.r.t. the axis $y = -x$. Note also that this solution may be defined for all $t \geq 1.5$.

(C2)

$$\omega_t^{c_2}(x,y) := \begin{cases} \omega^c(x,y), & (x,y) \in \Omega_t^{(c,0)} \\ \omega^c(2t-x, -2t-y), & (x,y) \in \Omega_t^{(c,2)} \\ 0, & \text{else.} \end{cases}$$

This function is symmetric w.r.t. the axes $y = -x$ and $y = x + 6$, and thus has all diagonal symmetry of Ω_t. It can be defined for all $t \geq 1.5$.

(C4)

$$\omega_t^{c_4}(x,y) := \begin{cases} \omega^c(x,y), & (x,y) \in \Omega_t^{(c,0)} \\ \omega^c(-y, x-2t), & (x,y) \in \Omega_t^{(c,1)} \\ \omega^c(2t-x, -2t-y), & (x,y) \in \Omega_t^{(c,2)} \\ \omega^c(y+2t, -x), & (x,y) \in \Omega_t^{(c,3)} \\ 0, & \text{else.} \end{cases}$$

This approximation exhibits full symmetry of the domain Ω_t. We have to require $t \geq 3$ in this case.

Edgebumps

Analogously to the cornerbump solutions we define, for $t \geq 3$, four subdomains of Ω_t, now containing the centre parts of the edges,

$$\Omega_t^{(e,0)} := (t-3, t+3) \times (0,1)$$
$$\Omega_t^{(e,1)} := (2t, 2t+1) \times (-t-3, -t+3)$$
$$\Omega_t^{(e,2)} := (t-3, t+3) \times (-2t-1, -2t)$$
$$\Omega_t^{(e,3)} := (-1, 0) \times (-t-3, -t+3),$$

see also Figure 9.1 (2), and put rotated and shifted versions of ω^e in $\Omega_t^{(e,i)}$, $i \in \{0, \dots, 3\}$. Extending by zero in the remaining part of Ω_t yields several types of edgebump-solutions. Note that in all cases $t \geq 3$ is necessary.

(E1)

$$\omega_t^{e_1}(x,y) := \begin{cases} \omega^e(x-t+3, y), & (x,y) \in \Omega_t^{(e,0)} \\ 0, & \text{else.} \end{cases}$$

By construction, $\omega_t^{e_1}$ is symmetric w.r.t. the axis $x = t$.

(E2)

$$\omega_t^{e_2}(x,y) := \begin{cases} \omega^e(x-t+3, y), & (x,y) \in \Omega_t^{(e,0)} \\ \omega^e(-x+t-3, -y-2t), & (x,y) \in \Omega_t^{(e,2)} \\ 0, & \text{else.} \end{cases}$$

This function is symmetric w.r.t. to the axes $x = t$ and $y = -t$.

(E4)

$$\omega_t^{e_4}(x,y) := \begin{cases} \omega^e(x-t+3, y), & (x,y) \in \Omega_t^{(e,0)} \\ \omega^e(-y+3-t, x-2t), & (x,y) \in \Omega_t^{(e,1)} \\ \omega^e(-x+t-3, -y-2t), & (x,y) \in \Omega_t^{(e,2)} \\ \omega^e(y+t+3, -x), & (x,y) \in \Omega_t^{(e,3)} \\ 0, & \text{else.} \end{cases}$$

This approximation exhibits full symmetry of the domain Ω_t.

Note that the construction of approximate solutions is similar to the idea that is used in Theorem 8, where $\sum_{i=1}^{n} U_{x_{R_i}, R}$ is a sum of rotated and translated versions of a ground state solution, and can be interpret as approximate solution.

9.2 Defect Computation

Recall that the defect of an approximate solution $\omega_t \in H_0^1(\Omega_t)$ can be estimated by

$$\| -\Delta\omega_t - |\omega_t|^3 \|_{H^{-1}(\Omega_t)} \le \|\nabla\omega_t - \rho_t\|_{L^2(\Omega_t)} + C_2 \| \operatorname{div}\rho_t + |\omega_t|^3 \|_{L^2(\Omega_t)}, \qquad (9.2)$$

where $\rho_t \in H(\operatorname{div}, \Omega_t)$ is an approximate minimizer of $\|\nabla\omega_t - \rho_t\|_{L^2(\Omega_t)}^2 + C_2\|\operatorname{div}\rho_t + |\omega_t|^3\|_{L^2(\Omega_t)}^2$. Our first aim is to construct such an approximation ρ_t by using only approximations of $\nabla\omega^c$ and $\nabla\omega^e$, respectively.

Cornerbumps

Let $\rho^c = \begin{pmatrix} \rho_1^c \\ \rho_2^c \end{pmatrix} \in H(\operatorname{div}, \Omega^T)$ be an approximation of $\nabla\omega^c$ satisfying $-\operatorname{div}(\rho^c) \approx |\omega^c|^3$ and $\rho_1^c(3,y) = \rho_2^c(x,-3) = 0$ for $x,y \in (0,1)$, i.e. the normal component of ρ^c is zero at $x=3$ and $y=-3$, respecively, which guarantees that the zero extension of ρ^c into $\Omega_t \backslash \Omega^T$ is in $H(\operatorname{div}, \Omega_t)$ (see e.g. the procedure in section 8.2.2). With the following definitions, using ρ^c as a building block, we obtain approximations of $\nabla\omega_t^{c_i}$ in $H(\operatorname{div}, \Omega_t)$:

(C1-1)

$$\rho_t^{c_1}(x,y) := \begin{cases} \rho^c(x,y), & (x,y) \in \Omega_t^{(c,0)} \\ 0, & \text{else,} \end{cases}$$

(C2-1)

$$\rho_t^{c_2}(x,y) := \begin{cases} \rho^c(x,y), & (x,y) \in \Omega_t^{(c,0)} \\ \begin{pmatrix} -\rho_1^c(2t-x, -2t-y) \\ -\rho_2^c(2t-x, -2t-y) \end{pmatrix}, & (x,y) \in \Omega_t^{(c,2)} \\ 0, & \text{else,} \end{cases}$$

(C4-1)

$$\rho_t^{c_2}(x,y) := \begin{cases} \rho^c(x,y), & (x,y) \in \Omega_t^{(c,0)} \\ \begin{pmatrix} \rho_2^c(-y, x-2t) \\ -\rho_1^c(-y, x-2t) \end{pmatrix}, & (x,y) \in \Omega_t^{(c,1)} \\ \begin{pmatrix} -\rho_1^c(2t-x, -2t-y) \\ -\rho_2^c(2t-x, -2t-y) \end{pmatrix}, & (x,y) \in \Omega_t^{(c,2)} \\ \begin{pmatrix} -\rho_2^c(y+2t, -x) \\ \rho_1^c(y+2t, -x) \end{pmatrix}, & (x,y) \in \Omega_t^{(c,3)} \\ 0, & \text{else.} \end{cases}$$

Edgebumps

Similarly to the proceeding for cornerbumps we start with an approximation $\rho^e = \begin{pmatrix} \rho_1^e \\ \rho_2^e \end{pmatrix} \in$ $H(\mathrm{div}, \Omega^e)$ of $\nabla \omega^e$, which satisfies $-\mathrm{div}(\rho^e) \approx |\omega^e|^3$ and $\rho_1^e(0,y) = \rho_1^e(6,y) = 0$ for $y \in (0,1)$. As before this implies that the normal component of ρ^e at $x = 0$ and $x = 6$, respectively, is zero. Since ω^e is a Finite Element function, we may search for ρ_1^e, ρ_2^e in the Finite Element space, too. We are now able to define approximations of $\nabla \omega_t^{e_i} \in H(\mathrm{div}, \Omega_t)$ in a similar way as we did for the cornerbump solutions:

(E1-1)

$$\rho_t^{e_1}(x,y) := \begin{cases} \rho^e(x-t+3, y), & (x,y) \in \Omega_t^{(e,0)} \\ 0, & \text{else,} \end{cases}$$

(E2-1)

$$\rho_t^{e_2}(x,y) := \begin{cases} \rho^e(x-t+3, y), & (x,y) \in \Omega_t^{(e,0)} \\ \begin{pmatrix} -\rho_1^e(-x+t-3, -y-2t) \\ -\rho_2^c(-x+t-3, -y-2t) \end{pmatrix}, & (x,y) \in \Omega_t^{(e,2)} \\ 0, & \text{else,} \end{cases}$$

(E4-1)

$$\rho_t^{e_2}(x,y) := \begin{cases} \rho^e(x-t+3, y), & (x,y) \in \Omega_t^{(e,0)} \\ \begin{pmatrix} \rho_2^e(-y+3-t, x-2t) \\ -\rho_1^e(-y+3-t, x-2t) \end{pmatrix}, & (x,y) \in \Omega_t^{(e,1)} \\ \begin{pmatrix} -\rho_1^e(-x+t-3, -y-2t) \\ -\rho_2^e(-x+t-3, -y-2t) \end{pmatrix}, & (x,y) \in \Omega_t^{(e,2)} \\ \begin{pmatrix} -\rho_2^e(y+2t, -x) \\ \rho_1^e(y+2t, -x) \end{pmatrix}, & (x,y) \in \Omega_t^{(e,3)} \\ 0, & \text{else.} \end{cases}$$

Due to the construction of $\omega_t^{c_i}$, $\omega_t^{e_i}$ and $\rho_t^{c_i}$, $\rho_t^{e_i}$, $i = 1, 2, 4$, (9.2) leads to

$$
\begin{aligned}
\| -\Delta\omega_t^{c_1} - |\omega_t^{c_1}|^3 \|_{H^{-1}(\Omega_t)} &\leq \|\nabla\omega^c - \rho^c\|_{L^2(\Omega^T)} + C_2 \|\operatorname{div}(\rho^c) + |\omega^c|^3\|_{L^2(\Omega^T)} \\
\| -\Delta\omega_t^{e_1} - |\omega_t^{e_1}|^3 \|_{H^{-1}(\Omega_t)} &\leq \|\nabla\omega^e - \rho^e\|_{L^2(\Omega^e)} + C_2 \|\operatorname{div}(\rho^e) + |\omega^e|^3\|_{L^2(\Omega^e)} \\
\| -\Delta\omega_t^{c_2} - |\omega_t^{c_2}|^3 \|_{H^{-1}(\Omega_t)} &\leq \sqrt{2}\left(\|\nabla\omega^c - \rho^c\|_{L^2(\Omega^T)} + C_2 \|\operatorname{div}(\rho^c) + |\omega^c|^3\|_{L^2(\Omega^T)} \right) \\
\| -\Delta\omega_t^{e_2} - |\omega_t^{e_2}|^3 \|_{H^{-1}(\Omega_t)} &\leq \sqrt{2}\left(\|\nabla\omega^e - \rho^e\|_{L^2(\Omega^e)} + C_2 \|\operatorname{div}(\rho^e) + |\omega^e|^3\|_{L^2(\Omega^e)} \right) \\
\| -\Delta\omega_t^{c_4} - |\omega_t^{c_4}|^3 \|_{H^{-1}(\Omega_t)} &\leq 2\left(\|\nabla\omega^c - \rho^c\|_{L^2(\Omega^T)} + C_2 \|\operatorname{div}(\rho^c) + |\omega^c|^3\|_{L^2(\Omega^T)} \right) \\
\| -\Delta\omega_t^{e_4} - |\omega_t^{e_4}|^3 \|_{H^{-1}(\Omega_t)} &\leq 2\left(\|\nabla\omega^e - \rho^e\|_{L^2(\Omega^e)} + C_2 \|\operatorname{div}(\rho^e) + |\omega^e|^3\|_{L^2(\Omega^e)} \right).
\end{aligned}
\tag{9.3}
$$

Note that upper bounds for $\|\nabla\omega^c - \rho^c\|_{L^2(\Omega^T)}$ and $\|\operatorname{div}(\rho^c) + |\omega^c|^3\|_{L^2(\Omega^T)}$ have already been computed and are displayed in section 8.2.4. The corresponding terms involving ω^e and ρ^e can easily be computed exactly using a quadrature rule of sufficiently high degree, since all occurring functions are piecewise polynomial. For the computation of an embedding constant $C_2 = C_2(\Omega_t)$ for all $t \geq \hat{t}$ we use Lemma 7, thereby obtaining $C_2(\Omega_t) = C_2(\Omega_{\hat{t}})$ for all $t \geq \hat{t}$. Thus we are now able to compute the defect for $\omega_t^{c_i}$, $\omega_t^{e_i}$ for $i = 1, 2, 4$ and all $t > \hat{t}$ (we choose $\hat{t} = 1.5$ for $\omega_t^{c_i}$ and $i = 1, 2$ and $\hat{t} = 3$ in the remaining cases).

9.3 Bound for the Inverse of the Linearization

By construction of the approximate solutions $\omega_t^{c_i}$, $\omega_t^{e_i}$ we have

$$
\omega_t^{c_i} \in H_0^1(\Omega_t, \operatorname{sym}^{c_i}), \quad \omega_t^{e_i} \in H_0^1(\Omega_t^{e_i}, \operatorname{sym}^{e_i}), \qquad (i = 1, 2, 4)
$$

where

$$
\begin{aligned}
H_0^1(\Omega_t, \operatorname{sym}^{c_1}) &:= \{ u \in H_0^1(\Omega_t) : u \text{ symmetric w.r.t. } y = -x \} \\
H_0^1(\Omega_t, \operatorname{sym}^{c_2}) &:= \{ u \in H_0^1(\Omega_t) : u \text{ symmetric w.r.t. } y = -x, y = x + 6 \} \\
H_0^1(\Omega_t, \operatorname{sym}^{c_4}) &:= \{ u \in H_0^1(\Omega_t) : u \text{ symmetric w.r.t. } y = -x, y = x + 6, x = t, y = -t \} \\
H_0^1(\Omega_t, \operatorname{sym}^{e_1}) &:= \{ u \in H_0^1(\Omega_t) : u \text{ symmetric w.r.t. } x = t \} \\
H_0^1(\Omega_t, \operatorname{sym}^{e_2}) &:= \{ u \in H_0^1(\Omega_t) : u \text{ symmetric w.r.t. } x = t, y = -t \} \\
H_0^1(\Omega_t, \operatorname{sym}^{e_4}) &:= H_0^1(\Omega_t, \operatorname{sym}^{c_4}).
\end{aligned}
$$

We will also use the notation $H_0^1(\Omega_t, \operatorname{sym})$ if the underlying symmetry is clear from the context.

Our aim is now to compute constants $K_t^{c_i}$, $K_t^{e_i}$, $i = 1, 2, 4$ satisfying

$$
\|v\|_{H_0^1(\Omega_t)} \leq K_t^{c_i} \left\| L_{\omega_t^{c_i}}[v] \right\|_{H^{-1}(\Omega_t)} \quad \text{for all } v \in H_0^1(\Omega_t, \operatorname{sym}^{c_i}), \text{ for all } t \geq \hat{t}, \tag{9.4}
$$

$$
\|v\|_{H_0^1(\Omega_t)} \leq K_t^{e_i} \left\| L_{\omega_t^{e_i}}[v] \right\|_{H^{-1}(\Omega_t)} \quad \text{for all } v \in H_0^1(\Omega_t, \operatorname{sym}^{e_i}), \text{ for all } t \geq \hat{t}. \tag{9.5}
$$

We have seen earlier that for for the computation of a constant K satisfying $\|v\|_{H_0^1(\Omega_t)} \leq K\|L_w[v]\|_{H^{-1}(\Omega_t)}$ for all $v \in H_0^1(\Omega_t)$ (with $w \in H_0^1(\Omega_t)$ given) it is sufficient and necessary to compute bounds for the smallest eigenvalues of

$$
\int_{\Omega_t} [\nabla u \cdot \nabla\varphi + u\varphi]\, dx = \kappa \int_{\Omega_t} (1 + 3|w|w)\, u\varphi\, dx \quad \text{for all } \varphi \in H_0^1(\Omega_t).
$$

Therefore, we will now compute uniform enclosures for the smallest eigenvalues of

$$\int_{\Omega_t} [\nabla u \cdot \nabla \varphi + u\varphi] \, dx = \kappa \int_{\Omega_t} (1 + 3|\omega_t|\omega_t) \, u\varphi \, dx \quad \text{for all } \varphi \in H_0^1(\Omega_t, \text{sym}), \qquad (9.6)$$

corresponding to eigenfunctions in $H_0^1(\Omega_t, \text{sym})$ where $\omega_t \in \{\omega_t^{c_i}, \omega_t^{e_i} : i = 1, 2, 4\}$ and $t \geq \hat{t}$.

In chapter 5 we have introduced and explained methods to obtain upper and lower eigenvalue bounds, thus we will now only comment on the settings and choices to be made for applying these methods. For lower eigenvalue bounds we start with a base problem that can be connected via a homotopy with the eigenvalue problem (9.6). It is obviously identical to problem (5.31), given by:

$$\int_{\Omega_t} [\nabla u \cdot \nabla \varphi + u\varphi] \, dx = \kappa^{(0)} \underbrace{\int_{\Omega_t} (1 + \overline{c}) u\varphi \, dx}_{=N_0(u,\varphi)} \qquad \text{for all } \varphi \in H_0^1(\Omega_t, \text{sym}), \qquad (9.7)$$

where $\overline{c} : \Omega_t \to \mathbb{R}$ depends on the choice of ω_t, is piecewise constant and such that

$$\overline{c} \geq 3|\omega_t|\omega_t \quad \text{in } \Omega_t. \qquad (9.8)$$

Clearly we can choose $\overline{c} = 0$ in all subdomains where $\omega_t \equiv 0$, and such that it exhibits the same symmetry as ω_t. In particular, $\overline{c}$ will depend only on ω^c and ω^e, respectively.

9.3.1 Domain decomposition

Keeping the symmetry of the approximate solutions in mind we can restrict ourselves to half, quarter or eighth domain of Ω_t, with Neumann boundary conditions on the new parts of the boundary.
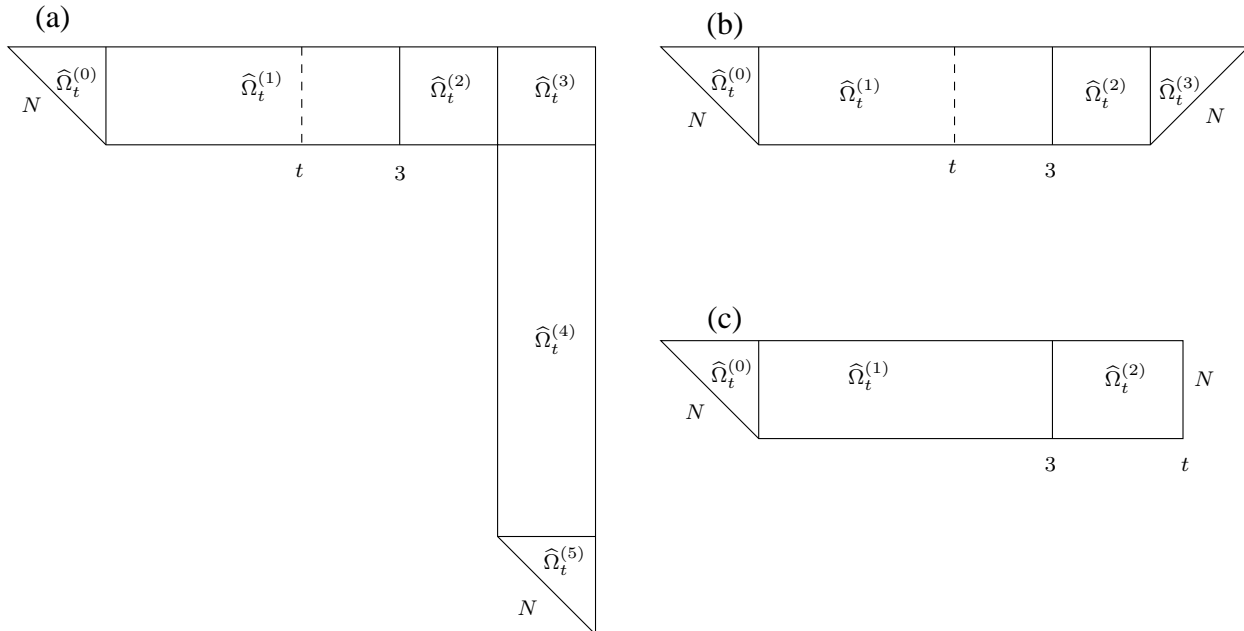
Figure 9.2: Computational domains and domain decomposition for cornerbumps in (a) case $i = 1$, (b) case $i = 2$ and (c) case $i = 4$

Figure 9.2 shows the computational domains and the splitting in subdomains $\widehat{\Omega}_t^{(j)}$ that will be used during the domain decomposition in case $\omega_t = \omega_t^{c_i}$, $i = 1, 2, 4$ is a cornerbump solution.

(a)

$\widehat{\Omega}_t^{(3)}$ $\widehat{\Omega}_t^{(2)}$ $\widehat{\Omega}_t^{(1)}$ N

N

$t-3$ t

(b)

$\widehat{\Omega}_t^{(3)}$ $\widehat{\Omega}_t^{(2)}$ $\widehat{\Omega}_t^{(1)}$ N

$t-3$ t

$\widehat{\Omega}_t^{(4)}$

N

(c)

$\widehat{\Omega}_t^{(3)}$ $\widehat{\Omega}_t^{(2)}$ $\widehat{\Omega}_t^{(1)}$ N

$t-3$ t

$\widehat{\Omega}_t^{(4)}$

$\widehat{\Omega}_t^{(5)}$ $\widehat{\Omega}_t^{(6)}$ N
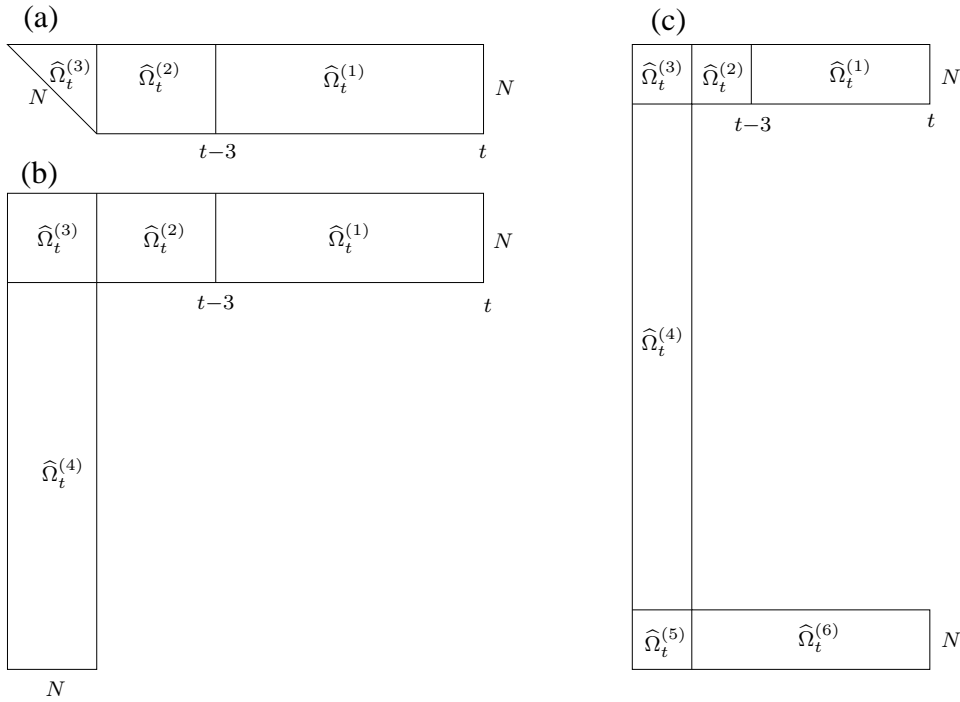
Figure 9.3: Computational domains and domain decomposition for edgebumps in (a) case $i = 4$, (b) case $i = 2$ and (c) case $i = 1$

Figure 9.3 shows the same for the edgebump solutions $\omega_t = \omega_t^{ei}$, $i = 1, 2, 4$. In all pictures N indicates parts of the boundary of $\widehat{\Omega}_t = \mathrm{int}\left(\bigcup_{j=0}^{k} \overline{\widehat{\Omega}_t^{(j)}}\right)$ ($k \geq 3$ to be chosen accordingly) where Neumann boundary conditions are imposed. Solid lines mark boundaries of the subdomains $\widehat{\Omega}_t^{(j)}$. The definitions of $\widehat{\Omega}_t^{(j)}$ are as follows:

Cornerbumps:

(a) $\widehat{\Omega}_t^{(0)} = \mathrm{conv}\{(0,0), (0,1), (-1,1)\}$
$\widehat{\Omega}_t^{(1)} = (0, t) \times (0, 1)$
$\widehat{\Omega}_t^{(2)} = (0, 3) \times (0, 1)$
$\widehat{\Omega}_t^{(3)} = (2t, 2t+1) \times (0, 1)$
$\widehat{\Omega}_t^{(4)} = (2t, 2t+1) \times (-2t, 0)$
$\widehat{\Omega}_t^{(5)} = \mathrm{conv}\{(2t, -2t), (2t+1, -2t),$
$\qquad\qquad (2t+1, -2t-1)\}$

(b) $\widehat{\Omega}_t^{(0)} = \mathrm{conv}\{(0,0), (0,1), (-1,1)\}$
$\widehat{\Omega}_t^{(1)} = (0, 3) \times (0, 1)$
$\widehat{\Omega}_t^{(2)} = (3, 2t) \times (0, 1)$
$\widehat{\Omega}_t^{(3)} = \mathrm{conv}\{(2t, 0), (2t+1, 1), (2t, 1)\}$

(c) $\widehat{\Omega}_t^{(0)} = \mathrm{conv}\{(0,0), (0,1), (-1,1)\}$
$\widehat{\Omega}_t^{(1)} = (0, 3) \times (0, 1)$
$\widehat{\Omega}_t^{(2)} = (3, t) \times (0, 1)$

Edgebumps:

(a) $\widehat{\Omega}_t^{(1)} = (t-3, t) \times (0, 1)$
$\widehat{\Omega}_t^{(2)} = (0, t-3) \times (0, 1)$
$\widehat{\Omega}_t^{(3)} = \mathrm{conv}\{(0,0), (0,1), (-1,1)\}$

(b) $\widehat{\Omega}_t^{(1)} = (t-3, t) \times (0, 1)$
$\widehat{\Omega}_t^{(2)} = (0, t-3) \times (0, 1)$
$\widehat{\Omega}_t^{(3)} = (-1, 0) \times (0, 1)$
$\widehat{\Omega}_t^{(4)} = (-1, 0) \times (-2t, 0).$

(c) $\widehat{\Omega}_t^{(1)} = (t-3, t) \times (0, 1)$
$\widehat{\Omega}_t^{(2)} = (0, t-3) \times (0, 1)$
$\widehat{\Omega}_t^{(3)} = (-1, 0) \times (0, 1)$
$\widehat{\Omega}_t^{(4)} = (-1, 0) \times (-2t, 0)$
$\widehat{\Omega}_t^{(5)} = (-1, 0) \times (-2t-1, -2t)$
$\widehat{\Omega}_t^{(6)} = (0, t) \times (-2t-1, -2t).$

For the domain decomposition we have to consider the eigenvalue problems

$$\begin{cases} -\Delta u + u &= \lambda(1 + \overline{c})u &\text{in} \quad \widehat{\Omega}_t^{(j)} \\ u &= 0 &\text{on} \quad \Gamma_D^{(j)} := \partial\Omega_t \cap \partial\widehat{\Omega}_t^{(j)} \\ \frac{\partial u}{\partial\nu} &= 0 &\text{on} \quad \partial\widehat{\Omega}_t^{(j)}\backslash\Gamma_D^{(j)} \end{cases} \qquad (9.9)$$

for $j \in \{0, \ldots, 6\}$. Recall that $\overline{c} \equiv 0$ in all subdomains where $\omega_t \equiv 0$. With the splitting made in figures 9.2 and 9.3, and by definition of ω_t in (C1)-(C3) and (E1)-(E2), respectively, we immediately see that $\overline{c} \equiv 0$ in $\widehat{\Omega}_t^{(j)}$ for all $j > 1$. Using a separation ansatz we can easily see that the eigenvalues of (9.9) for $j = 1, 3, 5$ are bounded from below by $\frac{\pi^2}{2} + 1$ (cf. section 6.2.2 when $\widehat{\Omega}^j$ is a triangle), whereas a lower bound for all eigenvalues of (9.9) for $j = 2, 4, 6$ is given by $\pi^2 + 1$. Since we are aiming at bounds for eigenvalues neighbouring 1, the eigenvalues contributed by $\widehat{\Omega}_t^{(j)}$, $j > 1$, are not of interest for us (provided that there are eigenvalues of (9.9) for $j = 0, 1$ which are smaller than $\frac{\pi^2}{2} + 1$).

Therefore it remains to consider the eigenvalue problem (9.9) for $j = 1$ and $j = 0$, the latter one only in the case that ω_t is a cornerbump function. We first fix the choice of $\overline{c}$:

Cornerbumps

We have $\widehat{\Omega}_t^{(0)} = \text{conv}\{(0,0), (0,1), (-1,1)\}$ and $\widehat{\Omega}_t^{(1)} = (0,3) \times (0,1)$. Since $\omega_t^{c_i} = \omega^c$ in $\overline{\widehat{\Omega}_t^{(0)} \cup \widehat{\Omega}_t^{(1)}}$, we can choose $\overline{c}$ independently of i in this subdomain. Analogously to the proceeding in section 6.2.2 we define $\overline{c}$ to be constant in $\widehat{\Omega}_t^{(0)}$ and piecewise constant in $\widehat{\Omega}_t^{(1)}$:

$$\overline{c}(x,y) := \begin{cases} c_0 := \max_{\overline{\widehat{\Omega}_t^{(0)}}} 3|\omega^c|\omega^c, & (x,y) \in \overline{\widehat{\Omega}_t^{(0)}} \\ c_1 := \max_{[0,1]\times[0,1]} 3|\omega^c|\omega^c, & (x,y) \in (0,1] \times (0,1) \\ c_2 := \max_{[1,3]\times[0,1]} 3|\omega^c|\omega^c, & (x,y) \in (1,3] \times (0,1). \end{cases}$$

Note that $c_0 > c_1 > c_2$, since ω^c is the basic corner bump.

Edgebumps

We have $\widehat{\Omega}_t^{(1)} = (t-3, t) \times (0,1)$. Choosing

$$\overline{c}(x,y) := \begin{cases} c_1 := \max_{[0,2]\times[0,1]} 3|\omega^e|\omega^e, & (x,y) \in (t-3, t-1] \times (0,1) \\ c_2 := \max_{[2,3]\times[0,1]} 3|\omega^e|\omega^e, & (x,y) \in (t-1, t] \times (0,1), \end{cases}$$

we see that problem (9.9) for $j = 1$ is equivalent to

$$\begin{cases} -\Delta u + u &= \lambda(1 + c^t)u &\text{in } (0,3) \times (0,1) \\ u(x,0) = u(x,1) &= 0, &x \in (0,3) \\ \frac{\partial u}{\partial x}(0,y) = \frac{\partial u}{\partial x}(3,y) &= 0, &y \in (0,1), \end{cases}$$

where $c^t(x) = \overline{c}(x + t - 3)$. Note that $c_1 < c_2$ in this case.

Eigenvalues of (9.9) for $j = 0$ have already been computed in section 5.3. For $j = 1$ we will (as before) use a separation ansatz $u(x,y) = v(x)w(y)$ with $v(x) = v_1(x)$ for $x \in (0, \delta)$, $v(x) = v_2(x)$ for $x \in (\delta, 3)$ and v_1, v_2, w smooth functions. We choose $\delta = 1$ in case of cornerbumps and $\delta = 2$ in case of edgebump-solutions. In addition to the boundary conditions we require u to be continuously differentiable at $x = \delta$. As in the treatment of problem (6.7) in section 6.2.2 (page

54 ff.) this leads to transcendental equations, whose solutions are eigenvalues of (9.9) for $j = 1$. For the details we refer to the equations for (6.7), where the parameter s in that problem has to be replaced by 3 to obtain (9.9) for $j = 1$.

Let $\lambda_1 \leq \lambda_2 \leq \ldots \leq \lambda_q$ denote the union of all eigenvalues of problem (9.9) ($j = 0, 1$ for cornerbumps or $j = 0$ for edgebumps), counted by multiplicity, below a prescibed value $C_L < \frac{\pi^2}{2} + 1$. Moreover denote by $\kappa_1^{(0)} \leq \kappa_2^{(0)} \leq \ldots \leq \kappa_q^{(0)}$ the smallest eigenvalues of (9.7), counted by multiplicity, which correspond to eigenfunctions in $H_0^1(\Omega_t, \mathrm{sym})$. Since eigenvalues of (9.9) for $j > 1$ are larger than $\frac{\pi^2}{2} + 1$, Lemma 5 implies $\lambda_k \leq \kappa_k^{(0)}$ for all $j = 1, \ldots, q$ and moreover $\kappa_{q+1}^{(0)} > C_L$.

The following two tables summarize the results and include also upper bounds $\hat{\kappa}_j^{(0)}$ for the base eigenvalues. These upper bounds can be computed using the Rayleigh-Ritz method when "good" ansatz functions are known. Their construction is addressed in the next section.

j	λ_j	$\hat{\kappa}_j^{(0)}$
1	0.082911	0.181162
2	0.358674	0.480723
3	0.522312	0.698175
4	0.634437	0.845235
5	0.910201	1.027073
6	1.080058	1.435944
7	1.185964	1.525085
8	1.737490	1.935357
9	1.737490	1.975972
10	1.791883	2.070920
11	2.013254	2.277388
12	2.356533	2.750397
13	2.433678	2.862914
14	2.564780	3.000295

j	λ_j	$\hat{\kappa}_j^{(0)}$
1	0.138285	0.138287
2	0.287006	0.287008
3	0.474108	0.474110
4	0.627807	0.627810
5	0.644585	0.644587
6	1.003982	1.003987
7	1.028832	1.028844
8	1.181200	1.181214
9	1.211802	1.211816
10	1.568845	1.568862
11	1.586584	1.586603
12	1.803839	1.803898
13	1.952124	1.952190
14	1.994569	1.994635

Table 9.1: Lower bounds for the base problem in case of cornerbump-functions.

Table 9.2: Lower bounds for the base problem in case of edgebump-functions.

9.4   Upper Bounds and Homotopy

In analogy to the setting in section 5.2 we define for $s \in [0, 1]$:

$$N_s(u, \varphi) = \int_{\Omega_t} (1 + (1-s)\bar{c} + s3|\omega_t|\omega_t)u\varphi\,dx \quad (u, \varphi \in H_0^1(\Omega_t, \mathrm{sym})),$$

and the family of eigenvalue problems connecting (9.7) and (9.6) is given by

$$\langle u, \varphi \rangle_{H_0^1(\Omega_t)} = \kappa^{(s)} N_s(u, \varphi) \quad \text{for all } \varphi \in H_0^1(\Omega_t, \mathrm{sym}). \tag{9.10}$$

In order to find a suitable a-priori lower bound to start the homotopy, we have to find an index $n \in \{1, \ldots, q\}$ such that $\hat{\kappa}_n^{(0)} \leq \lambda_{n+1} < \kappa_{n+1}^{(0)}$, where $\hat{\kappa}_n^{(0)}$ denotes an upper bound for $\kappa_n^{(0)}$. Therefore we have to compute upper bounds for the first p eigenvalues of (9.7), which can as before be done using the Rayleigh-Ritz method. To apply this method, we have to choose suitable testfunctions $v_1, \ldots, v_q \in H_0^1(\Omega_t)$ having the same symmetry properties as ω_t. We will briefly comment on a possible construction of these test functions that can also be used in the homotopy and the Lehmann-Goerisch method.

Cornerbumps

Denote by $H_0^1(\Omega^T, \mathrm{sym})$ the subspace of $H_0^1(\Omega^T)$ containing all functions symmetric w.r.t. $y = -x$. Moreover, for some $s \in [0, 1]$, let $w = (1 - s)\bar{c} + s\omega^c \in H_0^1(\Omega^T, \mathrm{sym})$ and let $v_1^c, \ldots, v_q^c \in H_0^1(\Omega^T, \mathrm{sym})$ be approximate eigenfunctions of

$$\int_{\Omega^T} [\nabla u \cdot \nabla \varphi + u\varphi] \, dx = \tau \underbrace{\int_{\Omega^T} [1 + w(x)] \, u\varphi \, dx}_{=:N_s^c(u,\varphi)} \quad \text{for all } \varphi \in H_0^1(\Omega^T, \mathrm{sym}). \quad (9.11)$$

Using the same definitions as in $(C1), (C2)$ and $(C4)$ (construction of ω^{c_i}), with ω^c replaced by v_k^c $(k = 1, \ldots, q)$ we can define approximate eigenfunctions $v_1^{c_i}, \ldots, v_q^{c_i} \in H_0^1(\Omega_t, \mathrm{sym}^{c_i})$ $(i = 1, 2, 4)$ which are zero in the same subdomains as $\omega_t^{c_i}$ $(i = 1, 2, 4)$.

Due to symmetry of $v_1^{c_i}, \ldots, v_q^{c_i} \in H_0^1(\Omega_t)$ we have for the quantities in the Rayleigh-Ritz method:

$$\langle v_k^{c_i}, v_l^{c_i} \rangle_{H_0^1(\Omega_t)} = i \langle v_k^c, v_l^c \rangle_{H_0^1(\Omega^T)}$$

$$N_s(v_k^{c_i}, v_l^{c_i}) = \int_{\Omega_t} (1 + w(x)) v_k^{c_i} v_l^{c_i} \, dx = i N_s^c(v_k^c, v_l^c),$$

for $i = 1, 2, 4$, and analogously for the terms in the Lehmann-Goerisch method. Thus in the course of the homotopy and for the computation of upper eigenvalue bounds we have to work only on the domain Ω^c (or even more efficiently on the half domain $\mathrm{conv}\{(0, 0), (3, 0), (3, 1), (-1, 1)\}$).

Finally our considerations show that the computations are independent of t and we can therefore compute constants $K_t^{c_i, \mathrm{sym}}$, $i = 1, 2, 4$ satisfying (9.4).

Edgebumps

Analogously to the cornerbump-case denote by $H_0^1(\Omega^e, \mathrm{sym})$ the subspace of $H_0^1(\Omega^e)$ containing all functions symmetric w.r.t. $x = 3$. Let $w = (1 - s)\bar{c} + s\omega^e \in H_0^1(\Omega^e, \mathrm{sym})$ for some $s \in [0, 1]$ and let $v_1^e, \ldots, v_q^e \in H_0^1(\Omega^e, \mathrm{sym})$ be approximate eigenfunctions of

$$\int_{\Omega^e} [\nabla u \cdot \nabla \varphi + u\varphi] \, dx = \tau \underbrace{\int_{\Omega^e} [1 + w(x)] \, u\varphi \, dx}_{=:N_s^e(u,\varphi)} \quad \text{for all } \varphi \in H_0^1(\Omega^e, \mathrm{sym}). \quad (9.12)$$

With the definitions in (E1), (E2) and (E4) (replacing ω^e by $v_1^e, \ldots, v_q^e$) we can again define approximate eigenfunctions $v_1^{e_i}, \ldots, v_q^{e_i} \in H_0^1(\Omega_t, \mathrm{sym}^{e_i})$ being zero in the same subdomains as $\omega_t^{e_i}$ $(i = 1, 2, 4)$.

By construction we have

$$\langle v_k^{e_i}, v_l^{e_i}\rangle_{H_0^1(\Omega_t)} = i\,\langle v_k^e, v_l^e\rangle_{H_0^1(\Omega^e)}$$

$$N_s(v_k^{e_i}, v_l^{e_i}) = \int_{\Omega_t} (1 + w(x))v_k^{e_i} v_l^{e_i}\, dx = iN_s^e(v_k^e, v_l^e),$$

showing that during the homotopy or for the computation of upper bounds we have to work only with the domain Ω^e. Thus we will obtain constants $K_t^{e_i,\mathrm{sym}}$, $i = 1, 2, 4$ satisfying (9.5).

Remark 13. During the homotopy we have to compute also approximations of the gradients of $v_k^{c_i}$ and $v_k^{e_i}$. As in section 9.2 these can be constructed from approximations ρ_k^c of ∇v_k^c and ρ_k^e of ∇v_k^e, respectively, by zero extension outside the corners or edges of Ω_t. For the resulting gradient to be in $H(\mathrm{div}, \Omega_t)$ we have to impose Dirichlet boundary conditions for the first component of ρ_k^c at $x = 3$ and the second component of ρ_k^c at $y = -3$, as well as for the first component of ρ_k^e at $x = 0$ and $x = 6$.

9.5 Numerical Results

Cornerbumps

From the results (8.19) and (8.20) in section 8.2.4 for the unbounded L-shaped domain we have

$$\|\nabla\omega^c - \rho^c\|_{L^2(\Omega^T)} \leq 0.000781513$$
$$\|\,\mathrm{div}(\rho^c) + |\omega^c|^3\|_{L^2(\Omega^T)} \leq 0.002897424,$$

which, using (9.3), leads to

$$\| - \Delta\omega_t^{c_1} - |\omega_t^{c_1}|^3\|_{H^{-1}(\Omega_t)} \leq 0.00169663 =: \delta_t^{c_1} \quad \text{for all } t \geq 1.5$$
$$\| - \Delta\omega_t^{c_2} - |\omega_t^{c_2}|^3\|_{H^{-1}(\Omega_t)} \leq 0.00239940 =: \delta_t^{c_1} \quad \text{for all } t \geq 1.5$$
$$\| - \Delta\omega_t^{c_4} - |\omega_t^{c_4}|^3\|_{H^{-1}(\Omega_t)} \leq 0.00338548 =: \delta_t^{c_1} \quad \text{for all } t \geq 3.$$

For the eigenvalue problem (9.6) with ω_t replaced by $I_{V_{\tilde{N}}}(\omega_t^{c_i})$, $i = 1, 2, 4$ (see also Remark 7), we have the uniform eigenvalue bounds for all $t \geq \hat{t}$ ($\hat{t} = 1.5$ for $i = 1, 2$, $\hat{t} = 3$ for $i = 4$):

$$\kappa_1 \leq 0.35262$$
$$\kappa_2 \geq 1.36740.$$

From (8.21) we have

$$\|\omega^c\|_{L^4(\Omega^T)} \leq 3.014332566,$$

which implies

$$\|\omega_t^{c_1}\|_{L^4(\Omega_t)} = \|\omega^c\|_{L^4(\Omega^T)} \leq 3.014332566$$
$$\|\omega_t^{c_2}\|_{L^4(\Omega_t)} = \sqrt[4]{2}\|\omega^c\|_{L^4(\Omega^T)} \leq 3.584665734$$
$$\|\omega_t^{c_4}\|_{L^4(\Omega_t)} = \sqrt[4]{4}\|\omega^c\|_{L^4(\Omega^T)} \leq 4.262909995.$$

After using Lemma 1 once again, this yields the constants $K_t^{c_i, \text{sym}}$, $i = 1, 2, 4$ satisfying (9.4):

$$K_t^{c_1, \text{sym}} = 3.722882891 \quad \text{for all } t \geq 1.5$$
$$K_t^{c_2, \text{sym}} = 3.723601721 \quad \text{for all } t \geq 1.5$$
$$K_t^{c_4, \text{sym}} = 3.724806373 \quad \text{for all } t \geq 3.$$

Finally, with $C_4(\Omega_t)$ denoting the embedding constant for the embedding $H_0^1(\Omega_t) \hookrightarrow L^4(\Omega_t)$ we have by Lemma 7: $C_4(\Omega_t) = C_4(\Omega_{\hat{t}})$ for all $t \geq \hat{t}$ ($\hat{t} = 1.5$ for $i = 1, 2$, $\hat{t} = 3$ for $i = 4$) and with the results displayed in Table 6.1 we get

$$C_4(\Omega_{1.5}) = 0.461477761$$
$$C_4(\Omega_3) = 0.460583805.$$

Now we can look for $\alpha_t^{c_i} > 0$ such that

$$\delta_t^{c_i} < \frac{\alpha_t^{c_i}}{K_t^{c_i}} - 3 \left(C_4(\Omega_t)\right)^3 \left(\alpha_t^{c_i}\right)^2 \left(\|\omega_t^{c_i}\|_{L^4} + \tfrac{1}{3} C_4(\Omega_t)\alpha_t^{c_i}\right), \quad i = 1, 2, 4 \quad \text{for all } t \geq \hat{t},$$

and obtain that this inequality is satisfied for

$$\alpha_t^{c_1} = 0.006460701 \quad \text{for all } t \geq 1.5$$
$$\alpha_t^{c_2} = 0.009282265 \quad \text{for all } t \geq 1.5$$
$$\alpha_t^{c_4} = 0.013466675 \quad \text{for all } t \geq 3.$$

Therefore - after checking $\|\omega_t^{c_i}\|_{H_0^1(\Omega_t)} = \sqrt{i}\|\omega^c\|_{H_0^1(\Omega^T)} > \alpha_t^{c_i}$, $i = 1, 2, 4$ - we obtain for all $t \geq \hat{t}$ the existence of non-trivial solutions $u_t^{c_i} \in H_0^1(\Omega^{c_i}, \text{sym}^{c_i})$ to problem (3.10) such that

$$\|u_t^{c_i} - \omega_t^{c_i}\|_{H_0^1(\Omega_t)} \leq \alpha_t^{c_i} \qquad i = 1, 2, 4.$$

Edgebumps

For the basic edge-bump we obtain the results

$$\|\nabla\omega^e - \rho^e\|_{L^2(\Omega^e)} \leq 0.002138790$$
$$\|\operatorname{div}(\rho^e) + |\omega^e|^3\|_{L^2(\Omega^e)} \leq 0.004722495,$$

and thus, using (9.3),

$$\| - \Delta\omega_t^{e_1} - |\omega_t^{e_1}|^3\|_{H^{-1}(\Omega_t)} \leq 0.003623987 =: \delta_t^{e_1} \quad \text{for all } t \geq 3$$
$$\| - \Delta\omega_t^{e_2} - |\omega_t^{e_2}|^3\|_{H^{-1}(\Omega_t)} \leq 0.005125091 =: \delta_t^{e_2} \quad \text{for all } t \geq 3$$
$$\| - \Delta\omega_t^{e_4} - |\omega_t^{e_4}|^3\|_{H^{-1}(\Omega_t)} \leq 0.007247973 =: \delta_t^{e_4} \quad \text{for all } t \geq 3.$$

Uniform bounds for the eigenvalue problem (9.6) with ω_t replaced by $I_{V_{\tilde{N}}}(\omega_t^{e_i})$, $i = 1, 2, 4$ for all $t \geq 3$ are given by

$$\kappa_1 \leq 0.34915$$
$$\kappa_2 \geq 1.51840.$$

Together with $\|\omega^e\|_{L^4(\Omega^e)} \leq 1.320091540$, implying

$$\|\omega_t^{e_1}\|_{L^4(\Omega_t)} = \|\omega^e\|_{L^4(\Omega^e)} \leq 1.320091540$$
$$\|\omega_t^{e_2}\|_{L^4(\Omega_t)} = \sqrt[4]{2}\|\omega^e\|_{L^4(\Omega^e)} \leq 1.569862252$$
$$\|\omega_t^{e_4}\|_{L^4(\Omega_t)} = \sqrt[4]{4}\|\omega^e\|_{L^4(\Omega^e)} \leq 1.866891359,$$

the eigenvalue bounds yield the following constants $K_t^{e_i}$, $i = 1, 2, 4$ satisfying (9.5) (after using Lemma 1 once again)

$$K_t^{e_1,\text{sym}} = 2.929314798 \quad \text{for all } t \geq 3$$
$$K_t^{e_2,\text{sym}} = 2.929521043 \quad \text{for all } t \geq 3$$
$$K_t^{e_4,\text{sym}} = 2.929867970 \quad \text{for all } t \geq 3.$$

Suitable $\alpha_t^{e_i}$ satisfying

$$\delta_t^{e_i} < \frac{\alpha_t^{e_i}}{K_t^{e_i}} - 3(C_4(\Omega_t))^3 \left(\alpha_t^{e_i}\right)^2 \left(\|\omega_t^{e_i}\|_{L^4} + \tfrac{1}{3}C_4(\Omega_t)\alpha_t^{e_i}\right), \quad i = 1, 2, 4 \quad \text{for all } t \geq 3$$

are now given by

$$\alpha_t^{e_1} = 0.010757705 \quad \text{for all } t \geq 3$$
$$\alpha_t^{e_2} = 0.015346977 \quad \text{for all } t \geq 3$$
$$\alpha_t^{e_4} = 0.022036766 \quad \text{for all } t \geq 3.$$

Note that $C_4(\Omega_t) = C_4(\Omega_3)$ for all $t \geq 3$ as already explained in the previous paragraph. Therefore - after checking again $\|\omega_t^{e_i}\|_{H_0^1(\Omega_t)} = \sqrt{i}\|\omega^e\|_{H_0^1(\Omega^e)} > \alpha_t^{e_i}$, $i = 1, 2, 4$ - we obtain for all $t \geq 3$ the existence of non-trivial solutions $u_t^{e_i} \in H_0^1(\Omega^{e_i}, \text{sym}^{e_i})$ to problem (3.10) such that

$$\|u_t^{e_i} - \omega_t^{e_i}\|_{H_0^1(\Omega_t)} \leq \alpha_t^{e_i} \qquad i = 1, 2, 4.$$

Multiplicity

Similar as in section 6.4.2 we can prove

$$\|u_t^{(1)} - u_t^{(2)}\|_{H_0^1(\Omega_t)} > 0 \quad \text{for all } t \geq 3,$$

where $u_t^{(1)}, u_t^{(2)} \in \{u_t^{c_i}, u_t^{e_i} : i = 1, 2, 4\}$, $u_t^{(1)} \neq u_t^{(2)}$, as well as

$$\|u_t^{c_1} - u_t^{c_2}\|_{H_0^1(\Omega_t)} > 0 \quad \text{for all } t \geq 1.5.$$

Let moreover $(u_t)_{t \in [1.5,3]}$ denote the fourpeakcorner solution branch, whose existence had already been proven in Theorem 6. By showing

$$\|u_t^{c_i} - u_t\|_{H_0^1(\Omega_t)} > 0 \quad \text{for all } t \in [1.5, 3], \ i = 1, 2,$$

which is indeed satisfied, Theorem 10 is proved.

Smoothness of solution branches

We will finally prove

Theorem 11. *The solution branches $(u_t^{c_i})_{t\in[\hat{t},\infty)}$ and $(u_t^{e_i})_{t\in[\hat{t},\infty)}$, $i = 1,2,4$, are continuously differentiable.*

For the notion of differentiability of the branches we refer to the definitions in setion 7.2 (see Theorem 7 and Remark 11). The proof of Theorem 11 is almost identical to the proof of Theorem 7, but with significant simplification in some steps:

- Continuity of the mapping defined in (7.48) follows immediately due to the construction of the approximate solutions $\omega_t^{c_i}$ and $\omega_t^{e_i}$, $i = 1,2,4$

- The mappings $t \mapsto \alpha_t^{c_i}, t \mapsto \alpha_t^{e_i}$, $i = 1,2,4$ are constant and therefore clearly lower semi-continuous. Moreover the existence of some t-independent $\eta > 0$ such that (2.8) holds with $\alpha_t^{c_i} + \eta$ instead of $\alpha_t^{c_i}$, $i = 1,2,4$, and $\alpha_t^{e_i} + \eta$ instead of $\alpha_t^{e_i}$, $i = 1,2,4$, respectively, is trivial.

Remark 14. It is clear that the method explained in this chapter is not limited to the cornerbump and edgebump functions we constructed. One could also construct solutions having bumps in two adjacent corner parts or edges of the domain, three bumps, mixture of corner- and edgebumps and many more.

A Appendix

A.1 Complete Tables for Verified Results

Fourpeakcorner

t	$\overline{\kappa}_1$	$\underline{\kappa}_2$	K_t	δ_t	α_t	$\max \psi$
0.208984375	0.35886	1.46450	3.15489	0.0257979	-	0.0206708
0.23828125	0.35862	1.36796	3.72039	0.0201304	-	0.0147278
0.267578125	0.35837	1.29394	4.40575	0.0162102	-	0.0104117
0.296875	0.35805	1.24784	5.03974	0.0133682	-	0.0078930
0.326171875	0.35759	1.23600	5.24225	0.0112234	-	0.0072413
0.35546875	0.35700	1.25520	4.92280	0.0095729	-	0.0081590
0.384765625	0.35637	1.28913	4.46259	0.0083061	0.0529693	-
0.4140625	0.35579	1.32103	4.11833	0.0733333	0.0376470	-
0.443359375	0.35528	1.34409	3.90901	0.0057125	0.0302737	-
0.47265625	0.35485	1.35813	3.79517	0.0059516	0.0258406	-
0.501953125	0.35449	1.36588	3.73632	0.0054263	0.0227653	-
0.53125	0.35419	1.36966	3.70819	0.0049660	0.0204041	-
0.560546875	0.35393	1.37139	3.69581	0.0045563	0.0184645	-
0.58984375	0.35372	1.37191	3.69147	0.0041917	0.0168223	-
0.619140625	0.35355	1.37195	3.69149	0.0038717	0.0154279	-
0.6484375	0.35340	1.37157	3.69441	0.0035973	0.0142616	-
0.677734375	0.35328	1.37118	3.69733	0.0033684	0.0133000	-
0.70703125	0.35318	1.37074	3.70026	0.0031830	0.0125299	-
0.736328125	0.35309	1.37030	3.70320	0.0030377	0.0119315	-
0.765625	0.35302	1.36993	3.70615	0.0029272	0.0114808	-
0.794921875	0.35296	1.36943	3.70984	0.0028459	0.0111551	-
0.82421875	0.35290	1.36900	3.71281	0.0027881	0.0109250	-
0.853515625	0.35286	1.36872	3.71504	0.0027487	0.0107688	-
0.8828125	0.35282	1.36847	3.71728	0.0027233	0.0106701	-
0.9121093750	0.35279	1.36833	3.71805	0.0027079	0.0106086	-
0.94140625	0.35276	1.36793	3.72104	0.0026998	0.0105842	-
0.970703125	0.35274	1.36796	3.72108	0.0026965	0.0105701	-
1	0.35272	1.36782	3.72185	0.0026960	0.0105702	-
1.0625	0.35269	1.36762	3.72334	0.0026984	0.0105839	-
1.125	0.35267	1.36748	3.72482	0.0026996	0.0105930	-

1.1875	0.35265	1.36738	3.72556	0.0027001	0.0105967	-
2.25	0.35264	1.36723	3.72630	0.0027001	0.0105984	-
1.3125	0.35263	1.36718	3.71786	0.0026998	0.0105701	-
1.375	0.35263	1.36714	3.72704	0.0026993	0.0105967	-
1.4375	0.35263	1.36712	3.72704	0.0026988	0.0105940	-
1.5	0.35262	1.36710	3.72704	0.0026982	0.0105912	-
1.5625	0.35262	1.36709	3.72779	0.0026976	0.0105908	-
1.625	0.35262	1.36707	3.72779	0.0026971	0.0105881	-
1.6875	0.35262	1.36707	3.72779	0.0026965	0.0105856	-
1.75	0.35262	1.36706	3.72779	0.0026960	0.0105832	-
1.8125	0.35262	1.36705	3.72778	0.0026955	0.0105810	-
1.875	0.35262	1.36705	3.72778	0.0026951	0.0105790	-
1.9375	0.35262	1.36705	3.72778	0.0026947	0.0105771	-
2	0.35262	1.36704	3.72778	0.0026943	0.0105754	-
2.0625	0.35262	1.36704	3.72778	0.0026940	0.0105739	-
2.125	0.35262	1.36704	3.72778	0.0026937	0.0105726	-
2.1875	0.35262	1.36704	3.72778	0.0026934	0.0105714	-
2.25	0.35262	1.36703	3.72778	0.0026932	0.0105702	-
2.3125	0.35262	1.36703	3.72778	0.0026930	0.0105693	-
2.375	0.35262	1.36703	3.72778	0.0026928	0.0105684	-
2.4375	0.35262	1.36703	3.72778	0.0026927	0.0105677	-
2.5	0.35262	1.36703	3.72778	0.0026925	0.0105670	-
2.5625	0.35262	1.36703	3.72778	0.0026924	0.0105665	-
2.625	0.35262	1.36703	3.72778	0.0026923	0.0105660	-
2.6875	0.35262	1.36703	3.72778	0.0026922	0.0105656	-
2.75	0.35262	1.36703	3.72778	0.0026922	0.0105653	-
2.8125	0.35262	1.36703	3.72778	0.0026921	0.0105650	-
2.875	0.35262	1.36703	3.72778	0.0026921	0.0105649	-
2.9375	0.35262	1.36702	3.72778	0.0026920	0.0105647	-
3	0.35262	1.36702	3.72779	0.0026920	0.0105647	-

Fourpeakedge

t	$\overline{\kappa}_1$	$\underline{\kappa}_2$	K_t	δ_t	α_t	$\max \psi$
0.501953125	0.35423	1.06716	15.97879	0.0041423	-	0.0007329
0.53125	0.35286	1.24676	5.05846	0.0034592	0.0203114	-
0.560546875	0.35209	1.36622	3.73308	0.0030727	0.0122322	-
0.58984375	0.35153	1.46354	3.15902	0.0028470	0.0093761	-
0.619140625	0.35111	1.53966	2.85439	0.0027271	0.0080405	-
0.6484375	0.35077	1.56669	2.76567	0.0026737	0.0076181	-
0.677734375	0.35049	1.55988	2.78736	0.0026586	0.0076371	-
0.70703125	0.35027	1.55267	2.81061	0.0026642	0.0077214	-
0.736328125	0.35009	1.54664	2.83046	0.0026802	0.0078276	-
0.765625	0.34994	1.54170	2.84700	0.0027014	0.0079404	-
0.794921875	0.34981	1.53768	2.86107	0.0027252	0.0080550	-
0.82421875	0.34971	1.53442	2.87292	0.0027508	0.0081690	-
0.853515625	0.34962	1.53165	2.88209	0.0027779	0.0082802	-
0.8828125	0.34954	1.52943	2.88992	0.0028066	0.0083929	-
0.912109375	0.34948	1.52763	2.89637	0.0028370	0.0085074	-
0.94140625	0.34943	1.52609	2.90216	0.0028695	0.0086265	-
0.970703125	0.34939	1.52487	2.90627	0.0029042	0.0087476	-
1	0.34935	1.52380	2.91018	0.0029412	0.0088759	-
1.0625	0.34929	1.52222	2.91602	0.0028330	0.0085558	-
1.125	0.34925	1.52113	2.92002	0.0027784	0.0083971	-
1.1875	0.34922	1.52036	2.92292	0.0027499	0.0083163	-
1.25	0.34920	1.51987	2.92472	0.0027142	0.0082100	-
1.3125	0.34918	1.51947	2.92618	0.0026816	0.0081119	-
1.375	0.34917	1.51926	2.92691	0.0026644	0.0080603	-
1.4375	0.34916	1.51895	2.92802	0.0026621	0.0080561	-
1.5	0.34916	1.51908	2.92764	0.0026696	0.0080783	-
1.5625	0.34916	1.51902	2.92764	0.0026841	0.0081235	-
1.625	0.34915	1.51897	2.92802	0.0027053	0.0081907	-
1.6875	0.34915	1.51893	2.92803	0.0027340	0.0082804	-
1.75	0.34915	1.51897	2.92804	0.0027713	0.0083975	-
1.8125	0.34915	1.51890	2.92806	0.0028187	0.0085461	-
1.875	0.34915	1.51894	2.92810	0.0028772	0.0087300	-
1.9375	0.34915	1.51886	2.92851	0.0029480	0.0089540	-
2	0.34915	1.51888	2.92858	0.0030319	0.0092189	-
2.0625	0.34915	1.51884	2.92866	0.0031298	0.0095286	-

2.125	0.34915	1.51884	2.92875	0.0032422	0.0098853	-
2.1875	0.34915	1.51892	2.92850	0.0033696	0.0102895	-
2.25	0.34915	1.51885	2.92901	0.0035123	0.0107472	-
2.3125	0.34915	1.51884	2.92918	0.0036706	0.0112552	-
2.375	0.34915	1.51885	2.92936	0.0038445	0.0118161	-
2.4375	0.34915	1.51880	2.92957	0.0040340	0.0124306	-
2.5	0.34915	1.51865	2.93055	0.0042391	0.0131032	-
2.5625	0.34915	1.51878	2.93044	0.0044596	0.0138252	-
2.625	0.34915	1.51871	2.93072	0.0046955	0.0146047	-
2.6875	0.34915	1.51857	2.93178	0.0049465	0.0154449	-
2.75	0.34915	1.51878	2.93136	0.0052125	0.0163329	-
2.8125	0.34915	1.51870	2.93173	0.0054932	0.0172829	-
2.875	0.34915	1.51850	2.93287	0.0057884	0.0182967	-
2.9375	0.34915	1.51867	2.93292	0.0060980	0.0193619	-
3	0.34915	1.51868	2.93337	0.0064216	0.0204903	-

Onepeakcorner

t	$\overline{\kappa}_1$	$\underline{\kappa}_2$	K_t	δ_t	α_t
0.501953125	0.35262	1.36707	3.72550	0.0047839	0.0190828
0.53125	0.35262	1.36705	3.72560	0.0041881	0.0165515
0.560546875	0.35262	1.36704	3.72564	0.0036825	0.0144421
0.58984375	0.35262	1.36693	3.72642	0.0032471	0.0126552
0.619140625	0.35262	1.36702	3.72572	0.0028745	0.0111404
0.6484375	0.35262	1.36698	3.72600	0.0025596	0.0098762
0.677734375	0.35262	1.36689	3.72665	0.0022972	0.0088327
0.70703125	0.35262	1.36718	3.72449	0.0020819	0.0079760
0.736328125	0.35262	1.36717	3.72455	0.0019080	0.0072924
0.765625	0.35262	1.36722	3.72418	0.0017697	0.0067501
0.794921875	0.35262	1.36702	3.72566	0.0016613	0.0063301
0.82421875	0.35262	1.36708	3.72522	0.0015779	0.0060044
0.853515625	0.35262	1.36715	3.72470	0.0015146	0.0057581
0.8828125	0.35262	1.36712	3.72493	0.0014677	0.0055765
0.912109375	0.35262	1.36709	3.72516	0.0014336	0.0054445
0.94140625	0.35262	1.36708	3.72525	0.0014093	0.0053506

0.970703125	0.35262	1.36715	3.72474	0.0013923	0.0052843
1	0.35262	1.36702	3.72570	0.0013807	0.0052407
1.0625	0.35262	1.36702	3.72571	0.0013667	0.0051864
1.125	0.35262	1.36702	3.72571	0.0013593	0.0051577
1.1875	0.35262	1.36702	3.72571	0.0013553	0.0051423
1.25	0.35262	1.36702	3.72571	0.0013531	0.0051335
1.3125	0.35262	1.36702	3.72571	0.0013517	0.0051282
1.375	0.35262	1.36702	3.72571	0.0013509	0.0051248
1.4375	0.35262	1.36702	3.72571	0.0013502	0.0051224
1.5	0.35262	1.36702	3.72571	0.0013498	0.0051205

Onepeakedge

t	$\overline{\kappa}_1$	$\underline{\kappa}_2$	K_t	δ_t	α_t
0.501953125	0.34980	1.53720	2.86448	0.0021935	0.0064033
0.53125	0.34971	1.53469	2.87327	0.0020107	0.0058791
0.560546875	0.34963	1.53237	2.88145	0.0018845	0.0055204
0.58984375	0.34956	1.53033	2.88869	0.0017995	0.0052810
0.619140625	0.34950	1.52851	2.89519	0.0017422	0.0051220
0.6484375	0.34945	1.52717	2.89999	0.0017023	0.0050115
0.677734375	0.34940	1.52589	2.90458	0.0016729	0.0049319
0.70703125	0.34937	1.52481	2.90846	0.0016501	0.0048701
0.736328125	0.34933	1.52387	2.91183	0.0016315	0.0048201
0.765625	0.34931	1.52278	2.91576	0.0016161	0.0047805
0.794921875	0.34928	1.52234	2.91731	0.0016033	0.0047448
0.82421875	0.34926	1.52177	2.91933	0.0015932	0.0047176
0.853515625	0.34924	1.52133	2.92088	0.0015855	0.0046972
0.8828125	0.34923	1.52089	2.92242	0.0015804	0.0046844
0.912109375	0.34922	1.52059	2.92345	0.0015779	0.0046784
0.94140625	0.34921	1.52031	2.92441	0.0015779	0.0046800
0.970703125	0.34920	1.52005	2.92529	0.0015806	0.0046893
1	0.34919	1.51976	2.92628	0.0015857	0.0047065
1.0625	0.34918	1.51949	2.92569	0.0014423	0.0042745
1.125	0.34917	1.51934	2.92615	0.0014085	0.0041739
1.1875	0.34916	1.51915	2.92678	0.0013897	0.0041182

1.25	0.34916	1.51905	2.92709	0.0013685	0.0040551
1.3125	0.34915	1.51903	2.92712	0.0013496	0.0039985
1.375	0.34915	1.51838	2.92950	0.0013392	0.0039705
1.4375	0.34915	1.51870	2.92828	0.0013365	0.0039610
1.5	0.34915	1.51881	2.92786	0.0013392	0.0039682
1.5625	0.34915	1.51877	2.92799	0.0013455	0.0039875
1.625	0.34915	1.51874	2.92810	0.0013554	0.0040173
1.6875	0.34915	1.51870	2.92824	0.0013692	0.0040588
1.75	0.34915	1.51893	2.92738	0.0013875	0.0041123
1.8125	0.34915	1.51888	2.92757	0.0014108	0.0041825
1.875	0.34915	1.51886	2.92765	0.0014398	0.0042696
1.9375	0.34915	1.51892	2.92744	0.0014750	0.0043748
2	0.34915	1.51887	2.92765	0.0015168	0.0045007
2.0625	0.34915	1.51884	2.92779	0.0015656	0.0046475
2.125	0.34915	1.51891	2.92756	0.0016216	0.0048159
2.1875	0.34915	1.51891	2.92760	0.0016852	0.0050075
2.25	0.34915	1.51885	2.92787	0.0017565	0.0052229
2.3125	0.34915	1.51882	2.92804	0.0018356	0.0054620
$\frac{38}{16}$	0.34915	1.51884	2.92803	0.0019225	0.0057247
2.4375	0.34915	1.51882	2.92818	0.0020172	0.0060119
2.5	0.34915	1.51864	2.92893	0.0021197	0.0063246
2.5625	0.34915	1.51857	2.92928	0.0022300	0.0066606
2.625	0.34915	1.51866	2.92905	0.0023479	0.0070193
2.6875	0.34915	1.51298	2.95052	0.0024734	0.0074590
2.75	0.34915	1.51830	2.93062	0.0026063	0.0078136
2.8125	0.34915	1.51880	2.92887	0.0027467	0.0082392
2.875	0.34915	1.51850	2.93014	0.0028943	0.0086969
2.9375	0.34915	1.51878	2.92925	0.0030490	0.0091714
3	0.34915	1.51871	2.92966	0.0032109	0.0096732

Twopeakoppcorner

t	$\overline{\kappa}_1$	$\underline{\kappa}_2$	K_t	δ_t	α_t
0.501953125	0.35264	1.36689	3.72722	0.0160981	0.1054400
0.53125	0.35264	1.36688	3.72730	0.0135297	0.0709231
0.560546875	0.35263	1.36677	3.72813	0.0113996	0.0546435
0.58984375	0.35263	1.36677	3.72814	0.0096303	0.0436372
0.619140625	0.35262	1.36687	3.72742	0.0081618	0.0355496
0.6484375	0.35262	1.36677	3.72819	0.0069463	0.0294037
0.677734375	0.35262	1.36676	3.72830	0.0059446	0.0246219
0.70703125	0.35262	1.36708	3.72596	0.0051237	0.0085325
0.736328125	0.35262	1.36708	3.72601	0.0044549	0.0178981
0.765625	0.35262	1.36713	3.72569	0.0039136	0.0155638
0.794921875	0.35262	1.36709	3.72605	0.0034785	0.0137265
0.82421875	0.35262	1.36702	3.72665	0.0031316	0.0122840
0.853515625	0.35262	1.36710	3.72614	0.0028576	0.0111542
0.8828125	0.35262	1.36686	3.72803	0.0026440	0.0102880
0.912109375	0.35262	1.36704	3.72680	0.0024801	0.0096200
0.94140625	0.35262	1.36704	3.72692	0.0023570	0.0091240
0.970703125	0.35262	1.36711	3.72654	0.0022671	0.0087616
1	0.35262	1.36699	3.72758	0.0022034	0.0085089
1.0625	0.35262	1.36702	3.72571	0.0014085	0.0053480
1.125	0.35262	1.36702	3.72571	0.0013825	0.0052473
1.1875	0.35262	1.36702	3.72571	0.0013678	0.0051905
1.25	0.35262	1.36702	3.72571	0.0013596	0.0051589
1.3125	0.35262	1.36702	3.72571	0.0013551	0.0051414
1.375	0.35262	1.36702	3.72571	0.0013526	0.0051316
1.4375	0.35262	1.36702	3.72571	0.0013511	0.0051258
1.5	0.35262	1.36702	3.72571	0.0013502	0.0051223

Twopeakoppedge

t	$\overline{\kappa}_1$	$\underline{\kappa}_2$	K_t	δ_t	α_t
0.501953125	0.34983	1.53786	2.86108	0.0025267	0.0074174
0.53125	0.34973	1.53514	2.87054	0.0023319	0.0068555
0.560546875	0.34965	1.53269	2.87913	0.0022042	0.0064916
0.58984375	0.34957	1.53056	2.88665	0.0021258	0.0062726
0.619140625	0.34951	1.52866	2.89341	0.0020805	0.0061511
0.6484375	0.34945	1.52728	2.89834	0.0020558	0.0060872
0.677734375	0.34941	1.52596	2.90308	0.0020432	0.0060591
0.70703125	0.34937	1.52485	2.90707	0.0020375	0.0060503
0.736328125	0.34934	1.52391	2.91046	0.0020359	0.0060529
0.765625	0.34931	1.52281	2.91444	0.0020373	0.0060655
0.794921875	0.34928	1.52236	2.91605	0.0020410	0.0060801
0.82421875	0.34926	1.52179	2.91810	0.0020469	0.0061024
0.853515625	0.34924	1.52135	2.91968	0.0020550	0.0061303
0.8828125	0.34923	1.52090	2.92130	0.0020653	0.0061653
0.912109375	0.34922	1.52061	2.92233	0.0020780	0.0062060
0.94140625	0.34921	1.52032	2.92336	0.0020930	0.0062541
0.970703125	0.34920	1.52005	2.92432	0.0021104	0.0063094
1	0.34919	1.51976	2.92536	0.0021303	0.0063725
1.0625	0.34918	1.51949	2.92569	0.0014423	0.0042745
1.125	0.34917	1.51934	2.92615	0.0014085	0.0041739
1.1875	0.34916	1.51915	2.92678	0.0013897	0.0041182
1.25	0.34916	1.51905	2.92709	0.0013685	0.0040551
1.3125	0.34915	1.51903	2.92712	0.0013496	0.0039985
1.375	0.34915	1.51838	2.92950	0.0013392	0.0039705
1.4375	0.34915	1.51869	2.92832	0.0013365	0.0039610
1.5	0.34915	1.51881	2.92786	0.0013392	0.0039682
1.5625	0.34915	1.51877	2.92799	0.0013455	0.0039875
1.625	0.34915	1.51874	2.92810	0.0013554	0.0040173
1.6875	0.34915	1.51870	2.92824	0.0013692	0.0040588
1.75	0.34915	1.51893	2.92738	0.0013875	0.0041123
1.8125	0.34915	1.51888	2.92757	0.0014108	0.0041825
1.875	0.34915	1.51886	2.92765	0.0014398	0.0042696
1.9375	0.34915	1.51892	2.92744	0.0014750	0.0043748
2	0.34915	1.51887	2.92765	0.0015168	0.0045007
2.0625	0.34915	1.51884	2.92779	0.0015656	0.0046475

2.125	0.34915	1.51891	2.92756	0.0016216	0.0048159
2.1875	0.34915	1.51891	2.92760	0.0016852	0.0050075
2.25	0.34915	1.51885	2.92787	0.0017565	0.0052229
2.3125	0.34915	1.51882	2.92804	0.0018356	0.0054620
2.375	0.34915	1.51884	2.92803	0.0019225	0.0057247
2.4375	0.34915	1.51882	2.92818	0.0020172	0.0060119
2.5	0.34915	1.51864	2.92893	0.0021197	0.0063246
2.5625	0.34915	1.51857	2.92928	0.0022300	0.0066606
2.625	0.34915	1.51866	2.92905	0.0023479	0.0070193
2.6875	0.34915	1.51298	2.95052	0.0024734	0.0074590
2.75	0.34915	1.51830	2.93062	0.0026063	0.0078136
2.8125	0.34915	1.51880	2.92888	0.0027467	0.0082392
2.875	0.34915	1.51850	2.93014	0.0028943	0.0086969
2.9375	0.34915	1.51878	2.92925	0.0030490	0.0091714
3	0.34915	1.51871	2.92966	0.0032109	0.0096732

A.2 Positivity Check

We will explain how to compute enclosures for the range of approximate solutions ω_t in order to prove their nonnegativity in Ω_t. This will be necessary to omit the modulus in various computations. These calculations also apply for proving nonnegativity of the computed approximate solution in the unbounded L-shaped domain.

Note that during our computations we used pure Finite Element functions as well as approximations which are improved by corner singular functions, i.e. which are of the form $\omega_t = \sum_{i=1}^{4} \tilde{a}_i \lambda_i \gamma_i + v$ (see section 3.2.3 for the definitions of λ_i and γ_i). In the following we will (as done before) consider a shifted version of Ω_t such that the upper left re-entrant corner is located at $(0,0)$. Then local polar coordinates, centered at this corner, are given by (r, φ), $\varphi \in (0, \frac{3\pi}{2})$,

$$r = \sqrt{x^2 + y^2}$$

$$\varphi = \begin{cases} \arctan(\frac{y}{x}), & x > 0, y > 0 \\ \frac{\pi}{2}, & x = 0, y > 0 \\ \arctan(\frac{y}{x}) + \pi, & x < 0 \\ \frac{3\pi}{2}, & x = 0, y < 0 \end{cases}$$

We will show how to compute an enclosure for the range of ω_t on some elements K such that $K \subset ((-1, t) \times (-t, 1)) \cap \Omega_t$. All other elements can be treated similarly since $\lambda_i \gamma_i$ is given by a suitable rotation and shift of $\lambda_1 \gamma_1$ for $i = 2, 3, 4$.

First we recall some notations for Finite Elements that were introduced in section 3.1: The reference elements are given by $\hat{K}^t = \text{conv}\{(0,0), (0,1), (1,0)\}$ and $\hat{K}^q = (0,1)^2$. Reference shape

functions in $\hat{K}^t$ are denoted by $\hat{s}_j^t$, $j = 1, \ldots, 5$ and are defined in (3.2). For reference shape functions in $\hat{K}^q$ we use the analogous notation $\hat{s}_j^q$, $j = 0, \ldots, 7$ and refer to the definition in (3.3). Local shape functions on an element K are then denoted by s_j^K, $j = 0, \ldots, m$ (with $m = 5$ in case K is a triangle and $m = 7$ in case K is a rectangle, respectively), for their definition see (3.5).

Remark 15. If edgebump functions (onepeakedge, twopeakedge, fourpeakedge, see Figure 6.1) are considered, the corresponding computational domains (see Figure 6.6) can be discretized using solely rectangles. This is not possible in the cornerbump function cases, where the computational domains contain only the half corner $\operatorname{conv}\{(0,0), (0,1), (-1,1)\}$. Then also triangles occur in the discretization.

In the following we omit the index t.

Pure Finite Element function

If K is a triangle we can compute the exact range as follows: Let $c_0, \ldots, c_5$ be the nodal values of $\omega|_K$, i.e.

$$\omega|_K = \sum_{i=0}^{5} c_i s_i^K.$$

By construction, the transformation mapping K on the reference cell $\hat{K}^t$, preserves the range of the Finite Element function and therefore we have

$$\omega|_K(K) = \hat{v}(\hat{K}^t) \qquad \text{where} \qquad \hat{v} = \sum_{i=0}^{5} c_i \hat{s}_i^t.$$

Clearly, $\hat{v}$ can also be written as $\hat{v}(\hat{x}, \hat{y}) = e_0 + e_1\hat{x} + e_2\hat{y} + e_3\hat{x}\hat{y} + e_4\hat{x}^2 + e_5\hat{y}^2$. It is easy to compute $\min_{\hat{K}^t} \hat{v}$ and $\max_{\hat{K}^t} \hat{v}$ and therefore the range $\hat{v}(\hat{K}^t) = [\min_{\hat{K}^t} \hat{v}, \max_{\hat{K}^t} \hat{v}]$. However, since there is no compact formula for $\min_{K^t} \hat{v}$ and $\max_{K^t} \hat{v}$ and one has to consider several cases depending on the coefficients of $\hat{v}$, we will leave out the details.

If K is a rectangle we have

$$\omega|_K = \sum_{i=0}^{7} c_i s_i^K,$$

and therefore with the same argument as before

$$\omega|_K(K) = \hat{v}(\hat{K}^q), \qquad \text{where} \qquad \hat{v} = \sum_{i=1}^{7} c_i \hat{s}_i^q.$$

Writing

$$\hat{v}(\hat{x}, \hat{y}) = e_0 + e_1\hat{x} + e_2\hat{y} + e_3\hat{x}\hat{y} + e_4\hat{x}^2 + e_5\hat{y}^2 + e_6\hat{x}^2\hat{y} + e_7\hat{x}\hat{y}^2,$$

with $e_1, \ldots, e_7$ being linear combinations of $c_1, \ldots, c_7$, the most simple enclosure for the range is then given by

$$\omega|_K(K) \subset e_0 + e_1[0, 1] + e_2[0, 1] + e_3[0, 1] + e_4[0, 1] + e_5[0, 1] + e_6[0, 1] + e_7[0, 1]. \qquad \text{(A.1)}$$

The expression on the right-hand-side can not be reduced further, since in general $a[0,1]+b[0,1] \neq (a+b)[0,1]$ for $a, b \in \mathbb{R}$. Consider e.g. $a = -1$ and $b = 1$: Then $-1 \cdot [0,1] + 1 \cdot [0,1] = [-1,1]$ but $(-1+1)[0,1] = 0$.

If the enclosure given by (A.1) does only contain non-negative values, we are done. This is indeed satisfied in most elements. If the enclosure contains also negative values we can refine the above procedure by splitting the reference element in n^2 subsquares $\hat{K}_{ik}^q = [ih, (i+1)h] \times [kh, (k+1)h]$, where $n \in \mathbb{N}$ is suitably chosen, $h = \frac{1}{n}$ and $i, k = 0, \dots, n-1$. An enclosure for the range $\hat{v}(\hat{K}^q)$ is then given by

$$\hat{v}(\hat{K}^q) \subset \bigcup_{i,k=1}^{n} \hat{v}(\hat{K}_{ik}^q)$$

and enclosures for $\hat{v}(\hat{K}_{ik}^q)$ can be calculated by

$$e_0 + e_1[x_i] + e_2[y_k] + e_3[x_i][y_k] + e_4[x_i]^2 + e_5[y_k]^2 + e_6[x_i]^2[y_k] + e_7[x_i][y_k]^2,$$

where we used the notation $[x_i] := [ih, (i+1)h]$ and $[y_k] := [kh, (k+1)h]$.

However, also this refinement will not yield the desired enclosures if K is an element touching the boundary, where we have Dirichlet boundary conditions. In this case the enclosure will certainly contain zero and due to overestimation possibly also negative values. As an example how to treat these cases we will consider the elements $K = (x_p, x_p + d) \times (0, e)$ and $K = (-1, -1 + d) \times (1 - e, 1)$. The first element touches the boundary of $\partial\Omega$ at the upper edge of the inner hole and the second is the element at the "outer" corner $(-1, 1)$, see also Figure A.1. Note that other elements touching the boundary can be treated similarly as the element in case FE1. Indeed, using a suitable rearrangement of the coefficients, the same formulas can be used.

Case FE1: $K = (x_p, x_p + d) \times (0, e)$, $x_p \geq 0$.

In this case we have $c_0 = c_1 = c_4 = 0$, and therefore

$$\begin{aligned}
\hat{v}(\hat{x}, \hat{y}) &= -c_2 \hat{x}\hat{y}(3 - 2\hat{x} - 2\hat{y}) - c_3 \hat{y}(1 - \hat{x})(1 + 2\hat{x} - 2\hat{y}) \\
&\quad + 4c_5 \hat{x}\hat{y}(1 - \hat{y}) + 4c_6 \hat{x}\hat{y}(1 - \hat{x}) + 4c_7 \hat{y}(1 - \hat{x})(1 - \hat{y}) \\
&= \hat{y}\left(e_0 + e_1\hat{x} + e_2\hat{y} + e_3\hat{x}\hat{y} + e_4\hat{x}^2\right) \\
&=: \hat{y}p(\hat{x}, \hat{y}).
\end{aligned}$$

Since $\hat{y}$ is positive in $(0, 1)$ we are left to check that $p(\hat{K}^q)$ is contained in the nonnegative real numbers. This could in principle be done using (A.1), but since p is linear in $\hat{y}$ and quadratic in $\hat{x}$, we can even compute $\min_{\hat{K}^q} p$ and $\max_{\hat{K}^q} p$ without much effort and therefore also $p(\hat{K}^q) = [\min_{\hat{K}^q} p, \max_{\hat{K}^q} p]$.

Case FE2: $K = (-1, -1 + d) \times (1 - e, 1)$.

Now we have $c_0 = c_2 = c_3 = c_6 = c_7 = 0$ and thus

$$\begin{aligned}
\hat{v}(\hat{x}, \hat{y}) &= -c_1 \hat{x}(1 - \hat{y})(1 - 2\hat{x} + 2\hat{y}) + 4c_4 \hat{x}(1 - \hat{x})(1 - \hat{y}) + 4c_5 \hat{x}\hat{y}(1 - \hat{y}) \\
&=: \hat{x}(1 - \hat{y})p(\hat{x}, \hat{y}).
\end{aligned}$$

Again, since $\hat{x}(1 - \hat{y}) \geq 0$ in $\hat{K}^q$ we are left to consider $p(\hat{K}^q)$. Here, p is bilinear and takes its minimal and maximal value, respectively, in one of the corners of $\hat{K}^q$.

Remark 16. Clearly a necessary condition for non-negativity of a Finite Element function is non-negativity of all nodal values. This is indeed satisfied for all our approximate solutions.
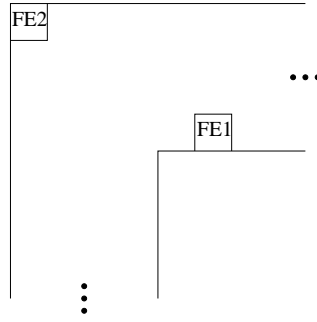
Figure A.1: Position of sample elements (Finite Element case)

Sum of corner singular function and Finite Element function

Let the approximate solution now be given by

$$\omega = \sum_{i=1}^{4} \tilde{a}_i \lambda_i \gamma_i + v,$$

with cut-off functions λ_i, γ_i as defined in (3.15) and a Finite Element function v. For elements $K \subset ((-1,t) \times (-t,1)) \cap \Omega_t$ we have by construction of λ_i (see (4.5) and (4.6)):

$$\omega = \tilde{a}_1 \underbrace{\lambda_1 \gamma_1}_{=\tilde{w}_1} + v$$

and $\gamma_1(r,\varphi) = r^{\frac{2}{3}} \sin(\frac{2}{3}\varphi)$. In the following, we omit the index 1 and for simplicity of presentation we consider the case $t = 1$, i.e. $\lambda(x,y) = (1 - x^2)^2 (1 - y^2) \chi_{[-1,1]^2}(x,y)$ (note that the general case $\lambda(x,y) = \left(1 - \frac{x^2}{t^2}\right)^2 \left(1 - \frac{y^2}{t^2}\right)^2$ can be treated analogously).

Clearly, the corner singular part is non-negative in Ω and positive in $\Omega \cap (-1,1)^2$. If also the Finite Element part is non-negative in some element K, we are ready. The range computations can be done as explained in the previous subsection. However, there will be elements for which the regular part $v|_K$ is negative or the range-enclosure contains negative values. In this case we have to compute range-enclosures of both the corner singular part and v. We will here show some special examples of elements and the corresponding procedures to prove non-negativity. For the positions of the sample elements see also Figure A.2

Case S1: $\overline{K} \subset \Omega \cap \{(x,y) \in \mathbb{R}^2 : x < 0, y > -x\}$, $K = \text{conv}\{(x_p, y_p), (x_p + d, y_p),$
$$(x_p, y_p + d)\}.$$

We have $x_p, x_p + d < 0$ and obtain for all $(x,y) \in K$:

$$\tilde{w}(x,y) \geq \underbrace{\left(1 - x_p^2\right)^2 \left(1 - (y_p + d)^2\right)^2 \left((x_p + d)^2 + y_p^2\right)^{\frac{1}{3}} \sin\left(\frac{2}{3} \arctan\left(\frac{y_p}{x_p + d}\right) + \frac{2}{3}\pi\right)}_{=:m},$$

$$\tilde{w}(x,y) \leq \underbrace{\left(1 - (x_p + d)^2\right)^2 \left(1 - y_p^2\right)^2 \left(x_p^2 + (y_p + d)^2\right)^{\frac{1}{3}} \sin\left(\frac{2}{3} \arctan\left(\frac{y_p}{x_p}\right) + \frac{2}{3}\pi\right)}_{=:M}.$$

The minimal and maximal values for $\sin\left(\frac{2}{3}\varphi\right)$ are due to the fact that $y > -x$ for $(x, y) \in K$. Denote by $[v_m, v_M]$ the computed range for the regular part, then $\omega(K) \subset [\tilde{a}m, \tilde{a}M] + [v_m, v_M]$. This enclosure is indeed sufficient in all our applications to obtain non-negative range enclosures.

Case S2: $K = \text{conv}\{(0, d), (-d, d), (0, 0)\}$.

This is the triangle element at the re-entrant corner $(0, 0)$. Here the procedure from the first case will not work, since $\tilde{w} = 0$ at the corner and the range of the regular part contains negative values. Due to Dirichlet boundary conditions we have:

$$\omega(x, y) = \tilde{a}(1 - x^2)^2(1 - y^2)^2 r^{\frac{2}{3}}\sin\left(\frac{2}{3}\varphi\right) + c_0(1 - \hat{x} - \hat{y})(1 - 2\hat{x} - 2\hat{y}) + c_1\hat{x}(2\hat{x} - 1)$$
$$+ 4c_3\hat{x}(1 - \hat{x} - \hat{y}) + 4c_4\hat{x}\hat{y} + 4c_5\hat{y}(1 - \hat{x} - \hat{y})$$

where $\hat{x} = -\frac{x}{d}$ and $\hat{y} = \frac{d-y}{d} = 1 - \frac{y}{d}$. Thus $1 - \hat{x} - \hat{y} = \frac{x+y}{d}$, and using polar coordinates $x = r\cos\varphi$ and $y = r\sin\varphi$ we obtain

$$\omega(r\cos\varphi, r\sin\varphi) = r^{\frac{2}{3}}\left[\tilde{a}(1 - r^2\cos^2\varphi)^2(1 - r^2\sin^2\varphi)^2\sin\left(\frac{2}{3}\varphi\right)\right.$$
$$+ \frac{r^{\frac{1}{3}}}{d^2}\left(c_0(\cos\varphi + \sin\varphi)(-d + 2r\cos\varphi + 2r\sin\varphi)\right.$$
$$- c_1\cos\varphi(-2r\cos\varphi - d) - 4c_3\cos\varphi(r\cos\varphi + r\sin\varphi)$$
$$\left.\left. - 4c_4\cos\varphi(d - r\sin\varphi) + 4c_5(d - r\sin\varphi)(\cos\varphi + \sin\varphi)\right)\right]$$
$$=: r^{\frac{2}{3}}w^{(pc)}(r, \varphi).$$

Note that we have $K \subset \{(r\cos\varphi, r\sin\varphi) : r \in [0, \sqrt{2}d], \varphi \in [\frac{\pi}{2}, \frac{3\pi}{4}]\}$. Using interval arithmetic we can thus compute $w^{(pc)}([0, \sqrt{2}d] \times [\frac{\pi}{2}, \frac{3\pi}{4}])$ and obtain an enclosure for $\omega(K)$.

Case S3: $\overline{K} \subset \Omega \cap (-1, 1)^2$, $K = (x_p, x_p + d) \times (y_p, y_p + e)$, $x_p \geq 0$, $x_p + d \leq 1$.

An enclosure for the range of the regular part can be computed using (A.1). For the singular part we have the following estimates (for all $(x, y) \in K$):

$$\tilde{w}(x, y) \geq \left(1 - (x_p + d)^2\right)^2\left(1 - (y_p + e)^2\right)^2\left(x_p^2 + y_p^2\right)^{\frac{1}{3}}\sin\left(\frac{2}{3}\arctan\left(\frac{y_p}{x_p+d}\right)\right)$$
$$\tilde{w}(x, y) \leq \left(1 - x_p^2\right)^2\left(1 - y_p^2\right)^2\left((x_p + d)^2 + (y_p + e)^2\right)^{\frac{1}{3}}\sin\left(\frac{2}{3}\arctan\left(\frac{y_p+e}{x_p}\right)\right).$$

To check positivity we sum up the two ranges, leading to non-negative range enclosures in all applications.

Case S4: $K = (0, d) \times (0, e)$

The procedure of Case S3 will not work here, since both the singular and the regular part of the approximation satisfy Dirichlet boundary conditions and the enclosure given by (A.1) will contain negative values due to overestimation. However, since for the regular part we have $c_0 = c_1 = c_4 = 0$ we can use a similar trick as in case S2:

$$\omega(x, y) = \tilde{a}(1 - x^2)^2(1 - y^2)^2 r^{\frac{2}{3}}\sin\left(\frac{2}{3}\varphi\right) - c_2\hat{x}\hat{y}(3 - 2\hat{x} - 2\hat{y})$$
$$- c_3\hat{y}(1 - \hat{x})(1 + 2\hat{x} - 2\hat{y}) + 4c_5\hat{x}\hat{y}(1 - \hat{y}) + 4c_6\hat{x}\hat{y}(1 - \hat{x})$$
$$+ 4c_7\hat{y}(1 - \hat{x})(1 - \hat{y}),$$

where $\hat{x} = \frac{x}{d}$, $\hat{y} = \frac{y}{e}$. Using $r \sin \varphi = y$, we obtain

$$\omega(x,y) = r^{\frac{2}{3}} \sin \varphi \left[\tilde{a}(1-x^2)^2(1-y^2)^2 \frac{\sin\left(\frac{2}{3}\varphi\right)}{\sin\varphi} + \frac{r^{\frac{1}{3}}}{e}\left(-c_2\hat{x}(3-2\hat{x}-2\hat{y})\right.\right.$$

$$\left.\left. -c_3(1-\hat{x})(1+2\hat{x}-2\hat{y}) + 4c_5\hat{x}(1-\hat{y}) + 4c_6\hat{x}(1-\hat{x}) + 4c_7(1-\hat{x})(1-\hat{y})\right)\right]$$

$$=: r^{\frac{2}{3}} \sin \varphi \left[\tilde{a}(1-x^2)^2(1-y^2)^2 \frac{\sin\left(\frac{2}{3}\varphi\right)}{\sin\varphi} + \frac{r^{\frac{1}{3}}}{e}\hat{p}(\hat{x},\hat{y})\right].$$

The range of the polynomial part $\hat{p}$ can be computed exactly by calculating $m := \min_{\hat{K}^q} \hat{p}$ and $M = \max_{\hat{K}^q} \hat{p}$. For the singular part we can use the estimate:

$$\tilde{a}(1-x^2)^2(1-y^2)^2 \frac{\sin\left(\frac{2}{3}\varphi\right)}{\sin\varphi} \geq \frac{2\tilde{a}}{3}\left(1-d^2\right)^2\left(1-e^2\right)^2 =: C.$$

Note that $\frac{\sin(\frac{2}{3}\varphi)}{\sin(\varphi)}$ has a removable singularity at $\varphi = 0$ and $\lim_{\varphi \to 0} \frac{\sin(\frac{2}{3}\varphi)}{\sin(\varphi)} = \frac{2}{3}$, $\frac{\sin(\frac{2}{3}\varphi)}{\sin(\varphi)} \geq \frac{2}{3}$ for $\varphi \in [0, \frac{\pi}{2}]$. If $C + \frac{\left((x_p+d)^2+(y_p+e)^2\right)^{\frac{1}{6}} m}{e} \geq 0$, non-negativity of the approximate solution in K is proved. Indeed, this inequality is satisfied in our applications.

Case S5: $K = (x_p, x_p + d) \times (0, e)$, $x_p > 0$.

The first idea is to treat these elements as the corner element in case S4. Unfortunately, this does not work for all elements. Therefore we present another solution here. Obviously, the approximate solution is zero on the boundary of Ω. We compute the partial derivative of ω with respect to y and check its positivity using interval arithmetic. If the derivative is positive in K, ω itself must be positive in K. Indeed, this sufficient condition is satisfied in our applications.

Case S6: $K = (x_p, x_p + d) \times (1 - e, 1)$, $x_p > 0$.

In this case it turned out to be sufficient to compute a range enclosure for the regular part as explained in case FE1.
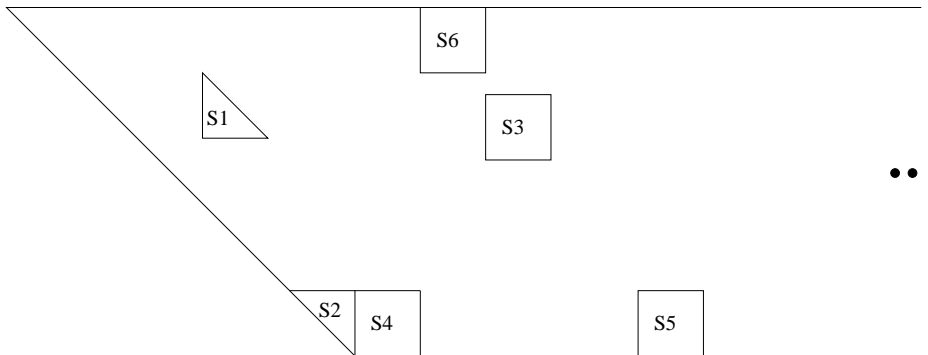

Figure A.2: Position of sample elements

Again note that all other elements can be treated similarly: For elements not touching the boundary a similar procedure as in case S1 or S3 can be used, where only the estimates of the maximal and

minimal values of the corner singular part have to be adapted accordingly. For elements touching the boundary at the outer square we refer to case S6 and for other boundary elements to the cases S4 and S5 (where in S5 possibly the derivative w.r.t to x has to be considered, e.g. for elements at the left inner square boundary).

A.3 Construction of Cubature Rules

At many points in this thesis we have to compute enclosures (or upper bounds) for integrals of Finite Element functions, i.e. for integrals of polynomials over triangles and rectangles in $\mathbb{R}^2$. For small polynomial degree one can find examples for cubature rules which are sufficient to integrate these polynomials exactly (e.g. [28, Chapter 15]). However, in our computations we need cubature rules which can integrate also polynomials of higher degree and thus we will in this section explain how we constructed suitable cubature rules to do so.

A.3.1 Cubature on a rectangle

We will first explain how to construct a cubature rule on the unit square $[0, 1]^2$ which is exact for polynomials of the form $p(x, y) = \sum_{k=0}^{M_1} \sum_{l=0}^{M_2} c_{kl} x^k y^l$ $(c_{kl} \in \mathbb{R})$. We start with considering quadrature rules on the interval $[0, 1]$:

For $n \in \mathbb{N}$, let $x_1, \ldots, x_n \in [0, 1]$ be nodes and $w_1, \ldots, w_n \in \mathbb{R}$ weights of the quadrature rule

$$Q_n(f) := \sum_{k=1}^n w_k f(x_k) \approx \int_0^1 f(x)\,dx, \qquad f : [0, 1] \to \mathbb{R}.$$

We will also write $Q_n[x_1, \ldots, x_n; w_1, \ldots, w_n; f]$ if the nodes and weights of Q_n are not clear from the context.

Q_n is said to be of order m if $Q_n(x^k) = \int_0^1 x^k\,dx$ for all $k = 0, \ldots, m$, i.e. Q_n is exact for all polynomials of degree smaller than or equal to m. It is well known that the order of a quadrature rule with n nodes cannot exceed $2n - 1$ and that this order is attained for Gaussian quadrature rules.

Analogously we define a cubature formula C_n on $[0, 1]^2$ with nodes $(x_1, y_1), \ldots, (x_n, y_n)$ and weights $w_1, \ldots, w_n$, which approximates the integral of a function $f : [0, 1]^2 \to \mathbb{R}$ over $[0, 1]^2$:

$$C_n(f) := \sum_{k=1}^n w_i f(x_i, y_i) \approx \int_{[0,1]^2} f(x, y)\,d(x, y).$$

Let $Q_{n_1}^{(x)}[\hat{x}_1, \ldots, \hat{x}_{n_1}; \alpha_1, \ldots, \alpha_{n_1}; f]$ and $Q_{n_2}^{(y)}[\hat{y}_1, \ldots, \hat{y}_{n_2}; \beta_1, \ldots, \beta_{n_2}; f]$ be quadrature rules of order M_1 and M_2, respectively. The tensor-product cubature rule given by these two is denoted by

$C_{n_1 n_2}\{Q_{n_1}^{(x)}, Q_{n_2}^{(y)}\}$ and has the following $n_1 n_2$ nodes and weights

$$
\begin{aligned}
(x_1, y_1) &= (\hat{x}_1, \hat{y}_1), & w_1 &= \alpha_1 \beta_1 \\
(x_2, y_2) &= (\hat{x}_1, \hat{y}_2), & w_2 &= \alpha_1 \beta_2 \\
&\vdots \\
(x_{n_2}, y_{n_2}) &= (\hat{x}_1, \hat{y}_{n_2}), & w_{n_2} &= \alpha_1 \beta_{n_2} \\
(x_{n_2+1}, y_{n_2+1}) &= (\hat{x}_2, \hat{y}_1), & w_{n_2+1} &= \alpha_2 \beta_1 \\
&\vdots \\
(x_{2n_2}, y_{2n_2}) &= (\hat{x}_2, \hat{y}_{n_2}), & w_{2n_2} &= \alpha_2 \beta_{n_2} \\
&\vdots \\
(x_{n_1 n_2}, y_{n_1 n_2}) &= (\hat{x}_{n_1}, \hat{y}_{n_2}), & w_{n_1 n_2} &= \alpha_{n_1} \beta_{n_2}.
\end{aligned}
$$

Thus, for any $f : [0,1]^2 \to \mathbb{R}$ we have

$$
C_{n_1 n_2}(f) = \sum_{l=1}^{n_1 n_2} w_l f(x_l, y_l) = \sum_{j=1}^{n_1} \sum_{k=1}^{n_2} \alpha_j \beta_k f(\hat{x}_j, \hat{y}_k).
$$

For a polynomial $x^p y^q$ with $0 \le p \le M_1$ and $0 \le q \le M_2$ the cubature rule gives

$$
\begin{aligned}
C_{n_1 n_2}(x^p y^q) &= \sum_{j=1}^{n_1} \sum_{k=1}^{n_2} \alpha_j \beta_k \, \hat{x}_j^p \, \hat{y}_k^q = \sum_{j=1}^{n_1} \alpha_j \hat{x}_j^p \sum_{k=1}^{n_2} \beta_k \hat{y}_k^q = Q_{n_1}^{(x)}(x^p) Q_{n_2}^{(y)}(y^q) \\
&= \int_0^1 x^p \, dx \int_0^1 y^q \, dy = \int_{[0,1]^2} x^p y^q \, d(x, y),
\end{aligned}
$$

and the second last equation holds due to the given orders of $Q_{n_1}^{(x)}$ and $Q_{n_2}^{(y)}$. Therefore all polynomials of this form are integrated exactly.

To obtain a tensor-product cubature rule with smallest possible number of nodes (and weights) we construct it from quadrature rules with the same property, i.e. Gaussian quadrature rules.

Gauss-Legendre quadrature

In this section we will shortly recall the definition of the Gauss-Legendre quadrature on the interval $[-1, 1]$.

For $n \in \mathbb{N}_0$ let P_n be the n-th Legendre polynomial, which can be expressed using the Rodrigues-formula

$$
P_n(x) = \frac{1}{2^n n!} \frac{d^n}{dx^n} (x^2 - 1)^n. \tag{A.2}
$$

P_n is a polynomial of degree n and has n simple real zeros, denoted by $x_1, \ldots, x_n$, which will serve as nodes of the Gauss-Legendre quadrature. The weights can be computed by

$$
w_i = \int_{-1}^1 \prod_{\substack{j=1 \\ j \neq i}}^n \frac{x - x_j}{x_i - x_j} \, dx = \frac{2}{(1 - x_i^2)(P_n'(x_i))^2} \qquad (i = 1, \ldots, n), \tag{A.3}
$$

the latter formula following e.g. from [27, (9.4)] together with some basic properties of the Legendre polynomials.

The order of the Gauss-Legendre quadrature rule is $2n - 1$, i.e. to integrate polynomials x^q with $0 \leq q \leq M$ exactly one has to use the corresponding rule with $n = \lceil \frac{M+1}{2} \rceil$ nodes and weights. The tensor-product rule $C_{n_1 n_2}\{Q_{n_1}^{(x)}, Q_{n_2}^{(y)}\}$ will therefore be exact for polynomials $x^p y^q$ with $0 \leq p \leq M_1$ and $0 \leq q \leq M_2$ if $Q_{n_1}^{(x)}$ and $Q_{n_2}^{(y)}$ are chosen to be the Gauss-Legendre quadrature rules with $n_1 = \lceil \frac{M_1+1}{2} \rceil$ and $n_2 = \lceil \frac{M_2+1}{2} \rceil$ nodes and weights, respectively.

A.3.2 Cubature on a triangle

Let T be the triangle given by the points $(0,0)$, $(1,0)$ and $(0,1)$. For a function $f : T \to \mathbb{R}$ we want to construct a cubature formula which approximates the integral $\int_T f(x, y) \, d(x, y)$. Since $T = \{(x, y) \in \mathbb{R}^2 : 0 \leq x \leq 1, \ 0 \leq y \leq 1 - x\}$ we can use the substitution $y = t(1 - x)$ with $0 \leq x, t \leq 1$ to obtain

$$\int_T f(x, y) \, d(x, y) = \int_0^1 \int_0^{1-x} f(x, y) \, dy \, dx = \int_0^1 \int_0^1 \underbrace{f(x, t(1 - x))(1 - x)}_{=:g(x,t)} \, dt \, dx.$$

Since the integral on the right-hand-side is an integral over $[0, 1]^2$, we can use the tensor-product ansatz described in the previous subsection to construct so called conical cubature rules on the triangle T: Let $Q_{n_1}^{(x)}[\hat{x}_1, \ldots, \hat{x}_{n_1}; \alpha_1, \ldots, \alpha_{n_1}; f]$ and $Q_{n_2}^{(t)}[\hat{t}_1, \ldots, \hat{t}_{n_2}; \beta_1, \ldots, \beta_{n_2}; f]$ be quadrature rules for the interval $[0, 1]$ of order M_1 and M_2, respectively, then (with the definition of g as in the above formula)

$$\int_0^1 \int_0^1 g(x, t) \, dt \, dx \approx \sum_{j=1}^{n_1} \sum_{k=1}^{n_2} \alpha_j \beta_k g(\hat{x}_j, \hat{t}_k) = \sum_{j=1}^{n_1} \sum_{k=1}^{n_2} \alpha_j \beta_k (1 - \hat{x}_j) f(\hat{x}_j, \hat{t}_k(1 - \hat{x}_j)).$$

The conical cubature rule for the triangle T is therefore given by the $n_1 n_2$ nodes (x_i, y_i) and weights w_i ($i = 1, \ldots, n_1 n_2$), where

$$\begin{aligned} x_{(j-1)n_2+k} &= \hat{x}_j \\ y_{(j-1)n_2+k} &= \hat{t}_k(1 - \hat{x}_j) \\ w_{(j-1)n_2+k} &= \alpha_j \beta_k (1 - \hat{x}_j) \qquad \text{for } j = 1 \ldots, n_1, k = 1, \ldots, n_2. \end{aligned}$$

Note that this cubature rule does not integrate all polynomials $x^p y^q$ with $0 \leq p \leq M_1$ and $0 \leq q \leq M_2$ over T exactly, but only the ones with $0 \leq q \leq M_2$ and $0 \leq p + q + 1 \leq M_1$. To construct a conical cubature rule for T which is exact for polynomials $x^p y^q$ with $0 \leq p \leq \widetilde{M}_1$ and $0 \leq q \leq \widetilde{M}_2$, the number of nodes and weights for the quadrature rules must at least be $n_2 = \lceil \frac{\widetilde{M}_2+1}{2} \rceil$ and $n_1 = \lceil \frac{\widetilde{M}_1+\widetilde{M}_2+2}{2} \rceil$ (with n_1 and n_2 attaining these minimal values if Gauss-Legendre quadrature rules are used).

A.3.3 Verified cubature formulas

In order to obtain verified enclosures for the integrals computed by one of the above cubature rules we have to use interval arithmetic. This requires verified enclosures for both the nodes and weights

of the cubature rules, which, by the above formulas, can be constructed from nodes and weights of the corresponding quadrature rules.

In all our applications we used Gauss-Legendre quadrature rules, where the nodes are given by the zeros $x_1, \ldots, x_n$ of the Legendre polynomials P_n, defined in (A.2), and the weights can be computed using the formula (A.3). For small values of n the zeros can be computed in closed form and the expressions can be found in many textbooks. However for larger values ($n > 5$) we have to compute enclosures for these zeros, which can be done rigorously using an Interval Newton method. Finally the weights can be computed using interval arithmetic and (A.3), and the cubature nodes and weights are then given by the formulas in the previous sections.

A.4 Some norm estimates and computations

In the following we omit the index t.

We want to apply Lemma 1 to $u = \omega$ and $\tilde{u} = \breve{\omega}^{(2)}$. Recall that $\breve{\omega}^{(2)} = I_{V_{\tilde{N}}}(\omega)$ and $\breve{\omega} = I_{V_N}(\omega)$, where $\tilde{N} < N$. We will also need the piecewise polynomial approximation $\hat{\omega}$ of ω that was defined in (4.7) and is given by

$$\hat{\omega}(x, y) = \sum_{i=1}^{4} \tilde{a}_i \lambda_i(x, y) I_{V_N}(\gamma_i).$$

Assume that we have already computed a bound K, such that

$$\|v\|_{H_0^1} \leq \|L_{\breve{\omega}^{(2)}}[v]\|_{H^{-1}} \qquad \text{for all } v \in H_0^1(\Omega).$$

We set $p_1 = 4$, $p_2 = 2$, $p_3 = p_4 = 8$. Obviously $\frac{1}{p_1} + \frac{1}{p_2} + \frac{1}{p_3} + \frac{1}{p_4} = 1$ is satisfied. Now, in order to satisfy the assumptions of Lemma 1 (b) we have to compute

$$\kappa = K \left[3C_4^2 \left(\|\omega\|_{L^4} + \|\breve{\omega}^{(2)}\|_{L^4} \right) \|\omega - \breve{\omega}^{(2)}\|_{L^2} \right] \tag{A.4}$$

and check that $\kappa < 1$ is satisfied. Note that it is sufficient to compute an upper bound $\bar{\kappa}$ for the right hand-side of (A.4), check $\bar{\kappa} < 1$, and use the conclusion of Lemma 1 (b) with $\bar{\kappa}$ instead of κ.

We will briefly comment on the techniques to compute (or estimate) the norm-quantities occuring in (A.4).

a) To compute an upper bound for $\|\omega - \breve{\omega}^{(2)}\|_{L^2}$ we use triangle inequality:

$$\|\omega - \breve{\omega}^{(2)}\|_{L^2} \leq \|\omega - \hat{\omega}\|_{L^2} + \|\hat{\omega} - \breve{\omega}\|_{L^2} + \|\breve{\omega} - \breve{\omega}^{(2)}\|_{L^2}.$$

Since $\hat{\omega} - \breve{\omega}$ as well as $\breve{\omega} - \breve{\omega}^{(2)}$ are piecewise polynomial, their L^2-norms can be computed exactly using quadrature rules of sufficiently high degree, applied elementwise. For the first summand we can write

$$\|\omega - \hat{\omega}\|_{L^2}^2 = \sum_K \int_K (\omega - \hat{\omega})^2 \, d(x, y)$$

$$\leq \sum_K \sum_{i=1}^{4} \tilde{a}_i^2 \left(\max_K \lambda_i(x, y) \right)^2 \int_K (\gamma_i - I_{V_N} \gamma_i)^2 \, d(x, y). \tag{A.5}$$

All quantities on the right-hand-side, or upper bounds for them, have already been computed in the course of the defect computation.

b) For the computation of $\|\omega\|_{L^4}$ we use triangle inequality again:

$$\|\omega\|_{L^4} \le \|\omega - \hat{\omega}\|_{L^4} + \|\hat{\omega}\|_{L^4},$$

and for the first summand we have the estimate

$$\|\omega - \hat{\omega}\|_{L^4}^4 \le \max_{\overline{\Omega}}(\omega - \hat{\omega})^2 \|\omega - \hat{\omega}\|_{L^2}^2. \tag{A.6}$$

An upper bound for $\|\omega - \hat{\omega}\|_{L^2}^2$ is already known and the term $\max_{\overline{\Omega}}(\omega - \hat{\omega})^2$ can be computed without much additional effort using interval arithmetic. In principle, one could also use a similar estimate as in (A.5) to bound $\|\omega - \breve{\omega}\|_{L^4}^4$ directly. However, this would require upper bounds for the integrals $\int_K (\gamma_i - I_{V_N}\gamma_i)^4 \, d(x, y)$, and computing tight upper bounds for these integrals is too costly for our purposes.

Bibliography

[1] N. ACKERMAN, M. CLAPP, AND F. PACELLA, *Self-focusing Multibump Standing Waves in Expanding Waveguides*, Milan Journal of Mathematics, 79 (2011), pp. 221–232.

[2] ——, *Alternating Sign Multibump Solutions of Nonlinear Elliptic Equations in Expanding Tubular Domains*, Communications in Partial Differential Equations, 38 (2013), pp. 751–779.

[3] G. ALEFELD AND J. HERZBERGER, *Einführung in die Intervallrechnung*, Bibliographisches Institut, 1974.

[4] K. APPEL AND W. HAKEN, *Every planar map is four colorable*, Bulletin of the American Mathematical Society, 82 (1976), pp. 711–712.

[5] D. N. ARNOLD, D. BOFFI, AND R. S. FALK, *Approximation by Quadrilateral Finite Elements*, Mathematics of Computation, 71 (2002), pp. 909–922.

[6] R. G. BARTLE, *Newton's Method in Banach Spaces*, Proceedings of the American Mathematical Society, 6 (1955), pp. 827–831.

[7] T. BARTSCH, M. CLAPP, M. GROSSI, AND F. PACELLA, *Asymptotically radial solutions in expanding annular domains*, Mathematische Annalen, 352 (2012), pp. 485–515.

[8] H. BEHNKE, U. MERTINS, M. PLUM, AND C. WIENERS, *Eigenvalue Inclusions via Domain Decomposition*, Proceedings of The Royal Society: Mathematical, Physical and Engineering Sciences, 456 (2000), pp. 2717–2730.

[9] F. BLOMQUIST, W. HOFSCHUSTER, AND W. KRÄMER, *C-XSC-Langzahlarithmetiken für reelle und komplexe Intervalle basierend auf den Bibliotheken MPFR und MPFI*, Preprint BUW-WRSWT 2011/1, Universität Wuppertal.

[10] J. BORWEIN AND M. P. SKERRITT, *An Introduction to Modern Mathematical Compu-ting: With Maple^{TM}*, Springer, 2011.

[11] S. BRENNER AND L. R. SCOTT, *The Mathematical Theory of Finite Element Methods*, Springer, 2008.

[12] B. BREUER, J. HORÁK, P. J. MCKENNA, AND M. PLUM, *A computer-assisted existence and multiplicity proof for travelling waves in a nonlinearly supported beam*, Journal of Differential Equations, 224 (2006), pp. 60–97.

[13] B. BREUER, P. J. MCKENNA, AND M. PLUM, *Multiple solutions for a semilinear boundary value problem: a computational multiplicity proof*, Journal of Differential Equations, 195 (2003), pp. 243–269.

[14] J. BYEON, *Existence of Many Nonequivalent Nonradial Positive Solutions of Semilinear Elliptic Equations on Three-Dimensional Annuli*, Journal of Differential Equations, 136 (1997), pp. 136–165.

[15] F. CATRINA AND Z. Q. WANG, *Nonlinear elliptic equations on expanding symmetric domains*, Journal of Differential Equations, 156 (1999), pp. 153–181.

[16] K. C. CHANG, *Methods in nonlinear analysis*, Springer, 2005.

[17] G. CHEN, J. ZHOU, AND W. N. NI, *Algorithms and Visualization for Solutions of Nonlinear Elliptic Equations*, International Journal of Bifurcation and Chaos, 10 (2000), pp. 1565–1612.

[18] Y. S. CHOI AND P. J. MCKENNA, *A Mountain Pass Method for the Numerical Solution of Semilinear Elliptic Problems*, Nonlinear Analysis, Theory, Methods & Applications, 20 (1993), pp. 417–437.

[19] P. G. CIARLET, *The Finite Element Method for Elliptic Problems*, North-Holland, 1978.

[20] C. V. COFFMAN, *A Non-linear Boundary Value Problem with Many Positive Solutions*, Journal of Differential Equations, 54 (1984), pp. 429–437.

[21] L. DAMASCELLI, M. GROSSI, AND F. PACELLA, *Qualitative properties of positive solutions of semilinear elliptic equations in symmetric domains via the maximum principle*, Annales de l'Institut Henri Poincare (C) Non Linear Analysis, 16 (1999), pp. 631–652.

[22] E. N. DANCER, *The Effect of Domain Shape on the Number of Positive Solutions of Certain Nonlinear Equations*, Journal of Differential Equations, 74 (1988), pp. 120–156.

[23] ——, *On the number of positive solutions of some weakly nonlinear equations on annular regions*, Mathematische Zeitschrift, 206 (1991), pp. 551–562.

[24] ——, *Superlinear problems on domains with holes of asymptotic shape and exterior problems*, Mathematische Zeitschrift, 227 (1998), pp. 475–491.

[25] E. N. DANCER AND S. YAN, *Multibump solutions for an elliptic problem in expanding domains*, Communications in Partial Differential Equations, 27 (2002), pp. 23–55.

[26] M. DAUGE, Y. LAFRANCHE, AND N. RAYMOND, *Quantum Waveguides with Corners*, in ESAIM: Proceedings, vol. 35, 2012, pp. 14–45.

[27] P. DEUFLHARD AND A. HOHMANN, *Numerische Mathematik I*, Walter de Gruyter, 2002.

[28] G. ENGELN-MÜLLGES, K. NIEDERDRENK, AND R. WODICKA, *Numerik-Algorithmen*, Springer, 10 ed., 2011.

[29] I. ERGATOUDIS, B. M. IRONS, AND O. C. ZIENKIEWICZ, *Curved, Isoparametric, "Quadrilateral" Elements for Finite Element Analysis*, International Journal of Solids and Structures, 4 (1968), pp. 31–42.

[30] B. GIDAS, W. M. NI, AND L. NIRENBERG, *Symmetry and related properties via the maximum principle*, Communications in Mathematical Physics, 68 (1979), pp. 209–243.

[31] D. GILBARG AND N. S. TRUDINGER, *Elliptic Partial Differential Equations of Second Order*, Springer, 2001.

[32] P. GRISVARD, *Elliptic Problems in Nonsmooth Domains*, no. 24 in Monographs and Studies in Mathematics, Pitman, 1985.

[33] ———, *Singularities in Boundary Value Problems*, no. 22 in Research Notes in Applied Mathematics, Springer, 1992.

[34] M. GROSSI, *A uniqueness result for a semilinear elliptic equation in symmetric domains*, Advances in Differential Equations, 5 (2000), pp. 193–212.

[35] R. HAMMER, M. HOCKS, U. KULISCH, AND D.RATZ, *Numerical Toolbox for Verified Computing I*, Springer, 1993.

[36] K. HASHIMOTO, K. NAGATOU, AND M. T. NAKAO, *Numerical verification of stationary solutions for Navier-Stokes problems*, Journal of Computational and Applied Mathema-tics, 199 (2007), pp. 445–451.

[37] H. HEUSER, *Funktionalanalysis*, Teubner, 4th ed., 2006.

[38] V. HOANG, M. PLUM, AND C. WIENERS, *A computer-assisted proof for photonic band gaps*, Zeitschrift für angewandte Mathematik und Physik, 60 (2009), pp. 1035–1052.

[39] W. HOFSCHUSTER AND W. KRÄMER, *C-XSC 2.0: A C++ Library for Extended Scientific Computing*, in Numerical Software with Result Verification, 2004.

[40] T. KATO, *Perturbation Theory for Linear Operators*, vol. 132 of Grundlehren der mathematischen Wissenschaften, Springer, 1976.

[41] H. B. KELLER, *Numerical Solution of Bifurcations and Nonlinear Eigenvalue Problems*, in Applications of Bifurcation Theory, Academic Press, 1977, pp. 359–384.

[42] ———, *Constructive methods for bifurcation and nonlinear eigenvalue problems*, in Computing Methods in Applied Sciences and Engineering, Springer, 1979, pp. 241–251.

[43] R. KLATTE, U. KULISCH, A. WIETHOFF, C. LAWO, AND M. RAUCH, *C-XSC A C++ Class Library for Extended Scientific Computing*, Springer, 1993.

[44] J. R. LAHMANN AND M. PLUM, *A computer-assisted instability proof for the Orr-Sommerfeld equation with Blasius profile*, Zeitschrift für Angewandte Mathematik und Mechanik, 84 (2004), pp. 188–204.

[45] Y. Y. LI, *Existence of Many Positive Solutions of Semilinear Elliptic Equations on Annulus*, Journal of Differential Equations, 83 (1990), pp. 348–367.

[46] S. S. LIN, *Existence of Many Positive Nonradial Solutions for Nonlinear Elliptic Equations on an Annulus*, Journal of Differential Equations, 103 (1993), pp. 338–349.

[47] ———, *Asymptotic Behavior of Positive Solutions to Semilinear Elliptic Equations on Expanding Annuli*, Journal of Differential Equations, 120 (1995), pp. 255–288.

[48] MAPLESOFT, *Maple Webpage*, March 2014. `http://www.maplesoft.com/products/Maple/`.

[49] P. J. MCKENNA, F. PACELLA, M. PLUM, AND D. ROTH, *A Computer-Assisted Uniqueness Proof for a Semilinear Elliptic Boundary Value Problem*, in Inequalities and Applications 2010, vol. 161, Springer, pp. 31–52.

[50] ——, *A Uniqueness Result for a Semilinear Elliptic Problem: A Computer-assisted Proof*, Journal of Differential Equations, 247 (2009), pp. 2140–2162.

[51] T. MINAMOTO, M. T. NAKAO, AND Y. YAMAMOTO, *Numerical verification method for solution of the perturbed Gelfand equation*, Methods and Applications of Analysis, 7 (2000), pp. 251–262.

[52] M. T. NAKAO, *Numerical verifications of solutions for nonlinear hyperbolic equations*, Interval Computations, 4 (1994), pp. 64–77.

[53] M. T. NAKAO AND Y. WATANABE, *On computational proofs of the existence of solutions to nonlinear parabolic problems*, Journal of Computational and Applied Mathematics, 50 (1994), pp. 401–410.

[54] ——, *Numerical Verification Methods for Solutions of Semilinear Elliptic Boundary Value Problems*, Nonlinear Theory and Its Applications, 2 (2011), pp. 2–31.

[55] S. A. NAZAROV AND B. A. PLAMENEVSKY, *Elliptic Problems in Domains with Piecewise Smooth Boundaries*, Walter de Gruyter, 1994.

[56] M. PLUM, *Computer-Assisted Existence Proofs for Two-Point Boundary Value Problems*, Computing, 46 (1991), pp. 19–34.

[57] ——, *Existence and enclosure results for continua of solutions of parameter-dependent nonlinear boundary value problems*, Journal of Computational and Applied Mathematics, 60 (1995), pp. 187–200.

[58] ——, *Existence and Multiplicity Proofs for Semilinear Elliptic Boundary Value Problems by Computer Assistance*, Jahresbericht der DMV, 110 (2008), pp. 19–54.

[59] M. PLUM AND C. WIENERS, *New solutions of the Gelfand problem*, Journal of Mathematical Analysis and Applications, 269 (2002), pp. 588–606.

[60] S. I. POHOZAEV, *On the eigenfunctions of the equation $\Delta u + \lambda f(u) = 0$*, Doklady Akademii Nauk SSR, 165 (1965), pp. 36–39.

[61] P. H. RABINOWITZ, *Minimax Methods in Critical Point Theory with Applications to Differential Equations*, American Mathematical Society, 1984.

[62] S. M. RUMP, *INTLAB - INTerval LABoratory*, in Developments in Reliable Compu-ting, Kluwer Academic Publishers, 1999, pp. 77–104. `http://www.ti3.tuhh.de/rump/`.

[63] Y. WATANABE, *A numerical verification method for two-coupled elliptic partial differential equations*, Japan Journal of Industrial and Applied Mathematics, 26 (2009), pp. 233–247.

[64] H. F. WEINBERGER, *Variational Methods for Eigenvalue Approximation*, Society for Industrial and Applied Mathematics, 1974.

[65] C. WIENERS, *A geometric data structure for parallel finite elements and the application to multigrid methods with block smoothing*, Computing and Visualization in Science, 13 (2010), pp. 161–175.